THERMAL HISTORY OF THE MEGUMA TERRANE:

A STUDY BASED ON ^{40}Ar-^{39}Ar AND FISSION TRACK DATING.

BY

PETER ELIAS

SUBMITTED IN PARTIAL FULFILLMENT OF THE REQUIREMENTS
FOR THE DEGREE OF DOCTOR OF PHILOSOPHY

AT

DALHOUSIE UNIVERSITY
HALIFAX, NOVA SCOTIA
SEPTEMBER, 1986.

DALHOUSIE UNIVERSITY

FACULTY OF GRADUATE STUDIES

The undersigned hereby certify that they have read and recommend to the Faculty of Graduate Studies for acceptance a thesis entitled " Thermal History of the Meguma Terrane: A Study Based on ^{40}Ar-^{39}Ar and Fission Track Dating"

by Peter Elias

in partial fulfillment of the requirements for the degree of Doctor of Philosophy.

(C)

Dated October 28, 1986

External Examiner

Research Supervisor

Examining Committee

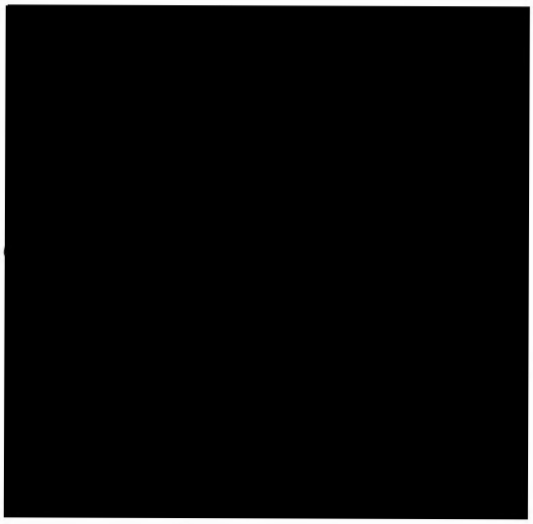

DALHOUSIE UNIVERSITY

Date 23 Dec., 1986

Author PETER ELIAS

Title Thermal History of the Meguma Terrane:

A Study Based on ^{40}Ar-^{39}Ar and Fission Track Dating

Department or School GEOLOGY

Degree PhD Convocation February Year 1987

Permission is herewith granted to Dalhousie University to circulate and to have copied for non-commercial purposes, at its discretion, the above title upon the request of individuals or institutions.

Signature of Author

THE AUTHOR RESERVES OTHER PUBLICATION RIGHTS, AND NEITHER THE THESIS NOR EXTENSIVE EXTRACTS FROM IT MAY BE PRINTED OR OTHERWISE REPRODUCED WITHOUT THE AUTHOR'S WRITTEN PERMISSION.

THE AUTHOR ATTESTS THAT PERMISSION HAS BEEN OBTAINED FOR THE USE OF ANY COPYRIGHTED MATERIAL APPEARING IN THIS THESIS (OTHER THAN BRIEF EXCERPTS REQUIRING ONLY PROPER ACKNOWLEDGMENT IN SCHOLARLY WRITING) AND THAT ALL SUCH USE IS CLEARLY ACKNOWLEDGED.

TABLE OF CONTENTS

	PAGE
LIST OF FIGURES	x
LIST OF TABLES	xiv
LIST OF ABBREVIATIONS	xvi
ABSTRACT	xvii
ACKNOWLEDGEMENTS	xviii

CHAPTER 1	1
INTRODUCTION	1
1.1. GENERAL STATEMENT	1
1.2. LOCATION AND ACCESS	2
1.3. PREVIOUS WORK AND GEOLOGICAL SETTING	2
1.3.1. THE ACADIAN EVENT	17
1.3.2. THE ALLEGHANIAN EVENT	20
1.3.3. THE MESOZOIC EVENT	20
1.4. SCOPE OF THE THESIS	23

CHAPTER 2 25

PRINCIPLES AND PROCEDURES 25

2.1. INTRODUCTION 25

2.2. K-Ar SYSTEMATICS 25

2.2.1. CONVENTIONAL K-Ar DATING 25

2.2.2 ^{40}Ar-^{39}Ar MODIFICATION 26

2.2.2.1. FLUX MONITORS (STANDARDS) 31

2.2.2.2. CORRECTION FOR INTERFERING ISOTOPES . . 32

2.3. PRINCIPLES OF FISSION TRACK DATING 37

2.4. DIFFUSION AND CLOSURE TEMPERATURE. 40

2.5. A DISCUSSION OF DIFFUSION EXPERIMENTS 49

2.6. THERMOCHRONOMETRY AND METHODS OF DERIVING T_c 51

2.6.1. THE BERGER-YORK PROCEDURE FOR DERIVING T_c 52

2.6.2. THE HARRISON-MCDOUGALL METHOD 56

2.6.3. OTHER METHODS OF DERIVING T_c 57

2.7. LABORATORY PROCEDURE 58

2.7.1. MINERAL SEPARATION 58

2.7.2. FISSION TRACK DATING PROCEDURE 58

2.7.3. ARGON DATING PROCEDURE 59

CHAPTER 3 62

EVALUATION OF SPECTRA AND DERIVATION OF CLOSURE TEMPERATURES 62

3.1. INTRODUCTION 62

3.2. CONCORDANT AND DISCORDANT SPECTRA 63

3.3. DISCORDANCE FACTORS 65

3.4. A MODEL FOR ARGON RELEASE DURING STEP HEATING . 66

3.5. INFORMATION CONTAINED IN ^{40}Ar-^{39}Ar SPECTRA 73

3.6. THE EFFECTS OF RECOIL ON THE SPECTRA OF SLATES 79

3.7. THE RELATIONSHIP BETWEEN $^{37}Ar/^{39}Ar$ AND Ca/K IN AMPHIBOLES. 85

3.8. GENERAL OBSERVATIONS ON MICA SPECTRA 87

3.9. DERIVATION OF CLOSURE TEMPERATURES 92

3.9.1. ARRHENIUS PLOTS 92

3.9.2. MUSCOVITE 104

3.9.3. BIOTITE 105

3.9.4. K-FELDSPAR 106

3.9.5. SUMMARY 107

CHAPTER 4 109

DATA BASE AND REGIONAL INTERPRETATION 109

4.1. GENERAL INTRODUCTION 109

4.1.1. THE POSSIBLE ROLE OF EXTRANEOUS ARGON IN THE MEGUMA TERRANE 112

4.2. DATA BASE AND INTERPRETATION FROM THE REGIONAL METAMORPHIC TERRANE 115

4.2.1. INTRODUCTION 115

4.2.2. SUMMARIZED GEOLOGY OF THE RMT 116

4.2.3. SLATES 126

4.2.4. AMPHIBOLES FROM THE RMT 136

4.2.5. MICAS FROM THE REGIONAL METAMORPHIC TERRANE 147

4.2.5.1. VARIATION OF MICA APPARENT AGES WITHIN THE MEGUMA TERRANE 148

4.2.5.2. A DOMAIN IN THE WHITE ROCK FORMATION . 157

4.2.5.3. SUMMARY OF 'AGE VARIATION' STUDIES . . 168

4.2.5.4. OLDER MICAS 169

4.2.5.5. YOUNGER MICAS 180

4.2.5.6. SUMMARY OF MICA DATA FROM THE RMT . . . 197

4.2.6. FISSION TRACK DATA 198

4.3. DATA BASE AND INTERPRETATION FROM THE SOUTHERN SATELLITE PLUTONS 199

4.3.1. INTRODUCTION 199

4.3.2. BARRINGTON PASSAGE PLUTON 206

4.3.3. BALD MOUNTAIN PLUTON 216

4.3.4. THE SHELBURNE PLUTON 221

4.3.5. PORT MOUTON PLUTON 231
4.3.6. THE QUINAN PLUTON 236
4.3.7. THE UPPER CLYDE RIVER PEGMATITE 236
4.3.8. SUMMARY OF DATA FROM THE SSP 239
4.4. DATA BASE AND SIGNIFICANCE OF ARGON DATA FROM FELDSPARS AND FISSION TRACK DATA FROM APATITES 240
4.4.1. INTRODUCTION 240
4.4.2. THE SOUTH MOUNTAIN BATHOLITH 242
4.4.3. THE SOUTHERN SATELLITE PLUTONS 253
4.4.4. SUMMARY OF K-FELDSPAR/FISSION TRACK DATA . 259
4.4.5. INFERENCE FROM PLAGIOCLASE 260
4.5. THERMAL MODELS FOR THE MEGUMA TERRANE 261
4.5.1. SMB MODEL 1 262
4.5.2. SMB MODEL 2. 270
4.5.3. SMB MODEL 3 270
4.5.4. DISCUSSION OF SMB MODELS 270
4.5.4.1. ARGON DIFFUSION CURVES FOR K-FELDSPAR . 272
4.5.4.2. COMBINATION OF KINETIC DATA FROM K-FELDSPAR AND APATITE 273
4.5.5. SSP MODEL 1 (ONE OVERPRINT). 277
4.5.6. SSP MODEL 2 (TWO OVERPRINTS) 282
4.5.7. DISCUSSION OF SSP MODELS 286
4.5.8. RMT COMPOSITE MODEL 1 287
4.5.9. RMT COMPOSITE MODEL 2 287
4.5.10. DISCUSSION OF RMT MODELS 292

CHAPTER 5 SUMMARY 293
5.1. INTRODUCTION 293
5.2. MAIN CONCLUSIONS 293
5.3. IMPLICATIONS OF TECTONOTHERMAL EVENTS 299
IN THE MEGUMA TERRANE 299
5.3.1. THE ACADIAN EVENT 299
5.3.2. THE ALLEGHANIAN EVENT (MARITIME DISTURBANCE) 300
5.3.3. THE MESOZOIC EVENT 305

APPENDIX A. SUMMARY TABLES FROM ARGON ANALYSES 307
APPENDIX B. MICROPROBE ANALYSES 360
APPENDIX C. OTHER DATA (XRD, PETROGRAPHY) 368
REFERENCES. 387

LIST OF FIGURES

	PAGE
1-1. Geologic Time Scale	4
1-2. Location map of study area.	6
1-3. Histogram of early geochronological data from the Meguma terrane (after Reynolds et al., 1981).	9
1-4. Paleozoic stratigraphy of the study area	12
1-5. Map outlining the relationship between plutons and the metamorphic zones.	16
2-1(a). Arrangement of standards and unknowns in canister for irradiation.	29
2-1(b). Typical curve from which 'J' is derived.	29
2-2. Experimental 'J' curve derived from standards MMhb-1 and NS-231, irradiated in the same canister (can. 53).	34
2-3. Models for which solutions to the diffusion equation have been obtained.	43
2-4. Schematic diagram illustrating the relationship between temperature and argon retention in a K-bearing mineral.	47
2-5. Schematic diagram outlining the diffusion profile for isothermal heating (T1) and heating at several temperatures (T1,T2,T3...).	55
3-1. Schematic diagram illustrating possible distribution of sites where radiogenic argon may reside in a K-bearing mineral.	71
3-2. Schematic diagram illustrating typical argon concentration gradient expected in a mineral that suffered episodic loss or cooled very slowly.	75
3-3. Photomicrograph of slate sample NS71-139.	81
3-4. Photomicrograph of slate sample NS72-31.	81
3-5. Photomicrograph of slate sample NS72-33.	83

3-6. Age spectra of amphiboles, showing variation of Ca/K with argon release. 89

3-7. Arrhenius plots for muscovite, biotite and K-feldspar. 94

3-8. Plot of biotite activation energy vs Fe/(Fe+Mg). 103

3-9. Plot of Closure temperature vs IDF. 103

4.2-1. Diagram illustrating P-T conditions of regional metamorphism in the Meguma terrane. 120

4.2-2. Map of 'complex domain' in southwest Nova Scotia. 123

4.2-3. Photomicrograph of metapelite from the 'Complex Domain', showing advanced chloritization of biotite. 125

4.2-4. Sample location for slates. 128

4.2-5. Age spectra for slates. 131

4.2-6. Sample locations for amphiboles. 139

4.2-7. Rim-to-core analyses of amphiboles from the RMT and the SSP. 141

4.2-8. Age spectra for amphiboles from the RMT. 145

4.2-9. Map of White Rock domain. 159

4.2-10. Photomicrograph of sheared metapelite from the White Rock Domain. 161

4.2.-11. Photomicrograph of sheared metapelite from the White rock Domain. 161

4.2-12. Photomicrograph of sheared metapelite from the White Rock Domain, showing post-tectonic chlorite overgrowth. 163

4.2-13. Distribution of 'older micas' in the RMT. 171

4.2-14. Histogram of apparent ages of 'older' biotites. 173

4.2-15. Age spectra of 'older' micas. 175

4.2-16. Distribution of 'younger micas' in the RMT. 182

4.2-17. Histogram of apparent ages of 'younger' biotites. 184

4.2-18. Age spectra of 'younger' micas. 186

4.2-19. Photomicrograph of sheared and altered metapelite from the 'Complex Domain' showing well-developed C-S fabric. 192

4.2-20. Photomicrograph of metapelite from the 'Complex Domain,' where muscovite has replaced biotite and staurolite. 192

4.2-21. Photomicrograph of metapelite showing muscovite and chlorite (c) replacing staurolite (st). 194

4.3-1. Photomicrograph of mylonitized monzogranite from the Seal Island pluton. 202

4.3-2. Photomicrograph of mylonitic monzogranite from the Seal Island pluton. 204

4.3-3. Sample locations for the SSP. 209

4.3-4. Age spectra of samples from the Barrington Passage pluton. 212

4.3-5. Age spectra of samples from the Bald Mountain pluton. 220

4.3-6. Map of Shelburne Domain 223

4.3-7. Age spectra of samples from the Shelburne pluton. 225

4.3-8. Age spectra of samples from the Port Mouton pluton. 233

4.3-9. Age spectra of samples from the Quinan pluton, and Upper Clyde River pegmatite. 238

4.4-1. Location map for fission track and feldspar samples. 245

4.4-2. Age spectra of samples from the SMB. 250

4.4-3. Age spectra of samples from the SSP. 257

4.4-4. SMB Model 1. 265

4.4-5. SMB Model 2. 267

4.4-6. SMB Model 3. 269

4.4-7. Time-temperature curves for argon loss from K-feldspars and fission track annealing of apatite (SMB). 275

4.4-8. SSP Model 1. 279

4.4-9. SSP Model 2. 281

4.4-10. Time-temperature curves for argon loss from K-feldspars and fission track annealing of apatite (SSP). 284

4.4-11. RMT Composite model 1. 289

4.4-12. RMT Composite model 2. 291

5-1. Summary of geologic events in the Meguma terrane. 295

LIST OF TABLES

	Page
1-1. Evidence for an Acadian event in the Meguma and elsewhere in the Appalachians.	18
1-2. Evidence for an Alleghanian event	21
2-1(a). Isotopes generated during neutron irradiation.	35
2-1(b). Argon isotope ratios from irradiated salts of Ca and K.	35
2-2. Solutions to the diffusion equations.	44
3-1. Discordance factors defined in this study.	67
3-2. PDF values for some samples which produced highly concordant spectra.	68
3-3. Derived closure temperatures and activation energies for muscovite, biotite and K-feldspar.	100
4.2-1. Estimates of metamorphic temperatures and pressures in the Meguma terrane	118
4.2-2. Ages and discordance factors of slates.	129
4.2-3. Ages and discordance factors for amphiboles from the RMT.	145
4.2-4. Data for biotites from the RMT.	150
4.2-5. Rank correlation coefficients between apparent age and various parameters.	154
4.2-6. Summarized results from stepwise regression of biotite data.	154
4.2-7. Some chemical data for biotite from the White Rock Domain.	164
4.2-8. Ages and discordance factors for samples from the White Rock Domain.	164
4.2-9. Ages and discordance factors for 'older' micas	178
4.2-10. Ages and discordance factors for 'younger' micas.	190
4.3-1. Ages and discordance factors for samples from the SSP.	207
4.3-2. Chemical data for Bald Mountain muscovites.	218

4.4-1. Fission track data for the SMB 247

4.4-2. Ages and discordance factors for samples from the SMB. 248

4.4-3. Fission track data for the SSP. 255

4.4-4. Time-temperature constraints for thermal models for the SMB, the SSP and the RMT. 263

LIST OF ABBREVIATIONS

ABBREVIATIONS FOR PLUTONS

BM - Bald Mountain

BP - Barrington Passage

PM - Port Mouton

Q - Quinan

Sh - Shelburne

UC - Upper Clyde River Pegmatite.

ABBREVIATIONS USED ON AGE SPECTRA AND SAMPLE LOCATION MAPS.

Ap = apatite (fission track)

Bi, B = Biotite

Hb, H = Hornblende

K = K-feldspar

M = Muscovite

P = Plagioclase Ph = Phlogopite

W = Whole Rock

All $^{40}Ar^{39}Ar$ ages are incremental total gas ages, except those in parentheses, which are plateau ages.

ABSTRACT

The Meguma terrane experienced a complex tectonothermal history. ^{40}Ar-^{39}Ar data on slates, amphiboles, and micas indicate that regional metamorphism was initiated about 400 Ma ago. Plutons were intruded approximately 386-360 Ma ago. The Southern Satellite plutons appear to be of similar age to the South Mountain batholith. An overprinting event which peaked about 320-300 Ma ago was much more extensive than previously considered. Information from fission track dating of apatite, and K-feldspar age spectra have been combined to put constraints on the timing, duration, and temperature of overprinting. The effects were most severe in the southwest, where domains of economic mineralization are located. Although opening of the Bay of Fundy rift about 210 Ma ago was accompanied by basaltic magmatism, the thermal effects of this event were mild in the Meguma terrane. Fission track ages from apatite suggest that final cooling below 100 degrees C occurred about 190-170 Ma, soon after magmatism associated with opening of the present Atlantic Ocean.

Overprinted mica and K-feldspar samples seem incapable of yielding meaningful data on closure temperature by the vacuum diffusion technique of Berger and York (1981). Quantification of discordance in ^{40}Ar-^{39}Ar age spectra provides a useful framework for evaluating information contained in such spectra, and for testing reproducibility in the ^{40}Ar-^{39}Ar step-heating technique.

ACKNOWLEDGEMENTS

Thanks to Dr G.K. Muecke for introducing me to the Meguma, and for providing much useful advice. I am grateful to Dr P.H. Reynolds for supervision and providing financial support towards the research. For helpful advice, I am grateful to all other members of the Faculty at Dalhousie Geology Department, especially Drs D.B. Clarke and P.E. Schenk for many 'brief' discussions. I extend heartfelt thanks to Lorraine Elias for typing most of the manuscript. Special thanks to the Geology Department support staff: G. Brown, A. Giddy, N. Keeping, K. Maxwell, R. McKay, D. Meggison, S. Parikh, K. Taylor, D. Van de Rijt, and C. Walls. My special appreciation to Casey Ravenhurst, Alex Grist, Dr M. Zentilli and Dr R. Parrish, who were instrumental in setting up the Fission Track laboratory. I am indebted to Dean Rogers and Songhi Hwang for logistic support and useful discussions in the field. Special thanks to Stephanie Woodend for providing samples and helpful discussions. Merci to Linda Richard for assistance in French. Thanks to R. Allen and B. Trim of the Physics Department for assistance with typing, and to F. Stefani for assistance with photography.

CHAPTER 1

INTRODUCTION

1.1. GENERAL STATEMENT

The Meguma terrane is one of several megatectonic units accreted to the eastern flank of the North American craton during the Paleozoic (Williams and Hatcher, 1982). It consists dominantly of clastic metasediments intruded by granitoid plutons which are overlain by a mixture of clastic sediments, carbonates, and evaporites. One distinctive feature of the Meguma terrane is that it contains several domains of economic mineralization, including major tin and gold deposits. As a first step towards tracing the ancestral affinities of the Meguma terrane, and understanding the processes responsible for the economic deposits, much effort has recently been directed towards understanding the deformational history, geochemistry, geochronology, metallogeny, metamorphism, and stratigraphy (e.g. Schenk, 1980, 1981; Clarke and Halliday, 1980; Reynolds et al., 1981; Keppie, 1982; Muecke, 1984; Zentilli and Reynolds, 1985). This study is part of that continuing research. By means of the principles of thermochronometry, constraints can be placed on tectonothermal events which

affected the Meguma terrane. The background is outlined below. To facilitate discussion of geochronologic data, absolute ages of stratigraphically dated units are referred to the time scale of Palmer, (1983, fig. 1-1).

1.2. LOCATION AND ACCESS

The study area, located in southwestern Nova Scotia, is outlined in fig. 1-2. Easy access is provided by Highway 103 and numerous branch roads. Some points in Shelburne County are accessible only through fair-weather gravel roads. Outcrop exposure is fair in coastal areas, but rather poor inland, where bedrock is covered with thick glacial overburden and peat bogs.

1.3. PREVIOUS WORK AND GEOLOGICAL SETTING

Recorded geologic work in the study area dates back to the early nineteenth century. The first substantial mapping program was undertaken by Bailey (1898). He recognized three units in what is now known as the Meguma Group. From bottom to top, they are: (1) quartzite unit, (2) banded argillite unit, and (3) black slate unit. Members of the Geological Survey of Canada continued field mapping in areas that were not previously described (Faribault, 1912; Faribault et al., 1938a, 1938b).

The first major geochronological survey was undertaken by Fairbairn et al. (1960) and Fairbairn et al. (1964).

Fig. 1-1.

Part of the Geologic Time Scale (after Palmer, 1983).

GEOLOGIC TIME SCALE

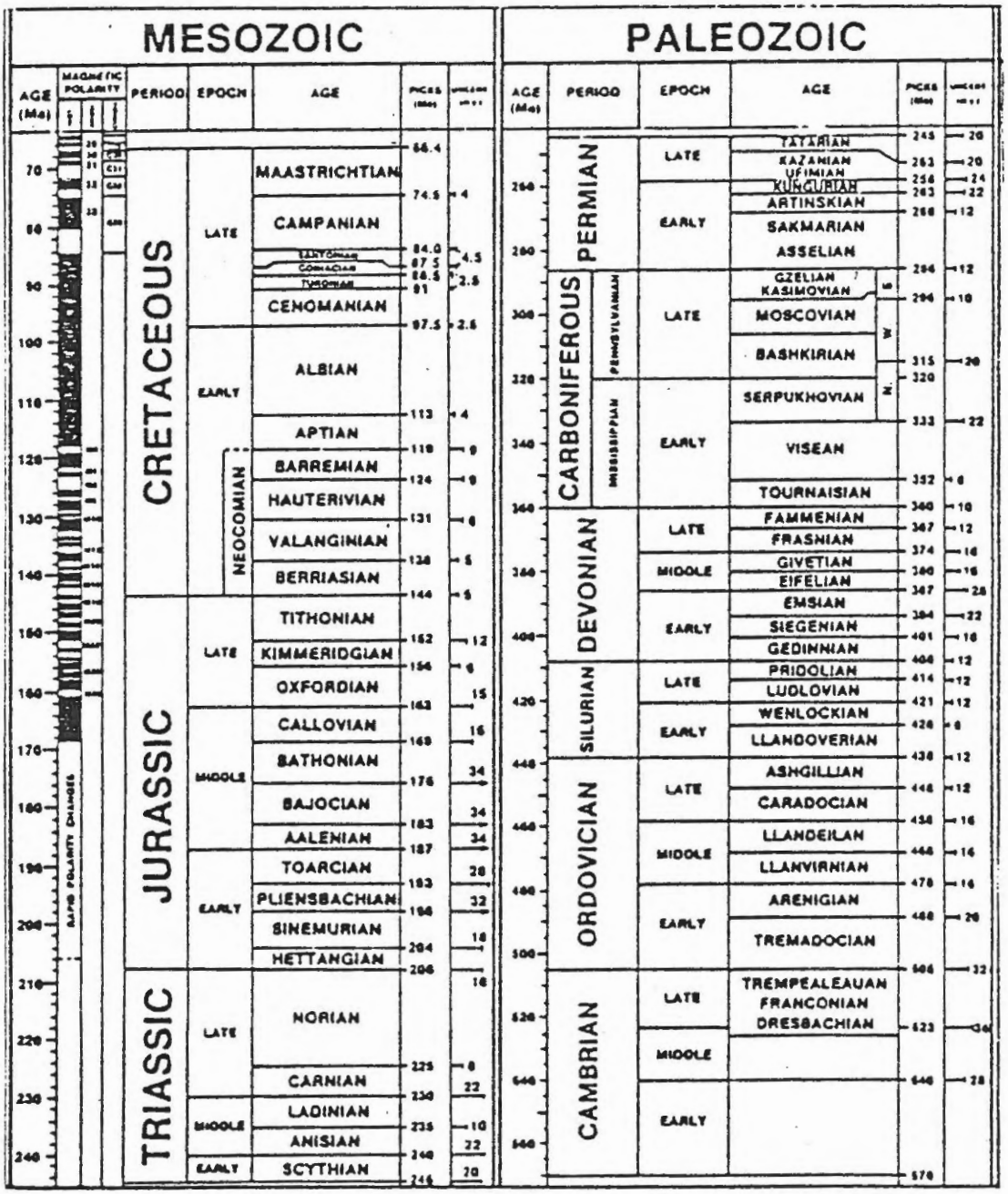

Fig. 1-2. Location map of tne study area

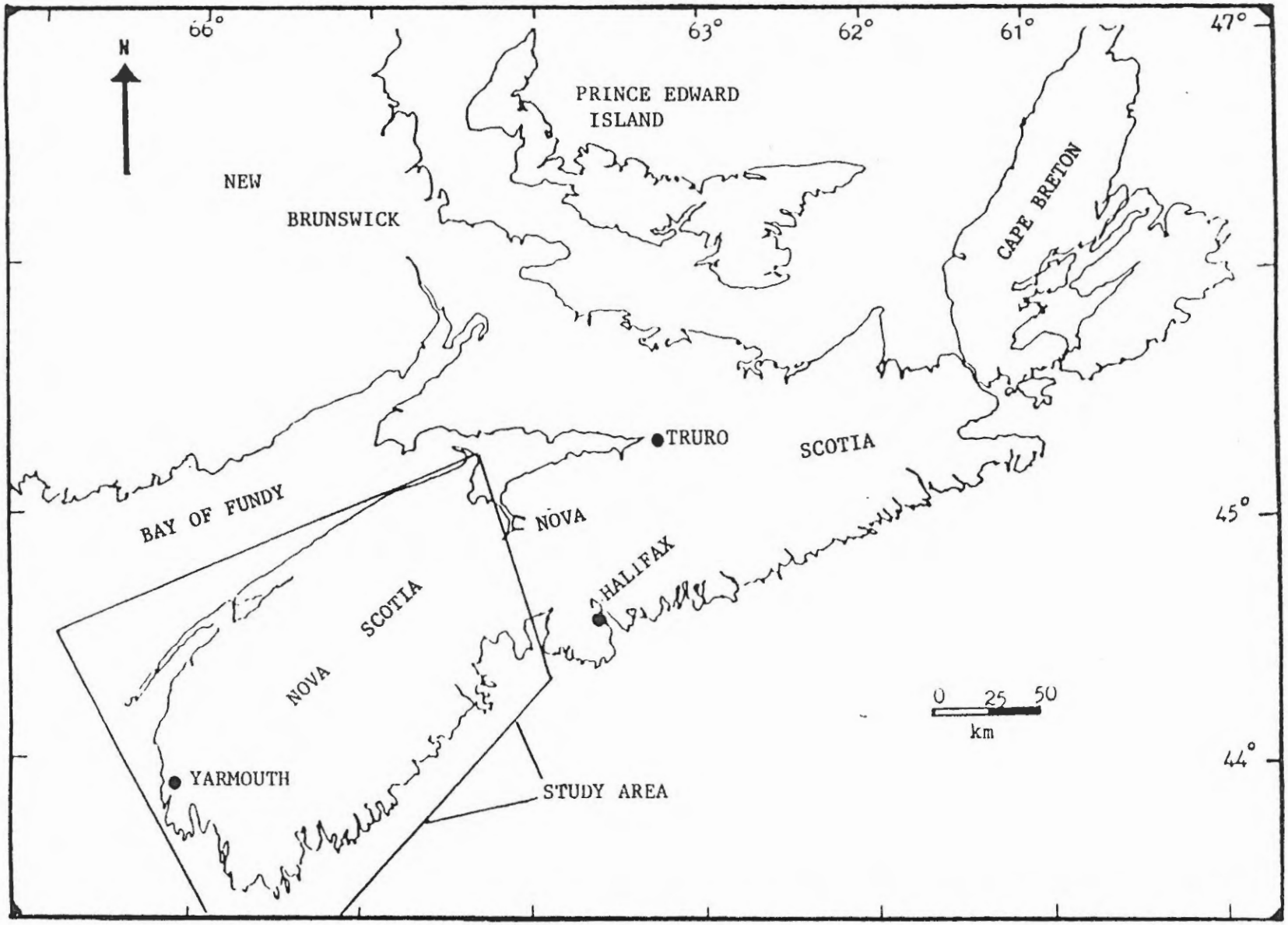
66°
63°
62°
61°
47°
N
PRINCE EDWARD
ISLAND
NEW
BRUNSWICK
CAPE BRETON
TRURO
SCOTIA
BAY OF FUNDY
NOVA
HALIFAX
45°
NOVA SCOTIA
0 25 50
km
44°
YARMOUTH
STUDY AREA

By means of conventional K-Ar and Rb-Sr methods, these workers acquired a considerable body of data which suggested Devonian-Carboniferous ages for most of the granitoid rocks in Nova Scotia. The results are summarized in Fig. 1-3. Although analytical precision may have played a role, the wide range of ages in these early studies suggests that the tectonothermal history of the Meguma terrane may have been complex.

Taylor (1965, 1967, 1969) mapped most of southwestern Nova Scotia on a scale of one inch to two miles. He clarified the stratigraphic relationships among the Lower Paleozoic Goldenville, Halifax and White Rock Formations, and determined that all three were conformable, as previously suggested by Crosby (1962). The maps produced by Taylor still provide the basis for more detailed work in the area. Smitheringale (1973) mapped north of the study area on a scale of 1:50,000, including large portions of the South Mountain Batholith. He cited the findings of Boucot (1960) that the fossil assemblage in the Devonian Torbrook Formation suggests that southwest Nova Scotia is of European Rhenish affinities.

Schenk (1970, 1978, 1980, 1981) conducted detailed sedimentological studies of the Meguma Group and concluded that the sediments were derived from a region located to the southeast. He noted several similarities and dissimilarities in the sedimentology, stratigraphy, and tectonic setting between the Meguma zone and western

Fig 1-3. Histogram of early geochronological data from the Meguma terrane (after Reynolds et al., 1981).

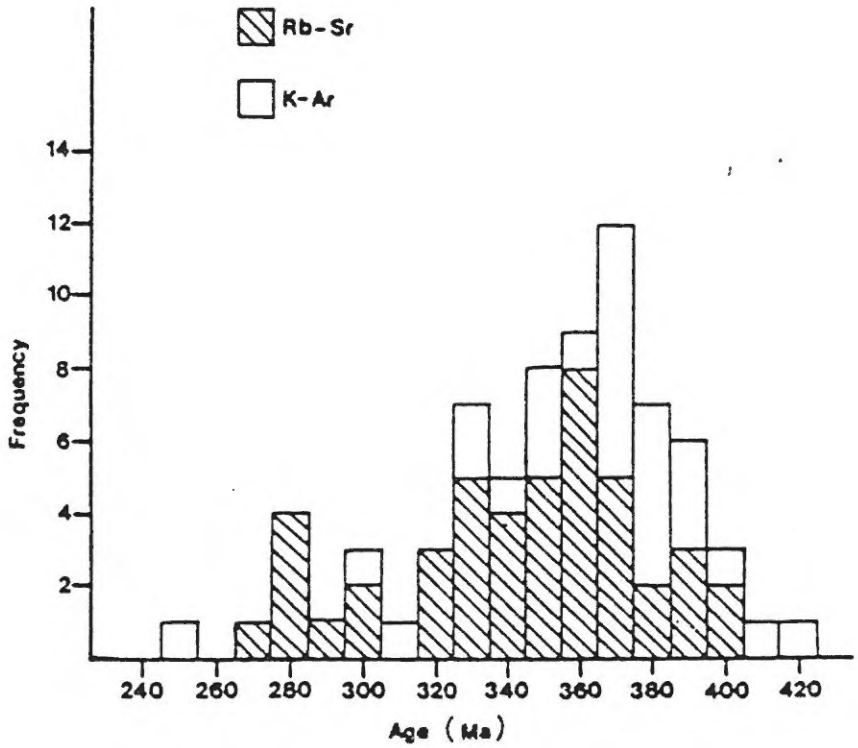
Rb-Sr
K-Ar
Frequency
14
12
10
8
6
4
2
240
260
280
300
320
340
360
380
400
420
Age (Ma)

Morocco. Schenk therefore suggested that the Saharan Shield may be a source of both sedimentary units, although he did not rule out other source areas like Western Europe or the Guyana Shield. The Paleozoic stratigraphy of the Meguma terrane is outlined in fig. 1-4 and map 2 (inside back cover).

Systematic documentation of metamorphism in the Meguma Group was first done by Taylor and Schiller (1966). They concluded that deformation preceded regional metamorphism, which reached almandine amphibolite facies. This was followed by granitoid intrusions with attendant contact metamorphism. Regional metamorphism was further described by Muecke (1973, 1984), and Clarke and Muecke (1980). Maps outlining the regional metamorphic zones (from chlorite to sillimanite zone) were produced by Keppie and Muecke (1979). A copy (map 1) is included in the folder in the back cover. Chu (1978) described regional metamorphism in the Goldenville and Halifax Formations in the Shelburne area. He concluded that regional metamorphism post-dates two episodes of regional deformation, and that regional metamorphism was followed by shearing associated with the generation of pseudotachylites and local retrograde metamorphism. Sarkar (1978) studied volcanism and metamorphism in the White Rock Formation, and suggested alkaline affinities for these rocks. Metamorphism in part of the Meguma Group in Yarmouth County was investigated by Cullen (1983). He concluded that regional metamorphism in

Fig. 1-4. Cambrian - Carboniferous stratigraphy of the Meguma terrane, (after Hacquebard, 1972; and Schenk, in press). For complete stratigraphy, see map 2 (Keppie, 1979) inside back cover.
SMB = South Mountain Batholith

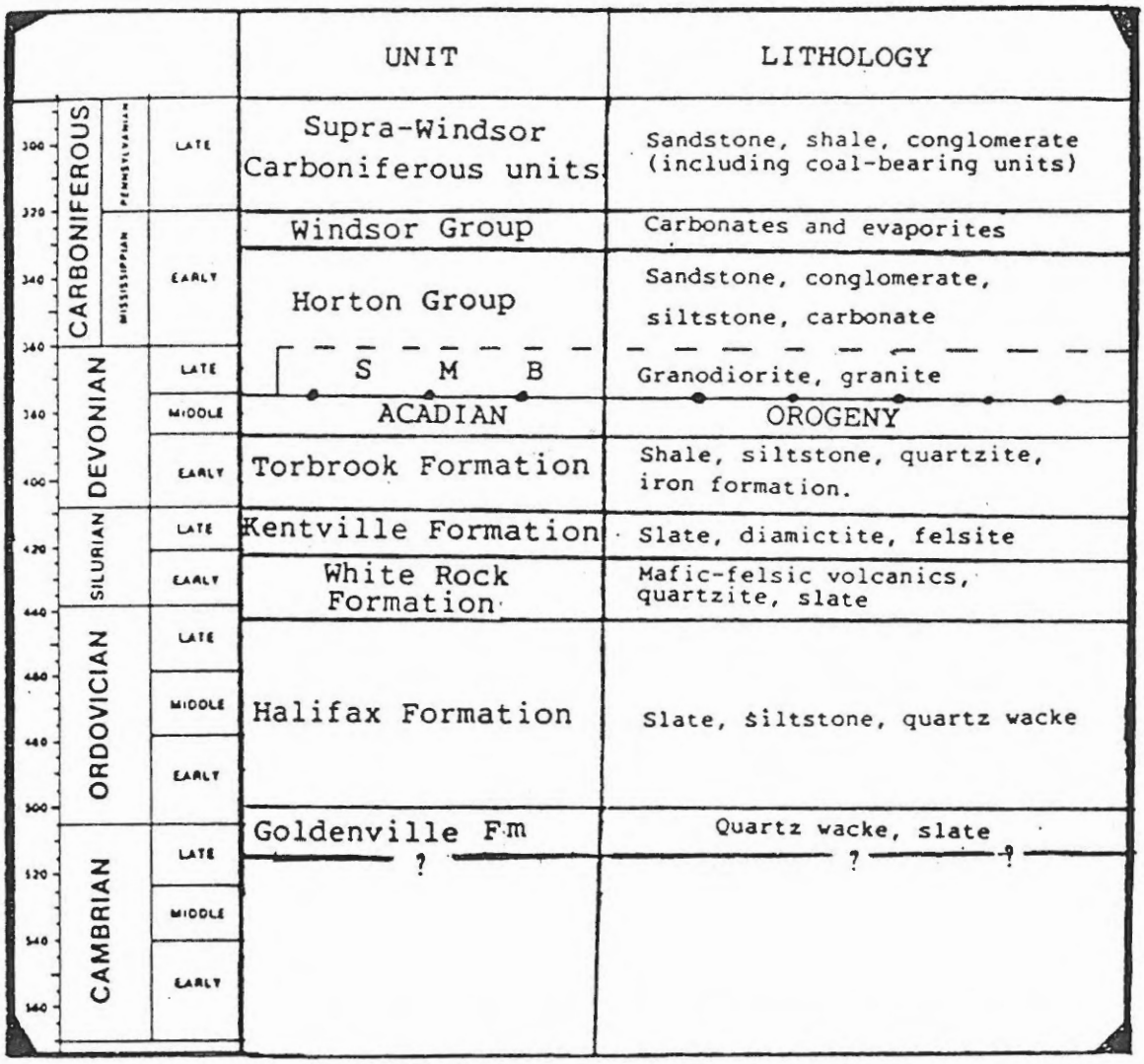
UNIT
LITHOLOGY
CARBONIFEROUS
PENNSYLVANIAN
MISSISSIPPIAN
DEVONIAN
SILURIAN
ORDOVICIAN
CAMBRIAN
LATE
EARLY
MIDDLE
300
320
340
360
380
400
420
440
460
480
500
520
540
560
Supra-Windsor Carboniferous units
Sandstone, shale, conglomerate (including coal-bearing units)
Windsor Group
Carbonates and evaporites
Horton Group
Sandstone, conglomerate, siltstone, carbonate
S M B
Granodiorite, granite
ACADIAN
OROGENY
Torbrook Formation
Shale, siltstone, quartzite, iron formation.
Kentville Formation
Slate, diamictite, felsite
White Rock Formation
Mafic-felsic volcanics, quartzite, slate
Halifax Formation
Slate, siltstone, quartz wacke
Goldenville Fm
Quartz wacke, slate
?
?
?
Nonconformity
Intrusive contact

the biotite zone occurred at relatively low pressure (ca. 0.3 GPa). Subsequent intrusion of the Wedgeport pluton superimposed a contact aureole on the regional metamorphic rocks. Regional metamorphism is further discussed in Chapter 4.

The structural history of the Meguma terrane is quite complex. The principal foliation (S_2), is associated with open to isoclinal folds, which were generated during the Acadian orogeny. For most of the Meguma terrane, the foliation trend is generally northeast, but this changes abruptly to north-northeast in the southwestern region (e.g. Keppie, 1979). Later deformation produced ductile and brittle shearing, crenulation cleavage, and faulting, which were superimposed on the main foliation, at least locally (Fyson, 1966; Keppie,1983; O'Brien, 1983; Hwang and Williams, 1985).

K-Ar and ^{40}Ar-^{39}Ar data on slates suggest that the initiation of regional metamorphism occurred about 410 Ma ago (Reynolds et al., 1973; Reynolds and Muecke, 1978). The age of intrusion of the South Mountain Batholith (SMB) has been constrained at 361-372 Ma by the Rb-Sr isochron method (Clarke and Halliday 1980). ^{40}Ar-^{39}Ar ages on micas produced an average cooling age of 367 Ma for the batholith (Reynolds et al., 1981). In contrast, ^{40}Ar-^{39}Ar mica ages for the southern satellite plutons average 312 Ma (Reynolds et al., 1981). To account for the contrasting apparent ages of the SMB and SSP, Reynolds et al., (1981) proposed three

alternative hypotheses, but their data did not permit a clear choice. They are:

(1) The SSP were intruded considerably later than the SMB.

(2) The SSP are of similar age to that of the SMB, but cooled much more slowly to argon retention temperatures in micas.

(3) The SSP are of similar age to that of the SMB, but were overprinted by a later tectonothermal event.

Fig. 1-5 illustrates the relationship between the SSP and the regional metamorphic zones.

Three orogenies are considered to have affected the Appalachians during the Paleozoic. They are (1) the Ordovician Taconic orogeny which resulted in closure of Iapetus ocean (Wilson, 1966; Williams, 1980); (2) the Devonian Acadian orogeny associated with regional deformation, regional metamorphism and large-scale plutonism; and (3) the Alleghanian orogeny of Permo - Carboniferous age, probably involving collision of Gondwana with North America (Riding, 1974; Keppie, 1982). The Meguma terrane is thought to have been joined to the Appalachian Orogen during the Devonian period (e.g. Schenk, 1978; Keppie 1982), and therefore did not experience the Taconic Orogeny. The only clearly documented evidence of significant pre-Devonian thermal activity in the Meguma terrane is the White Rock volcanics, which are

Fig. 1-5. Map outlining the relationship between plutons and regional metamorphic zones in the Meguma terrane, southwest Nova Scotia.

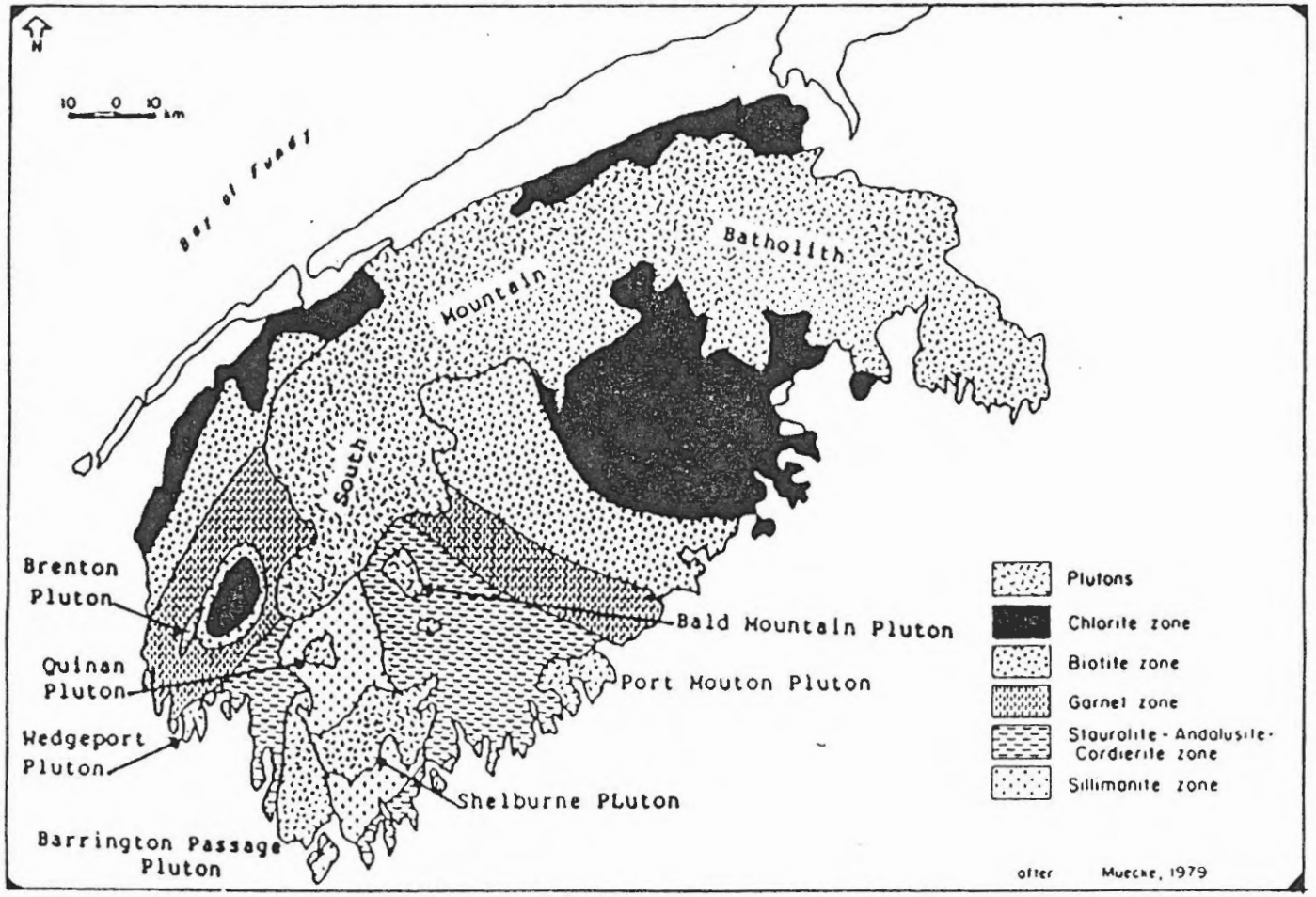
N
10 0 10 km
Bay of Fundy
South Mountain Batholith
Brenton Pluton
Quinan Pluton
Wedgeport Pluton
Barrington Passage Pluton
Shelburne PLuton
Port Mouton Pluton
Bald Mountain Pluton
Plutons
Chlorite zone
Biotite zone
Garnet zone
Staurolite - Andalusite - Cordierite zone
Sillimanite zone
after Muecke, 1979

stratigraphically dated as pre-Ludlovian (Late Silurian) to possibly Ordovician (Taylor, 1965).

1.3.1. THE ACADIAN EVENT

During the Devonian period a major tectonothermal event occurred in the Meguma terrane. Multiphase deformation is represented by open to isoclinal folds, associated with gold-bearing quartz veins (Fyson, 1966; Keppie, 1977; Keppie, 1983; O'Brien, 1983). The folding may have been accompanied by transcurrent movement along the Minas Geofracture (Keppie, 1982). Folding was followed by regional metamorphism (e.g. Taylor and Schiller, 1966; Muecke, 1974; Chu, 1978). A Devonian age (ca. 410-380 Ma) is suggested for the Acadian event by K-Ar and ^{40}Ar-^{39}Ar dates on slates and phyllites from various localities in the Meguma terrane (Reynolds et al., 1973; Reynolds and Muecke, 1978; Savell, 1980; Dallmeyer and Keppie, 1986). Ages of 362-373 Ma were obtained for micas from (1) metamorphic rocks, (2) granites, and (3) rocks dynamically recrystallized during shearing associated with movement of the Minas Geofracture (Dallmeyer and Keppie, 1984). These ages suggest that regional metamorphism and plutonism occurred within a short period in Devonian time, as suggested by Schenk (1978). The data of Dallmeyer and Keppie (1984) were, however, obtained outside the study area (in the northeastern part of the Meguma terrane).

Table 1-1. Evidence for an Acadian event in the Meguma terrane, and elsewhere in the Appalachians.

	TECTONIC OR THERMAL DISTURBANCE	APPARENT AGE	REFERENCE
MEGUMA	Regional metamorphism in Meguma	390-410 Devonian	Reynolds and Muecke,1978. Keppie,1977
	Transcurrent motion on Minas Geofracture	Devonian	Keppie,1982. Dallmeyer and Keppie,1984.
	Acadian folding in Meguma	Devonian	Keppie,1977.
	Intrusion of South Mountain Batholith	372-361	Clarke and Halliday,1980. Reynolds et al.,1981.
REST OF THE APPALACHIANS	Motion on Dover-Hermitage Fault	Devonian	Kennedy et al.,1982.
	Plutonism in Newfoundland	Devonian	Bell et al.,1977. Jayasinghe and Berger,1979. Strong,1980.
	Faulting and folding in New Brunswick	Devonian	Fyffe,1982. Ruitenberg and McCutcheon,1982.
	Plutonism in New Brunswick	Devonian	Fyffe et al.,1981a Fyffe et al.,1981b
	Deformation and high grade metamorphism in the Blue Ridge	380	Butler,1973
	Metamorphism and granite intrusion in the North Carolina Piedmont	Devonian	Butler and Fullagar,1978.

Interpretation derived from them requires testing on a regional scale.

Timing of the main phase of plutonism in the Meguma terrane is well constrained. The Meguma metasediments were post-tectonically intruded by the South Mountain Batholith (SMB), and several satellite plutons comprising approximately half of the outcrop area within the Meguma terrane. The age of deposition of the youngest sediments intruded by the SMB is Gedinnian-Emsian (ca. 408-387 Ma). The upper 30% of these sediments (Torbrook Formation) is not exposed (Smitheringale, 1973), which suggests that they may be somewhat younger than Emsian. The South Mountain Batholith is overlain by sediments of possible Tournaisian age (ca. 360-352 Ma). The Rb-Sr mineral-whole rock isochron ages of 372-361 Ma for the SMB (Clarke and Halliday, 1980) and the stratigraphic constraints sharply define this major plutonic component of the Acadian Orogeny in the Meguma terrane.

The Acadian Orogeny has been recorded elsewhere in the Appalachian Belt, although interpretations on its timing permit inclusion of some events much younger than Devonian. Granite plutonism has been dated in Newfoundland (e.g. Bell and Blenkinsop 1977), New England (e.g. Naylor 1971, Aleinikoff et al., 1985; Dallmeyer et al., 1982), and the Southern Appalachians (Fullagar and Butler, 1979). Table 1-1 summarizes evidence for an Acadian event in the Meguma terrane, and elsewhere in the Appalachians.

1.3.2. THE ALLEGHANIAN EVENT

As stated above, the Alleghanian Orogeny is one of the major tectonothermal events recorded in the Appalachians. Correlation of local thermal and tectonic perturbations assigned to this event along the length of the orogen is not well-documented, but recent work has added considerably to its definition (table 1-2).

In Nova Scotia, the Late Carboniferous intense shearing and faulting, defined as the Maritime Disturbance (Poole, 1967), is thought to be associated with the Alleghanian orogeny. Several other workers have reported thermotectonic activity of Late Carboniferous age in the Meguma terrane. Notable among these are: (1) hydrothermal alteration associated with polymetallic base metal mineralization in southwestern Nova Scotia (e.g. Hutchinson, 1982; Keppie et al., 1983; Zentilli and Reynolds, 1985); (2) intense shearing deformation on scales ranging from less than one meter to several kilometers (e.g. Belt, 1968; Reynolds et al., 1981; Giles, 1985; Dallmeyer and Keppie, 1986).

1.3.3. THE MESOZOIC EVENT

Rifting, block faulting, and basaltic magmatism are events ascribed to Triassic-Jurassic time (Crosby, 1962; Klein, 1962; Wark and Clarke, 1980; Keen and Cordsen, 1981; Bedard, 1985). The present Atlantic Ocean was opened, marginal basins were created, and deposition of sediments

Table 1-2. Evidence for an Alleghanian event in the Meguma terrane, and elsewhere in the Appalachians.

	TECTONIC OR THERMAL DISTURBANCE	APPARENT AGE	REFERENCE
MEGUMA	Maritime Disturbance	Late Carb.	Poole,1967
	Shearing of Brenton Pluton	320-330	Reynolds et al.,1981.
	Deerfield,Barrington shear zones	275-325	Dallmeyer and Keppie,1986.
	East Kemptville mineralization	295	Zentilli and Reynolds,1985.
	Brazil Lake Pegmatite	333	Hutchinson,1982.
	Wedgeport pluton	313-316	Keppie et al.,1983
	SMB reset	320	Reynolds et al.,1981.
	Tobiatic Fault Zone	271-300	Giles,1985
	Dunbrack mineralization	300	Reynolds et al.,1981
	Mylonitization of SMB	post-Devonian	Smith,1985.
	Mineralization of SMB (3 locations)	281-332	O'Reilly et al.,1985.
REST OF THE APPALACHIANS	Deformation in Stellarton Graben	Late Carboniferous	Yeo and Ruixing,1986
	Deformation in New Brunswick	Carboniferous	Rast and Currie,1976 Ruitenberg and McCutcheon,1982. Nance,1985. Nance and Warner,1986.
	Plutonism in Newfoundland	300-325	Bell and Blenkinsop,1977,1979.
	Metamorphism in the Narragansett Basin,RI	239-258	Dallmeyer,1982.
	Metamorphism in New England	Carboniferous to Permian	Zartman et al.,1970. Lux and Guidotti,1985.
	Metamorphism in Southern Piedmont	Carboniferous to Permian	Kulp and Eckelmann,1961.
	Plutonism in Southern Appalachians	Carboniferous to Permian	Fullagar and Butler,1979
	Plutonism in Maine	325	Aleinikoff et al.,1985.

into basins in the Bay of Fundy and the Atlantic continental margin was initiated. Whereas sedimentation commenced in the Bay of Fundy (Fundy Group) in Late Triassic time (Klein, 1962), accumulation of sediment in the present North Atlantic continental commenced in Middle-Late Jurassic (e.g. Keen and Cordsen, 1981; Tankard and Welsink, in press).

Extrusive and intrusive basaltic rocks are exposed in narrow strips along the northern and southern flanks of the study area (map 2). These rocks gave K-Ar apparent ages of about 200 Ma (Poole et al., 1970; Wark and Clarke, 1980). This phase of magmatism is associated with opening of the Bay of Fundy rift, into which Triassic-Jurassic sediments were deposited (map 2). Field mapping indicates that deformation of the Triassic-Jurassic rocks of the Bay of Fundy is confined to gentle open folds and minor faulting (Crosby, 1962; Smitheringale, 1973). Recent drilling and seismic interpretation, however, suggest major deformation, including formation of large-scale folds and thrust faults (Brown, in press). Although mafic dikes have been reported at several localities in southwestern Nova Scotia (Taylor, 1967, 1969), their ages and overall thermal effects on the Meguma terrane are not yet fully established. Biotite from a lamprophyre dike swarm cutting the Wedgeport pluton (southwest Nova Scotia), gave an ^{40}Ar-^{39}Ar plateau age of 225 Ma (Reynolds, 1986, personal comm.).

1.4. SCOPE OF THE THESIS

In order to answer some of the questions raised above, this study focuses on the following:

(1) ^{40}Ar-^{39}Ar dating of slates from the chlorite zone (fig. 1-5). These data are compared with those previously derived by Reynolds et al. (1973), and Reynolds and Muecke (1978). Since white micas in slates are formed at relatively low temperatures, they are likely to cool rapidly to argon retention temperatures and yield apparent ages close to the metamorphic event. Timing of regional metamorphism can be better defined.

(2) ^{40}Ar-^{39}Ar dating of available amphiboles in the "Regional Metamorphic Terrane" (RMT). Because of their high closure temperatures (e.g. Harrison, 1981), amphiboles are likely to start quantitative argon retention soon after crystallization, and to remain closed to subsequent mild tectonothermal events. Dating of amphiboles, like the slates, should help constrain the early thermal history of the Meguma terrane.

(3) ^{40}Ar-^{39}Ar dating of micas from the RMT. Even though micas have lower closure temperatures than amphiboles, they are dated because they set limits on the post-metamorphic cooling history of the RMT. When combined with apparent ages of coexisting amphiboles, data from micas can be used to identify domains within the RMT which experienced complex thermal histories.

(4) ^{40}Ar-^{39}Ar dating of amphiboles, micas and feldspars from the southern satellite plutons (SSP). This is done in order to resolve the apparent discrepancy between the SSP ages and those of the South Mountain Batholith (Reynolds et al., 1981). Because of the low closure temperatures of feldspars (e.g. Harrison and McDougall, 1982) they can be used to define late-stage cooling and mild tectonothermal events.

(5) Fission track dating of apatite from the SSP and RMT. The annealing temperature for apatite fission tracks is ~100 degrees C (e.g. Naeser, 1979). Data from this mineral should supplement the feldspar data in defining the latest cooling and mild tectonothermal events.

(6) Performing diffusion experiments on micas and K-feldspars to determine whether the technique described by Berger and York (1981) is capable of yielding meaningful results.

(7) Evaluation of these data in conjunction with other available information to elucidate the tectonothermal history of the Meguma terrane.

CHAPTER 2

PRINCIPLES AND PROCEDURES

2.1. INTRODUCTION

In this chapter, the theoretical basis for K-Ar systematics, fission track dating and diffusion experiments are briefly examined. Principles of thermochronometry are discussed. Laboratory procedures employed in applying these techniques to the Meguma Terrane are outlined.

2.2. K-Ar SYSTEMATICS

Most of the data in this study are based on the natural production of ^{40}Ar from ^{40}K, and its retention in minerals. The conventional K-Ar technique and the ^{40}Ar-^{39}Ar modification employed in this study are described below.

2.2.1. CONVENTIONAL K-Ar DATING

^{40}K spontaneously decays by the branching scheme. 11.2% of ^{40}K is converted by electron capture and B+ emission to ^{40}Ar. To obtain an age from a K-bearing phase, the potassium content is measured by flame photometry or

another similar method. ^{40}K is readily determined if it is assumed that the present-day isotopic composition of potassium is $^{40}K/K = 1.167 \times 10^{-4}$. From a separate aliquant of the sample, ^{40}Ar is determined by mass spectrometry, usually with the aid of an ^{38}Ar tracer. This method is capable of dating K-bearing phases of any grain size, but is subject to large errors if the sample is not homogeneous.

2.2.2 ^{40}Ar-^{39}Ar MODIFICATION

In a conventional Argon equation, the age t, is given by:

$$t = \frac{1}{\lambda} \ln [1 + \lambda/\lambda_\varepsilon \, {}^{40}Ar^*/{}^{40}K] \quad ..(1)$$

λ = total decay constant for ^{40}K.

λ_ε = decay constant for electron capture by ^{40}K.

$^{40}Ar^*$ = radiogenic ^{40}Ar.

Decay constants are as suggested by Steiger and Jager (1977).

In the ^{40}Ar-^{39}Ar method, a finite amount of ^{39}K is converted to ^{39}Ar by neutron bombardment in a nuclear reactor (Natural $^{39}K/^{40}K = 7.99 \times 10^3$). For the nuclear reaction $^{39}K(n, p)^{39}Ar$, the amount of ^{39}Ar produced is given by:

$$^{39}Ar = {}^{39}K \, \Delta T \int \phi(\varepsilon)\sigma(\varepsilon)d\varepsilon \quad .....(2)$$

$\phi(\varepsilon)$ = neutron flux with energy ε.

$\sigma(\varepsilon)$ = cross section for the reaction $^{39}K(n, p)^{39}Ar$ at

energy ε.

ΔT = duration of the reaction.

Since $^{40}K = (^{39}K)/(7.99 \times 10^3)$, equations (1), (2), yield:

$$^{40}K = (^{39}Ar)/(7.99 \times 10^3 \Delta T \int \phi(\varepsilon)\sigma(\varepsilon)d\varepsilon \ldots\ldots(3).$$

By substituting into equation (1), the age, t, becomes:

$$t = 1/\lambda \ln (\lambda/\lambda_\varepsilon \frac{^{40}Ar^*}{^{39}Ar} \times 7.99 \times 10^3 \Delta T \int \phi(\varepsilon)\sigma(\varepsilon)d\varepsilon + 1) \quad (4).$$

Because the value of $\int \phi(\varepsilon)\sigma(\varepsilon)d\varepsilon$ is not easily determined, unknown samples are irradiated with standard monitors (flux monitors), whose ages are assumed known. The apparent age of the unknown is then derived simply by proportionality, as outlined below.

A parameter, J, may be defined thus:

$$J = 7.99 \times 10^3 \lambda/\lambda_\varepsilon \Delta T \int \phi(\varepsilon)d\varepsilon \ldots\ldots(5)$$

Equation (4) now becomes :

$$t=1/\lambda \ln [1 + JR] \ldots\ldots(6) \quad (R = ^{40}Ar^*/^{39}Ar)$$

Or by rearrangement,

$$J = [\exp(\lambda t)-1]/R \ldots\ldots(7)$$

J is readily determined for a sample of known age (standard), provided the ratio $R= ^{40}Ar^*/^{39}Ar$ is measured. Conversely, the age, t, is readily determined for a sample

Fig. 2-1(a). Arrangement of standards and unknowns in canister for irradiation.

Fig 2-1(b). Typical curve from which 'J' is derived.

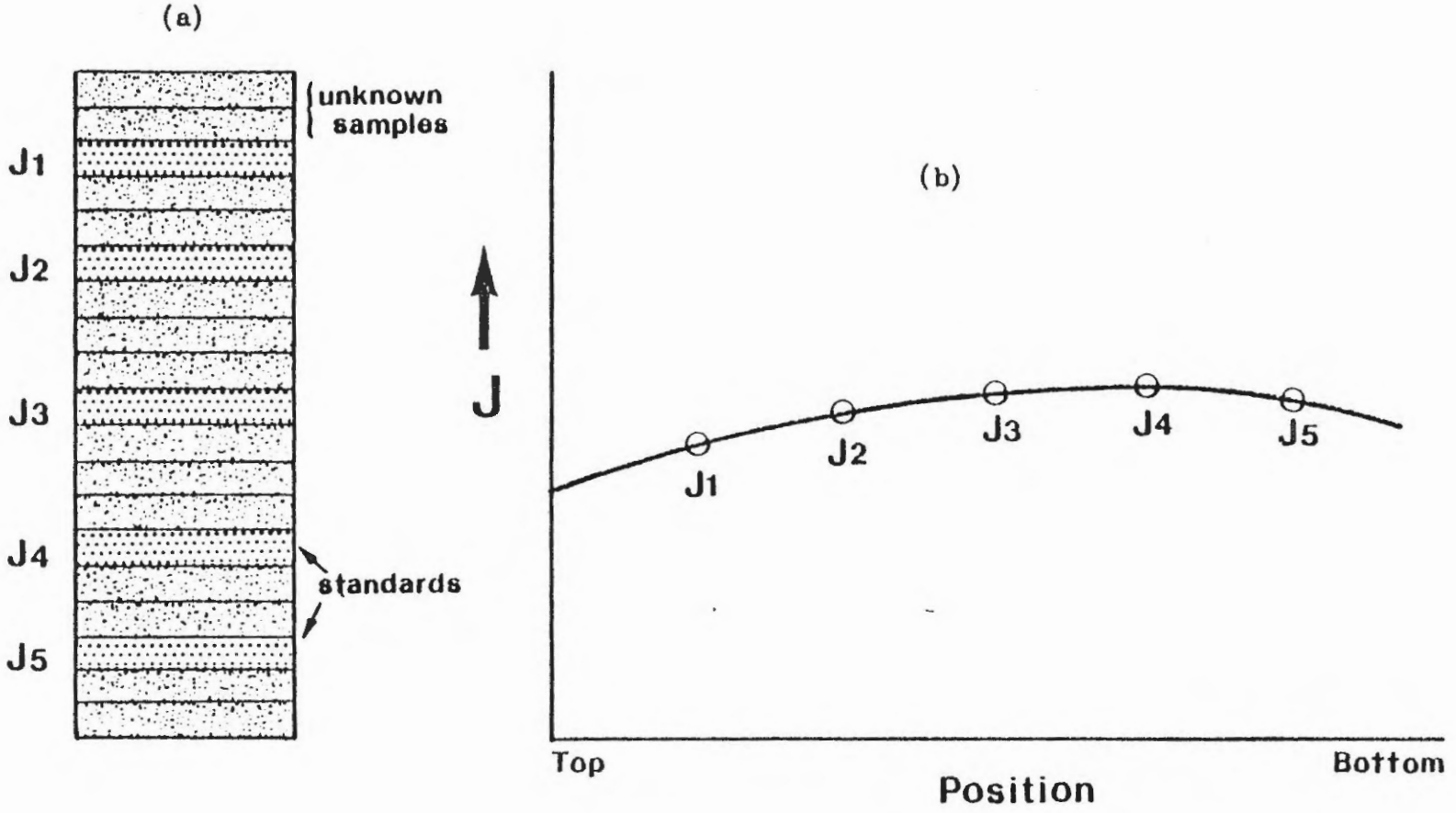
(a)
unknown samples
J1
J2
J3
J4
J5
standards
J
(b)
J1
J2
J3
J4
J5
Top
Bottom
Position

to which a J-value is assigned.

Fig. 2-1(a) shows a typical arrangement of standard monitors and unknown samples in a canister during irradiation. Because of a possible small flux gradient along the length of the canister, J is expected to vary concomitantly. A graph is made of these values (fig. 2-1(b), and an appropriate J value for each unknown sample is determined by interpolation.

With the ^{40}Ar-^{39}Ar method, analyses can be performed with smaller samples than in conventional K-Ar dating. Analyses are completed in single experiments, where isotopic ratios are measured. Hence, greater precision is attained with this method. Minor sample inhomogeneity is tolerable, and there is no need to prepare and calibrate an ^{38}Ar tracer system. The most important advantage is that an age spectrum (section 3.1) may be generated by heating the sample in a stepwise manner, and analysing the gas released at each step. This yields information not obtainable by the conventional K-Ar technique (Chapter 3). The most important disadvantage is that very fine grained samples may lose ^{39}Ar by recoil, producing anomalously high ages (e.g. section 3.6). The necessity of handling radioactive materials is a potential hazard.

2.2.2.1. FLUX MONITORS (STANDARDS)

Dalrymple et al., (1981) listed desirable criteria for minerals used as flux monitors.

(1) The mineral should have a uniform ratio of $^{40}Ar/^{40}K$.

(2) Both ^{40}K and ^{40}Ar should be homogenously distributed. This criterion and the one above are necessary because the age is determined by the conventional K-Ar method, where sample splitting is necessary. Calculation of the factor J assumes a reproducible $^{40}Ar/^{39}Ar$ ratio.

(3) The monitor should be of similar age and K/Ca ratio to the sample being dated. Wide disparity is undesirable, since these two parameters determine sample size and optimum irradiation dose. K/Ca disparity between standards and unknowns is important only when their ages are very different. For example, a 600 Ma old amphibole standard may be irradiated with a 500 Ma old mica unknown, in spite of their dissimilar K/Ca ratios. If a 3 Ga old mica were irradiated with a 10 Ma old amphibole, precision would be low, because of their contrasting neutron dose requirements.

(4) The monitor should be fairly coarse grained. Extremely fine grain size (<50μm) would likely increase the risks of releasing radioactive dust during sample handling and of recoil induced loss of ^{39}Ar (e.g. Turner and Cadogan, 1974).

(5) The monitor should be available in reasonable

quantity. This criterion is obviously required to ensure availability to laboratories for repeated analyses.

Two flux monitors were used during this study :

(1) NS-231 biotite collected from the South Mountain Batholith, Halifax County, Nova Scotia. Its conventional K-Ar age is 368+/-5Ma (Reynolds et al., 1973). It produced an age spectrum with a well defined plateau (fig. 4.4-2)

(2) MMhb-1 hornblende. This is a well-calibrated specimen collected from a syenite body in the Cambrian McClure Mountain Complex, Fremont County, Colorado, (Alexander et al., 1978;Roddick, 1983). The conventional K-Ar age accepted for this mineral is 520 +/- 8 Ma. Its ^{40}Ar-^{39}Ar age spectrum gave a well defined plateau (Harrison, 1981).

Both of these standards appear to meet the criteria listed above. They both produce plateau ages comparable to their conventional K-Ar ages, suggesting uniform distribution of $^{40}Ar/^{40}K$. When included in the same irradiation package, the two standards yielded J values that agreed within 1 %. (e.g. fig. 2-2).

2.2.2.2. CORRECTION FOR INTERFERING ISOTOPES

Neutron irradiation of K-bearing minerals is designed to produce ^{39}Ar from ^{39}K. Ideally this should be the only reaction, so that the measured $^{40}Ar/^{39}Ar$ is equivalent to $^{40}Ar/^{40}K$ in conventional K-Ar dating. However, other Ar

Fig. 2-2. Experimental 'J' curve derived from standards MMhb-1 and NS-231, irradiated in the same canister (can. 53).

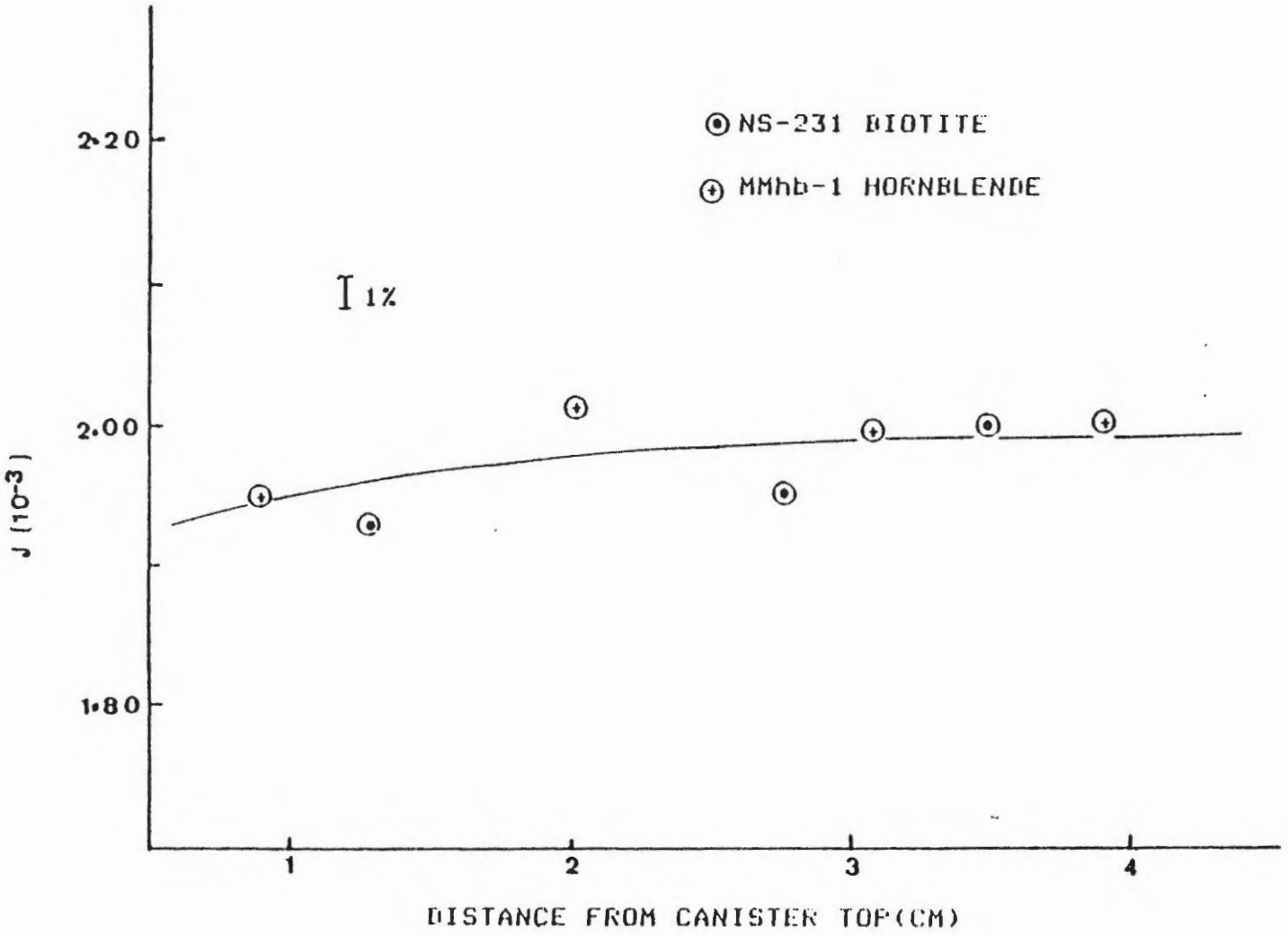
NS-231 BIOTITE
MMhb-1 HORNBLENDE
1%
2.20
2.00
1.80
J (10-3)
1
2
3
4
DISTANCE FROM CANISTER TOP(CM)

Table 2-1(a). Isotopes generated during neutron irradiation of K-bearing phases in a reactor (Brereton, 1970).

Argon Isotope Produced	Ca Reaction	K-Reaction
36	$^{40}Ca(n,n\alpha)$	
37	$^{40}Ca(n,\alpha)$	$^{39}K(n,nd)^{+}$
38	$^{42}Ca(n,n\alpha)$	$^{39}K(n,d)$; $^{41}K(n,\alpha)$
39	$^{42}Ca(n,\alpha)$; $^{43}Ca(n,n\alpha)$	$^{39}K(n,p)$; $^{40}K(n,d)$
40	$^{43}Ca(n,\alpha)^{+}$; $^{44}Ca(n,n\alpha)^{+}$	$^{40}K(n,p)$; $^{41}K(n,d)$

+ Negligible quantities

Table 2-1(b). Argon ratios from salts of Ca and K irradiated in the McMaster reactor (Mak et al., 1976).

Ar isotope ratios	Values
$(37/39)_{Ca}$	1.536×10^{3}
$(36/39)_{Ca}$	0.390
$(40/39)_{K}$	1.56×10^{-2}

isotopes are produced, and corrections must be made for them. Brereton (1970), listed the isotopes generated during neutron irradiation of minerals with K and Ca. They are shown in table 2-1(a). ^{37}Ar, ^{38}Ar, and ^{39}Ar are also produced by neutron activation of Ar isotopes, but the quantities are always small and therefore ignored (Brereton, 1970). From table 2-1(a), the following observations may be made: ^{38}Ar does not enter into the age calculation, and therefore need not be further considered. Quantities of K-derived ^{37}Ar and Ca-derived ^{40}Ar are small enough to be ignored. Correction for interfering isotopes is therefore confined to Ca-derived ^{36}Ar ($^{36}Ar_{Ca}$) and ^{39}Ar ($^{39}Ar_{Ca}$) and K-derived ^{40}Ar ($^{40}Ar_{K}$) (Mak et al., 1976).

Since all ^{37}Ar is assumed to be derived from Ca, the measure of $^{37}Ar_{Ca}$ can be used to estimate $^{39}Ar_{Ca}$ and $^{36}Ar_{Ca}$. The magnitude of interference produced in the McMaster reactor (section 2.7.3), was estimated by irradiating pure salts of Ca and K, of "zero" age (Mak et al., 1976). The values are listed in Table 2-1(b). The numbers 36, 37, 39 and 40 refer to Ar isotopes with those mass numbers.

In the absence of interference, the equation from which the $^{40}Ar/^{39}Ar$ ratio is derived is:

$$40^*/39 = (40/39)_m - 295.5\ (36/39)_m \quad \ldots \quad (8),$$

where * and m signify radiogenic and measured argon respectively. All contaminating argon is assumed to have the atmospheric ratio (40/36) = 295.5. For most analyses where Ca/K is very low (micas, K-feldspars), equation (8) is

adequate.

To correct for $^{36}Ar_{Ca}$, $^{39}Ar_{Ca}$, and $^{40}Ar_{K}$, equation (8) is modified to:

$$40^*/39 = (40/39)_m(1-f_1) - 295.5\,(36/39)_m(1-f_2) - (40/39)_K \quad \ldots\ldots\ldots\ldots\ldots (9).$$

$$f_1 = \frac{1}{1-[(37/39)_{Ca}/(37/39)_m]} \quad \ldots\ldots\ldots (10)$$

$$f_2 = \frac{1-[(36/39)_{Ca}/(36/39)_m]}{1-[(37/39)_{Ca}/(37/39)_m]} \ldots\ldots\ldots (11).$$

Since $(37/39)_{Ca} = 1.536 \times 10^3$ ($>> 1$), f_1 is always negative. When $(36/39)_m$ is small ($<<1$), the numerator in equation (11) is negative and f_2 is positive; this is the usual case. Where $(36/39)_m$ is large (high atmospheric contamination), f_2 may be negative. Since the half-life of ^{37}Ar is 35.1 days, a correction must be made for post-irradiation decay before calculating f_1 and f_2.

2.3. PRINCIPLES OF FISSION TRACK DATING

The uranium isotope ^{238}U undergoes spontaneous fission. The fission products are propelled through the host crystal (or glass) leaving damaged zones known as fission tracks. Once the host crystal is etched with a suitable chemical, the fission tracks are exposed for viewing with a petrographic microscope. Track density is proportional to uranium concentration, age, and etching efficiency. Hence,

if the uranium concentration and an etching efficiency can be determined, an apparent age can be calculated. Several techniques and various versions of the age equation have been employed, e.g. Fleischer et al., (1975); Naeser (1967); Gleadow (1981); Hurford and Green, (1982); Hurford and Green (1983).

In this study, the method is analogous to that used in ^{40}Ar-^{39}Ar dating, modified after Hurford and Green (1983). To estimate uranium content (^{235}U, proportional to total U), fresh tracks were induced in the specimen by thermal neutron bombardment in the McMaster reactor. The induced tracks were recorded in a low uranium muscovite external detector. To account for indeterminate factors associated with the reactor process, the sample canister was stacked with standards of known age, as well as those whose ages were to be determined. The standard selected for this study is apatite from the Fish Canyon Tuff. The age of the tuff has been determined as 27.79 +/- .07 Ma, on the basis of ^{40}Ar-^{39}Ar dating of amphibole, biotite, and sanidine (Kunk et al., 1985). This age has been calibrated against the flux monitor MMhb-1, upon which ^{40}Ar-^{39}Ar dates in this study are based (section 2.2.2.1). Dosimeter glasses (NBS glass SRM-963A, U = .823 +/- .002 ppm) were included to monitor the flux gradient and to construct the zeta calibration baseline (Hurford and Green, 1983). The age, t, is given by:

$$t = \frac{1}{\lambda_D} \ln[1 + \lambda_D Z(\rho_s/\rho_i) g \rho_D] \quad \ldots\ldots\ldots \quad (12).$$

where zeta (Z) = $\dfrac{\exp(\lambda_D t_{STD})-1}{\lambda_D(\rho_s/\rho_i)_{STD} g \rho_D}$

λ_D = total decay constant of ^{238}U (1.55125×10^{-10} a^{-1}).

ρ_s = spontaneous track density.

ρ_i = induced track density.

ρ_D = track density of dosimeter.

t_{STD} = age of standard.

g = geometry factor (.5).

The parameter zeta (Z) is somewhat analogous to J in ^{40}Ar-^{39}Ar dating, and takes into account neutron flux in the reactor, thermal neutron cross section, uranium concentration, etching efficiency, and counting bias, provided both standards and unknowns are treated the same way. Once zeta is found by interpolation between standards, the apparent age of the unknown can be calculated by one of two methods:

(a) The age is calculated by simply inserting the interpolated value of ρ_D and the mean value of zeta from a

given irradiation batch into equation (12).

(b) The age is calculated by inserting the interpolated value of ρ_D and the mean value of zeta from several determinations (several irradiation batches) into equation (12). Values for Zeta from individual determinations may be unreliable, because of underestimated errors in the procedure (e.g. Hurford and Green, 1983). The value of zeta can be specified with greater precision if standards are repeatedly calibrated against uranium glass dosimeters as described by Hurford and Green (1983). This procedure is adopted in this study. An average value for Z was calculated after four batches of samples were irradiated (12 determinations). Details of the procedure are given in section 2.7.2.

2.4. DIFFUSION AND CLOSURE TEMPERATURE.

The retention of argon in a K-bearing mineral is best described by diffusion theory. Thermally-driven diffusion is governed by the Arrhenius relationship:

$D = D_o \exp(-E/RT)$.....(a)

D = diffusion coefficient, a measure of diffusion rate.

D_o = diffusion coefficient at infinitely high temperature.

E = activation energy

R = gas constant

T = temperature (Kelvin)

Diffusion is also governed by Fick's Second Law, one version of which is:

$$dc/dt = D\left(\frac{d^2c}{dx^2} + \frac{d^2c}{dy^2} + \frac{d^2c}{dz^2} \right) \quad \ldots\ldots\ldots \quad (b)$$

where t = time over which diffusion occurs

c = concentration

x, y, z = Cartesian coordinates in space.

Equation (b) must be solved to derive 'E' and D_o (or D_o/a^2, see below). Solutions to the diffusion equation (b) have been derived and listed by several authors, e.g. Crank, 1957;Carslaw and Jager, 1959; Jost, 1960; Fechtig and Kalbitzer, 1966; Mussett, 1969. To facilitate calculation, the geometry of the system out of which diffusion occurs, has been modelled as one of the following (a) sphere, with radial diffusion; (b) cylinder of infinite length with radial diffusion; (c) infinite plane sheet with diffusion perpendicular to the sheet (see fig.2-3). In each case, the exact solution is in the form of an infinite series. For practical purposes, approximate solutions are given, e.g Fechtig and Kalbitzer, 1966; Musset, 1969. Some solutions are listed in table 2-2.

In the equations listed in table 2-2, f = cumulative fraction of gas removed up to a given temperature T. By rearrangement, equation (a) becomes:

$$\ln D = \ln D_o - E/RT \quad \ldots\ldots\ldots \quad (c)$$

Fig. 2-3. Models for which solutions to the diffusion equation have been obtained.

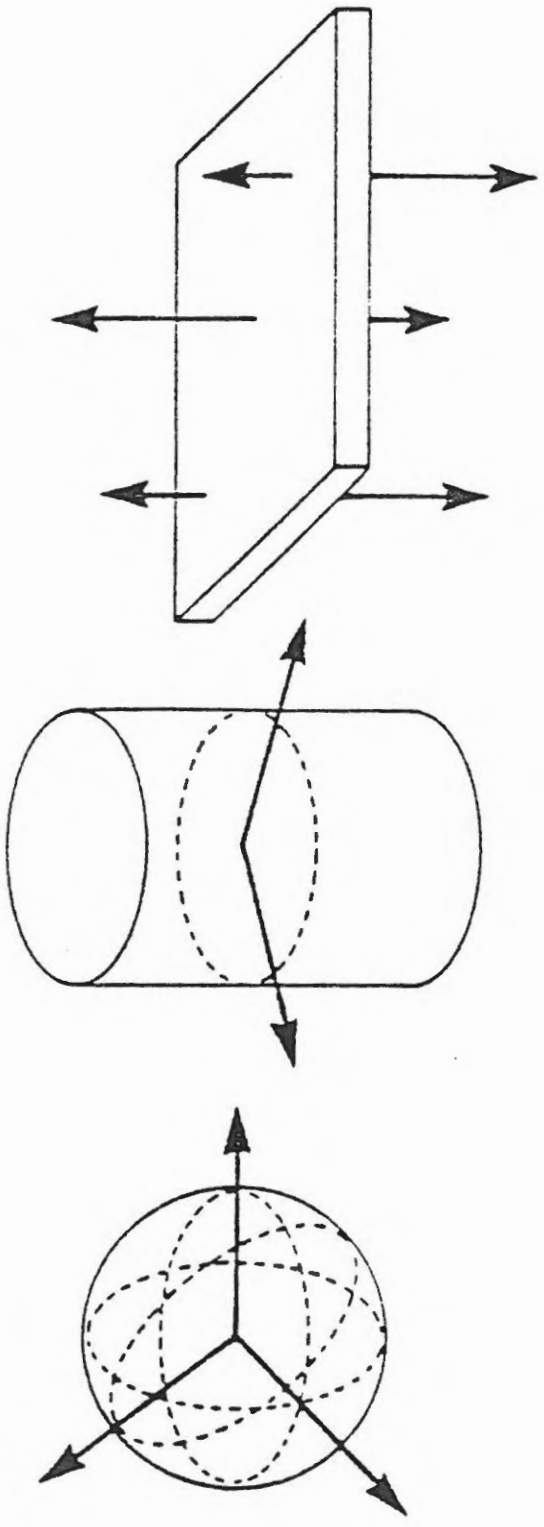

Table 2-2. Some approximate solutions to the diffusion equations (Mussett, 1969).

Shape	Validity	Solution
Sphere Radius a	$0.85 \leq f \leq 1$	$f = 1 - \frac{6}{\pi^2} \exp\left[\frac{-\pi^2 Dt}{a^2}\right]$
	$0 \leq f \leq 0.85$	$f = \frac{6}{\pi^{3/2}} \left[\frac{\pi^2 Dt}{a^2}\right]^{1/2} - \frac{3}{\pi^2} \left[\frac{\pi^2 Dt}{a^2}\right]$
Cylinder Radius a Length ∞	$0.6 \leq f \leq 1$	$f = 1 - \frac{4}{\alpha_n^2} \exp\left[\frac{-\alpha_n^2 Dt}{a^2}\right]$ where $\alpha_n = 2.405$
	$0 \leq f \leq 0.6$	$f = \frac{4}{\pi^{1/2}} \left[\frac{Dt}{a^2}\right]^{1/2} - \frac{Dt}{a^2}$
Sheet Thickness 2a Extent ∞	$0.45 \leq f \leq 1$	$f = 1 - \frac{8}{\pi^2} \exp\left[\frac{-\pi^2 Dt}{4a^2}\right]$
	$0 \leq f \leq 0.5$	$f = \frac{2}{\pi^{1/2}} \left[\frac{Dt}{a^2}\right]^{1/2}$

If $\log_e D$ is plotted vs $1/T$ (derived experimentally), both D_o and E are derived. A grain size parameter, a, can be included to give the relationship

$$\ln D/a^2 = \ln Do/a^2 - E/RT \quad \ldots\ldots\ldots\ldots \quad (d)$$

From equation (a), D increases exponentially with T. Therefore, although an isotopic system would not be completely closed at a precise temperature, the open-closed temperature interval is likely to be very small. Provided the cooling system is not held unduly long in the open-closed transitional interval, it is reasonable to speak of a single closure temperature. The concept of 'closure' to diffusion is illustrated in fig. 2-4. Dodson (1973) made the assumption that over a limited temperature range, cooling can be approximated by a linear increase of $1/T$ with respect to time. The exponential decrease in D is described by a time constant τ, which is the time taken for D to decrease by a factor of $1/e$, that is, for E/RT to increase by 1.

It follows that $E/RT = E/RT_o + t/\tau$ .... (e)

where t = time

T_o = temperature at t = 0

Equation (a) becomes:-

$D = Do \exp[-E/RT_o - T/\tau]$

From equation (e)

Fig. 2-4.

Schematic diagram illustrating the relationship between temperature and argon retention in a K-bearing mineral.

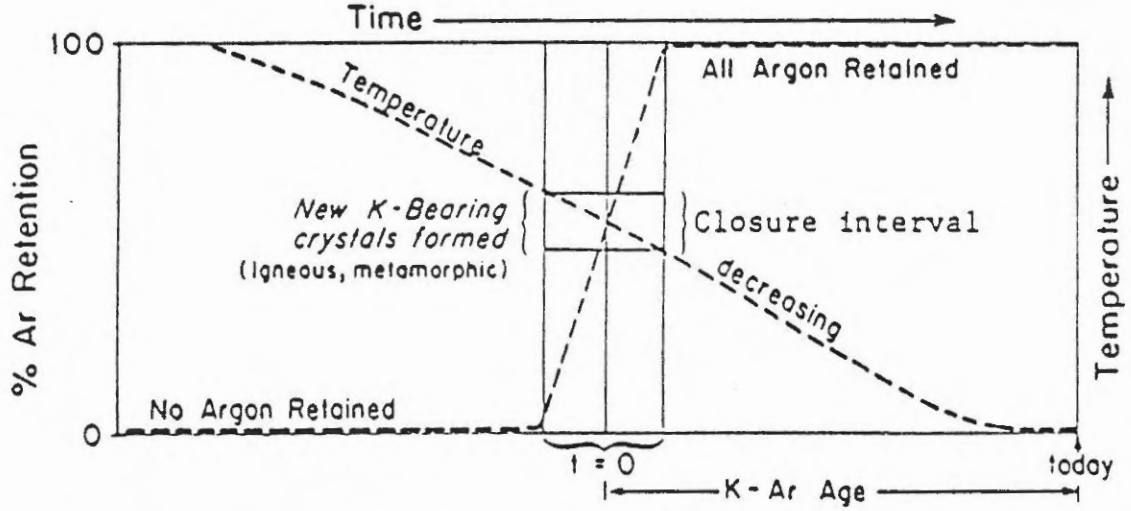

Argon Accumulation in K-Bearing Mineral with Simple History

$$t = E\tau/RT - E\tau/RT_o$$

$$dt/dT = 1/\dot{T} = -E\tau/RT^2 \quad \ldots\ldots\ldots\ldots \quad (f)$$

Therefore $\tau = -RT^2/E\dot{T}$ $\ldots\ldots\ldots\ldots$ (g)

Assuming slow cooling, temperature-controlled volume diffusion, and adapting the principles of heat conduction, Dodson (1973) derived the following equation for closure temperature, T_C:

$$E/RT_C = \ell n(A\tau D_o/a^2) \quad \ldots\ldots\ldots (h)$$

Where 'a' describes the dimensions of the volume through which diffusion occurs (e.g. radius of sphere/cylinder). 'A' is a constant = 55 for a sphere, 27 for a cylinder, 8.7 for a plane sheet.

By rearrangement of equations (g,h),

$$T_C = E/R \; \ell n\left[\frac{-ART_C^2D_o}{E\dot{T}a^2}\right] \quad \ldots\ldots \quad (i)$$

This equation can be solved iteratively. Since T_C is rather insensitive to the cooling rate T, a reasonable estimate of T is inserted on the right hand side. A solution is reached after a few iterations.

2.5. A DISCUSSION OF DIFFUSION EXPERIMENTS

Before the results of diffusion experiments are applied to geologic problems, it is important to document the boundary conditions assumed, and the possible limitations involved.

Harrison (1981) listed some criteria for meaningful diffusion experiments:

(1) The mineral phase should remain stable throughout the entire experiment.

(2) The effective diffusion radius is known or can be derived from the experiment.

(3) The shape of the volume from which diffusion proceeds should approximately conform to one of the geometric solutions to the diffusion equation.

(4) The grain size of the mineral aggregate should fall within a narrow range.

(5) Only one mineral phase should be present

(6) Initial distribution of argon within the mineral should be homogeneous.

The criteria listed above may be examined in turn.

(1) Should a mineral undergo any phase change during a diffusion experiment, its activation energy E, would not be constant, and no single solution would be found for the Arrhenius equation. Hydrous minerals like amphiboles and micas are known to undergo dehydration during vacuum heating. For this reason, such diffusion experiments have

been criticized (e.g. Harrison, 1981, 1984). K-feldspars are subject to perthite homogenization and polymorphic inversion during heating. To partly overcome problems associated with phase changes, data should be taken only for temperatures below which such transformations occur.

(2) Attempts have been made to calculate the effective diffusion radius of K-bearing phases (e.g. Harrison 1981; Harrison and McDougall, 1982). This calculation is, however, not explicitly required in some diffusion experiments. The compound term D/a^2 can be calculated without specifying the grain dimension a (e.g Berger and York, 1981; Hammerschmidt and Wagner, 1983).

(3) The shape of the presumed diffusion volume for any given mineral is not completely understood. It is frequently assumed that the mineral structure as observed petrographically is a reflection of its diffusion geometry. For example, perthitic K-feldspars are modelled as sheets whereas hornblende is modelled as a sphere or a cylinder (e.g. Harrison, 1981; Harrison and McDougall 1982).

(4) Since calculation of the diffusion coefficient D depends on the geometry of the volume from which diffusion proceeds, it is desirable to work with uniform grain size. Diffusion gradients may be imposed on a sample because of a complex thermal history. In such cases the sample grain size must exceed the effective diffusion radius for the gradient to be reflected in a diffusion experiment (Harrison, 1981). Samples with very fine grain size (<100

um) may experience ^{39}Ar loss during irradiation (e.g. Huneke and Smith, 1976; see section 3.6).

(5) Since each mineral has its own peculiar argon retention properties, it is highly desirable to prepare pure monomineralic separates for diffusion studies. The activation energy would not be a constant for a mixture of phases; no single solution can be found for the Arrhenius equation, and Dodson's formula cannot be solved.

(6) The approximate solutions to the diffusion equation (listed in table 2-2) require that the initial concentration of argon within the phase being studied be uniform. Therefore, samples that experienced complex thermal histories may yield spurious diffusion data. This was emphasized by Berger and York (1981).

2.6. THERMOCHRONOMETRY AND METHODS OF DERIVING T_c

The term thermochronometry was introduced by Berger and York (1981). It assumes that each isotopic system dated is associated with a characteristic closure temperature that can be estimated. With various values of age and T_c, the thermal history of an igneous or metamorphic terrane can be deduced. To perform thermochronometric studies, various techniques have been used to derive T_c. Some examples are outlined below.

2.6.1. THE BERGER-YORK PROCEDURE FOR DERIVING T_c

As outlined in section 2.4, Dodson's formula permits calculation of T_c if a method can be found to derive the activation energy E and the frequency factor Do/a^2. Berger and York (1981) proposed that the ^{40}Ar-^{39}Ar step heating technique could be regarded as a diffusion experiment, as well as a dating procedure.

The Berger-York method is a direct application of the theory described by Fechtig and Kalbitzer, (1966), and Mussett (1969). The mineral sample is heated at successively higher temperatures. The duration of each heating step, Δt_i, and the fraction of argon released, Δf_i, are recorded. From these data, D/a^2 is calculated. The experiment may be based on an equation of the form:

$$f^2 = \frac{4Dt}{\pi a^2} \quad \ldots\ldots\ldots\ldots\ldots\ldots \quad (j)$$

(Sheet model, Musset, 1969).

As outlined in fig 2-5, when a diffusion experiment is performed at several temperatures, T_1, T_2, T_3, the diffusion profiles a, b, c, are different for each temperature. The diffusion 'constant' varies with corresponding values D_1, D_2, D_3. over time Δt_1 Δt_2, Δt_3. The values are calculated as follows:

For Temperature T_1 over time Δt_1:

$(D\Delta t/a^2)_1 = (D_1 t_1/a^2)$

The value $(D_1 t_1/a^2)$ is calculated directly from

equation (j). $(D/a^2)_1$ is readily found since $(\Delta t)_1$ is known (actual duration of heating at T_1).

For temperature T_2 over time Δt_2

$(D\Delta t/a^2)_2 = (D_1 t_2/a^2) - (D_1 t_1/a^2)$

The value $(D_1 t_2/a^2)$ is derived from equation (j); it corresponds to point t_2 on profile (a), (fig. 2-5). This value would give the diffusion constant for t_2 if the experiment was conducted at the single temperature T_1. As for T_1, $(D/a^2)_2$ is readily found since $(\Delta t)_2$ is known (actual heating time at temperature T_2).

Similarly, for T_3:

$(D\Delta t/a^2)_3 = (D_1 t_3/a^2) - (D_1 t_2/a^2)$,

and so on for T_4, T_5, T_6...

When log (D/a^2) is plotted against $1/T_i$, the activation energy, E, is derived from the slope, and the frequency factor (Do/a^2) is obtained from the intercept (see section 3.8).

Since conditions in a vacuum contrast so sharply with those likely to be encountered in the geologic environment, the above procedure may give incorrect results. However, it has been argued by Berger and York (1981) that internally consistent results from the technique suggest that the method may be appropriate. Berger and York (1981) have recorded a wide range of closure temperatures for hornblende, biotite and feldspars. The mean values and

Fig. 2-5.

Schematic diagram outlining the diffusion profile for isothermal heating (T_1) and heating at several temperatures ($T_1, T_2, T_3...$).

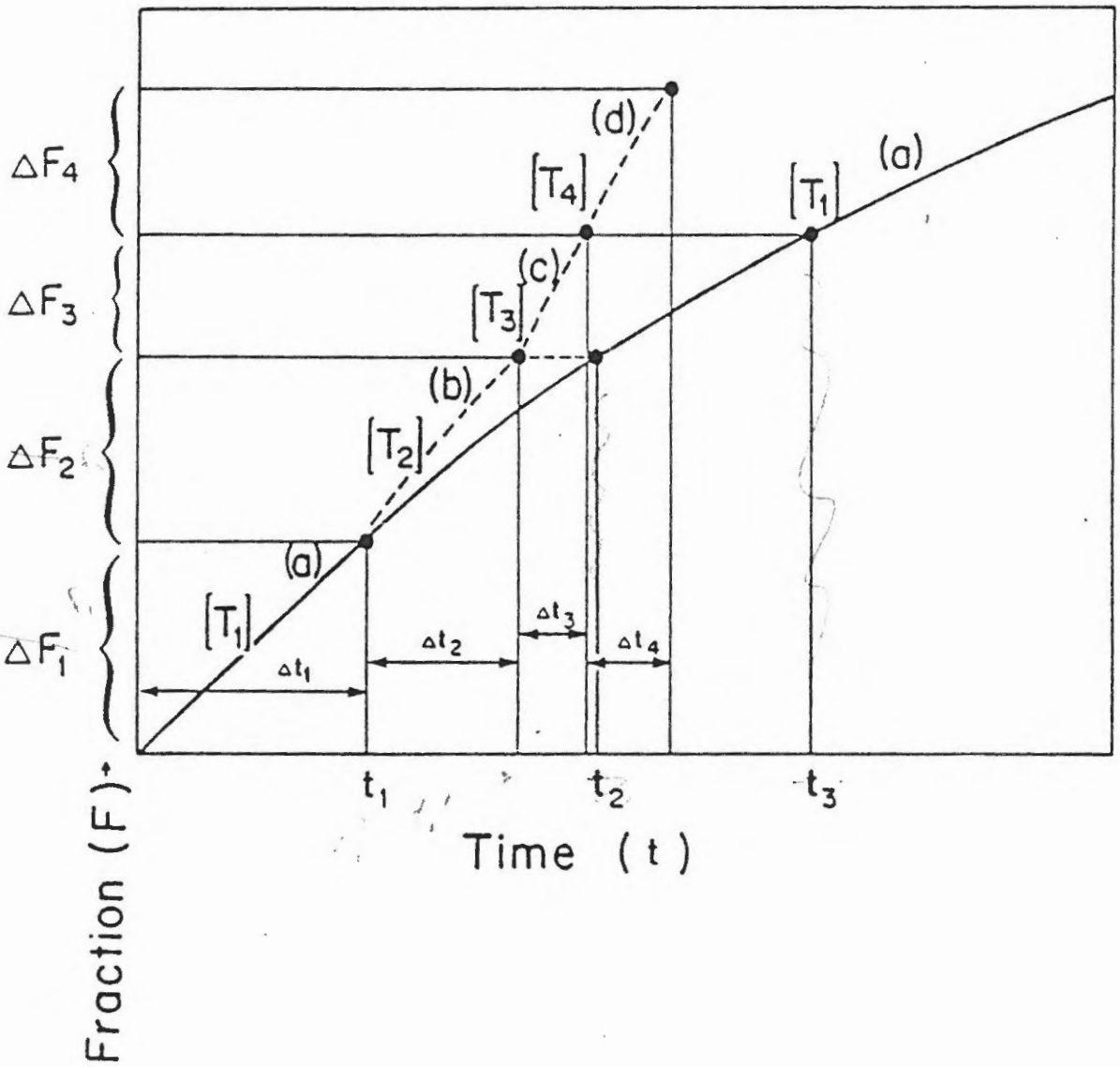
ΔF4
ΔF3
ΔF2
ΔF1
(d)
[T4]
[T1]
(a)
(c)
[T3]
(b)
[T2]
(a)
[T1]
Δt1
Δt2
Δt3
Δt4
t1
t2
t3
Time (t)
Fraction (F)

standard deviations are 685 +/- 46° C for hornblende, 373 +/- 17° C for biotite, 230 +/- 18° C for K-feldspar, and 193 +/- 32° C. for plagioclase. The large uncertainties (~10%) reflect the need for caution in applying these estimates to thermochronometry. It is clear, however that the method is capable of yielding results consistent with relative argon retentivity of the above minerals. Using the same technique on unirradiated Hercynian biotites, Hammerschmidt and Wagner (1983) calculated a closure temperature of 330° C for this mineral.

2.6.2. THE HARRISON–McDOUGALL METHOD

Harrison and McDougall (1982) applied the Berger-York technique to K-feldspar, deriving a closure temperature of 132 +/- 13° C. They argued, however, that hydrous minerals (micas, amphiboles) should not be treated in this manner, since they are dehydrated during vacuum extraction of argon. Dehydration leads to lattice changes, which affect diffusion calculations by producing phases which have different activation energies. Harrison (1981) conducted diffusion experiments on hornblende at about 1kb water pressure. Although this pressure is somewhat lower than expected in plutonic and regional metamorphic environments, it was presumed to be a reasonable simulation. Depending on grain size and cooling rate, closure temperatures for hornblende were estimated to be in the range 490-578 degrees° C.

Harrison et al (1985) performed diffusion experiments on biotite under hydrothermal conditions (15 kbars), and derived closure temperatures of 280 - 310 C, slightly lower than those obtained by Hammerschmidt and Wagner (1983).

2.6.3. OTHER METHODS OF DERIVING T_c

Attempts have been made to obtain closure temperatures from more direct geologic observations. This approach is especially applicable in active geothermal fields, where geothermal gradients are unusally high. Because high temperatures are attained at relatively shallow depths, thermal resetting of minerals can be observed by recovering samples in drill holes. Closure temperature for biotite has been estimated as 225° C (Turner and Forbes, 1976) and 400° C (Del Moro et al., 1983). The estimate for apatite fission track annealing is 105° C (Naeser and Forbes, 1976). Closure temperatures have also been estimated by comparison with other isotopic systems and metamorphic assemblages of known thermal stability. This method has been used to estimate a closure temperature of 350° C for muscovite and 300° C for biotite (Purdy and Jager, 1976). Similarly, a closure temperature of 480° C for hornblende and 345° C for biotite has been estimated by Dallmeyer(1978). These techniques assume that opening of an isotopic system is an exact reverse of closure. Complications associated with variables such as local partial pressure of argon,

permeability, and state of deformation, may invalidate this assumption.

2.7. LABORATORY PROCEDURE

2.7.1. MINERAL SEPARATION

Representative samples of up to a few kg in size were first trimmed of weathered surfaces, then comminuted in a steel jaw crusher. Where the grain size warranted, final pulverization was performed in a tungsten carbide shatter box. Appropriate size fractions were screened and thoroughly washed in tap water, then air dried. Mineral separation was completed in a Franz magnetic separator, or by means of heavy liquids (methylene iodide, tetrabromoethane). Hand picking of individual grains was sometimes necessary to attain high purity.

2.7.2. FISSION TRACK DATING PROCEDURE

For standards and samples, apatite grains were mounted in epoxy, polished and etched in 7% nitric acid for 30 seconds. A layer of clear low uranium muscovite was attached to the polished surface as an external detector. Muscovite detectors were also attached to uranium glass dosimeters. Pin holes were made through the mounts and detectors, to act as reference points for matching

spontaneous and induced tracks. Samples were interleaved with standards and dosimeters in aluminum canisters. Samples were irradiated as described in section 2.3. After irradiation, each muscovite external detector was etched in 48% HF for 28 seconds, and the exposed fission tracks were counted. Spontaneous fission tracks were counted in samples and standards at this time. Spontaneous and induced tracks were carefully matched on a grain - to - grain basis, by means of the pin holes and a graduated grid mounted on the microscope stage. Counting magnification was 400x for dosimeters, and 1000x for standards and samples. The size of the counting field was determined by an eyepiece graticule (5x5 grid). The size of the counting field was 55x55 um at 1000x, and 125x125 um at 400x. Ages were calculated as described in section 2.3, after Hurford and Green, 1983).

2.7.3. ARGON DATING PROCEDURE

Samples were packed into small thin-walled aluminum discs or simply wrapped in aluminum foil. Samples and standards were stacked in aluminum canisters. Most of the canisters were lined with 1.0 mm of cadmium metal to absorb thermal neutrons.

Samples were irradiated with fast neutrons in position 5C, in the core of the McMaster Reactor, Hamilton, Ontario. Irradiation typicallly lasted for 7.5 hours (15 MWH power),

but some samples received larger doses. Sample configuration in a typical canister is shown schematically in Fig 2.1.(a).

After irradiation, samples were stored for a few weeks to permit safer handling. Each sample was subsequently loaded into a quartz boat and placed in a quartz extraction tube connected to a glass vacuum line. The quartz tube was heated to a maximum of 1200 degrees C by means of a Lindberg (type 59344) furnace. Temperature within the furnace was monitored by a "Platinel" thermocouple. The gas was extracted in a stepwise fashion, usually at 50 degree intervals, purified over a Ti sponge getter, and leaked directly into the chamber of a substantially modified MS-10 mass spectrometer.

Analyses were accomplished by sequentially scanning for masses 36, 37, 39 and 40. Mass 37 was omitted for samples with low Ca/K ratios, and mass 38 was not recorded for any samples (section 2.2.2.2). A peak hopping procedure was executed automatically and the amplified signal fed into an on-line Apple 11e microcomputer. Each mass was measured 15 times. Peak positions were relocated before the first, sixth and eleventh measurements.

Amplified signals arriving from the mass spectrometer were digitized and the following mass ratios calculated: 36/39, 37/39, 40/39. The measured isotopic ratios often vary significantly over the duration of 15 determinations (about 45 minutes). Consequently, a linear extrapolation of

ratios was made back to zero time, when the gas was first let into the mass spectrometer. In calculating the ratio of $^{40}Ar/^{39}Ar$, a correction was made for the tailing of the ^{40}Ar peak at the ^{39}Ar position. Very occasionally, the ^{40}Ar tail was observed to extend over to the ^{36}Ar position, in which case a correction was performed manually.

After the above mentioned ratios were determined, appropriate corrections were made (section 2.2.2.2), and the age calculated according to equation (4) (section 2.2.). The complete data sets for all heating steps were stored on discs. They were subsequently retrieved to make summary sheets and age spectrum plots for each sample.

CHAPTER 3

EVALUATION OF SPECTRA AND DERIVATION OF CLOSURE TEMPERATURES

3.1. INTRODUCTION

This chapter focuses on techniques commonly used in the interpretation of age spectra. Some problems are highlighted and suggestions are made for improvements. To facilitate quantitative evaluation of spectra, some numerical parameters are introduced. The Berger - York method for deriving closure temperature is tested. Interpretation of the age data on a regional scale is deferred to Chapter 4. Three terms are defined:

Age spectrum: A graphic plot of apparent age versus fraction of gas released. The apparent age of each increment is displayed with appropriate error bars.

Plateau age (tp): The apparent age of that portion of the spectrum which defines a plateau (Section 3.2).

Total Fusion Age: The apparent age derived from the $^{40}Ar/^{39}Ar$ ratio after all argon is released in a single heating step.

Incremental Total Gas Age (t_T): The apparent age derived from the $^{40}Ar/^{39}Ar$ ratio after total gas release in

several steps. The ratios of all steps are compounded; each step is given weight commensurate with its percentage of the total.

Sigma (s): The uncertainty associated with an apparent age. By convention, 1s = uncertainty at the 68% confidence level; 2s = uncertainty at the 95% confidence level.

3.2. CONCORDANT AND DISCORDANT SPECTRA

A concordant spectrum is one in which the apparent age of every step is indistinguishable at the 95 % confidence level (Fleck et al. , 1977). ^{40}K and radiogenic ^{40}Ar are presumed to occupy similar lattice sites; therefore the release of ^{39}Ar (representing ^{40}K) is highly correlated with that of radiogenic ^{40}Ar. The entire spectrum is a plateau, where the apparent age of each step agrees with the total fusion age, the incremental total gas age, and the conventional K-Ar age.

Ideal concordant spectra have rarely been produced from terrestrial samples. Even in well defined, undisturbed samples, small fractions of the total ^{39}Ar yield ages substantially different from the plateau age (e.g. Dalrymple and Lanphere, 1974). These minor effects are usually ascribed to: (a) minor excess argon; (b) minor argon loss during sample preparation, (c) minor argon loss during irradiation (e.g. Harrison, 1983; Huneke and Smith, 1976). Since gas increments which represent small fractions of the

total may be unreliable, steps containing less than 3% of the total ^{39}Ar are ignored when determining a plateau (Fleck et al., 1977).

A spectrum is considered discordant if any step, containing more than 3% of the total ^{39}Ar does not lie on the plateau.

Fleck et al.(1977) emphasised the distinction between discordant spectra and spectra from tectonothermally disturbed samples. In some cases, disturbance may cause discordance (as outlined above), but this should not be automatically assumed. Thermally overprinted samples have been known to yield concordant spectra (e.g. Berger 1975), while some undisturbed samples have produced discordant spectra (Kunk et al., 1985). Even though most terrestrial samples do not produce ideal concordant spectra, many produce plateaus that are considered reliable and of geologic significance. These features are further discussed below.

Berger and York (1981) defined a reliable plateau as that part of a spectrum where five or more contiguous steps agree at the 95% confidence level (2s). A plateau has also been defined as that part of the spectrum where contiguous steps, constituting 50% or more of the total gas agree at the 95% confidence level (Fleck et al., 1977). The value of s depends on experimental conditions: the above definitions imply that analyses with large values of s (experimental uncertainty) have the best chance of producing plateaus.

According to these definitions, a spectrum may contain a plateau even though substantial portions of the gas give discordant ages. Although the presence or absence of a plateau can sometimes be used as a qualitative indicator of tectonothermal history, this distinction can be obscured by variation of conditions during the step-heating process.

3.3. DISCORDANCE FACTORS

To quantify deviation from ideal concordance in an age spectrum, three numerical parameters (DISCORDANCE FACTORS) are proposed: The term 'plateau' is as defined by Fleck et al., (1977).

1. DISCORDANCE NUMBER (DN): This is simply the difference between the mean plateau age and the incremental total gas age, expressed as a percentage of the incremental total gas age. For ideal concordance, DN = 0.

2. PLATEAU DISCORDANCE FACTOR (PDF): This is the summed difference between the mean plateau age and that of each individual step. Each step is weighted according to the percentage of ^{39}Ar it contains. For ideal concordance, PDF = 0.

3. INCREMENTAL TOTAL GAS DISCORDANCE FACTOR (IDF).This is analogous to PDF and is applied when a plateau does not exist. IDF is the summed difference between the t_T age and that of each individual step. Each step is weighted

according to its percentage of ^{39}Ar. The value of IDF is always greater than 0.

A related parameter, COMPOUND SIGMA, is defined as the summed errors (2s) of all steps. The error in each step is assigned weight according to the fraction of the total ^{39}Ar it contains. COMPOUND SIGMA (CS) gives a measure of interstep uncertainty (analytical precision).

For most samples, the parameters IDF and CS are adequate to describe both the deviation from ideal concordance, and interstep uncertainties at the 95% confidence level. They are employed in sections which follow. The equations which define these terms are listed in table 3-1.

For comparison with values from this study, PDF values have been calculated for five samples from published literature, which produced highly concordant spectra. These values which range from .24 to .81 are listed in table 3-2.

3.4. A MODEL FOR ARGON RELEASE DURING STEP HEATING

In order to critically evaluate ^{40}Ar-^{39}Ar age spectra, it is useful to consider some factors which affect the release of ^{39}Ar and ^{40}Ar. The location of radiogenic argon within a K-bearing mineral may be conveniently viewed in terms of sites of occupancy. Fitch et al., (1969) and Brereton (1972) suggested that there are three types of sites within K-bearing minerals in which ^{40}Ar resides:

Table 3-1. Discordance factors defined in this study.

$$DN = \frac{|t_T - t_P|}{t_T} \times 100$$

$$PDF = \sum_{i=1}^{n} \frac{f_i|(\Delta P)_i|}{t_P} \times 100$$

$$IDF = \sum_{i=1}^{n} \frac{f_i|(\Delta T)_i|}{t_T} \times 100$$

$$CS = \sum_{i=1}^{n} 2f_i\sigma_i$$

t_T = incremental total gas age.

t_P = plateau age.

f_i = fraction of ^{39}Ar in individual step.

σ_i = inter-step uncertainty on individual step.

$(\Delta P)_i$ difference between apparent age of individual step and the plateau age.

$(\Delta T)_i$ difference between apparent age of individual step and the incremental total gas age.

Table 3-2. PDF values for some biotite and hornblende samples which produced highly concordant age spectra.

Sample	Phase	Geologic Setting	PDF	Ref.
MMhb-1	Hb	McClure Mt Complex Colorado	0.24	Harrison, 1981.
4A	Hb	Hartland Stock,Maine	0.69	Dallmeyer et al 1982
4A	Bi	Hartland Stock,Maine	0.72	Dallmeyer et al 1982.
9400	Hb	Eldorado Stock Colorado	0.32	Berger, 1975.
22500	Bi	Eldorado Stock Colorado	0.81	Berger, 1975.

Type (1). Non-lattice sites. ^{40}Ar is adsorbed on surfaces (crystal faces, cracks, cleavages, intergranular boundaries), or loosely held in lattice imperfections (cavities, fluid inclusions).

Type (2): High Diffusion Probability lattice sites. ^{40}Ar is held within normal lattice, but close to grain boundaries, cavities, cracks, and other discontinuities; or in damaged lattice sites.

Type (3): Low diffusion probability sites. ^{40}Ar is held in undamaged lattice sites away from discontinuities.

Although it is recognized that this model may be an oversimplification the three categories probably cover the range of argon retention sites that may be found in a mineral. It provides a basis for discussion of argon release. The sites are shown schematically in fig. 3-1. The relative proportions of types 1, 2, and 3 will depend on the tectonothermal history of the rock, and may vary within individual samples. It was suggested by Brandt and Voronovskiy (1967) that after ^{40}Ar is produced from interlayer ^{40}K in micas, it recoils with an energy of about 30 eV, with 4π geometry. This ensures that about 93% of the ^{40}Ar produced is directed towards the mica crystal lattice. Since the bond energy is about 5 eV (Brandt and Voronovskiy, 1967), the ^{40}Ar atom has enough kinetic energy to become imbedded in the mica structure. These estimates suggest that about 93% of ^{40}Ar occupies type 3 sites for undisturbed micas. The other 7% remain in types 1 and 2

Fig. 3-1. Schematic diagram illustrating possible distribution of sites where radiogenic argon may reside in a K-bearing mineral.

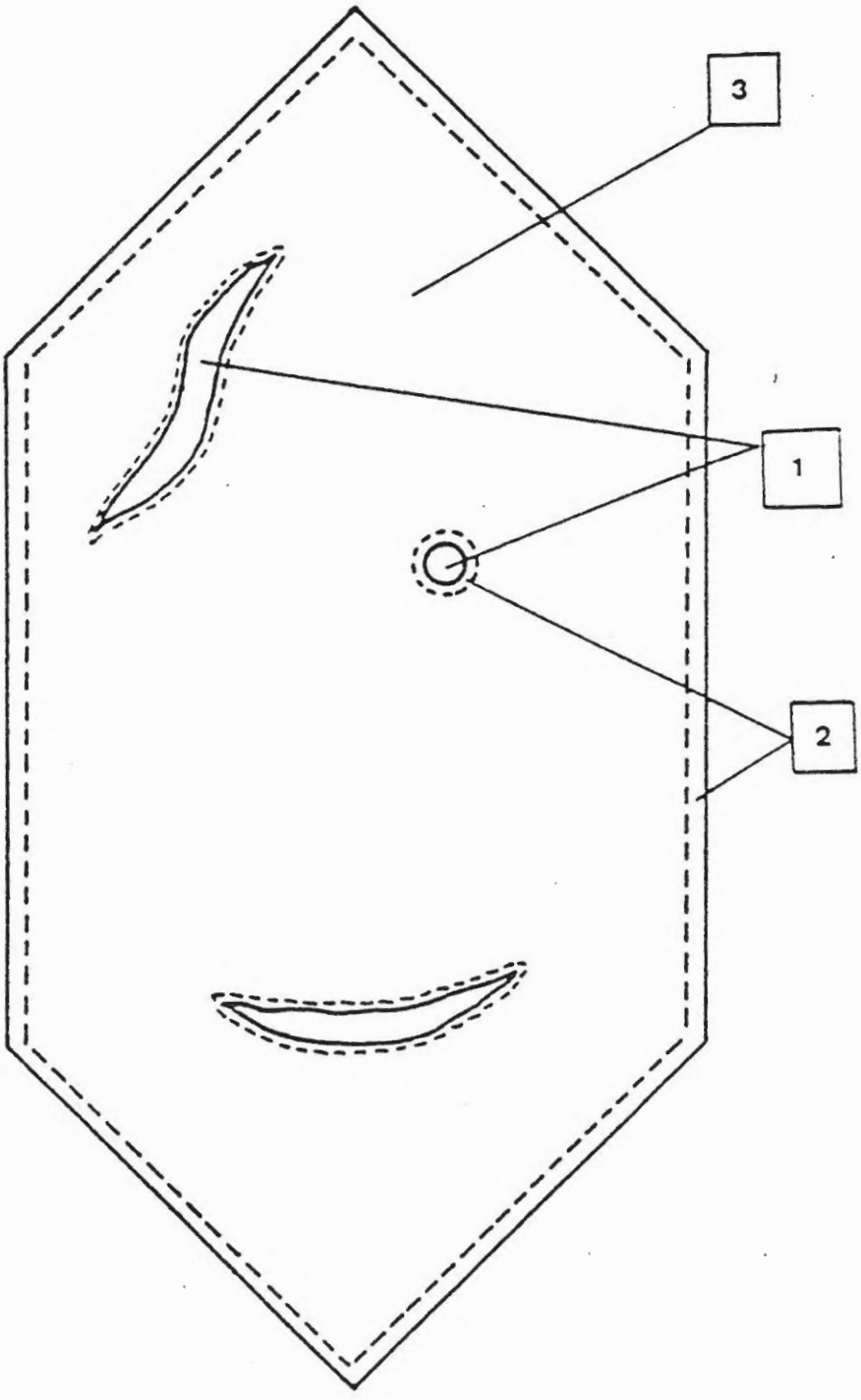
3
1
2

sites. If the mica lattice is subsequently disturbed by tectonothermal events, the proportion of sites may change drastically. Although this structural analysis is not appropriate to most other K-bearing minerals, it emphasizes the potential complexity of K-Ar systematics. Reactor-produced ^{39}Ar moves over a distance of 0.08 - 0.1 um (Brereton, 1972; Huneke and Smith, 1976), leading to redistribution among the three site types. In rocks which have had a simple tectonothermal history, only a small proportion of the sites are likely to be type 1 and type 2. Redistribution of reactor-produced ^{39}Ar would occur largely within type 3 sites. Subsequent step heating analysis should produce a high correlation between ^{39}Ar and ^{40}Ar, resulting in a plateau in the age spectrum. Small portions of the spectrum will be discordant, reflecting the small proportion of type 1 and type 2 sites. These observations are generally confirmed by experimental results, where the low temperature early steps give discordant ages followed by a plateau. (e.g. Dalrymple and Lanphere, 1974; Berger, 1975; Hurford and Hammerschmidt, 1985).

Disturbed samples are likely to have a high proportion of type 1 and type 2 sites. Redistribution of ^{39}Ar during irradiation should cause ^{39}Ar and ^{40}Ar to occupy different sites. The two isotopes will be poorly correlated during stepwise release, producing discordance in the age spectrum. Where tested, this model is supported by experimental results and field observations (e.g. Berger, 1975;

Dallmeyer, 1975; Hanson et al., 1975; Ozima et al., 1979; Harrison et al., 1985).

3.5. INFORMATION CONTAINED IN ^{40}Ar-^{39}Ar SPECTRA

When tested on meteorite samples (Turner, 1968), the ^{40}Ar-^{39}Ar step heating technique appeared capable of giving the following information:

(1)The time of original post-crystallization cooling from the plateau age of an undisturbed sample.

(2) The time of reheating from the plateau age of a sample completely outgassed by a secondary event.

(3) The time of reheating as well as the time of initial crystallization from a sample which suffered minor gas loss during a secondary event.

Results from terrestrial samples have been rather ambiguous. Few studies have been undertaken with samples whose thermal histories have been independently determined. In some cases, amphiboles seem capable of giving information on the time of original crystallization, the time and temperature of overprinting, and the fraction of gas lost during that secondary event (eg Harrison and McDougall, 1980). This follows from the model of Turner (1968, 1969), which assumes that a crystal that suffered partial loss of ^{40}Ar retains an argon concentration gradient from core to rim (fig 3-2). Analyses of such grains by the ^{40}Ar-^{39}Ar step heating technique should reflect the naturally induced

Fig. 3-2. Schematic diagram illustrating typical argon concentration gradient expected in a mineral that suffered episodic loss or cooled very slowly.

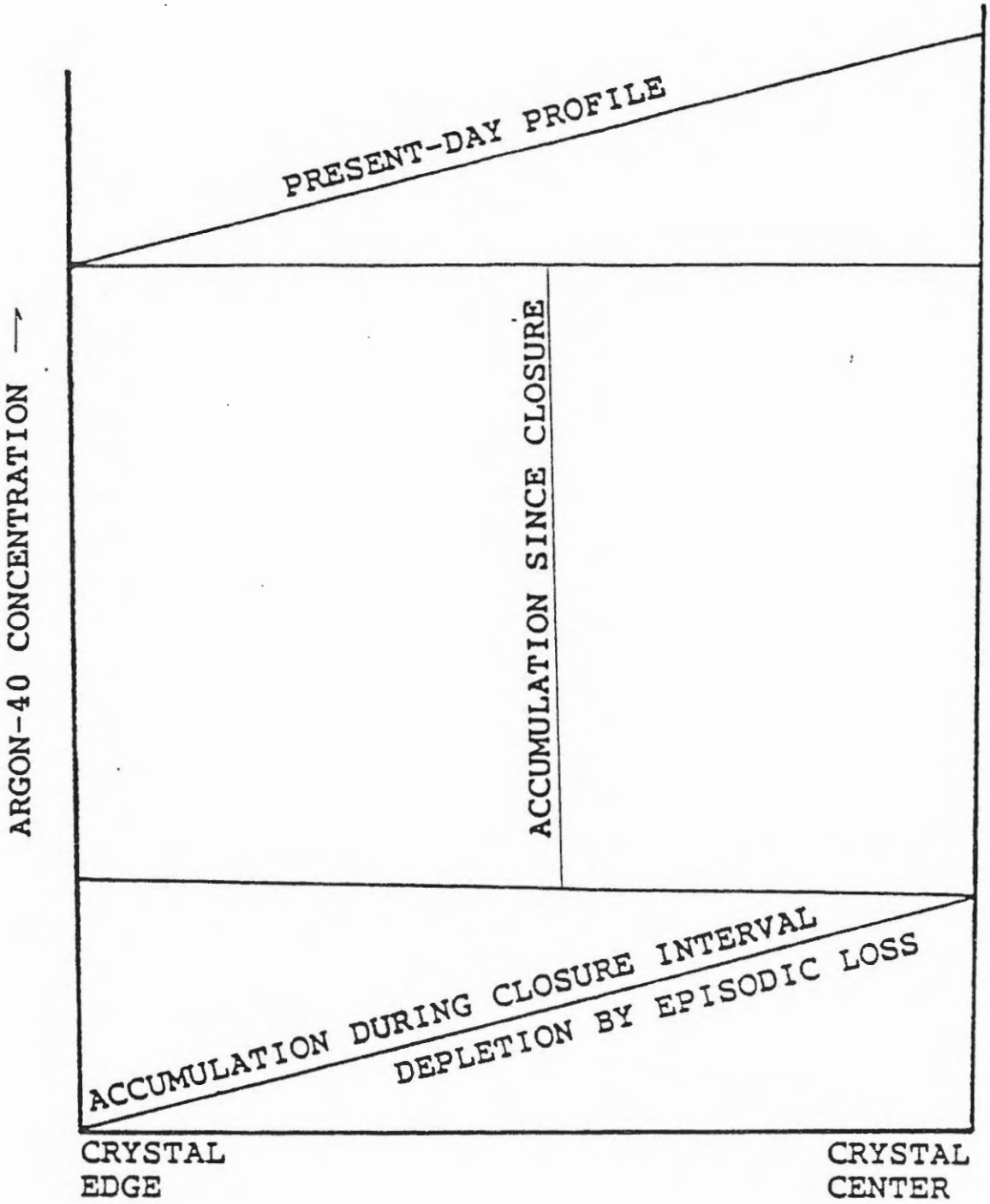
PRESENT-DAY PROFILE
ACCUMULATION SINCE CLOSURE
ACCUMULATION DURING CLOSURE INTERVAL
DEPLETION BY EPISODIC LOSS
ARGON-40 CONCENTRATION →
CRYSTAL EDGE
CRYSTAL CENTER

gradient. The rim of the crystal is presumably outgassed completely by the overprinting event: the first few steps of the age spectrum represent the rim and therefore should give the age of overprint. Apparent ages increase in successive steps as argon is removed from domains progressively closer to the center of the crystal. The apparent age of the last step should be close to the original cooling age for small losses (less than about 20%). For much larger ^{40}Ar losses, the original cooling age cannot be determined; the last step defines a minimum value. This ideal model requires two conditions to be fulfilled:

(1) The ^{40}Ar gradient must be maintained throughout the experiment. Loss of crystalline integrity by processes such as dehydration, polymorphic inversion, and excessive pulverization may obliterate the naturally induced gradient.

(2) It is necessary that the overprinting event did not also induce a gradient in K, which is known to be highly mobile in hydrothermal solutions. Further, it is necessary that the release of ^{39}Ar reflect the original (pre-overprint) distribution of ^{40}K. Redistribution of ^{39}Ar by recoil may distort the release pattern (see fig. 3-1).

It may be noted from fig. 3-2 that a concentration gradient may also be induced in a crystal by slow cooling through the transitional closure interval (section 2.4). Such gradients are indistinguishable from those produced by episodic loss (e.g. Harrison and McDougall, 1982).

Gerling et al., (1966) performed heating experiments on

amphiboles, which indicate that dehydration is almost complete in the temperature range 765-1005 degrees C. Amphiboles are converted to the pyroxene structure. They also found that most radiogenic argon from the same samples was released after dehydration. Harrison (1983) suggested that this behaviour of amphiboles ensures that naturally induced argon diffusion gradients are preserved. This may be an oversimplification, since dehydration and argon release partly overlap. Information from the low temperature end of the spectrum may be unreliable. The effects of the phase transformation after dehydration on an argon concentration gradient are uncertain. Since the change from amphibole to pyroxene can occur with minor rearrangement of the chain structure, the interpretation of Harrison (1983) may be valid in some cases. In contrast, argon release from micas is apparently accompanied by dehydration and delamination (Gerling et al., 1966; Brandt and Voronovskiy, 1967; Zimmerman, 1972). This implies that argon concentration profiles are unlikely to be preserved, although some thermally overprinted muscovites have been shown to produce staircase profiles in their spectra (e.g. Hanson et al., 1975). Harrison and Be (1983) employed the model of Turner (1968) to derive information on ^{40}Ar loss from detrital microcline. Homogenization of perthite lamellae and inversion of microcline to orthoclase should occur over the temperature range 500-1200 degrees C (e.g. Evernden et al., 1960; Abramov et al., 1972), but it is

uncertain how far these transformations reach during the short duration of a step heating experiment. Harrison (1983) suggested that most argon is released from perthitic microcline before any significant phase changes. This conclusion is, however, based on deductions from age spectra instead of direct measurements, and is contrary to the findings of Evernden et al., (1960). The following observations may be made on the information obtainable from terrestrial samples.

(1)Most samples from undisturbed volcanic rocks produce plateau ages equal to the time of crystallization (e.g. Hurford and Hammerschmidt, 1985; Kunk et al., 1985; McDougall, 1985).

(2)Samples from undisturbed plutonic and metamorphic rocks yield plateau ages lower than the time of original crystallization. The difference between the plateau age and the original crystallization age is inversely proportional to the cooling rate and the closure temperature of the mineral dated. (e.g. Dallmeyer et al., 1975 ; Berger and York, 1981).

(3) Samples completely outgassed during an overprinting event produce plateau ages lower than the time of that second event, (e.g. Berger, 1975; Hanson et al., 1975). As in (2), the age difference is inversely proportional to the cooling rate and the closure temperature.

(4) Samples partially outgassed during a secondary event may produce spectra of various shapes (Berger, 1975;

Hanson et al., 1975). Spectra from some overprinted amphiboles may give plateau ages (e.g. Berger, 1975; Harrison and McDougall, 1980). The significance of such plateau ages must be interpreted in conjunction with other geologic information. The model of Turner (1968) may be applied to amphiboles and K-feldspars with the reservations listed above.

(5) Samples containing excess argon sometimes give saddle shaped spectra (Lanphere and Dalrymple, 1976). This shape is difficult to explain and may not always be present (e.g. Foland, 1983). This is further discussed in Chapter 4.

3.6. THE EFFECTS OF RECOIL ON THE SPECTRA OF SLATES

Because of their complex nature, whole rock samples are rarely dated. Interpretation of their spectra is, therefore, poorly documented. White micas in slates are commonly less than 100um in size, and a substantial fraction are smaller than 20 um. This range in size provides ample opportunity for ^{39}Ar transfer to K-poor minerals (mainly quartz and chlorite). For example, samples NS72-31 and NS72-33 (Chapter 4) contain white micas with approximate mean dimensions of 30 um diameter, and 3 um thickness when viewed parallel to the 001 cleavage (figs. 3-3, 3-4, 3-5). Many grains are smaller than these. The shape of white micas in these samples can be approximated by a circular

Fig. 3-3.

Photomicrograph of slate sample NS71-139.
Note high quartz content and poor foliation.

Fig. 3-4.

Photomicrograph of slate sample NS72-31.
Note good foliation and range of white mica size.

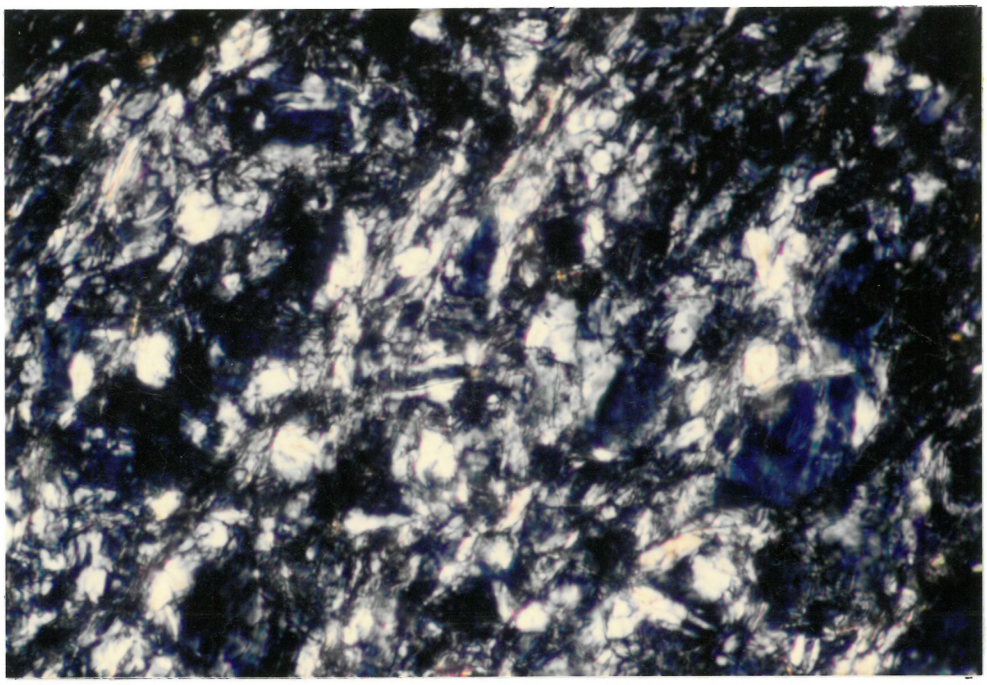

30 μm

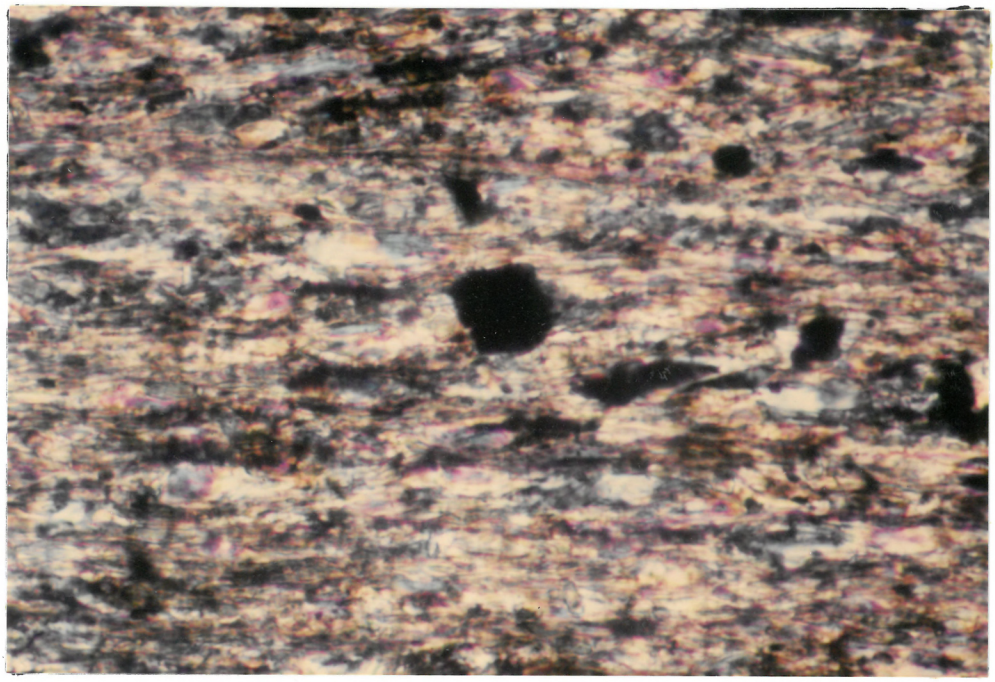

30 μm

Fig. 3-5.

Photomicrograph of slate sample NS72-33.
Note good foliation and range of white mica size.

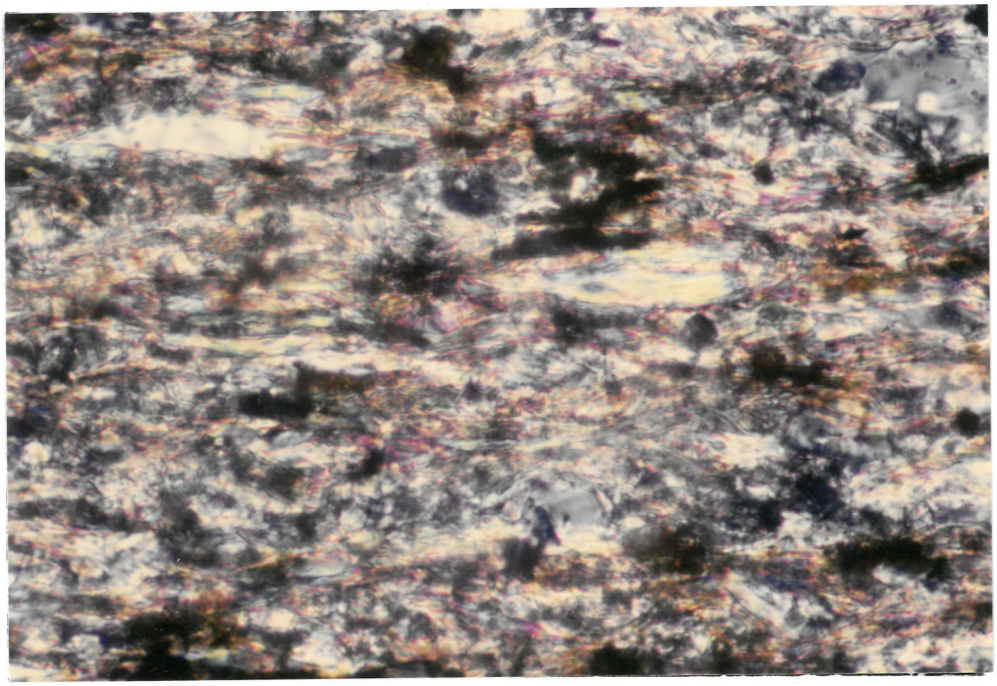

30μm

disc 30 um in diameter and 3 um in height. Assuming a peripheral 'damage zone' of 0.1 um (e.g. Brereton, 1972), such grains would lose 10% of their ^{39}Ar to recoil. By a similar model, grains of 30 um length and 1 um thickness would lose about 20% of their ^{39}Ar to recoil. These predicted losses are similar to those found experimentally by Hunziker et al., (1986) for illite extracted from pelites. Three size fractions, 6 - 20 um, 2 - 6 um, 0.6 - 2 um, were analysed by both conventional K-Ar and ^{40}Ar-^{39}Ar techniques. Apparent age differences indicate ^{39}Ar losses of 21.9%, 22.8%, and 35.6% respectively.

Since whole rock slate samples in this study were not crushed to sizes below 100 um (typically about 200 um), ^{39}Ar expelled from white mica was largely retained in the aggregate. The detailed shapes of the spectra are distorted, but the incremental total gas ages are not significantly affected. Recoil-induced discordance may be superimposed on geologically significant profiles, rendering interpretation of the spectra difficult. Because of the small grain size of white mica in slates, release of the argon can be expected at relatively low temperatures during step-heating. Experimental results support these predictions. All slate/siltstone spectra are highly discordant (Chapter 4). IDF ranges from 2.68 to 10.92. Except for sample PE85-138 (346 Ma), ages range from 368 Ma to 406 Ma, consistent with stratigraphic constraints (Chapter 1). The ^{40}Ar-^{39}Ar apparent ages of three of the

samples are indistinguishable from their conventional K-Ar ages (Chapter 4). These results would not be expected if significant amounts of ^{39}Ar were lost during irradiation. Except for samples KB1, KB3, and KB6, all samples release more than 50% of their total argon below 800 degrees C (Appendix A). The slower release of KB1, KB3, and KB6 has been ascribed by Savell (1980) to slightly lower permeability. This may be partly due to slightly greater grain size (Chapter 4). Release of argon from slates, phyllites, and illite/phengite separates, at relatively low temperatures, has been recorded elsewhere (e.g. Reynolds and Muecke, 1978; Dallmeyer, 1982; Hunziker et al., 1986). The extent to which early argon release is induced by recoil in very fine grained micas is uncertain. This can be tested by observing the release pattern of irradiated and unirradiated aliquants of the same sample.

3.7. THE RELATIONSHIP BETWEEN $^{37}Ar/^{39}Ar$ AND Ca/K IN AMPHIBOLES.

During neutron irradiation, ^{37}Ar is produced from $^{40}Ca(n, a)^{37}Ar$, whereas ^{39}Ar is produced from $^{39}K(n, p)^{39}Ar$. For a given neutron spectrum, therefore, $^{37}Ar/^{39}Ar$ is proportional to Ca/K. It is possible to evaluate a conversion factor $F= (Ca/K)/(^{37}Ar/^{39}Ar)$ for a given position in a reactor, where the neutron spectrum is reproducible.

The value for position 5C of McMaster reactor has been calculated using the standard hornblende sample MMhb-1, which has Ca/K =4.54 +/- 0.24 (Alexander et al., 1978). The calculated conversion factor is 1.86 +/- 0.12, which can be used to estimate Ca/K in the release pattern of 'unknown' samples in this study.

The $^{37}Ar/^{39}Ar$ ratio is sometimes regarded as a faithful reflection of Ca/K during step-heating. Variations in $^{37}Ar/^{39}Ar$ are usually ascribed to chemical zoning, where each domain supposedly releases Ar separately with characteristic $^{37}Ar/^{39}Ar$, reflecting its composition (e.g. Harrison and Fitzgerald, 1986).

A uniform $^{37}Ar/^{39}Ar$ ratio throughout an age spectrum requires complete correlation between the release of the two isotopes. The absence of complete correlation is not always caused by chemical zonation of the amphibole. The following factors may contribute to variation in $^{37}Ar/^{39}Ar$:

(1) Minor mica contamination. Since micas commonly contain more than 50 times the K-content of hornblende, even a minor mica contaminant would substantially distort the $^{37}Ar/^{39}Ar$ ratio.

(2) The reaction $^{40}Ca(n, a)^{37}Ar$ has a maximum recoil energy of 360 keV, 20% higher than that for $^{39}K(n, p)^{39}Ar$ (300 keV) (Brereton, 1972). Recoil redistribution is therefore unlikely to be the same for the two isotopes. This problem will be aggravated by the presence of crystal defects imposed by tectonothermal disturbance.

In the spectra of sample PE83-11 and PE84-130 (fig. 3-6), $^{37}Ar/^{39}Ar$ starts quite low for the first 20 % of the gas, then rises to a relatively uniform value. The initial value is 3-5 in sample PE83-11 which rises to 16-19 . For sample PE84-130 $^{37}Ar/^{39}Ar$ starts at 4-4.5, then rises to 11-12. The trend is similar for samples PE83-9 and PE84-114. In contrast, $^{37}Ar/^{39}Ar$ for sample PE84-64C, rises from an initial value of 9 to a uniform 12-13.5 (see Appendix A). The low initial $^{37}Ar/^{39}Ar$ values of the first four samples are probably due to minor biotite contamination. Sample 84-64C was not so affected since biotite does not occur in the rock. The inferred Ca/K values are similar to those obtained by microprobe analyses (fig. 3-6). Minor discrepancies are probably due to low precision in measuring K (s~8%), and the possible recoil problems discussed above. Both microprobe analyses and $^{37}Ar/^{39}Ar$ data from the age spectra indicate that the amphiboles dated in this study are not complexly zoned. It may be possible, therefore, to extract geologically meaningful information from the age spectra of these samples. (cf. Harrison and Fitzgerald, 1986).

3.8. GENERAL OBSERVATIONS ON MICA SPECTRA

Micas constitute 75% of the spectra generated in this study. (38 biotites, one phlogopite, and 18 muscovites). It is, therefore, necessary to assess criteria for

Fig. 3-6. Age spectra for amphiboles showing variation of Ca/K with argon release. The vertical bar represents the Ca/K ratio determined by microprobe analyses. The number below the sample number is the incremental total gas age. 'H' signifies hornblende.

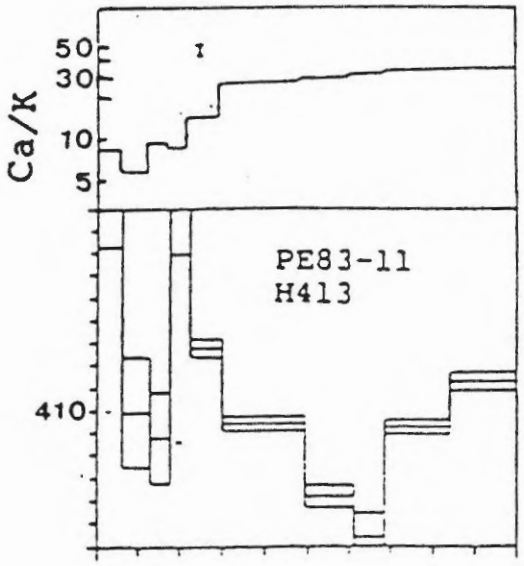
Ca/K
50
30
10
5
410
PE83-11
H413

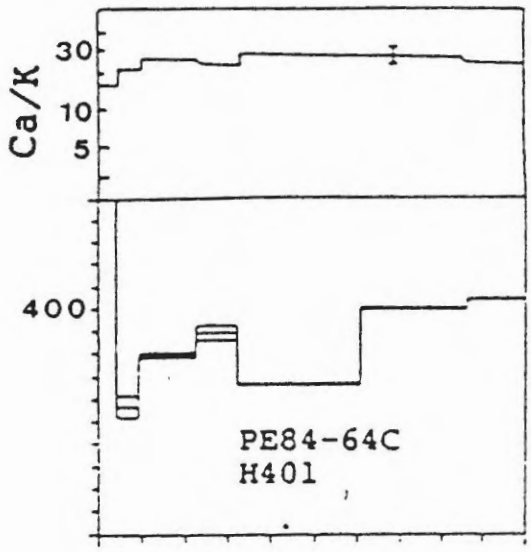
Ca/K
30
10
5
400
PE84-64C
H401

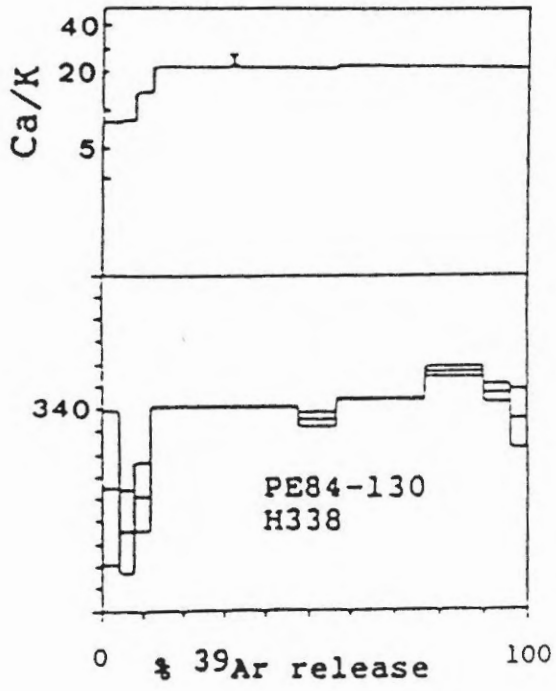
Ca/K
40
20
5
340
PE84-130
H338
0
% 39Ar release
100

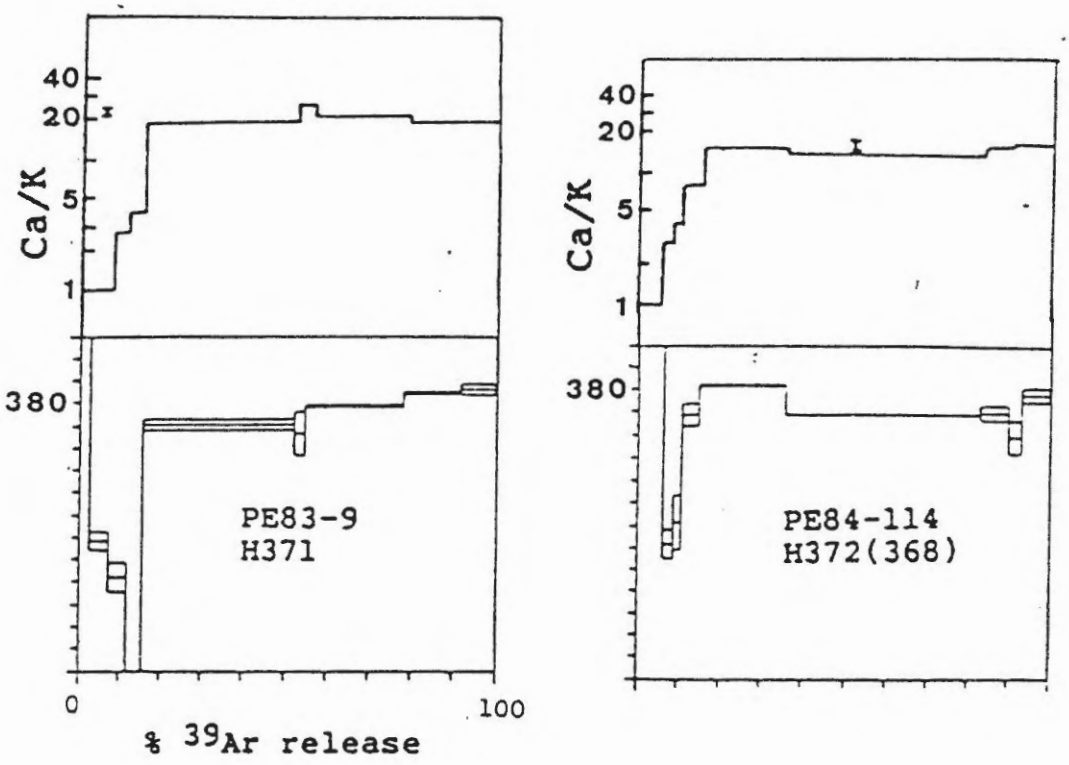
40
20
5
1
Ca/K
380
PE83-9
H371
0
100
% 39Ar release
40
20
5
1
Ca/K
380
PE84-114
H372(368)

evaluating them. ^{40}Ar-^{39}Ar experiments on biotites which were artificially heated or deformed, indicate that detailed shapes of spectra from such samples are not diagnostic (e.g. Ozima et al., 1979; Harrison et al., 1985). On the contrary Dallmeyer (1975, 1982) suggested that such spectra are characterized by anomalously low ages in their intermediate steps (saddle-shaped). Although spectra from some samples (e.g. PE84-41, PE84-72) display this feature, it is not very pronounced (figs. 4.2-15, 4.2-18). Some samples (e.g. muscovite PE48-77M, biotite PE82-9) display profiles similar to those described by Turner (1968), for partial argon loss: The earliest step gives the lowest age, while successive steps give progressively higher ages, approaching or attaining a plateau. Since the first few steps tend to be poorly defined, and vary considerably in apparent age, it is difficult to assign geolologic significance to them, as required by the Turner model. The varied texture of these spectra support the findings of Dallmeyer (1975), that the diffusion loss model of Turner (1968) is not applicable to micas. Since argon release in micas is accompanied by dehydration (section 3.5), it is likely that any geologically induced profile is modified during step heating.

3.9. DERIVATION OF CLOSURE TEMPERATURES

An attempt was made in this study to test the Berger-York technique (Section 2.6.1) for deriving closure temperature. As described in Chapter 2, the step-heating procedure was treated as a diffusion experiment. Experiments were performed on muscovite, biotite and K-feldspar. Of the three available models (section 2.5), the sphere is probably the least relevant; both feldspars and micas are highly anisotropic. The cylindrical model was chosen for the micas because diffusion is believed to proceed easiest parallel to the 001 cleavage, instead of perpendicular as required by the plane sheet model (e.g. Giletti, 1974). Both the cylindrical and sheet models were tested on the K-feldspars. A cooling rate of 1 degree/Ma is assumed.

3.9.1. ARRHENIUS PLOTS

Following the procedure outlined in Section 2.6.1, log D/a2 was plotted against 1/T for each sample. The plots are displayed in fig. 3-7. It can be seen that the plots are not linear throughout the range of experimental temperatures. For most samples, there is an abrupt change of slope at some point in the temperature range 650-850 degrees C (1000/K = 1.08 - .89). This implies a change in activation energy, which is probably accompanied by structural transformation (e.g. Gerling et al., 1966;

Fig. 3-7. Arrhenius plots for muscovite, biotite and K-feldspar.

"Non-linear" plots did not satisfy the criteria of section 3.9.1.

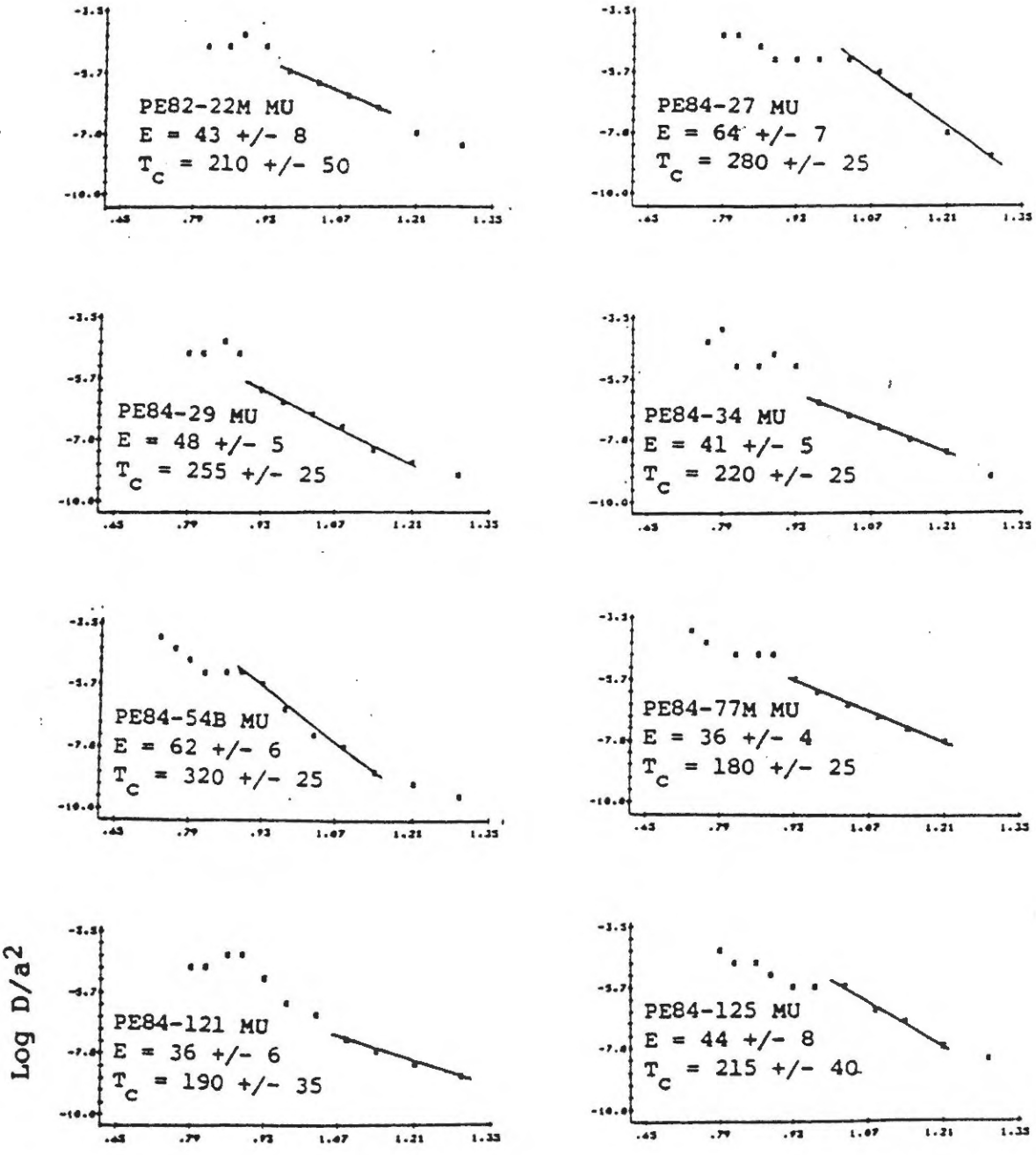
PE82-22M MU
E = 43 +/- 8
T_c = 210 +/- 50
PE84-27 MU
E = 64 +/- 7
T_c = 280 +/- 25
PE84-29 MU
E = 48 +/- 5
T_c = 255 +/- 25
PE84-34 MU
E = 41 +/- 5
T_c = 220 +/- 25
PE84-54B MU
E = 62 +/- 6
T_c = 320 +/- 25
PE84-77M MU
E = 36 +/- 4
T_c = 180 +/- 25
PE84-121 MU
E = 36 +/- 6
T_c = 190 +/- 35
PE84-125 MU
E = 44 +/- 8
T_c = 215 +/- 40
Log D/a2
1000/K

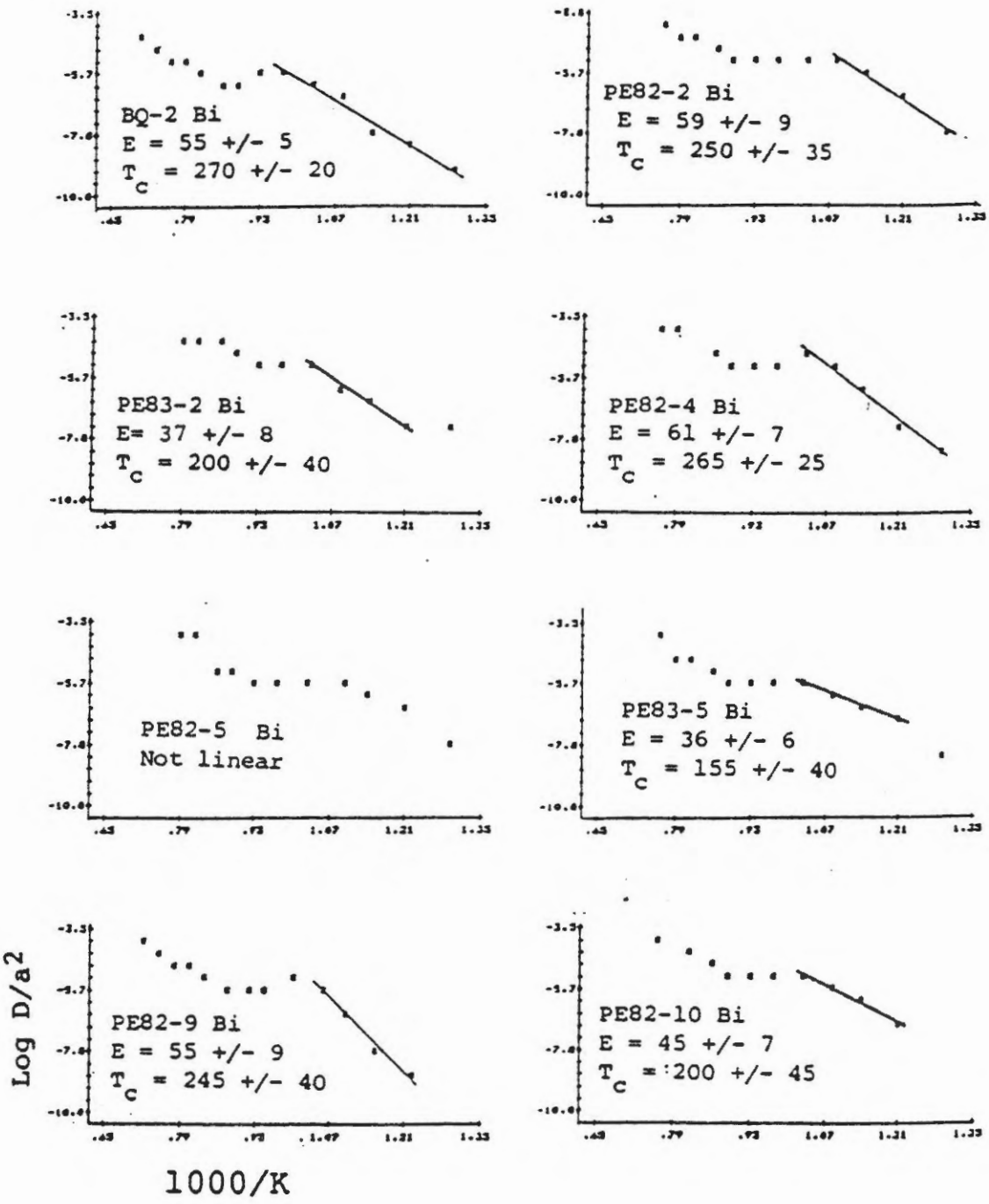
BQ-2 Bi
E = 55 +/- 5
T_c = 270 +/- 20
PE82-2 Bi
E = 59 +/- 9
T_c = 250 +/- 35
PE83-2 Bi
E= 37 +/- 8
T_c = 200 +/- 40
PE82-4 Bi
E = 61 +/- 7
T_c = 265 +/- 25
PE82-5 Bi
Not linear
PE83-5 Bi
E = 36 +/- 6
T_c = 155 +/- 40
PE82-9 Bi
E = 55 +/- 9
T_c = 245 +/- 40
PE82-10 Bi
E = 45 +/- 7
T_c = 200 +/- 45
Log D/a2
1000/K

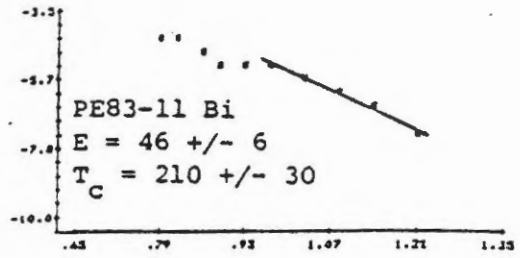

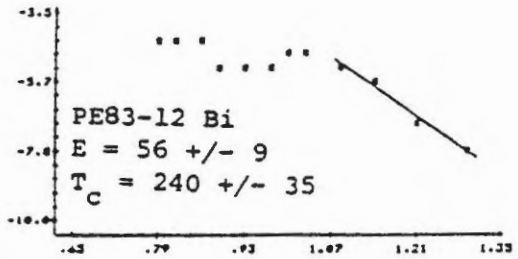

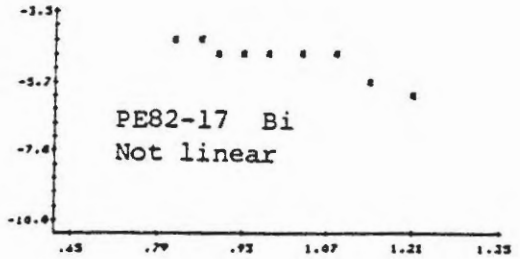

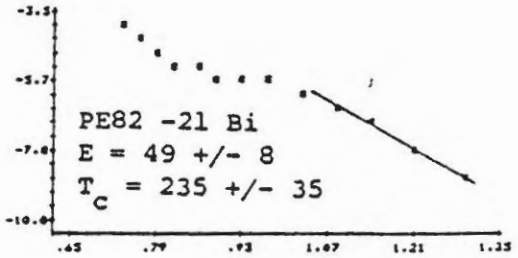

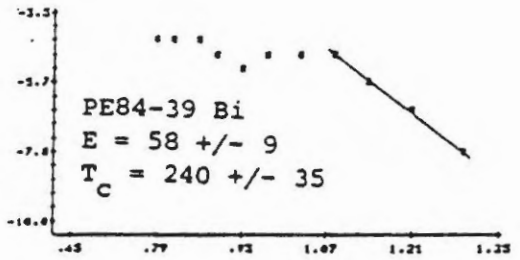

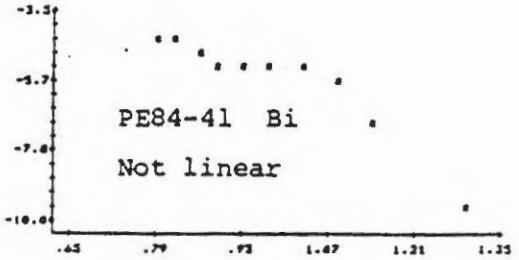

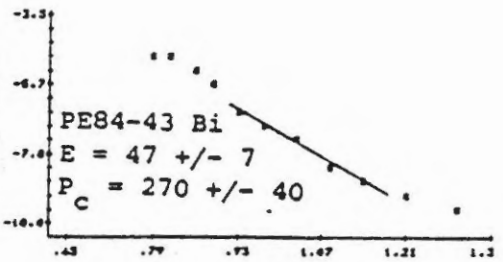

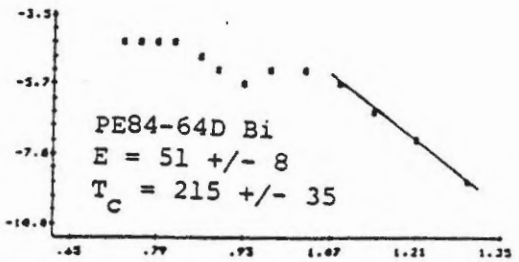

Log D/a2

1000/K

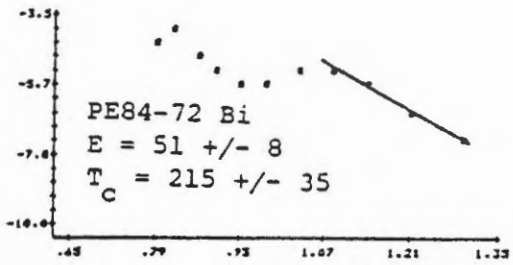
PE84-72 Bi
E = 51 +/- 8
T_c = 215 +/- 35

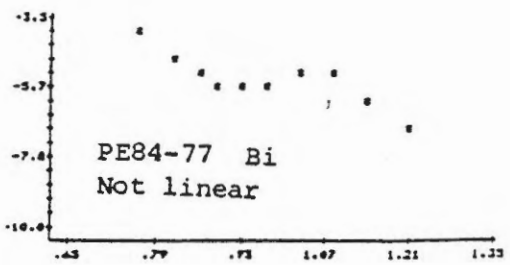
PE84-77 Bi
Not linear

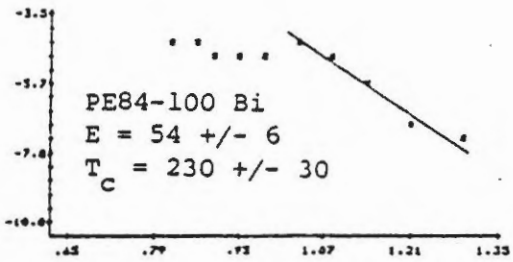
PE84-100 Bi
E = 54 +/- 6
T_c = 230 +/- 30

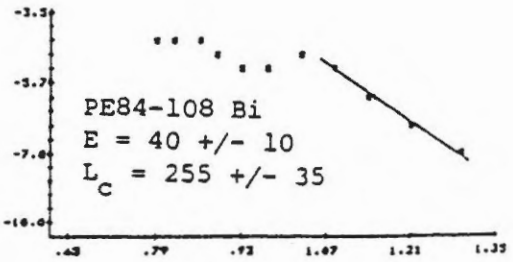
PE84-108 Bi
E = 40 +/- 10
L_c = 255 +/- 35

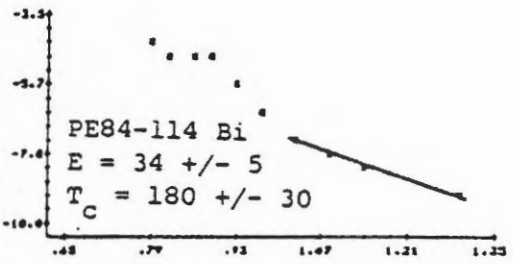
Log D/a2
PE84-114 Bi
E = 34 +/- 5
T_c = 180 +/- 30
1000/K

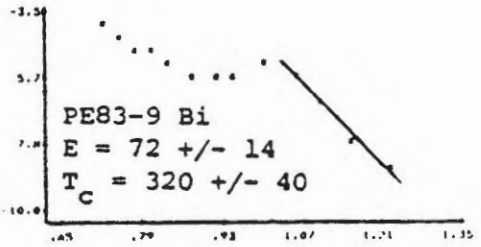
PE83-9 Bi
E = 72 +/- 14
T_c = 320 +/- 40

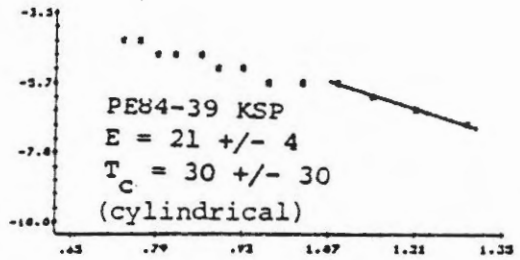

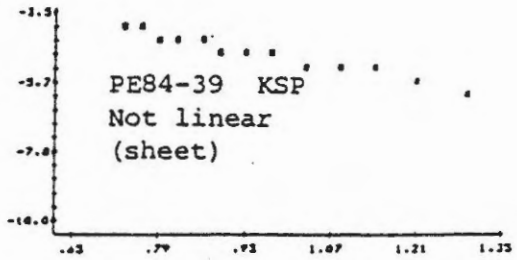

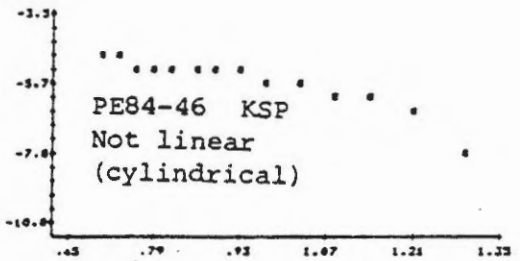

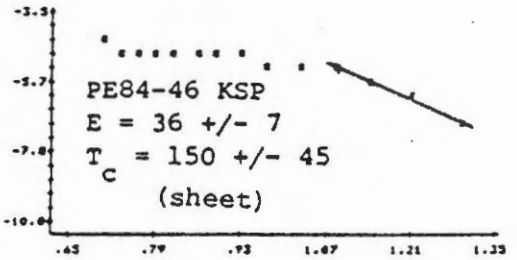

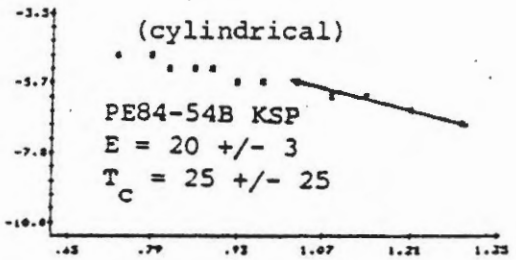

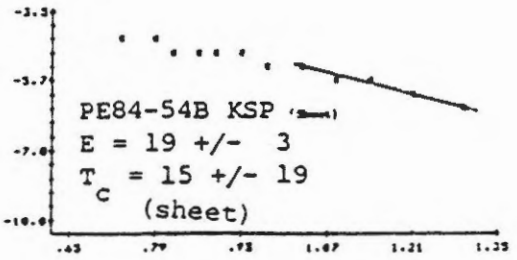

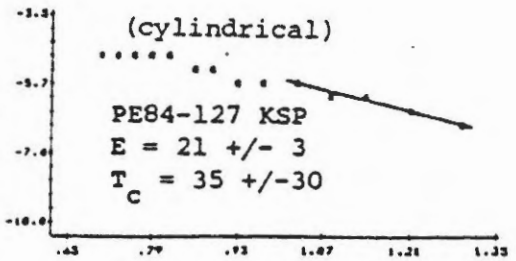

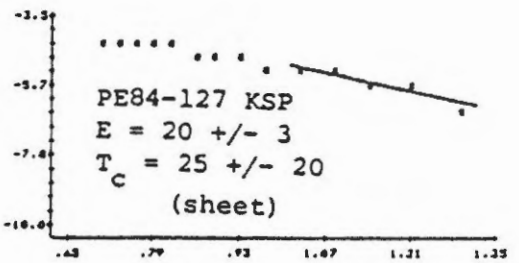

Log D/a2

1000/K

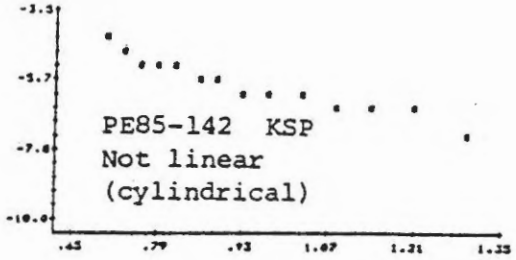
PE85-142 KSP
Not linear
(cylindrical)

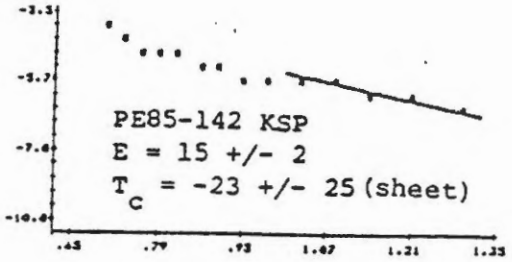
PE85-142 KSP
E = 15 +/- 2
T_c = -23 +/- 25 (sheet)

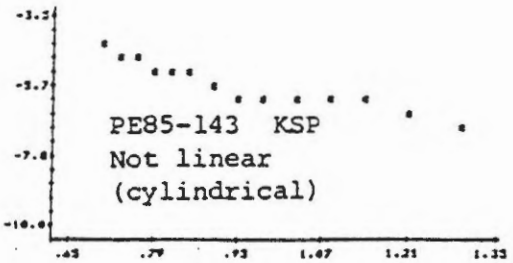
PE85-143 KSP
Not linear
(cylindrical)

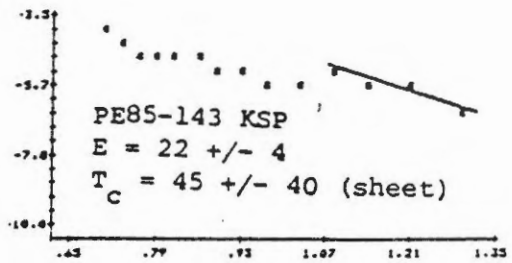
PE85-143 KSP
E = 22 +/- 4
T_c = 45 +/- 40 (sheet)

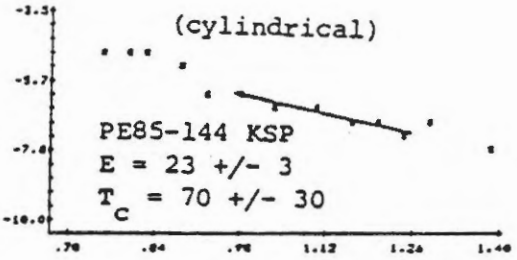
(cylindrical)
PE85-144 KSP
E = 23 +/- 3
T_c = 70 +/- 30

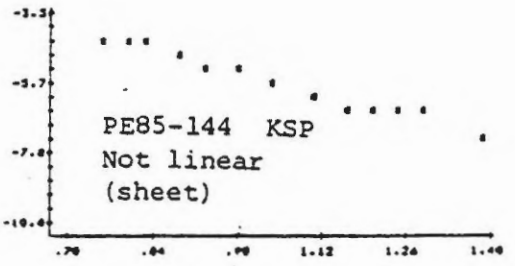
PE85-144 KSP
Not linear
(sheet)

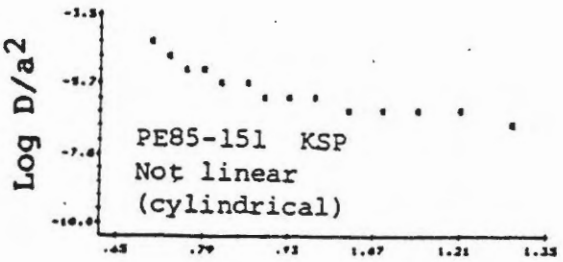
Log D/a2
PE85-151 KSP
Not linear
(cylindrical)
1000/K

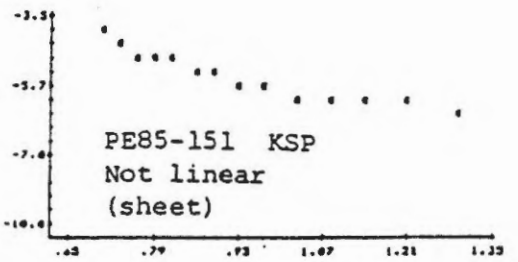
PE85-151 KSP
Not linear
(sheet)

Table 3-3. Derived closure temperatures and activation energies for muscovite, biotite and K-feldspar.

MINERAL	SAMPLE NUMBER	E (kcal/mol)	Tc (°C)	MODEL
BIOTITE	BQ-2	55 +/- 5	270 +/- 20	CYLINDRICAL
	PE82-2	59 +/- 9	250 +/- 35	
	PE83-2	37 +/- 8	200 +/- 40	
	PE82-4	61 +/- 7	265 +/- 25	
	PE83-5	36 +/- 6	155 +/- 40	
	PE82-9	55 +/- 9	245 +/- 40	
	PE83-9	72 +/- 14	320 +/- 40	
	PE82-10	45 +/- 7	200 +/- 45	
	PE83-11	46 +/- 6	210 +/- 30	
	PE83-12	56 +/- 9	240 +/- 35	
	PE82-21	49 +/- 8	235 +/- 35	
BIOTITE	PE84-39	58 +/- 9	240 +/- 35	CYLINDRICAL
	PE84-43	47 +/- 7	270 +/- 40	
	PE84-64D	51 +/- 8	215 +/- 35	
	PE84 72	51 +/- 8	215 +/- 35	
	PE84-100	54 +/- 6	230 +/- 30	
	PE84-108	60 +/- 10	255 +/- 35	
	PE84-114	34 +/- 5	180 +/- 30	

MINERAL	SAMPLE NUMBER	E (kcal/mol)	Tc (°C)	MODEL
K-FELDSPAR	PE84-39	21 +/- 4	30 +/- 30	CYLINDRICAL
	PE84-54B	20 +/- 3	25 +/- 25	
	PE84-127	21 +/- 3	35 +/- 30	
	PE85-144	23 +/- 3	70 +/- 30	
K-FELDSPAR	PE84-46	36 +/- 7	150 +/- 45	SHEET
	PE84-54B	19 +/- 3	15 +/- 19	
	PE84-127	20 +/- 3	25 +/- 20	
	PE85-142	15 +/- 2	-23 +/- 25	
	PE85-143	22 +/- 4	45 +/- 40	
MUSCOVITE	PE82-22M	43 +/- 8	210 +/- 50	CYLINDRICAL
	PE84-27	64 +/- 7	280 +/- 25	
	PE84-29	48 +/- 5	255 +/- 25	
	PE84-34	41 +/- 5	220 +/- 25	
	PE84-77M	36 +/- 4	180 +/- 25	
	PE84-54B	62 +/- 6	320 +/- 25	
	PE84-121	36 +/- 6	190 +/- 35	
	PE84-125	44 +/- 8	215 +/- 40	

Fig. 3-8. Plot of biotite activation energy vs Fe/(Fe+Mg).

Fig.3-9. Plot of closure temperature vs IDF. for biotite.

'2' on the diagram signifies position where two data points coincide.

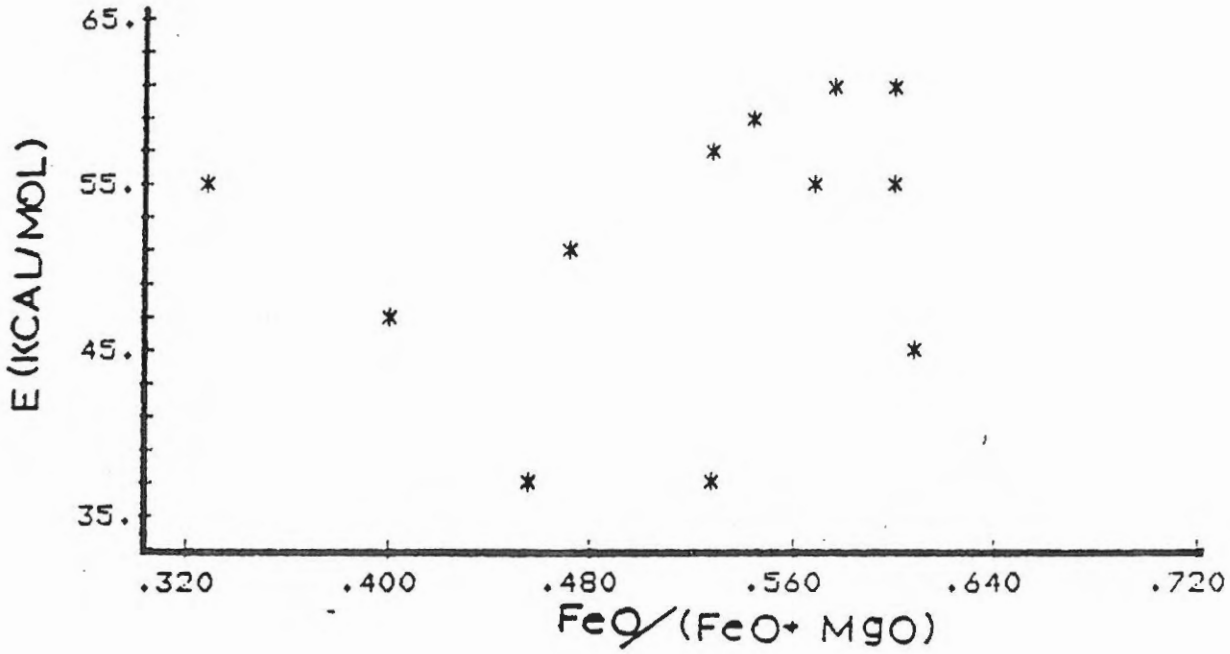
65.
55.
45.
35.
E (KCAL/MOL)
.320
.400
.480
.560
.640
.720
FeO/(FeO+MgO)

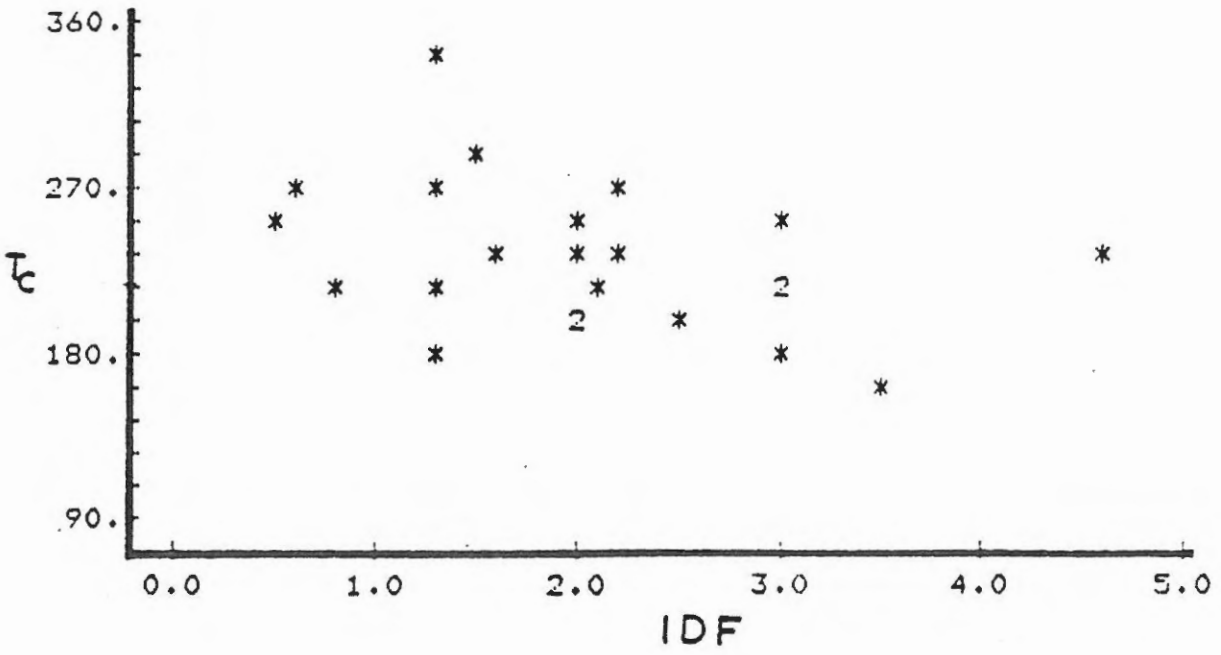
360.
270.
180.
90.
0.0
1.0
2.0
3.0
4.0
5.0
IDF

Foland, 1974). Polymorphic inversion and homogenization of perthitic microcline may occur over a wide temperature range (section 3.5). The same is true for dehydration and delamination of micas (e.g. Gerling et al., 1966). To avoid complicatons associated with possible phase changes, the following criteria are adopted for derivation of activation energy from the slope of the Arrhenius plots: (1) Points on the curve, corresponding to temperatures above 850 degrees are omitted. (2) The straight line portion of the curve below 850 degrees must be defined by at least four points.

3.9.2. MUSCOVITE

Of the 8 muscovite samples on which diffusion experiments were performed, all satisfied the criteria listed in section 3.9.1. They gave closure temperatures ranging from 180+/-25 degrees C to 320+/-25 degrees C, with an average of 234 +/- 33 degrees C. Results are displayed in Table 3-3. Activation Energies vary from 36+/-4 kcal/mol to 64+/-7 kcal/mol, giving a mean of 47+/-6 kcal/mol.

These values are significantly lower than others derived elsewhere by other methods. The average closure temperature is about 33% less than that estimated for muscovite deduced from metamorphic facies temperatures (Purdy and Jager, 1976). The average activation energy is 49% lower than that reported by Gerling (1984, technique not

described). The average value is only 14% lower than that derived by Brandt and Voronovskiy (1967, technique not described). Although the coarsest sample (PE84-54B) gave the highest T_C, there is no clear correlation between grain size and closure temperature. This implies either that diffusion was not by volume diffusion, or that the effective diffusion radius was smaller than the smallest grain size used. Very little is known about the effective diffusion radius for muscovite, but the value for biotite is thought to be about 200 um (Harrison et al., 1985). All of the muscovite samples were coarser than 200 um.

3.9.3. BIOTITE

Diffusion experiments were performed on 28 biotite samples. Eighteen satisfied the criteria listed above for an acceptable straight line on the Arrhenius plot. These samples produced closure temperatures ranging from 155 +/- 40 degrees C to 320 +/- 40 degrees C. The average value is 233+/-35 degrees C. Activation energies range from 34 +/- 5 to 72 +/- 14 kcal/mol, with a mean of 58 +/- 8 kcal/mol. The mean closure temperature is 32% lower than that obtained by Berger and York (1981) for biotite samples analysed under similar conditions. The mean activation energy is 27% lower for the same samples. Harrison et al., (1986) found a strong positive correlation between activation energy and the phlogopite content of biotite. Fig 3-8 shows a plot of

activation energies vs Fe/(Fe+Mg) for twelve biotite samples in this study. The correlation is poor (r=0.498), and opposite to the findings of Harrison et al., (1985). The rank correlation coefficient between T_c and IDF is r = -0.408. A significant correlation for 18 samples at the 95% confidence level should give $-0.399 < r < +0.399$ (Lewis, 1984). This weak, but significant correlation suggests that the same processes which produce discordance in biotite age spectra also contribute to lowering of the apparent T_c.

3.9.4. K-FELDSPAR

Diffusion experiments were performed on 8 K-feldspar samples. They are intermediate to maximum microcline (section 4.4). Since K-feldspars are often perthitic on a fine scale, they have been modelled as sheets by some investigators (e.g. Harrison and McDougall, 1982). This model would be applicable only if diffusion occurs perpendicular to the perthite lamellae. Should diffusion proceed parallel to the lamellae, the cylindrical model would apply. Both models were tried and the results compared.

Five K-feldspar samples satisfied the criteria for the sheet model. The average activation energy is 22 +/- 4 kcal/mol. Corresponding closure temperatures range from -23 degrees C to 150 +/- 45 degrees C. Four samples satisfied the criteria for the cylindrical model. Activation energies

are similar to those of the sheet model (21 +/- 3 kcal/mol). Closure temperature ranges from 30 +/- 30 degrees C to 70 +/- 30 degrees C.

Although the derived activation energies for microcline are quite uniform, they are about 30% lower than that calculated by Harrison and McDougall, (1982). The derived values for E are, however, quite similar to those obtained by Evernden et al., (1960), using the vacuum step heating technique, and assuming spherical geometry. The closure temperatures obtained for microcline by both models show too much variation to be considered reliable.

3.9.5. SUMMARY

Although these experiments seem capable of yielding consistent values for activation energies for microcline, (cf Harrison and McDougall, 1982), this is not so for micas. The derived closure temperatures show very wide and apparently unsystematic variation. The apparently low values for closure temperature cannot be accounted for simply by the slow cooling rate assumed (1 degree/Ma). For instance, a tenfold increase in the assumed cooling rate for biotite sample PE84-100 results in a 9% increase in T_c (from 230 to 250 ^{o}C). An assumed cooling rate of 100 degrees/Ma produces a T_c of 270 degrees C, 17% higher than that at 1 degree/Ma. Very large differences in assumed cooling rate would be required to produce uniform values for T_c. The

similarity in ages between hornblende and biotite from adjacent outcrops in the White Rock Formation (section 4.2.5.2), suggests that the cooling rate in the interval between the closure temperatures of these two minerals was substantially greater than 1 degree/Ma. From the calculations on sample PE84-100, it can be inferred that the derived average T_C for muscovite and biotite would be about 9-19% higher (i.e. 254 - 273 ^{o}C) if more realistic cooling rates (10-100 degrees/Ma) are adopted.

One of the boundary conditions of diffusion experiments is that the initial distribution of the diffusant be uniform in structurally equivalent sites. Apparently this boundary condition was not met (cf. section 3.4). As shown in Chapters 1 and 4, the Meguma terrane experienced at least one episode of tectonothermal overprinting. This may have caused sufficient lattice distortion to the samples to render them unsuitable for diffusion experiments. The selected lower portion of the curves may have been affected by loosely held argon (section 3.4), and not reflect diffusion behaviour that can be generally applied to these minerals.

CHAPTER 4

DATA BASE AND REGIONAL INTERPRETATION

4.1. GENERAL INTRODUCTION

This study records apparent ages ranging from 413 Ma to 170 Ma. An attempt is made in this chapter to interpret these data in the context of the geologic framework described in Chapter One. For convenience, data from the Regional Metamorphic Terrane (RMT) and the Southern Satellite Plutons (SSP) are treated separately. Each pluton is evaluated individually, after which the total data base is assessed. The implications of data from apatite fission track and K-feldspar ^{40}Ar-^{39}Ar analyses are also discussed. The inter-step errors on ^{40}Ar-^{39}Ar age spectra are as quoted on the summary sheets (Appendix A). They are 1s values (see below), and do not include a contribution from the standard. The 1s error for intralaboratory comparison of sample ages is 1%. This includes the uncertainty in J, (.7%). For comparison with ages obtained elsewhere, the estimated 1s error is 2%. This includes the uncertainty in the age of the standards. The 1s error on fission track ages are as

quoted in table 4.4-2. They were obtained by an error propagation technique which takes into account uncertainties in the counting procedure, the age of the standard, and the value of Zeta (Chapter 2). Absolute age estimates of stratigraphically dated units are based on the GSA time scale of Palmer, (1983).

To facilitate discussion, appropriate values for closure temperatures must be selected. Since no reliable values were derived from this study (Chapter 3), estimates will be taken from data published elsewhere.

(a) Hornblende: As stated in Chapter 2, estimates for hornblende closure temperature vary considerably, depending on assumed cooling rate, grain size, and experimental technique. Harrison (1981) calculated a closure temperature of 490-578 degrees C for hornblende with assumed cooling rates of 5-500 degrees/Ma. This calculation was based on observed gas loss in a contact aureole, as well as hydrothermal diffusion experiments. No significant difference was observed between hornblendes of contrasting Fe/(Fe+Mg) ratios, (.72, .36). Although this conflicts with predictions from vacuum experiments (e.g. Gerling et al., 1966), the close correspondence between data derived from laboratory and field observations, gives some reliability to the calculations of Harrison (1981). A value of 500 degrees C is here adopted. This corresponds to a cooling rate of about 5 degrees/Ma, and is similar to the closure temperature suggested by Dallmeyer (1978) from comparison

with metamorphic assemblages.

(b) Muscovite: Few studies have been done on the closure temperature of muscovite. Diffusion experiments suggest that it has activation energies similar to biotite (e.g. Brandt and Voronovskiy, 1967). The only available estimate is 350 degrees C (Purdy and Jager, 1976), which suggests that muscovite is slightly more retentive of argon. This value is tentatively adopted.

(c) Biotite: Of the various estimates for biotite closure temperature, most are very close to the value of 300 degrees C, suggested by Purdy and Jager (1976, see section 2. 6. 3). This value will be used in this study. The annealing temperature for fission tracks in apatite is assumed to be 100 degrees C (Naeser, 1979). Although this value may vary slightly with assumed cooling rates, it has been derived both from laboratory annealing experiments, and observations in geothermal fields. The closure temperature for K-feldspar is discussed in section 4. 4.

The following abbreviations are used in this Chapter.

SMB = South Mountain Batholith.

SSP = Southern Satellite Plutons

RMT = Regional Metamorphic Terrane

tT = Incremental Total Gas Age

IDF = Incremental Total Gas Discordance Factor (Chapter 3).

CS = Compound Sigma (Chapter 3)

s = 1 sigma (error at 99% confidence level).

2s = 2 sigma, (error at 95% confidence level).

F/FM = [total Fe]/[total Fe + Mg] (atomic %).

Ti/Al(iv) = Ti/[tetrahedral Al] (atomic %).

4.1.1. THE POSSIBLE ROLE OF EXTRANEOUS ARGON IN THE MEGUMA TERRANE

Before any evaluation is made of ^{40}Ar-^{39}Ar data, the possible contribution of excess argon should be assessed. Extraneous argon can be derived from two sources: (a) inherited argon, and (b) excess argon. Inherited argon is that portion which was generated in the sample prior to the event being dated. For example, detrital micas in a slate sample may contain inherited argon from some event prior to deposition. The term "excess argon" means argon that was trapped in the mineral, other than that which is produced by in situ decay of ^{40}K. Early research (e.g. Lanphere and Dalrymple, 1976) suggested that extraneous argon resides in special sites within the mineral lattice. These sites were expected to release argon in a fashion which produces characteristic patterns in their spectra. Intermediate temperature steps in the spectra produce relatively low apparent ages, resulting in 'saddle shaped' depressions. The conclusions of Lanphere and Dalrymple (1976) were based on one phlogopitic biotite, one plagioclase, and two pyroxene samples. Lanphere and Dalrymple also cited

examples of saddle shaped spectra from whole-rock basalt samples suspected of containing excess argon. Later studies (e.g. Harrison and McDougall, 1981; Harrison and Fitzgerald, 1986) suggest that the shape of spectra from plagioclase, pyroxenes, and amphiboles can be affected by complex exsolution features. It was suggested by Harrison and McDougall (1981) that the complexity of these minerals permit excess argon and radiogenic argon to occupy separate sites, which outgas separately. Such behaviour is, however, possible only if the exsolution features are preserved during step-heating. There is much uncertainty about this problem (section 3. 5). Other studies on biotites suspected to contain excess argon have produced spectra which are nearly flat for most of their release pattern (eg. Pankhurst et al., 1973; Roddick et al., 1980; Dallmeyer and Rivers, 1982; Foland, 1983). Furthermore, it has been shown that biotite samples which suffered ^{40}Ar loss by an overprinting event produce saddle - shaped spectra (Berger, 1975; Dallmeyer, 1975; Reynolds et al., 1981; Dallmeyer, 1982). It therefore appears that the saddle-shaped feature is not a reliable indicator of excess argon, at least for biotite. The probability of the occurrence of extraneous argon in a given terrane is best assessed by inference from its geologic constraints, instead of simply relying on the shape of individual spectra.

The geologic constraints within which this study is undertaken are outlined in Chapter 1. On the basis of

fossil evidence, the Halifax Formation, from which most of the slate and mica samples were taken, was deposited during the Tremadocian, about 500 Ma ago (Cumming, 1985). Fossil evidence also suggests that the depositional age of the youngest pre - metamorphic unit, the Torbrook Formation, is Siegenian to Emsian, about 395 Ma ago (Jensen, 1976). The regionally metamorphosed rocks were intruded by the SMB, producing hornfelses which overprint the regional fabric (Reynolds et al., 1973). Since the SMB is 372-361 Ma old (Clarke and Halliday, 1980), timing of regional metamorphism appears to be constrained between 372 and 395 Ma. Conceivably, this "window" could be wider if regional metamorphism was initiated prior to deposition of the Torbrook Formation. During regional metamorphism, the most likely source of extraneous argon would be detritus within the Halifax and underlying Goldenville Formations. The 'crustal residence' age of these two formations is 1773 +/- 95 Ma (Clarke and Halliday 1985). Detrital components with inherited argon (e.g. white mica) would lead to anomalously high ages for samples from the lowest grades (slates). Such components are likely to be completely outgassed at metamorphic temperatures prevailing at the biotite zone or higher. Substantial partial pressures of excess argon from these sources would result in ages much greater than 395 Ma. None of the samples dated in this study show ages (tT) above 406Ma, except for one poorly defined hornblende age of 413 Ma (section 4.2.3). It may be concluded that, except for

possibly some slate samples, inherited argon very likely did not affect any of the Meguma terrane samples. In all cases where mineral pairs were dated, apparent ages were similar, or in the order expected from estimated closure temperatures. Apparent ages of a few samples are 390 - 406 Ma. Since the estimated uncertainty in these ages is 2% (8 Ma), they seem reasonable within the stratigraphic constraints listed above. While these constraints rule out the influence of major amounts of excess argon, they cannot exclude the possibility of minor local contamination. Because pegmatites probably crystallize under high fluid pressures (e.g. Jahns and Burnham, 1969), samples from them may contain excess argon. Since amphiboles analysed in this study contain less than .5 wt% K_2O, even minor amounts of excess argon would result in anomalously high ages. Individual cases are examined below.

4.2. DATA BASE AND INTERPRETATION FROM THE REGIONAL METAMORPHIC TERRANE

4.2.1. INTRODUCTION

The RMT consists of three stratigraphic units: (1) the Goldenville Formation, which consists of metapsammites and minor metapelites; (2) the Halifax Formation, which is made

up dominantly of metapelites; and (3) the White Rock Formation, which consists of quartzites, metavolcanics, and minor metapelites. Metamorphic grade ranges from lower greenschist to upper amphibolite facies. Zone boundaries have been drawn by Keppie and Muecke (1979). These are shown on Map 1.

Three amphibole and thirty-nine mica samples from the RMT were dated by the ^{40}Ar-^{39}Ar method. One sample was dated by the apatite fission track technique. To facilitate evaluation, the samples are divided into five groups: (a) slates; (b) amphiboles; (c) older micas (d) younger micas; (e) apatite fission track. The dividing line between older and younger micas is taken as 360 Ma, the approximate age of the youngest phase of the SMB. Since intrusion of the SMB marks a major tectonothermal event in the Meguma terrane, which partly or completely reset some metamorphic ages (Reynolds and Muecke, 1978), the 360 Ma line is considered a reasonable choice. Any RMT ages younger than 360 Ma cannot be attributed simply to outgassing during the SMB intrusive event.

4.2.2. SUMMARIZED GEOLOGY OF THE RMT

As stated in Chapter 1, the Meguma terrane consists dominantly of flyschoid metasediments (Goldenville and Halifax Formations), with minor volcanics (Map 2). Although deformation is locally complex, rocks within the Halifax and

Goldenville Formations display a principal NE to NNE trending foliation (S_2), associated with folding during the Acadian orogeny (e.g. Keppie, 1977). The foliation is more pronounced in the metapelitic units, where it is defined mainly by parallel orientation of muscovite and lenticular quartz. Generally, porphyroblasts of biotite, staurolite, andalusite, cordierite, and sillimanite are weakly aligned with S_2, or randomly overgrow it. These features indicate that regional metamorphism was late syn- to post-tectonic with respect to regional deformation (e.g. Taylor and Schiller, 1966; Chu, 1978; Muecke, 1984).

Metamorphic grade ranges from lower greenschist to upper amphibolite facies. Details have been described by several authors (e.g. Taylor and Schiller, 1966; Chu, 1978; Sarkar, 1978; Cullen, 1983; Muecke, 1984). Keppie and Muecke (1979) defined the following metamorphic zones in the Meguma Terrane: (1) Chlorite zone (2) Biotite zone (3) Garnet zone (4) Staurolite-andalusite-cordierite zone, and (5) Sillimanite zone (Map 1). Metamorphic conditions were of low-pressure type, with pressures less than 4 kbars (Chu, 1978; Cullen, 1983; Muecke, 1984). This corresponds to a depth of 10-15 km, and is summarized in table 4.2-1 and fig. 4.2-1.

Retrograde metamorphism in the Meguma Terrane has been noted by previous workers (e.g. Taylor and Schiller 1966; Cullen, 1983). The mineral assemblages produced include chlorite, muscovite, epidote, and albite. The regional

Table 4.2-1. Estimates of metamorphic temperatures and pressures in the Meguma terrane (courtesy, G.K. Muecke).

MEGUMA METAMORPHISM

ZONE	T RANGE	PRESSURE
CHLORITE	300-430C	~2.5-3 KB
BIOTITE	430-470C	~3 KB
GARNET	470-520C	
ANDALUSITE, STAUROLITE, CORDIERITE	520-600C	~3 KB
SILLIMANITE	600-650C	3 KB MAX.

Fig. 4.2-1.

Diagram illustrating P-T conditions of regional metamorphism in the Meguma terrane.

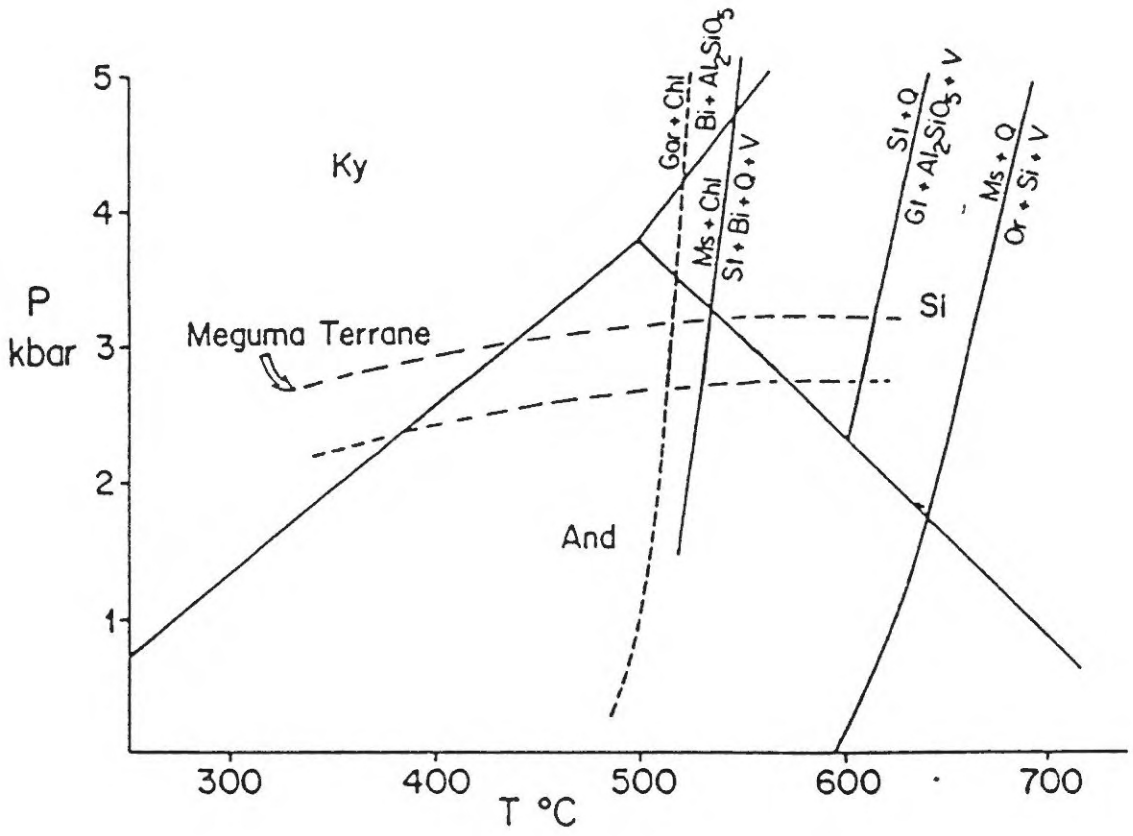
5
4
3
2
1
P
kbar
Ky
And
Si
Meguma Terrane
Gar + Chl
Bi + Al2SiO5
Ms + Chl
Si + Bi + Q + V
Si + Q
Gl + Al2SiO5 + V
Ms + Q
Or + Si + V
300
400
500
600
700
T °C

extent of this event is still poorly documented. Recent studies suggest such alteration is not only common in the metamorphic rocks, but is characteristically associated with economically important mineralization. Most of the documented domains of alteration are within or close to plutons (e.g. Chatterjee and Keppie, 1981; Richardson et al., 1982; O'Reilly et al., 1985; Zentilli and Reynolds, 1985). In many cases the alteration is associated with ductile shear zones that post-date plutonism and regional metamorphism. It is very likely that domains of post-metamorphic shearing and alteration observed in the plutons (see below) are more widespread in the RMT than previously realized. Observations by the author suggest that such a domain exists immediately south of the Shelburne and Barrington Passage plutons (fig. 4.2-2). A preliminary report by Hwang and Williams (1985) indicates that the domain was subject to a complex tectonothermal history. They identified ductile shear zones up to 100m wide. Where retrograde metamorphism is most advanced, the assemblage biotite - staurolite - cordierite - plagioclase - quartz has been replaced by an aggregate of chlorite, muscovite, quartz, albite and minor tourmaline (e.g. fig. 4.2-3). Most samples were selected from areas where visible effects of shearing and alteration are least severe. The few samples that are strongly sheared or severely altered are discussed in section 4.2.5.5.

Fig. 4.2-2. Location map of 'complex domain' in southwest Nova Scotia.

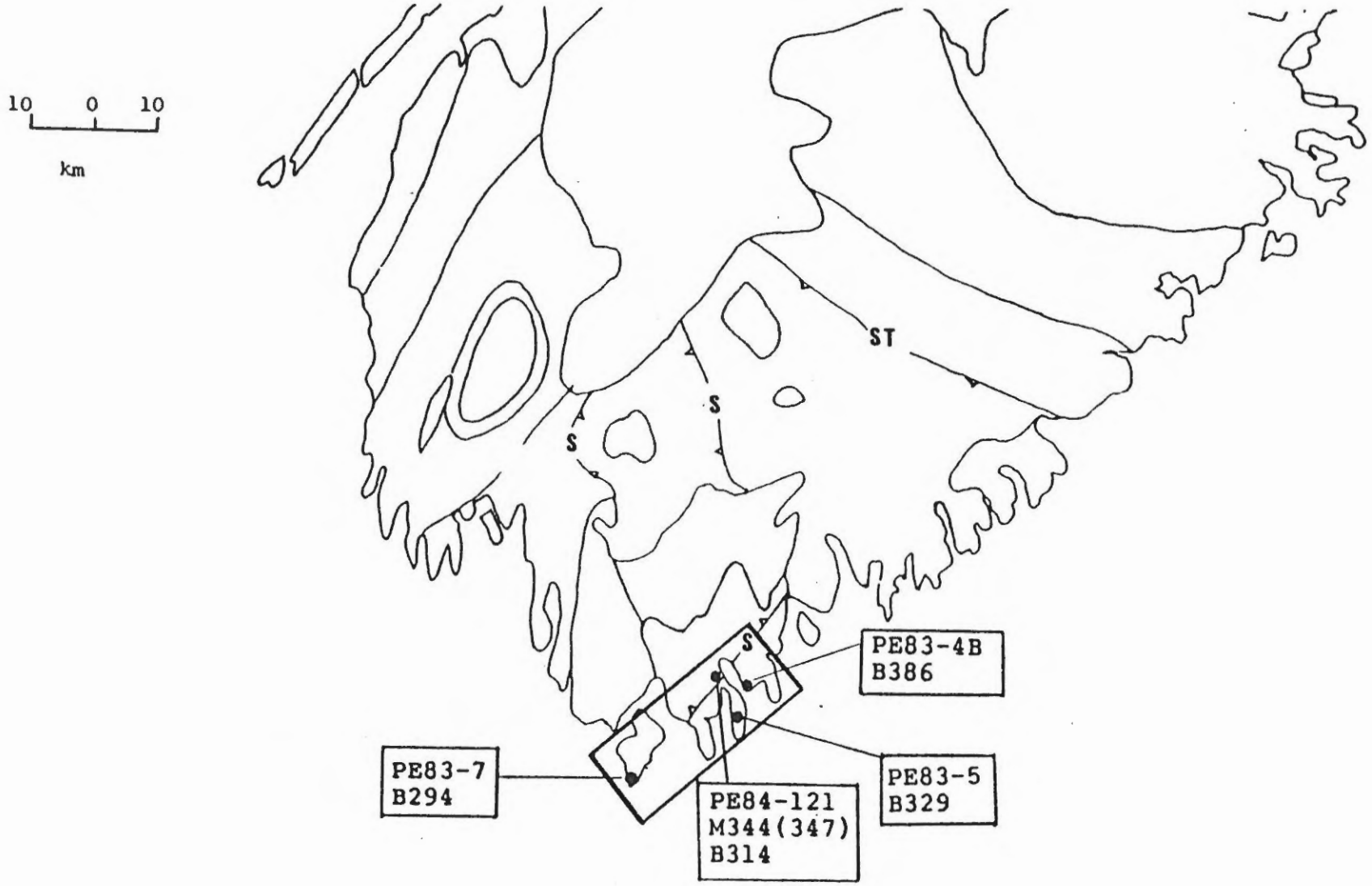
10 0 10
km
ST
S
S
S
PE83-4B
B386
PE83-7
B294
PE84-121
M344(347)
B314
PE83-5
B329

Fig. 4.2-3. Photomicrograph of metapelite from the 'Complex Domain', showing advanced chloritization of biotite. The groundmass is mainly sericite and quartz.

(Sample PE84-120).

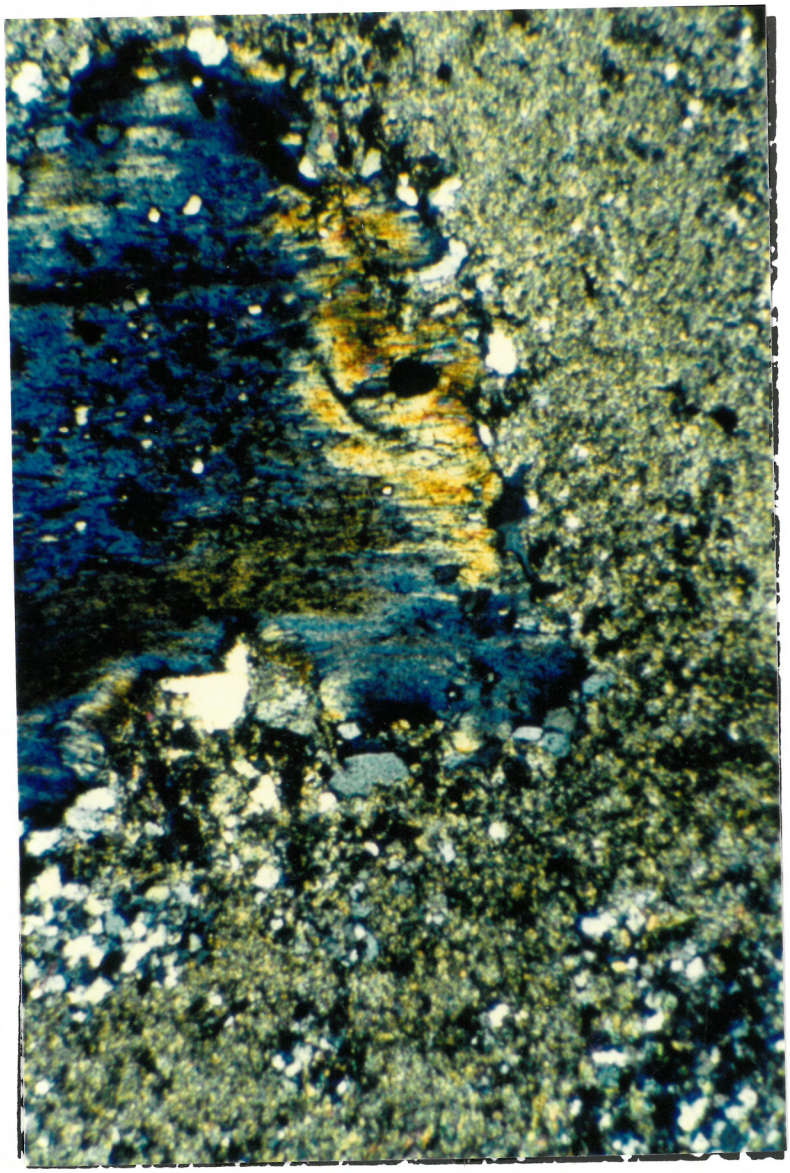

0.5 mm

4.2.3. SLATES

Eight slate/siltstone samples from the Halifax Formation (chlorite zone) were selected from areas where contact effects of the granitoid intrusions seemed minimal. Sample locations are shown in fig. 4.2-4. Data are displayed in table 4.2-2 and fig. 4.2-5.

Three of the samples (NS71-139, NS72-31, NS72-33) are replicates of samples previously analysed (Reynolds et al., 1973; Reynolds and Muecke, 1978). The analyses were repeated to obtain greater resolution in the spectra, and to calibrate the slate ages against the international standard flux monitor MMhb-1. A greater number of standards were included in the irradiation canister to reduce the uncertainty in J (from 1s = 2% to .7%). All three are fissile slates from the chlorite zone with white mica 10 to 30 um in diameter. The mica/quartz ratio of sample NS71-139 is about 2:1, whereas that of the other two is about 3:1. Samples NS72-31 and NS72-33 were obtained from locations about 3km from the SMB contact, whereas sample NS71-139 was located about 10 km from the SMB contact. In the order listed above, apparent ages (tT) from the present study (406, 390, 384 Ma) agree within analytical uncertainty with the conventional K-Ar ages (397, 392, 382 Ma, Reynolds et al., 1973). This suggests that no significant amounts of ^{39}Ar were lost during irradiation. The ^{40}Ar-^{39}Ar ages of Reynolds and Muecke, (1978) also agree (within analytical

Fig. 4.2-4. Sample location for slates.

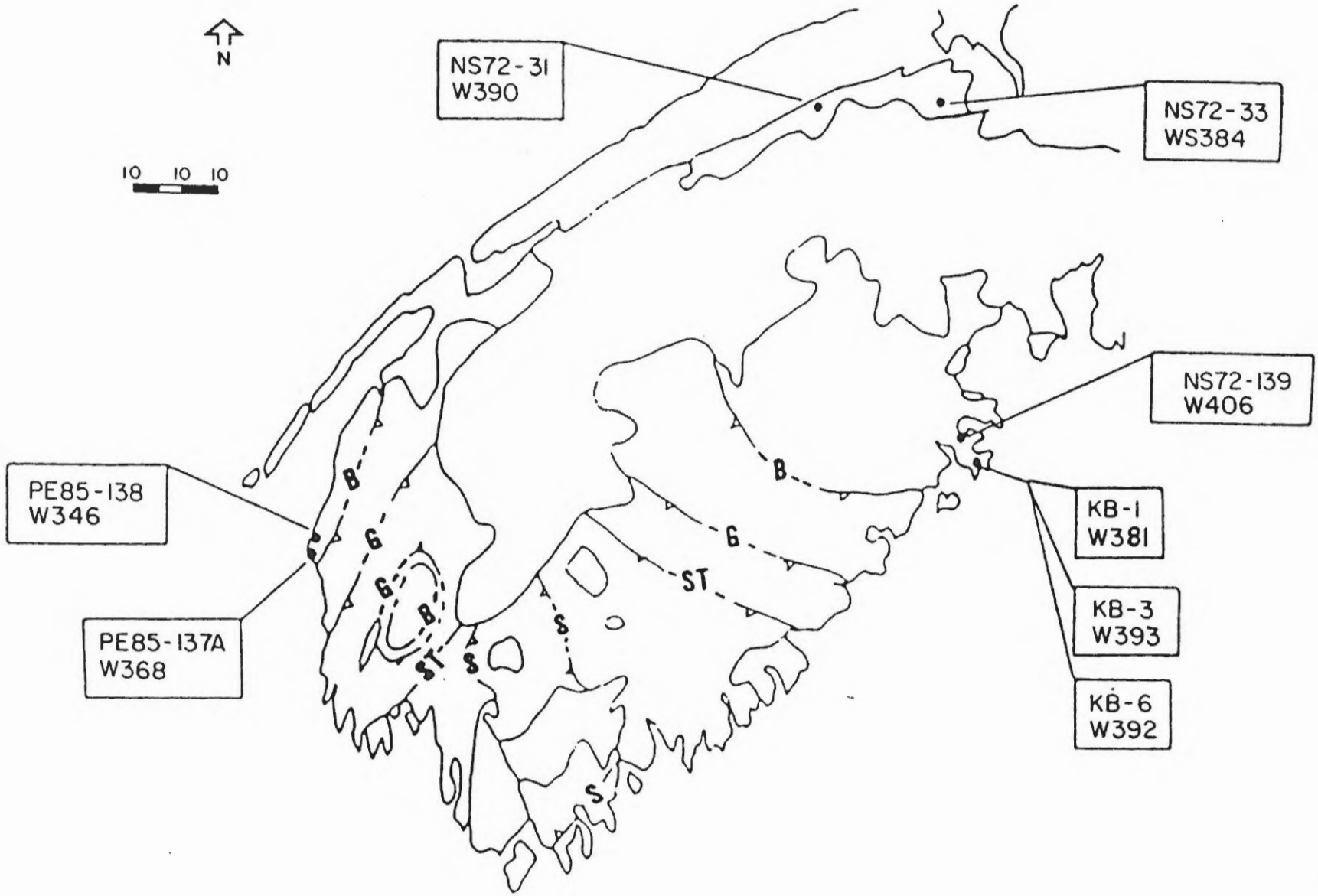
N
10 10 10
NS72-31
W390
NS72-33
WS384
NS72-139
W406
PE85-138
W346
PE85-137A
W368
KB-1
W381
KB-3
W393
KB-6
W392
B
G
ST
S

Table 4.2-2. Ages and discordance factors of slates.

SAMPLE	PHASE	AGE (Ma)	IDF	CS	
				Ma	%
NS71-139	Slt	406	3.41	3.9	1.0
NS72-31	Slt	390	4.22	1.8	.5
NS72-33	Slt	384	3.16	1.2	.3
KB-1	Slt	381	2.68	2.2	.6
KB-3	Slt	393	4.53	2.5	.6
KB-6	Slt	392	2.96	8.2	2.1
PE85-137A	Slt	368	10.92	5.2	1.4
PE85-138	Slt	346	7.95	3.8	1.1
NS71-139	Slt	390	3.45	3.9	.9 *
NS72-31	Slt	394	5.36	1.7	.4
NS72-33	Slt	399	2.61	3.4	.9

* Recalculated by Reynolds, 1985, (pers. comm).

** Reynolds and Muecke (1978).

Fig. 4.2-5. Age spectra of slates.
Bars on vertical axes represent 10 Ma.

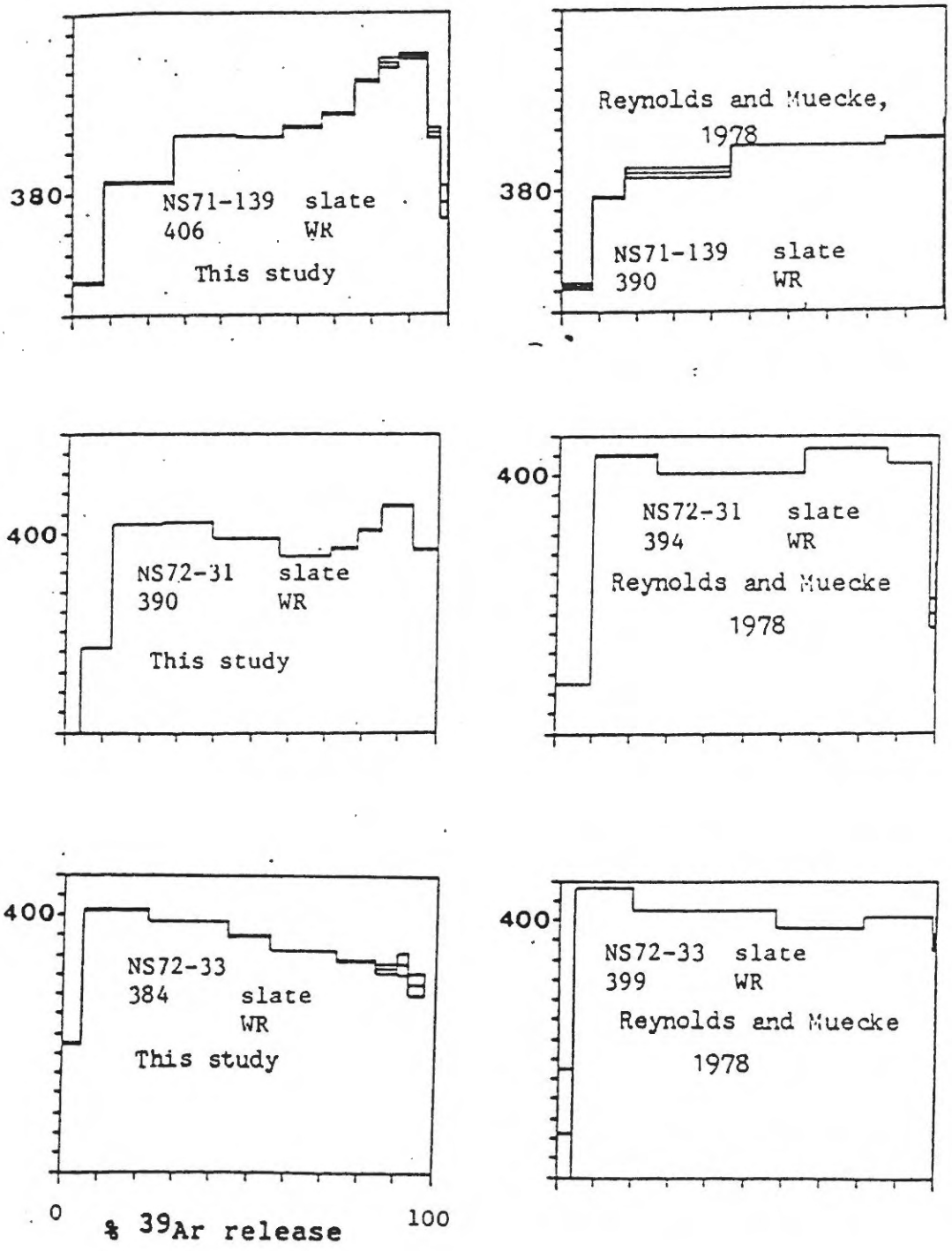
380
NS71-139 slate
406 WR
This study
380
Reynolds and Muecke,
1978
NS71-139 slate
390 WR
400
NS72-31 slate
390 WR
This study
400
NS72-31 slate
394 WR
Reynolds and Muecke
1978
400
NS72-33
384 slate
WR
This study
400
NS72-33 slate
399 WR
Reynolds and Muecke
1978
0
100
% 39Ar release

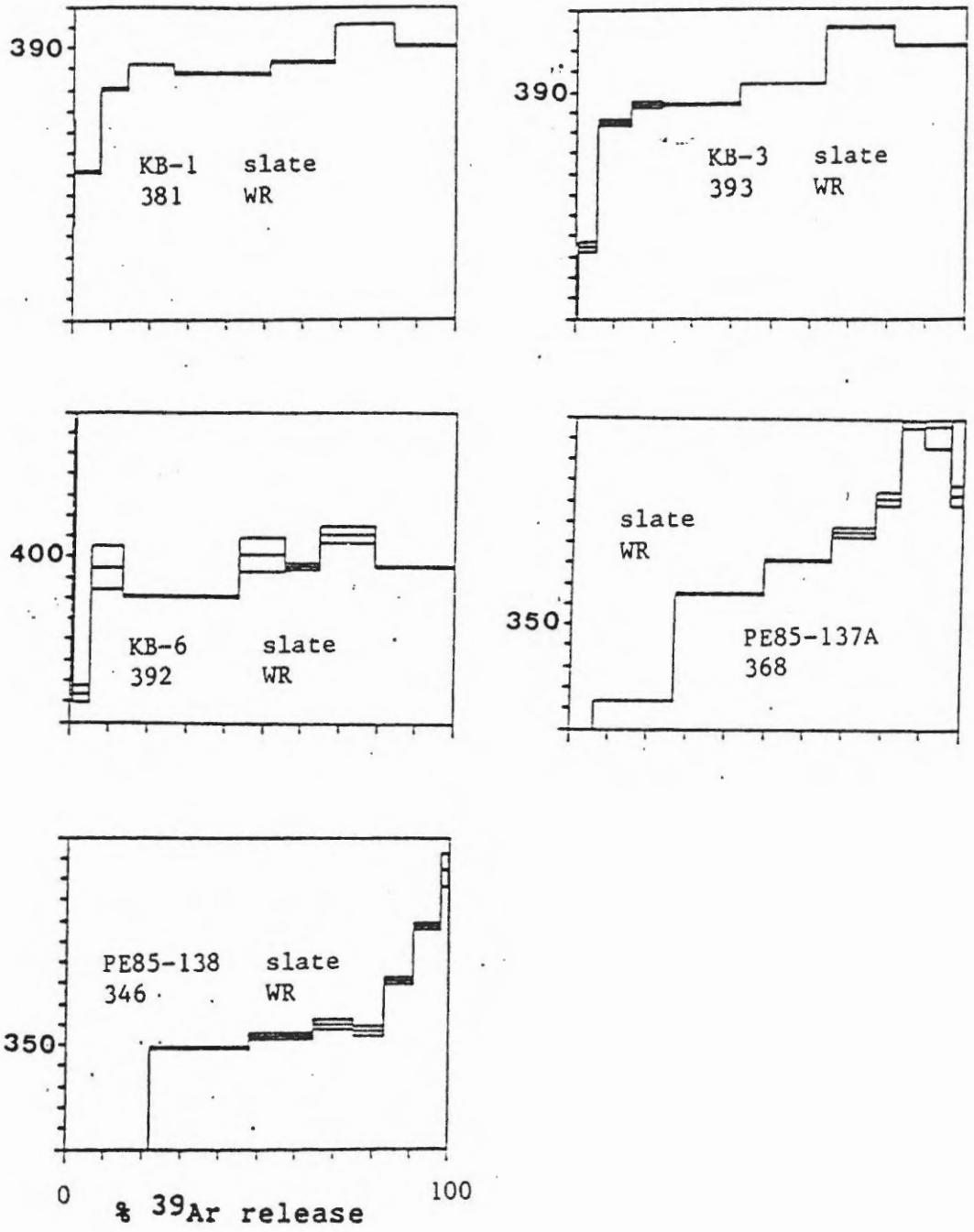
390
KB-1 slate
381 WR
390
KB-3 slate
393 WR
400
KB-6 slate
392 WR
slate
WR
350
PE85-137A
368
PE85-138 slate
346 WR
350
0
100
% 39Ar release

uncertainty), with the conventional K-Ar ages. The discrepancy in age between replicate analyses of samples NS71-139 and NS72-33 (4%) is probably due to improved analytical precision. Spectra from all three samples are highly discordant (IDF=3.16 - 4.22). The 'imperfect plateaus' reported by Reynolds and Muecke (1978), have not been reproduced in the new analyses, possibly because of higher resolution in the new spectra (fig. 4.2-5).

The relative order of discordance, however, has been reproduced (31>139 >33).

Both spectra for sample NS-71-139 display profiles suggestive of partial ^{40}Ar loss (e.g. Turner, 1968). Superficially, the spectra suggest an overprinting event at 330-335 Ma. The maximum ages suggested by the spectra are 405 Ma and 447 Ma respectively. Since the youngest pre-metamorphic unit in the Meguma Terrane (Torbrook Formation) is about 395 Ma, these high ages cannot be regarded as cooling ages (cf. Turner, 1968). It is possible that the high ages represent contributions from an inherited argon component. This is consistent with the greater detrital fraction (lower mica:quartz + feldspar) in this sample, and its slightly higher tT age (406 Ma). Alternatively, the high apparent ages in the high-temperature part of the age spectra may also be due to redistribution of argon isotopes during irradiation, or to the combined effects of recoil and inherited argon.

Three of the samples were collected and analysed by

Savell (1980). They were obtained from two adjacent outcrops at King's Bay, Lunenburg county, where slates grade into siltstones. These three samples reflect that gradation in their mica/quartz ratio and fissility. The samples in decreasing order of fissility and mica/quartz ratio are KB-1 (slate), KB-3 ("silty slate"), KB6 (siltstone). Mica:quartz ratios are approximately 1:1, 0.7:1, and 0.07:1 respectively. White mica ranges in size from 10um to 80um. These samples were analysed to test whether there were any compositional effects on the ^{40}Ar-^{39}Ar systematics of low grade metapelites. Savell (1980) found that siltstones tend to release argon at higher temperatures than more fissile, less silicious slates. The difference in these three samples is, however, quite subtle (Appendix A), but as a group, they seem to release most of their argon at higher temperatures than the other slate samples. This may be partly due to uncertainty in the extraction temperature calibration when these samples were analysed (P. H. Reynolds, 1986, personal comm.). All three spectra are highly discordant (IDF=2.68 - 4.53). Spectra from two of the samples KB-1 and KB-3 display a profile usually associated with partial loss of ^{40}Ar. This possibility cannot be excluded, since the Meguma terrane was affected by at least two later tectonothermal events (Chapter 1). As suggested in Chaper 3, redistribution of ^{39}Ar during irradiation may be responsible for much of the discordance observed. The apparent age of KB-1 is slightly lower (3%),

than those of the other two. This difference is marginally larger than the estimated error in ages (2s=2%). It is possible that this lower age in KB-1 may be due to a greater amount of $^{40}Ar^*$ loss. This is consistent with the greater fissility (greater permeability) of this sample. The loss may have been caused by intrusion of the SMB, as found for other slates in the Meguma terrane (Reynolds and Muecke, 1978).

Samples PE85-137A and PE85-138 were obtained from the chlorite zone in Digby County, over a distance of 5km. White mica is 10 - 30um in diameter in sample PE85-137A and 10 - 60um in diameter in sample PE85-138. Both samples have similar mica/quartz ratios (3:1), but sample PE85-138 displays a distinct crenulation fabric not seen in any of the other slates. This superimposed fabric may be related to observed shearing in the Mavilette gabbroic intrusive 2 km to the east (Calder and Barr, 1982). This fabric illustrates the polyphase nature of deformation in the Meguma terrane, (eg. Fyson, 1966; O'Brien, 1983; Hwang and Williams, 1985). These two samples produced the lowest ages among the slates analysed so far. There is also a sharp difference between the two ages (368 Ma, 346 Ma). The spectra are highly discordant (IDF= 10.92, 7.95), and both display profiles usually associated with ^{40}Ar loss. For sample PE85-137, it is difficult to assign geologic significance to either the lowest age step, 232 Ma or the highest step, 449 Ma. The corresponding ages for sample

PE85-138, 263 Ma and 434 Ma are also difficult to interpret. The apparent ages (tT) of samples PE 85-137A and PE85-138 are 368 Ma and 346 Ma respectively. This age contrast is probably not due to diachronous post-metamorphic cooling. The sharp difference in age (over 5 km) and the textural evidence of a superimposed foliation suggest that the more likely explanation is post-metamorphic ^{40}Ar loss. The effect was more severe in the vicinity of sample PE85-138, which is reflected in its secondary deformation.

In summary, the data from the slates confirm geologic observations and conclusions from previous studies that regional metamorphism occurred prior to the intrusion of the SMB. Two of the samples indicate substantial post-metamorphic ^{40}Ar loss. One of the samples (NS71-139) may be contaminated with inherited argon. The other five indicate an age for regional metamorphism of 381-393 Ma. These data are similar to those obtained from the northeastern section of the Meguma terrane, where whole rock slates and phyllites yielded discordant spectra with tT ages of 384-407 Ma (Keppie et al., 1985).

4.2.4. AMPHIBOLES FROM THE RMT

Three amphibole samples from the RMT were analysed. They are all from the White Rock Formation. This unit conformably overlies the Halifax Formation, and consists of mafic to felsic volcanics, interbedded with quartzites and

pelites, with a maximum thickness of 3km (Sarkar, 1978). Metamorphic grade reaches lower amphibolite facies. Deformation is represented by upright NNE trending folds, strike-slip faulting and local thrusting, some of which post date regional metamorphism (Sarkar, 1978). The three samples were extracted from metabasites about 7 km apart (fig. 4.2-6). The foliation is defined by parallel alignment of amphiboles, biotite, quartz lenses and chlorite. The foliation is strongest in sample PE84-64C and weakest in sample PE83-11. Amphibole is not significantly altered in any of the three samples. In sample PE84-64C, plagioclase is replaced by muscovite. Mild chlorite overgrowth is visible in sample PE84-130. Microprobe analyses reveal that the major element chemical composition of samples PE84-64C is uniform from rim to core (hornblende). Sample PE83-11 is is also uniform, but more actinolitic. Sample PE84-130 shows very little variation in Fe/(Fe+Mg), but appears to be slightly zoned with respect to Al/(Fe+Mg), (fig. 4.2-7). Variations in Ca/K has been discussed in section 3. 7. Chemical analyses are listed in Appendix B.

Amphibole age data are summarized in table 4.2-3 and fig. 4.2-8. The spectrum of PE84-64C shows a staircase pattern characteristic of partial ^{40}Ar loss (Turner 1968, Harrison, 1981). According to this interpretation, the apparent age of the last step (404 Ma) is the closest approximation to the time of cooling through argon retention

Fig. 4.2-6. Sample locations for amphiboles.

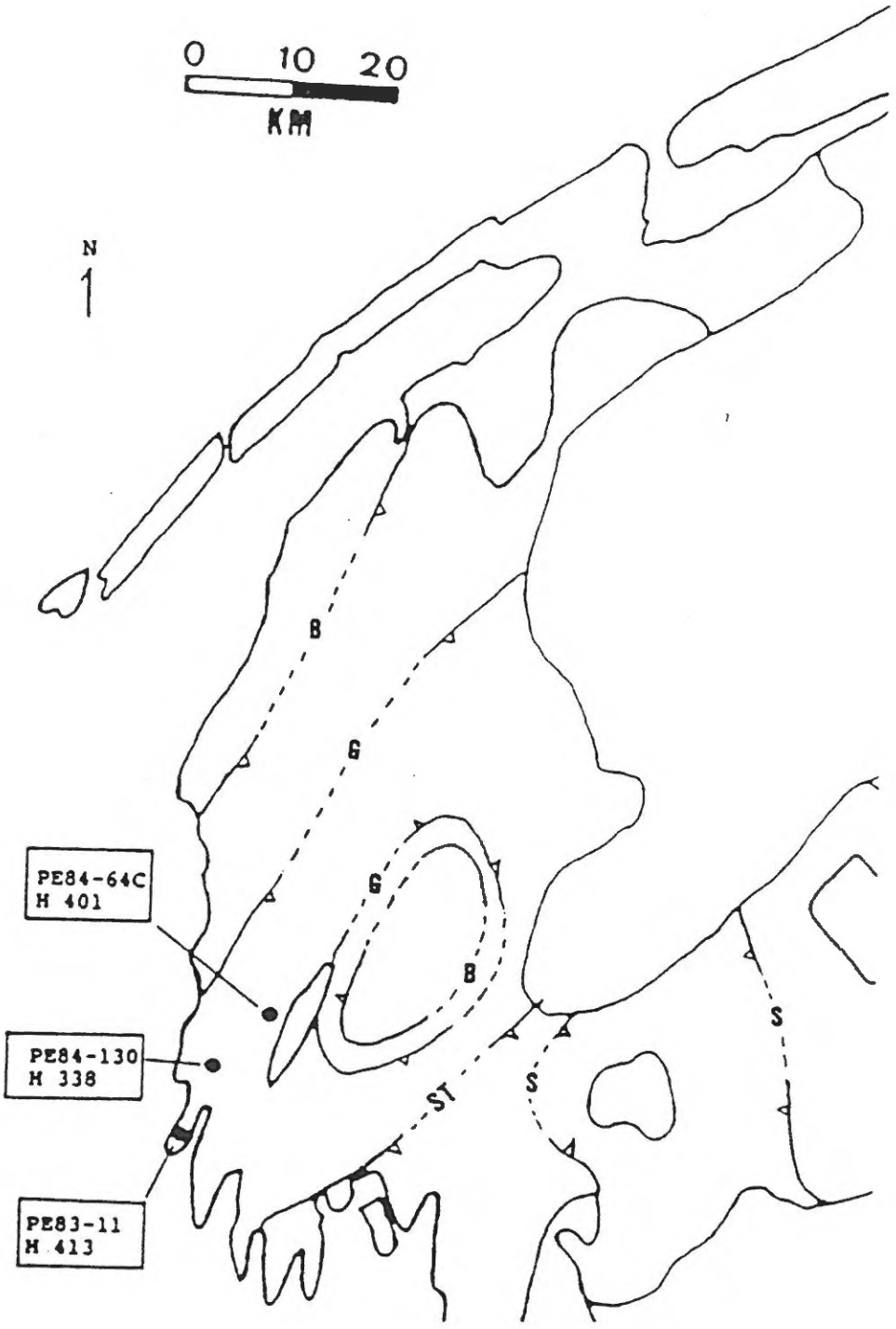
0 10 20
KM
N
1
B
G
G
B
S
S
ST
PE84-64C
H 401
PE84-130
H 338
PE83-11
H 413

Fig. 4.2-7. Rim-to-core analyses of amphiboles from the RMT (11, 64, 130), and the SSP (9, 114).
(a). F/FM. (b). Na/(Na+K). (c). Al/(Fe+Mg).
Note slight variation from rim to core.

(atomic ratios).

Analyses were spaced about 25 micrometers apart.
Vertical bar represents estimated analytical uncertainty.

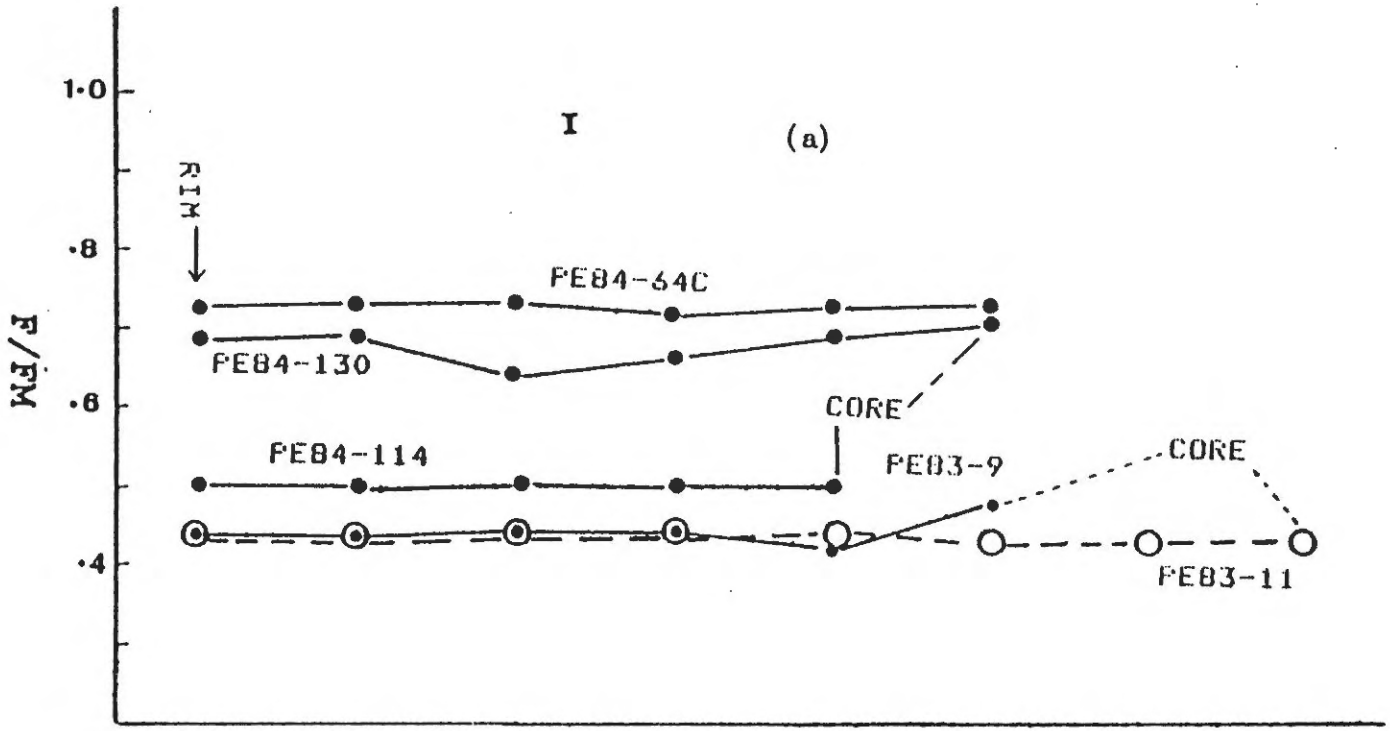
I
(a)
1·0
·8
·6
·4
F/FM
RIM
PE84-64C
PE84-130
CORE
PE84-114
PE83-9
CORE
PE83-11

(b)

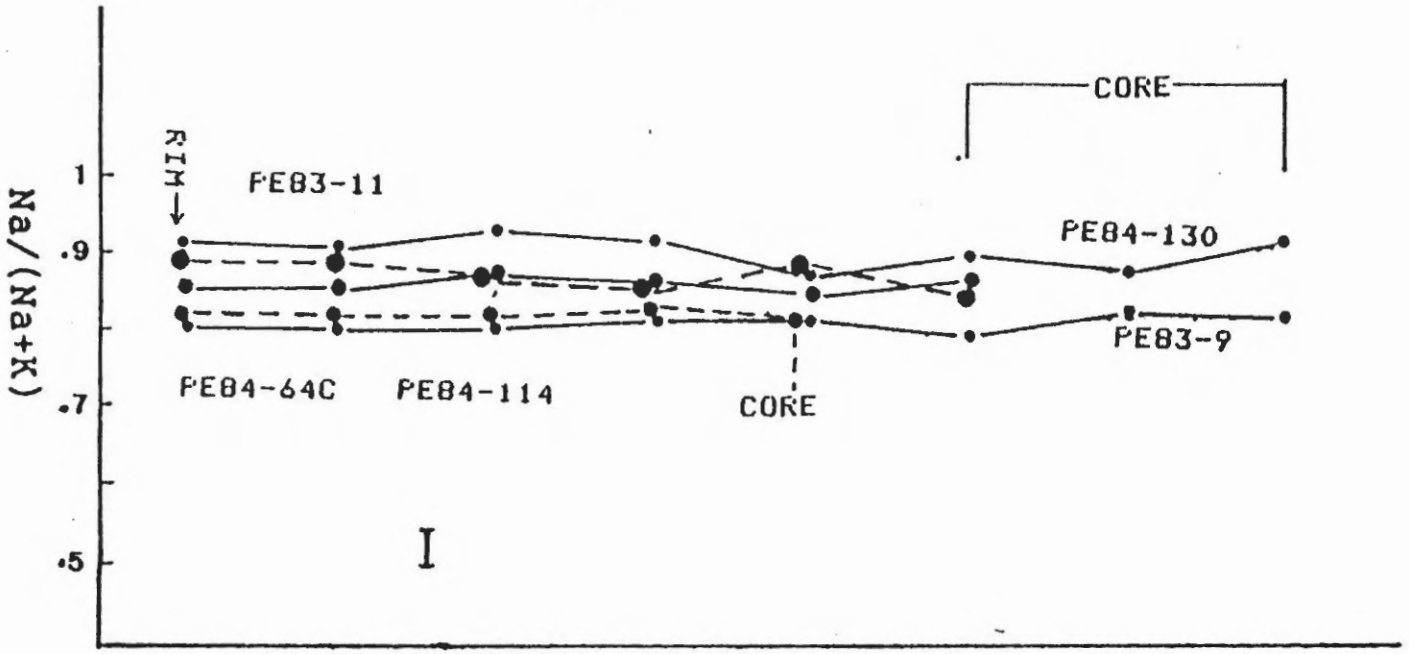
CORE
RIM
PE83-11
PE84-130
PE83-9
PE84-64C
PE84-114
CORE
Na/(Na+K)
1
.9
.7
.5

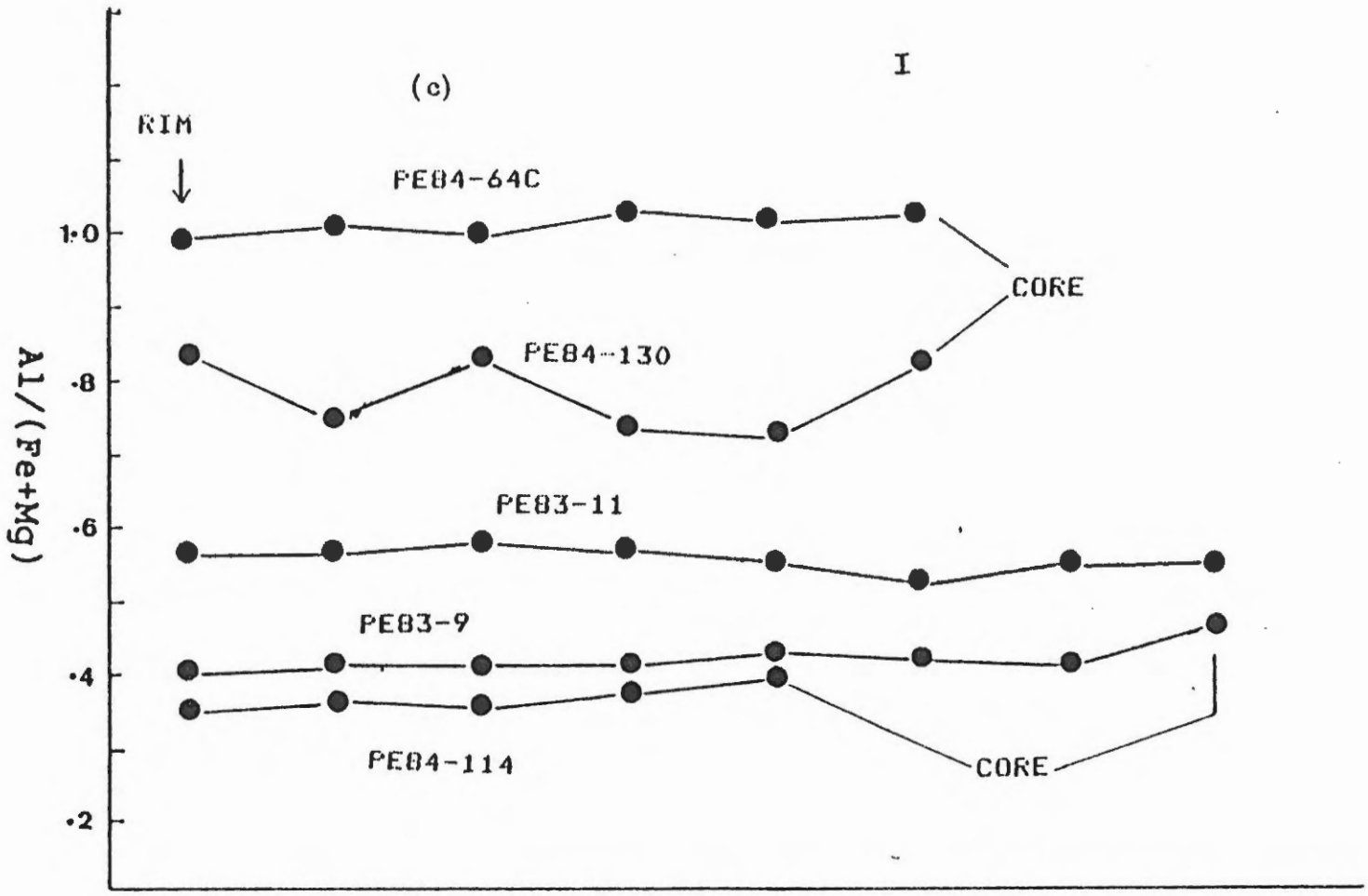
(c)
I
RIM
PE84-64C
CORE
PE84-130
PE83-11
PE83-9
PE84-114
CORE
Al/(Fe+Mg)
1·0
·8
·6
·4
·2

Fig. 4.2-8. Age spectra of amphiboles from the RMT. Bars on vertical axes represent 10 Ma.

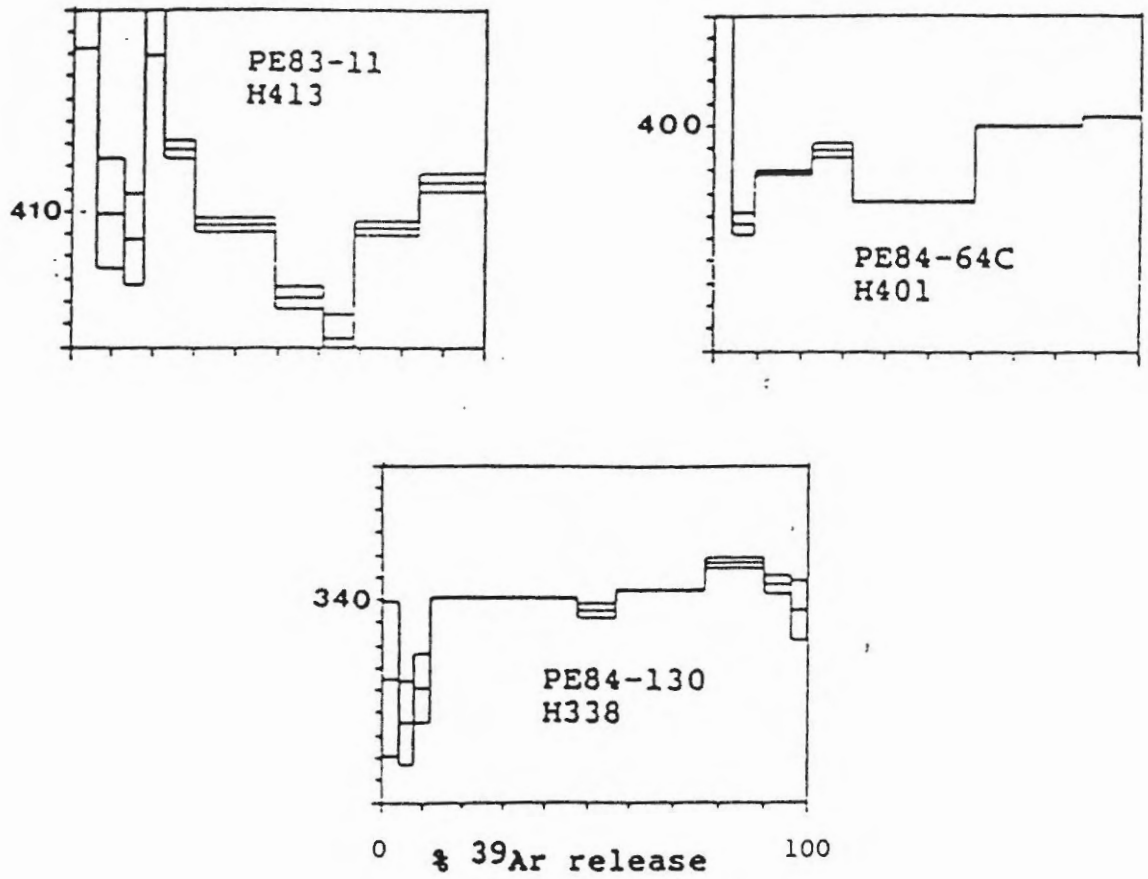

Table 4.2-3.
Ages and discordance factors for Amphiboles from the RMT.

SAMPLE	AGE (Ma)	IDF	CS	
			Ma	%
PE83-11	413	6.48	17.1	4.1
PE84-64C	401	7.97	4.0	1.0
PE84-130	338	3.08	9.9	2.9

temperatures in this mineral. This age is slightly older than that inferred from the slate data (section 4.2.3) for timing of regional metamorphism in the Meguma terrane. This age is also slightly older than that permitted by the stratigraphic constraints listed above. The discrepancy may be accounted for by the uncertainty in the age, (2s = 8Ma), or minor contamination with excess argon. The low temperature part of the spectrum (time of ^{40}Ar loss), is not well defined. The anomalously high age of the first step may be ascribed to minor excess argon or ^{39}Ar loss.

The spectrum of sample PE83-11 is highly discordant, with a very pronounced saddle. According to the model of Lanphere and Dalrymple (1976), this feature is indicative of excess argon (section 4.1.1). The cooling age indicated by the minimum in the saddle (353 Ma), is an unreasonably low estimate of the metamorphic cooling age. It is possible that this spectrum reflects ^{40}Ar loss on an excess argon profile (e.g. Harrison and McDougall, 1980b). The tT age of 413 Ma is poorly defined (CS = 4%), but is only slightly higher than that of sample PE84-64c, consistent with the suggestion of minor excess argon contamination.

The spectrum for sample PE84-130 displays a profile which resembles that associated with partial ^{40}Ar loss. The age maximum on the profile is 356 Ma, while the minimum is poorly defined, but close to 300 Ma. The age maximum clearly does not correspond to the time of regional metamorphism defined by any other sample. It is interpreted

as a lower limit to the cooling age, as would be expected if the sample suffered substantial ^{40}Ar loss during an overprinting event. This can explain the low tT age of 338 Ma.

If allowance is made for minor contamination by excess argon, ages from samples PE84-64C and PE83-11 are in agreement with the slate data: regional metamorphism occurred slightly before intrusion of the SMB. The apparent ^{40}Ar loss suffered by sample PE 84-130 is not reflected in any major chemical or physical difference between it and the other two samples. The sharp age contrast over a distance of 7 km, indicates that the overprinting event was of varying intensity. This is consistent with findings elsewhere in the Meguma terrane (e.g. section 4.2.3).

4.2.5. MICAS FROM THE REGIONAL METAMORPHIC TERRANE

Micas were extracted mainly from metapelites of the Halifax and White Rock Formations. A few samples were obtained from metapsammites and metabasites of the Goldenville and White Rock Formations respectively. Thirty-one samples were obtained from the following metamorphic zones of Keppie and Muecke (1979): biotite (11), garnet (7), staurolite-andalusite- cordierite (9), and sillimanite (4). In addition, one phlogopite (see below), and seven muscovite samples were obtained. The distribution

is shown in figs. 4.2-13 and 4.2-16. Two samples, PE84-97 and MC-1, included in the study, are not from the above formations. The phlogopite sample (PE84-97, Ann=16.5%) was obtained from a massive peridotite about 300 m^2 in area, in which phlogopite replaces orthopyroxene. The contacts with the country rocks are not exposed, but the massive nature suggests that intrusion was post-tectonic with respect to S_2. Phlogopite growth is interpreted as a metamorphic reaction, which justifies the inclusion of this sample with the RMT group. One of the biotite samples, MC-1, was obtained from a massive gabbronorite, (ca. 25 ha) in which biotite replaces pyroxene, and fibrolitic sillimanite overgrows plagioclase. No intrusive contact with the surrounding Goldenville Formation is exposed, but the gabbronorite is cut and partly enclosed by the Barrington Passage pluton (Taylor, 1967, Rogers, 1986). It is unclear whether biotite growth is due to regional metamorphism or to contact effects of the Barrington Passage pluton.

4.2.5.1. VARIATION OF MICA APPARENT AGES

WITHIN THE MEGUMA TERRANE

Previous geochronological studies in the Meguma terrane indicate that relatively low ^{40}Ar-^{39}Ar ages (less than 370Ma) on micas are associated with deformation or hydrothermal alteration (Reynolds et al., 1981; Zentilli and

Reynolds, 1985; Dallmeyer and Keppie, 1986). In view of the expanded data base, an attempt is made in this study to test whether any correlation exists between low ages and these suspected causes. Twenty-nine biotite samples from the RMT form the basis of this investigation. In addition to this general comparison, a detailed small-scale study is described.

The biotite samples have been classified into petrographic types on the basis of their relationship to the main NE to NNE foliation, S_2 (table 4.2-4). The categories are: (1) Type 1: Biotite which grew parallel to S_2, but is undeformed. (2) Type 2A: Biotite$^+$ which overgrew S_2 and is undeformed. (3) Type 2B: Biotite$^+$ which overgrew S_2, but was subsequently kinked and/or rotated. (4) Type 3: Biotite which was sheared into near parallism with a post-metamorphic foliation. The geologic setting of the biotite samples is described in section 4.2.2. The following hypothesis is tested: apparent age is a function of one or more variables (listed below). The following parameters are employed.

(1) Apparent age. It has been shown by several workers that the intensity of an overprinting event is reflected in the reduction of the apparent tT age (e.g. Berger, 1975; Dallmeyer, 1975; Hanson et al, 1975; Reynolds et al., 1981). Although regional metamorphism may have been diachronous, it is tentatively assumed the tT age is inversely proportional to the severity of overprinting. Apparent age is the

$^+$ or slightly aligned with S_2

Table 4.2-4. Data for biotite from the RMT.

Sample Number	Petrographic Class	Age (tT)	Saddle size	Alteration index	Deformation index	Distance from pluton(km)	Metamorphic grade *	IDF
PE85-162	03	401	4	1	8	05	2	1.81
PE85-161	03	394	4	1	7	05	2	4.20
PE83-004	2B	386	4	3	3	10	3	2.59
PE82-004	2A	374	2	0	0	33	1	2.19
PE84-064	03	373	4	1	8	05	2	2.06
PE84-072	2B	370	8	4	5	30	1	3.03
PE84-078	2B	370	2	1	3	38	1	3.95
PE84-100	2A	367	1	1	0	10	1	4.59
PE82-020	2A	364	1	0	0	10	4	2.24
PE82-005	2A	363	4	2	0	25	1	5.94
PE83-002	2A	363	1	1	4	05	2	2.03
PE84-076	2A	361	1	1	0	08	3	1.52
PE84-108	2A	358	1	2	1	25	1	1.97
PE82-002	03	356	1	1	4	30	1	0.54
PE83-012	2A	351	1	2	0	30	1	2.16
PE82-021	2B	350	4	1	3	08	4	2.23
PE82-010	01	349	1	1	0	25	1	2.12
PE84-033+	2A	348	1	2	0	15	2	1.81
PE82-017	2B	347	1	4	5	14	2	0.68
PE84-077+	03	347	1	2	4	17	4	3.03
PE82-009	2B	346	4	1	1	20	1	2.97
PE84-041	03	346	4	1	7	05	3	1.68
PE82-008	03	343	4	1	2	18	1	1.54
PE82-019	2B	338	1	1	3	03	3	0.38
PE82-018	2B	337	2	1	2	05	3	1.62
PE83-011	2A	336	4	1	0	08	2	1.31
MC-001	2A	334	1	1	0	01	4	8.49
PE83-005	2A	329	1	2	0	13	3	3.51
PE83-010	2B	319	2	2	3	08	3	2.02
PE84-121	2B	314	8	5	5	03	3	11.57
PE83-007	03	294	8	7	8	03	4	1.92

*Numbers represent metamorphic zones from biotite (1) through sillimanite (4). See Map 1.

+Not included in statistical analysis.

dependent variable.

(2) Alteration. The degree of chloritization is used as the index of alteration. Assigned values range from 1, for unaltered biotite, to 10, for a completely chloritized sample.

(3) Deformation. The degree of apparent strain in biotite is assigned arbitrary values ranging from 1 (undeformed), to 10 (highly strained).

(4) Distance from plutons. Previous work (e.g. Reynolds et al., 1981) suggest that plutonism in the Meguma terrane was later than regional metamorphism. It is therefore possible that low ages are caused by ^{40}Ar loss during intrusion of plutons, and to a first approximation, the effect may be assumed to be an inverse function of distance from the plutons.

(5) 'Saddle' in age spectra. Dallmeyer (1975), showed that spectra of thermally overprinted biotite samples may display 'saddles' (section 4.1.1). He suggested that the size of the saddle was related to the intensity of overprinting. He also showed that 7 of 11 samples studied bore no petrographic evidence of the overprint. The saddles were visually ranked on an arbitrary scale from 1 to 10.

(6) IDF. IF tectonothermal overprinting results in discordance, some correlation should be expected between the extent of discordance and the intensity of overprinting. The IDF parameter (section 3. 3) is a quantitative measure of discordance.

(7) Metamorphic grade. After regional metamorphism, domains of higher grade are likely to cool to argon retention temperatures later than their counterparts of lower grade. This should result in an inverse relationship between apparent age and metamorphic grade.

(8) Annite component. Experiments on argon diffusion in biotite indicate that the activation energy is inversely proportional to the annite (Fe) content (e.g. Harrison et al., 1985). If the activation energy is taken as a measure of resistance to overprinting, then an inverse correlation may be expected between annite content and apparent age (tT). The parameter Fe/(Fe+Mg) = (F/FM), was calculated (mol %) for 22 of the above samples (see Appendix B).

The database upon which the statistical analysis is based is displayed in table 4.2-4. Rank correlation ceofficients have been calculated to test the relationship between apparent age (tT) and (1) alteration (R = -0.311); (2) deformation (R = 0.127); (3) distance from pluton (R = 0.349); (4) metamorphic grade (R = -0.405); (5) Size of 'saddle' in the age spectrum (R = 0.013); IDF (R = 0.046);and F/(FM) (R = 0.631).

The above results (table 4.2-5) do not indicate any simple strong correlation between apparent ^{40}Ar deficit (represented by tT) and any of the parameters tested. For 29 samples, a significant correlation may exist (at 95%

confidence level) if r is greater than 0.31, or less than -0.31 (Lewis, 1984). The corresponding numbers for 22 samples (F/FM) are 0.36 and -0.36. Annite content of the biotites ranged from .403 to .669; a fair positive correlation between F/(FM) and tT (R=.631) within this range is indicated. This is discussed below. A weak positive correlation is indicated between tT and distance from plutons. Since post-plutonic overprinting was apparently most severe in and around the SSP (see below), the correlation may be reflecting this later event. There is a weak negative correlation between metamorphic grade and tT. This may indicate diachronous post-metamorphic cooling. It is also possible that a long-lived heat source was preferentially activated beneath the higher grade zones, which are also sites of intrusion for most of the SSP. This would explain why some of the lowest ages occur in, and close to the SSP (see below). It is possible that none of these variables is dominant over the range of the entire terrane .

Multivariate analysis by the stepwise regression technique (e.g. Thorndike, 1978), reveals that the three variables upon which age is most dependent are F/FM, deformation, and alteration. The combined correlation coefficient, R, is 0.712, which suggests a moderately strong correlation. The values of P which measure the relative contribution of each variable to the age deficit are listed in table 4.2-6. Also listed in table 4.2-6 are the values

Table 4.2-5. Rank correlation coefficients between apparent age and various parameters (Biotite from the RMT).

PARAMETER	R
Alteration index	-0.311
Deformation index	0.127
Distance from pluton	0.349
Metamorphic grade	-0.405
Saddle size	0.013
IDF	0.046
F/FM	0.631

Table 4.2-6. Summarized results from stepwise regression of biotite data from table 4.2-4.

PARAMETER	T	P
F/FM	2.35	0.031
Alteration index	-2.47	0.024
Deformation index	1.82	0.086
Value of T at:		
99% confidence limit = 2.55		
95% confidence limit = 1.73		

of T, which measure the magnitude and sign of the individual correlations with age. The theoretical values of T at the 99% and 95% confidence levels are also listed. The following observations can be made:

(1) When all three 'independent' variables are considered together, with age as the dependent variable, three variables best account for the observed variation in tT. The greatest influence is exerted by alteration (P = 0.024), and the least by deformation (P = 0.086). T values for all three 'independent' variables are significant at the 95% confidence level. The negative correlation between age and alteration is as would be expected since the alteration may lead to loss of ^{40}Ar relative to K - a very likely situation. The positive correlation between age and deformation may be a reflection of a complex deformational history, as suggested in section 4.2.2. Generally, it may be expected that the younger biotites represent recrystallization after deformation, whereas the older ones are relicts that survived the deformation. Petrographic examination of the samples, however, suggest that this interpretation may be an oversimplification. There are strongly deformed samples at both ends of the age range (table 4.2-4).

(2) When deformation is removed from the regression calculations, and the 'independent' variables are F/FM and alteration, the following observations can be made. The multiple correlation coefficient is slightly reduced

(R=0.646). In this case, F/FM (P=0.019) exerts the stronger influence on age.

The seven samples with the highest values for F/FM (>.590), are all older than 360 Ma, but do not belong to a single petrographic type. The five samples with the lowest values for F/FM (<.500), show no systematic pattern in age or petrographic type. Although the relationships are probably quite complex, it is possible that the older, iron rich biotites remained stable during a late overprinting event at moderate temperatures, while their Mg-rich counterparts were largely recrystallized. This would be expected from the known stability relationships in the phlogopite-annite series (e.g. Wones and Eugster,1965; Harrison et al., 1985). Alternatively, if the shearing occurred during the late stages or soon after metamorphism, biotite would remain stable, with ages which reflect post-metamorphic cooling. Variation in the time and temperature of overprinting events would tend to obscure meaningful trends. The inference is that although deformation seems to exert very little influence on age as an 'independent' variable (P=0.086), it has a strong influence on alteration. This indicates that deformation and alteration are not entirely independent variables. Indeed, these two variables are strongly associated at least locally in the Meguma terrane (section 4.2.5.5). Although the sampling procedure was designed to avoid the most deformed and altered samples, the results suggest that a

subtle interplay of these two factors may be responsible for the range in ages observed.

4.2.5.2. A DOMAIN IN THE WHITE ROCK FORMATION

In order to investigate the effects of post-metamorphic overprinting, five samples were dated from a small area (40,000 m^2) in the White Rock Formation. At the location shown in fig. 4.2-9, metabasites are interstratified with pelites.

The metabasites are cut by at least one post-tectonic chlorite-muscovite vein. The following were analysed: (a) biotite from three metapelite samples (PE84-64D, PE85-161, and PE85-162). Biotite is of similar chemical composition in the three samples (table 4.2-7); (b) hornblende from a metabasite sample (PE84-64C); and (c)muscovite from the post-metamorphic vein (PE84-65B). Data are shown in table 4.2-8.

The three metapelite samples have a strong foliation in which biotite is sheared into 'fish' structures with long tails. (e.g. Lister and Snoke, 1984). Although biotite is strongly sheared (fig. 4.2-10), it is not kinked, and there is little sign of retrograde alteration, which suggests that

Fig. 4.2-9. Map of White Rock domain.

For location, see fig. 4.2-13.

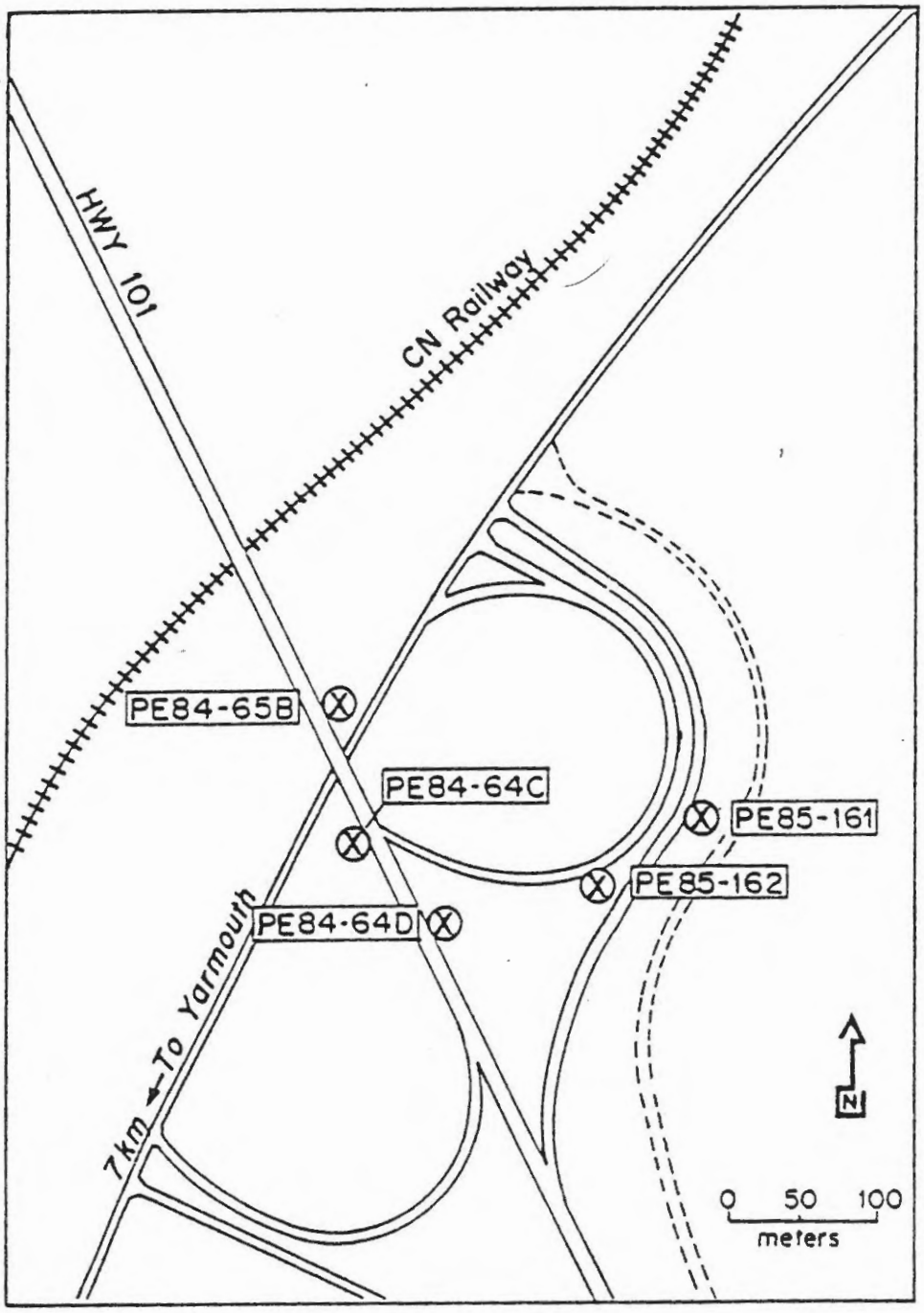
HWY 101
CN Railway
PE84-65B
PE84-64C
PE85-161
PE85-162
PE84-64D
7km ← To Yarmouth
N
0 50 100
meters

Fig. 4.2-10. Photomicrograph of sheared metapelite from the White Rock Domain. Note biotite 'fish', some of which are at extinction. The groundmass consists of muscovite and quartz. (Sample PE84-64D).

Fig. 4.2-11. Photomicrograph of sheared metapelite from the White Rock Domain. Inclusion trails in staurolite (partly at extinction) show sigmoidal continuity with the external foliation (upper right). Inclusion trails within other porphyroblasts are in straight continuity with, or at high angles to the external foliation (not shown). These textures suggest syntectonic growth of porphyroblasts. Note rotated unaltered biotite, and peripheral chloritization of staurolite. Euhedral garnet is partly enclosed by staurolite.

(Sample PE85-161).

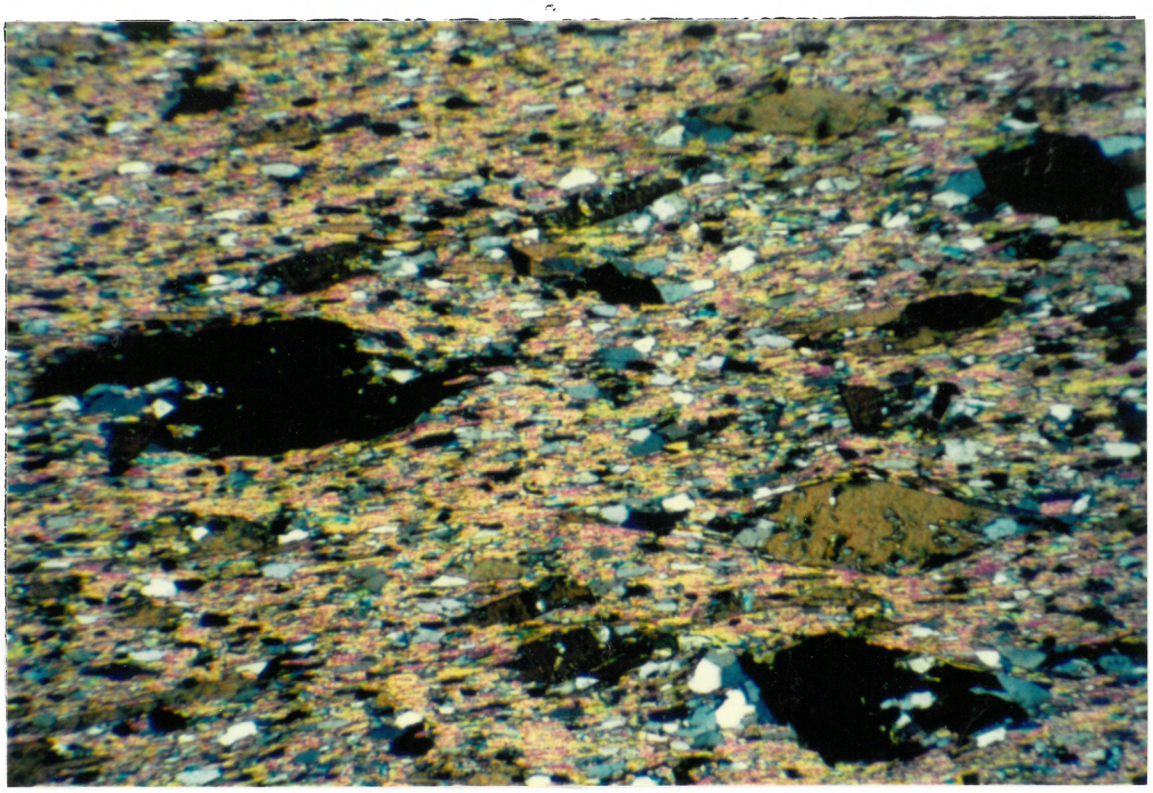

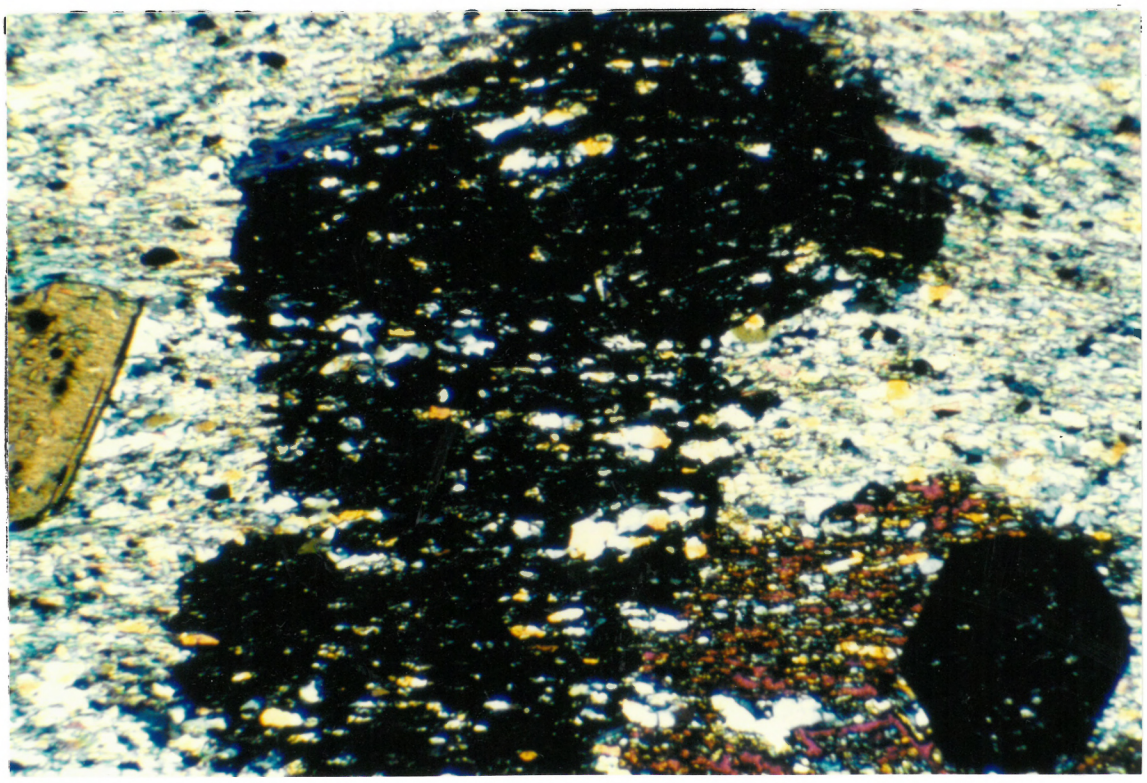

0.5 mm

Fig. 4.2-12. Photomicrograph of sheared metapelite from the White Rock Domain, showing post-tectonic chlorite overgrowth. Note strong foliation defined by micas and quartz. (Sample PE85-163).

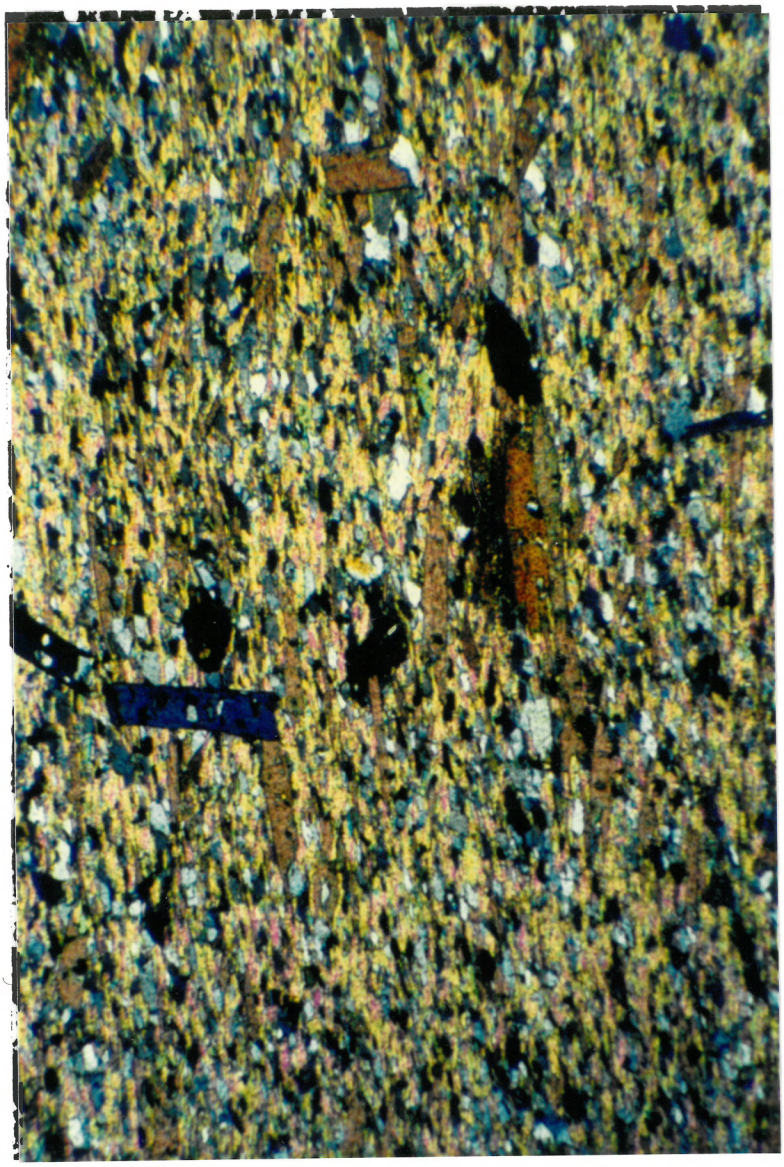

0.5 mm

Table 4.2-7. Chemical data for biotite from the White Rock Domain.

Sample	K/Al	K/(K+Na)	F/FM
PE84-64	.505	.969	.670
PE85-161	.496	.957	.590
PE85-162	.477	.980	.635

Table 4.2-8. Ages and discordance factors for samples from the White Rock Domain.

SAMPLE	PHASE	AGE (Ma)	IDF	CS Ma	CS %
PE84-64C	Hb	401	7.97	4.0	1.0
PE84-64D	Bi	373	2.06	2.9	0.8
PE85-161	Bi	394	4.20	2.2	0.6
PE85-162	Bi	401	1.81	1.8	0.4
PE84-65B	Mu	322	0.42	1.9	0.6

biotite was recrystallized during the deformation. This indicates that shearing occurred at moderately high temperatures. Inclusion trails in some garnet and staurolite porphyroblasts in these samples suggest that they were rotated, but the inclusion trails in others are apparently continuous with the external foliation (fig. 4.2-11). This relationship suggests that shearing could have commenced during growth of garnet and staurolite. Since the shearing clearly post-dates biotite growth, it may be at least partly post-metamorphic. Mild overgrowth of chlorite and muscovite apparently post-dates the shearing (fig. 4.2-12), and suggests that retrograde metamorphism was the latest in the sequence of events. The strong NNE foliation can be correlated with that in the nearby Brenton pluton (5km), where complete recrystallization of micas occurred about 320 Ma ago (O'Reilly, 1976). Hornblende Sample PE84-64C and its discordant spectrum have been described in section 4.2.1.

The three biotite samples all yield discordant spectra with saddles, which may be attributed to overprinting (e.g. Dallmeyer 1975, 1982). According to Dallmeyer (1975), the plateau portion of the spectrum in the last few steps may record the original cooling age. High temperature plateaus are poorly defined for these three samples. The last few steps show a lowering in apparent age, contrary to the findings of Dallmeyer (1975). If the highest apparent age is taken from this portion of the spectrum, it would

indicate cooling ages of 379 Ma, 409 Ma and 410 Ma for samples PE84-64D, PE85-161, PE85-162 respectively. Because of the following two reasons, these apparent cooling ages are unlikely to be meaningful. (1) Very sharp geothermal gradients during cooling would be required to produce a 30 Ma difference in biotite over a distance of about 100m. (2) Biotite would be required to have a higher closure temperature than hornblende, since the apparent cooling age of hornblende sample PE84-64c is 404 Ma. This is contrary to what is known about relative argon retentivities of these two minerals.

Dallmeyer (1975) suggested that the width of the 'saddle' and the accompanying reduction of the 'plateau' segment are proportional to the intensity of overprinting. Sample PE84-64D has the largest plateau segment (65.7%) and the lowest tT age (most apparent ^{40}Ar loss). The widest saddle was produced by sample PE85-161, with intermediate tT age.

The vein muscovite sample produced a well-defined plateau over 94% of its spectrum. The apparent plateau age is 322 Ma, identical with its tT age. This age is similar to the apparent age of shearing and recrystallization of the Brenton pluton 5 km to the east (Reynolds et al., 1981). This age is also similar to Rb-Sr ages of altered mineralized domains within the SMB (O'Reilly et al., 1985).

The following conclusions can be drawn from the above observations:

(1) Discordant spectra from biotite and hornblende are indicative of tectonothermal overprinting. The intensity of the secondary event is reflected in the lowering of the apparent age (tT). Considerable caution is required in assessing individual spectra from biotite (see section 4.2.5.1).

(2) The saddle feature is produced in the spectra of at least some overprinted biotite samples.

(3) Overprinted biotite samples may not yield meaningful ages in their high temperature steps.

(4) The width of the saddle cannot be taken as a measure of the intensity of overprinting.

(5) The intensity of overprinting (reflected in tT age) may vary sharply over small distances in the Meguma terrane.

(6) The maximum apparent age in a 'staircase' hornblende spectrum may be geologically meaningful (Chapter 3), but must be interpreted with caution.

The above data suggest at least two distinct tectonothermal events: (a) Regional metamorphism accompanied

by deformation about 370-400 Ma ago. (b) Overprinting about 320 Ma ago, involving retrograde metamorphism (represented by the chlorite-muscovite vein). It appears that whereas the micas of the nearby Brenton pluton were completely outgassed about 320 Ma ago, those of the White Rock domain suffered only minor argon loss. The 28 Ma range in apparent age among the three biotite samples is probably due to small variations in argon loss during the overprinting event. It is very likely that the effects of overprinting also vary on a regional scale, as suggested in sections 4.2.3 and 4.2.4. This variation is probably superimposed on diachroneity in the cooling pattern of the main regional metamorphic event.

4.2.5.3. SUMMARY OF 'AGE VARIATION' STUDIES

Although there are individual cases where association of cause and effect are obvious (described below), there appears to be no simple strong correlation between intensity of overprinting (age deficit), and the symptomatic features examined. It appears to be a common feature of the K-Ar systematics of biotite, that overprinting can occur without any obvious modification to the mineral (e.g. Berger, 1975; Dallmeyer, 1975; Reynolds et al., 1981; Criss et al., 1982).

Biotite is known to suffer substantial loss of K during hydrothermal alteration. Compared with the normal 8-10 wt% K_2O, altered 'biotite' may contain as little as 1 - 0.5 wt % K_2O (eg. Eggleton and Banfield, 1985; Dempster and Harte, 1986). Microprobe analyses on selected samples from the RMT reveal no such K loss (Appendix B). It has been shown, however, that biotite from hydrothermally altered rocks may not show any chemical modification (eg. Ferry, 1985). Since no clear straightforward correlation can be established between apparent ^{40}Ar loss and the parameters examined, it is concluded that the variation in mica ages is due to complex non-uniform overprinting. This is pursued in the sections that follow.

4.2.5.4. OLDER MICAS

The 'older micas' comprise thirteen biotites, one phlogopite and two muscovites (one of which was a fine grained impure separate containing quartz, chlorite and sericite). Sample locations are shown in fig. 4.2-13. All spectra from the older micas (fig. 4.2-15), with the exception of PE84-97, display one common feature: The low temperature steps give low apparent ages. Subsequent steps give ages which fall in a narrow range (10-20 Ma for most of the gas). Staircase features are not strongly pronounced and there is no consistent value for age minima or age maxima. A prominent saddle is superimposed on the mild

Biotite is known to suffer substantial loss of K during hydrothermal alteration. Compared with the normal 8-10 wt% K_2O, altered 'biotite' may contain as little as 1 - 0.5 wt % K_2O (eg. Eggleton and Banfield, 1985; Dempster and Harte, 1986). Microprobe analyses on selected samples from the RMT reveal no such K loss (Appendix B). It has been shown, however, that biotite from hydrothermally altered rocks may not show any chemical modification (eg. Ferry, 1985). Since no clear straightforward correlation can be established between apparent ^{40}Ar loss and the parameters examined, it is concluded that the variation in mica ages is due to complex non-uniform overprinting. This is pursued in the sections that follow.

4.2.5.4. OLDER MICAS

The 'older micas' comprise thirteen biotites, one phlogopite and two muscovites (one of which was a fine grained impure separate containing quartz, chlorite and sericite). Sample locations are shown in fig. 4.2-13. All spectra from the older micas (fig. 4.2-15), with the exception of PE84-97, display one common feature: The low temperature steps give low apparent ages. Subsequent steps give ages which fall in a narrow range (10-20 Ma for most of the gas). Staircase features are not strongly pronounced and there is no consistent value for age minima or age maxima. A prominent saddle is superimposed on the mild

Fig. 4.2-13. Distribution of 'older micas' in the RMT.

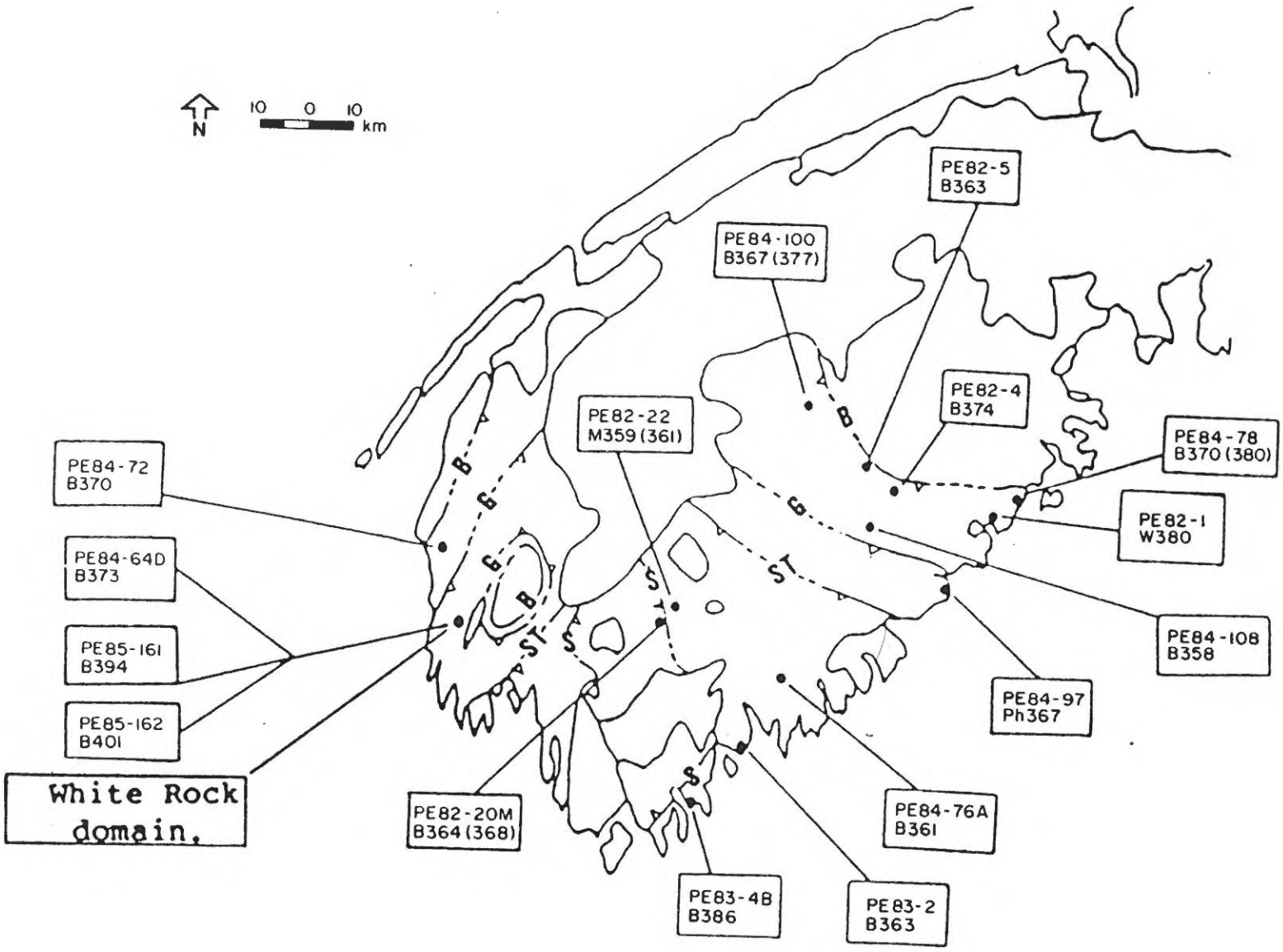
N
10 0 10
km
PE82-5
B363
PE84-100
B367(377)
PE82-4
B374
PE82-22
M359(361)
PE84-78
B370(380)
PE84-72
B370
PE82-1
W380
PE84-64D
B373
PE84-108
B358
PE85-161
B394
PE84-97
Ph367
PE85-162
B401
White Rock
domain.
PE82-20M
B364(368)
PE84-76A
B361
PE83-4B
B386
PE83-2
B363

Fig. 4.2-14.

Histogram of apparent ages of 'older' biotites.

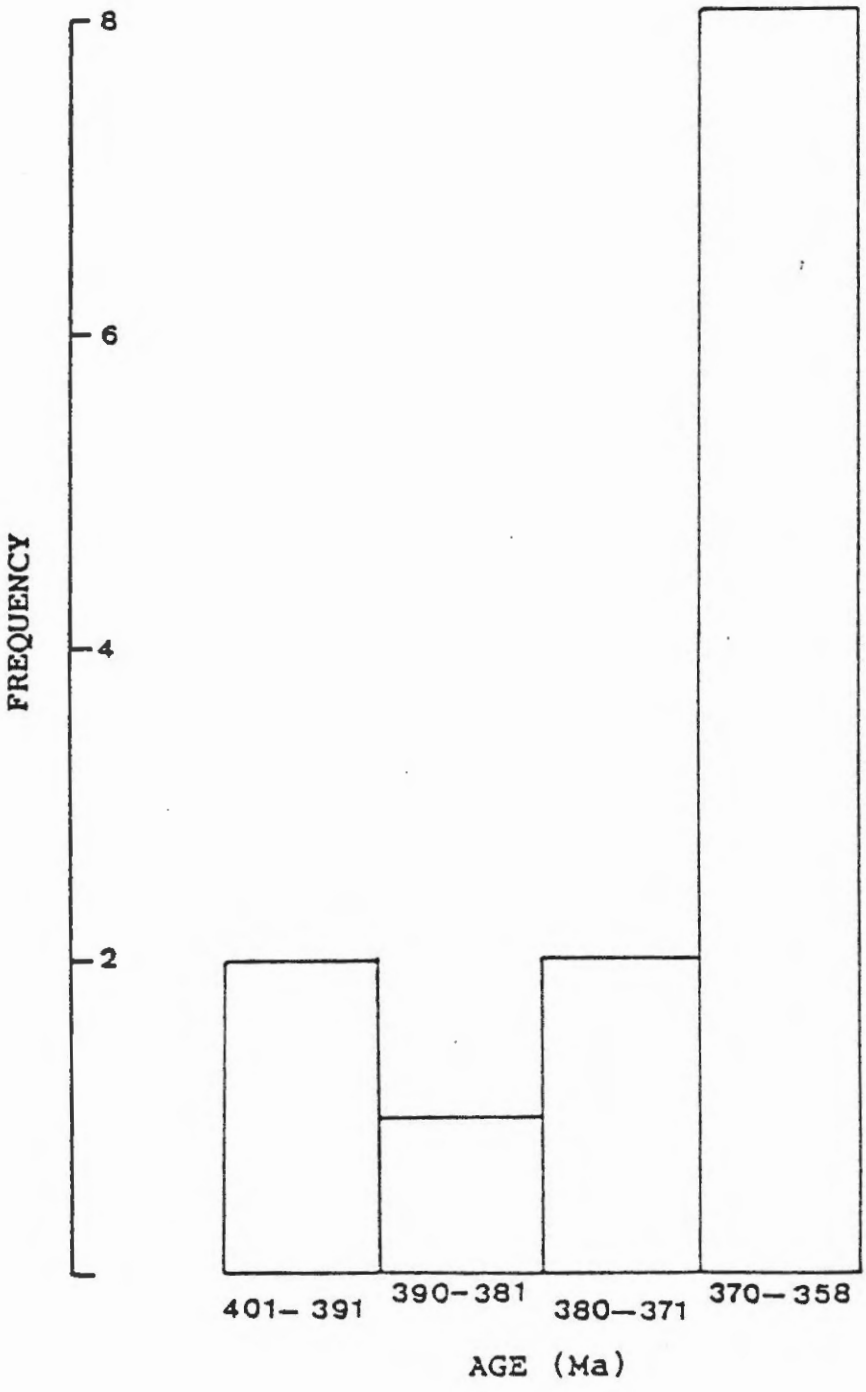
8
6
4
2
FREQUENCY
401– 391
390–381
380–371
370–358
AGE (Ma)

Fig. 4.2-15. Age spectra of 'older micas'.
Bars on vertical axes represent 10 Ma.

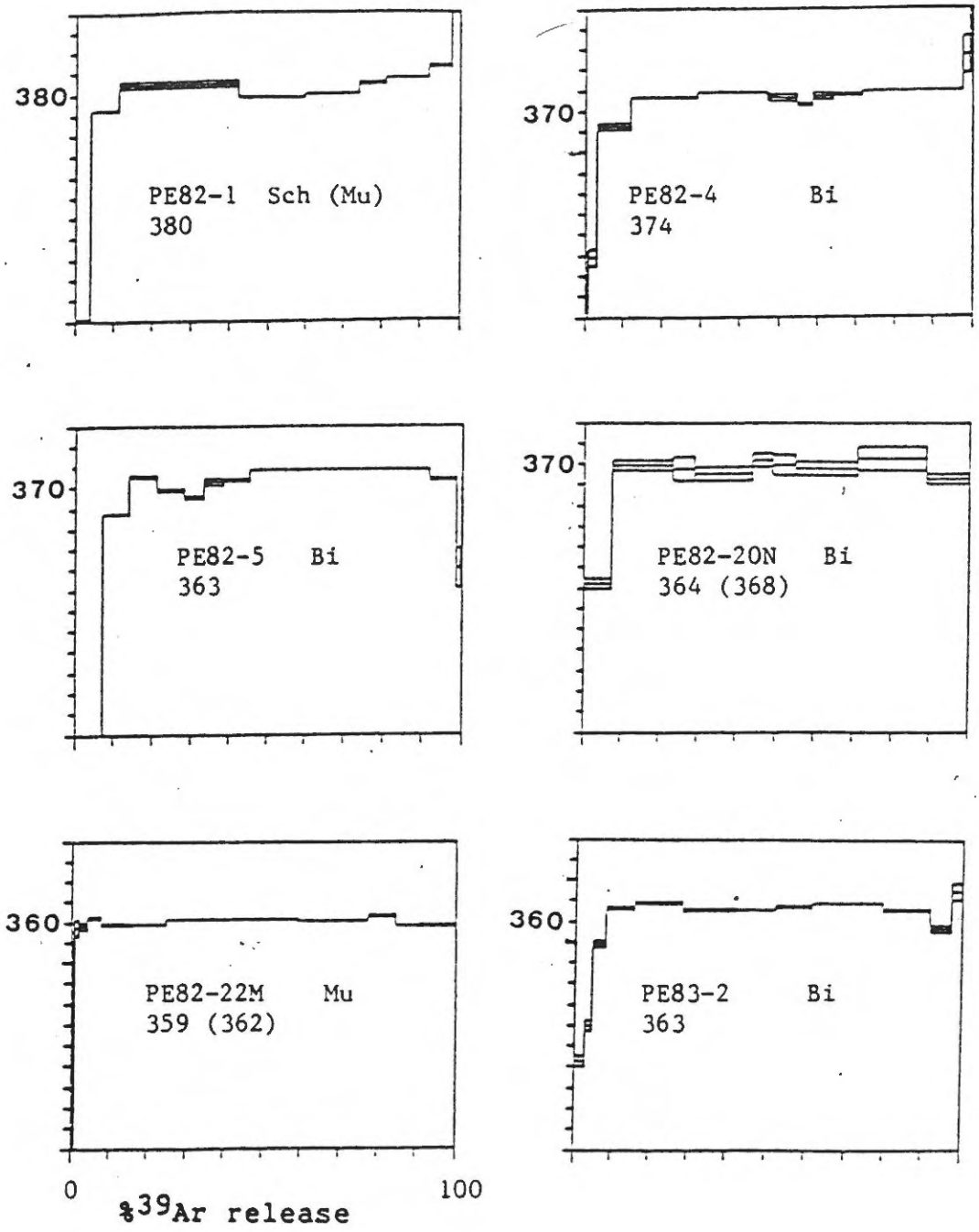
380
PE82-1 Sch (Mu)
380
370
PE82-4 Bi
374
370
PE82-5 Bi
363
370
PE82-20N Bi
364 (368)
360
PE82-22M Mu
359 (362)
360
PE83-2 Bi
363
0
100
%39Ar release

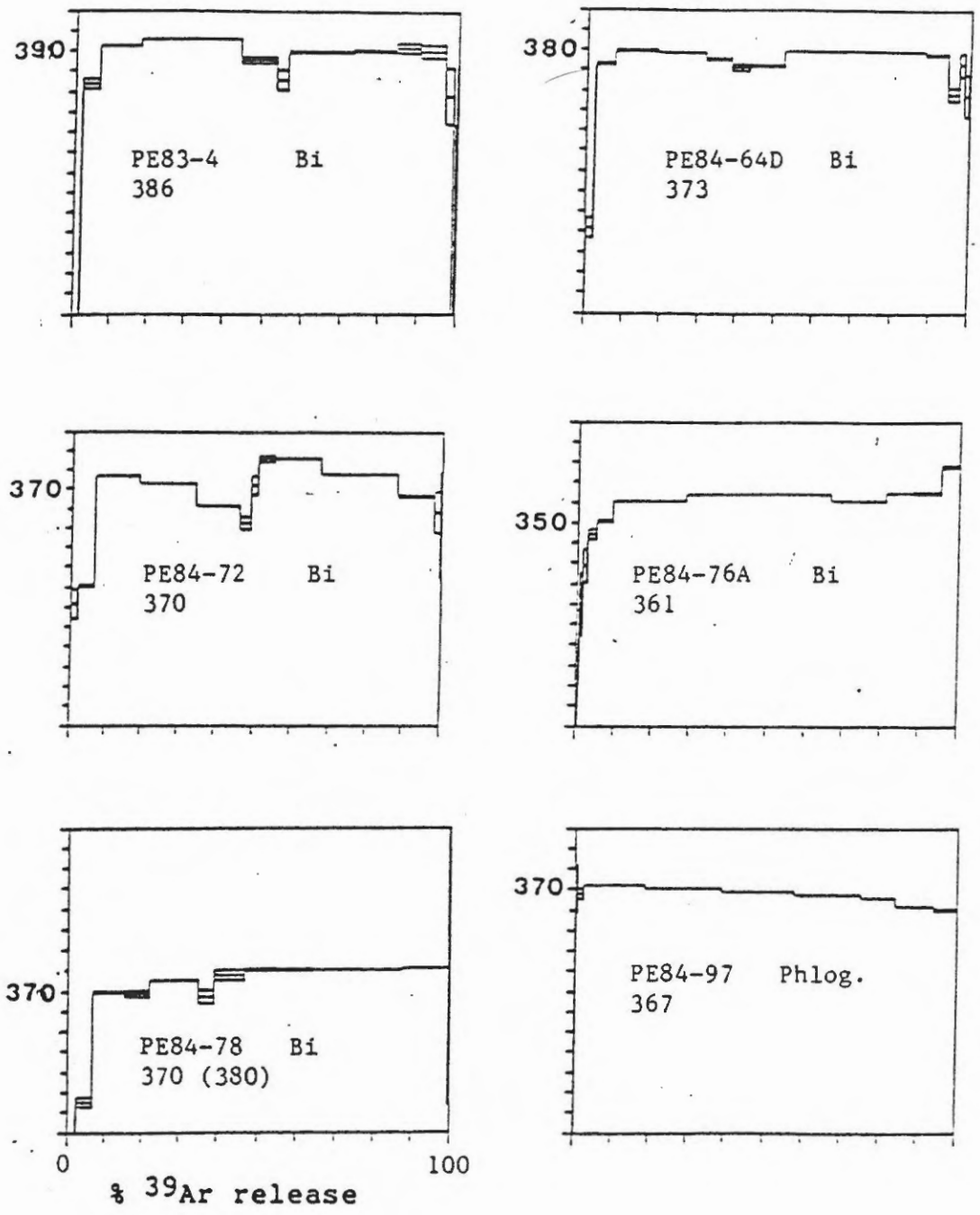
390
PE83-4 Bi
386
380
PE84-64D Bi
373
370
PE84-72 Bi
370
350
PE84-76A Bi
361
370
PE84-78 Bi
370 (380)
370
PE84-97 Phlog.
367
0
100
% 39Ar release

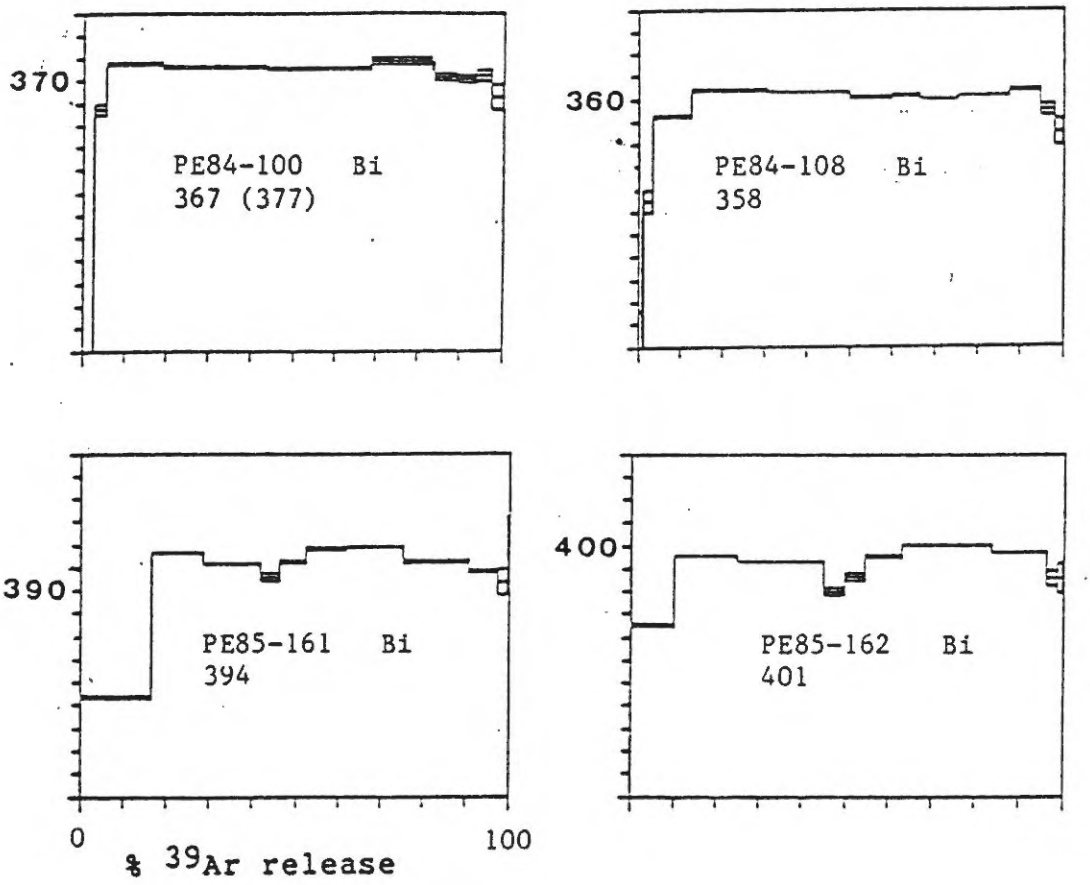
370
PE84-100 Bi
367 (377)
360
PE84-108 Bi
358
390
PE85-161 Bi
394
400
PE85-162 Bi
401
0
100
% 39Ar release

Table 4.2-9.

Ages and discordance factors for 'older' micas

SAMPLE	PHASE	AGE (Ma)	IDF	CS Ma	%
PE82-1	Sch(Mu)	380	2.81	2.2	0.6
PE82-4	Bi	374	2.19	2.7	0.7
PE82-5	BI	363	5.94	1.9	0.5
PE82-20N	Bi	364	2.24	8.1	2.2
PE82-22M	Mu	359	0.76	1.6	0.5
PE83-2	Bi	363	2.03	2.1	0.6
PE83-4B	Bi	386	2.59	4.7	1.2
PE84-64D	Bi	373	2.06	2.9	0.8
PE84-72	Bi	370	3.03	2.7	0.7
PE84-76A	Bi	361	1.52	2.3	0.6
PE84-78	Bi	370	3.95	3.9	1.1
Pe84-97	Phl	367	1.12	1.3	0.4
PE84-100	Bi	367	4.59	4.0	1.1
PE84-108	Bi	358	1.97	3.1	0.9
PE85-161	Bi	394	4.20	2.2	0.6
PE85-162	Bi	401	1.81	1.8	0.4

staircase profile in spectra from 6 biotite samples. These features suggest the samples experienced at least one episode of overprinting. As stated in Chapter 3, the coincidence of argon release with structural breakdown and dehydration of micas causes modification of naturally produced argon gradients. This may be the reason for poor definition of the staircase pattern. Indeed the staircase is reversed slightly for sample PE84-97 (phlogopite). There is no simple model to explain such a profile. Of the two muscovite samples one (PE82-22) gave a 3-step (60% ^{39}Ar) plateau age of 361 Ma. The other one PE82-1, gave no plateau but has the higher t_T (380 Ma). It is conceivable that discordance in the spectrum of sample PE82-1 (IDF = 2.74, table 4.2-9) was partly caused by the presence of minor sericite in the impure separate. The apparent age of biotite sample PE85-162 is 401 Ma (section 4.2.5.2). This overlaps with the deposition age of the youngest pre-metamorphic unit (Torbrook Formation, t = 395 Ma). Although this overlap can be accommodated by uncertainties in both the ^{40}Ar-^{39}Ar age and the boundaries of the geologic time scale (fig. 1-1), it is possible that this sample may be contaminated by minor excess argon. Apparent ages of the other 15 samples range from 358 Ma to 394 Ma (fig. 4.2-14). It is uncertain whether these samples suffered an overprint during post-metamorphic intrusion of plutons, or were affected by other events. This age range may partly be a reflection of diachronous post-metamorphic cooling.

However, they are interpreted to represent domains in the RMT which experienced the least effects of overprinting. It is interesting that most samples from the biotite zone (like the chlorite zone) apparently suffered only minor ^{40}Ar loss, and thus preserve ages close to the estimated time of the Acadian event (table 1-1). The age range of the older micas is very similar to plateau ages reported for regional metamorphic, plutonic and dynamically recrystallized micas in the northeastern Meguma Zone (Dallmeyer and Keppie 1984).

4.2.5.5. YOUNGER MICAS

The 'younger micas' consist of eighteen biotites and five muscovites from all metamorphic zones higher than chlorite (fig. 4.2-16). Ages range from 356 Ma to 294 Ma (fig. 4.2-17), and they do not belong to a single petrographic class (section 4.2.5.1). Biotite ages show a frequency concentration in the range 340-350 (fig. 4.2-17). There is no clear explanation for this age clustering. However, there are a few general and specific observations that can be made from the data summary (table 4.2-10) and the spectra displayed in fig. 4.2-18. Most of the spectra bear some evidence of an overprinting event. Twenty of the 23 spectra are characterized by low ages in their first few steps, which is usually ascribed to ^{40}Ar loss. This feature is missing from the spectrum of sample PE84-65 (muscovite from late vein), which is discussed in Section 4.2.5.2.

Fig. 4.2-16. Distribution of 'younger micas' in the RMT.

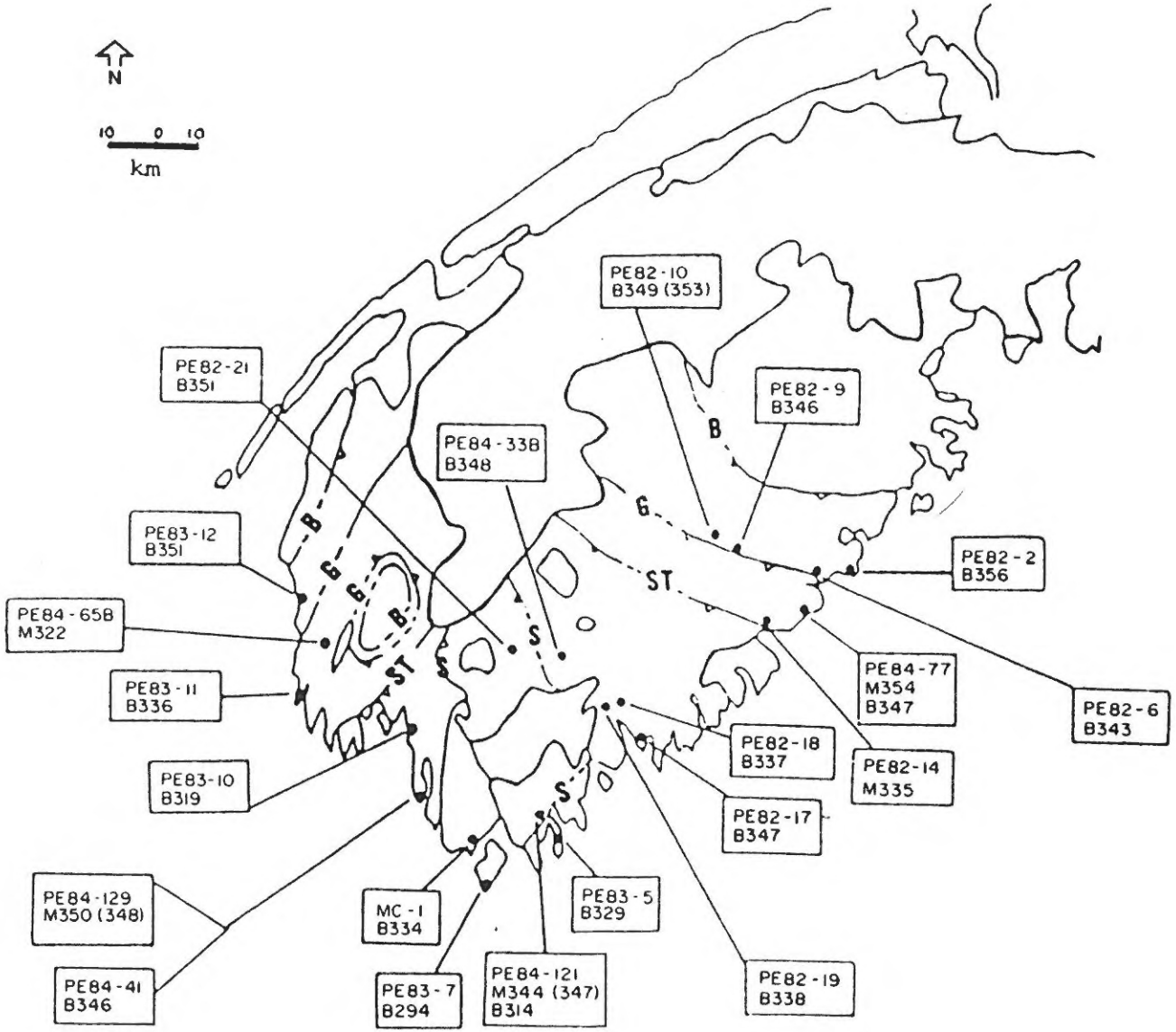
N
10 0 10
km
PE82-10
B349 (353)
PE82-21
B351
PE82-9
B346
PE84-338
B348
B
G
PE83-12
B351
PE82-2
B356
ST
PE84-658
M322
S
PE84-77
M354
B347
PE82-6
B343
PE83-11
B336
PE82-18
B337
PE82-14
M335
PE83-10
B319
PE82-17
B347
PE84-129
M350 (348)
MC-1
B334
PE83-5
B329
PE84-41
B346
PE83-7
B294
PE84-121
M344 (347)
B314
PE82-19
B338

Fig. 4.2-17.

Histogram of apparent ages of 'younger' biotites.

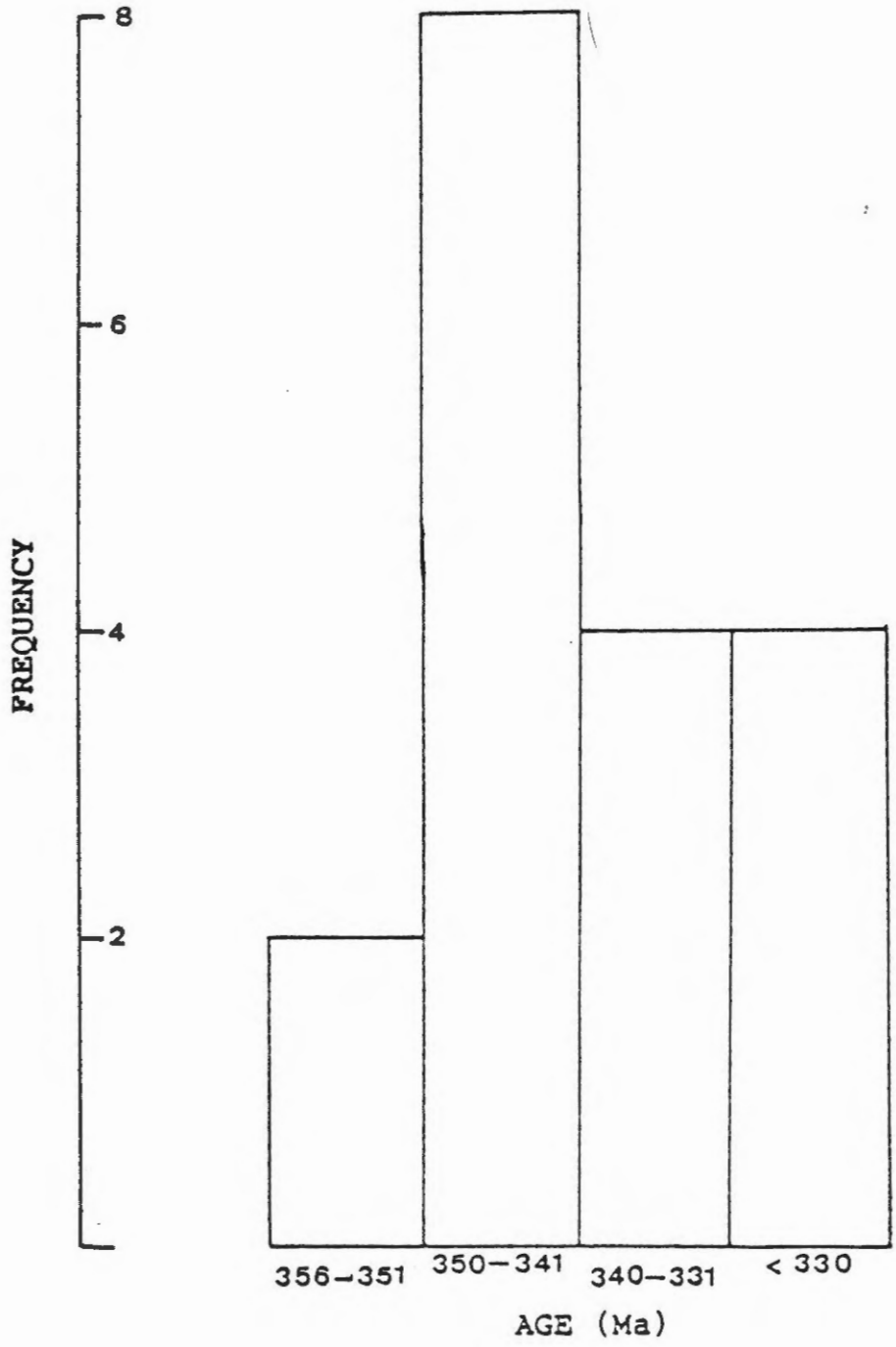
8
6
4
2
FREQUENCY
356–351
350–341
340–331
< 330
AGE (Ma)

Fig. 4.2-18. Age spectra of 'younger micas'. Bars on vertical axes represent 10 Ma.

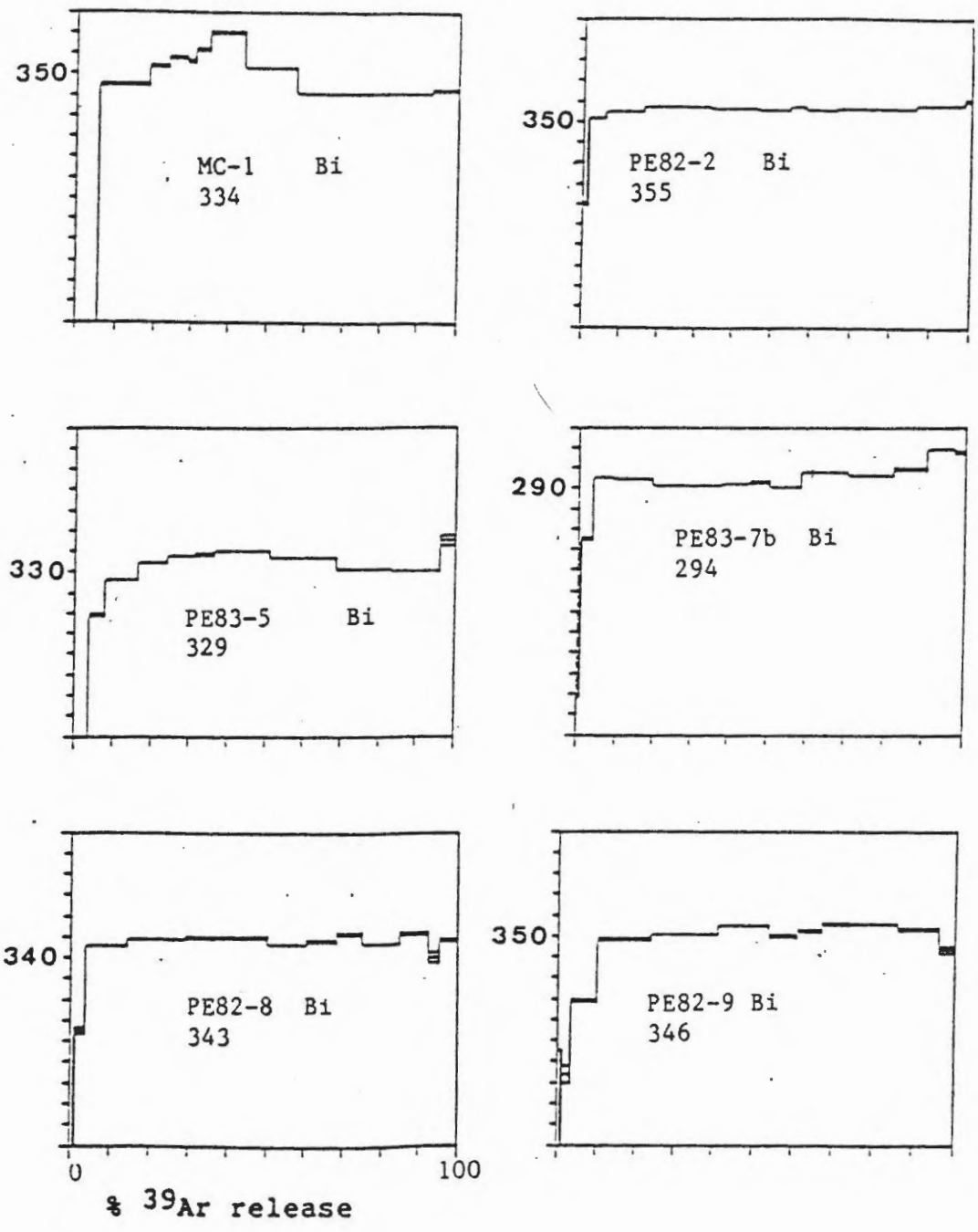
350
MC-1 Bi
334
350
PE82-2 Bi
355
330
PE83-5 Bi
329
290
PE83-7b Bi
294
340
PE82-8 Bi
343
350
PE82-9 Bi
346
0
100
% 39Ar release

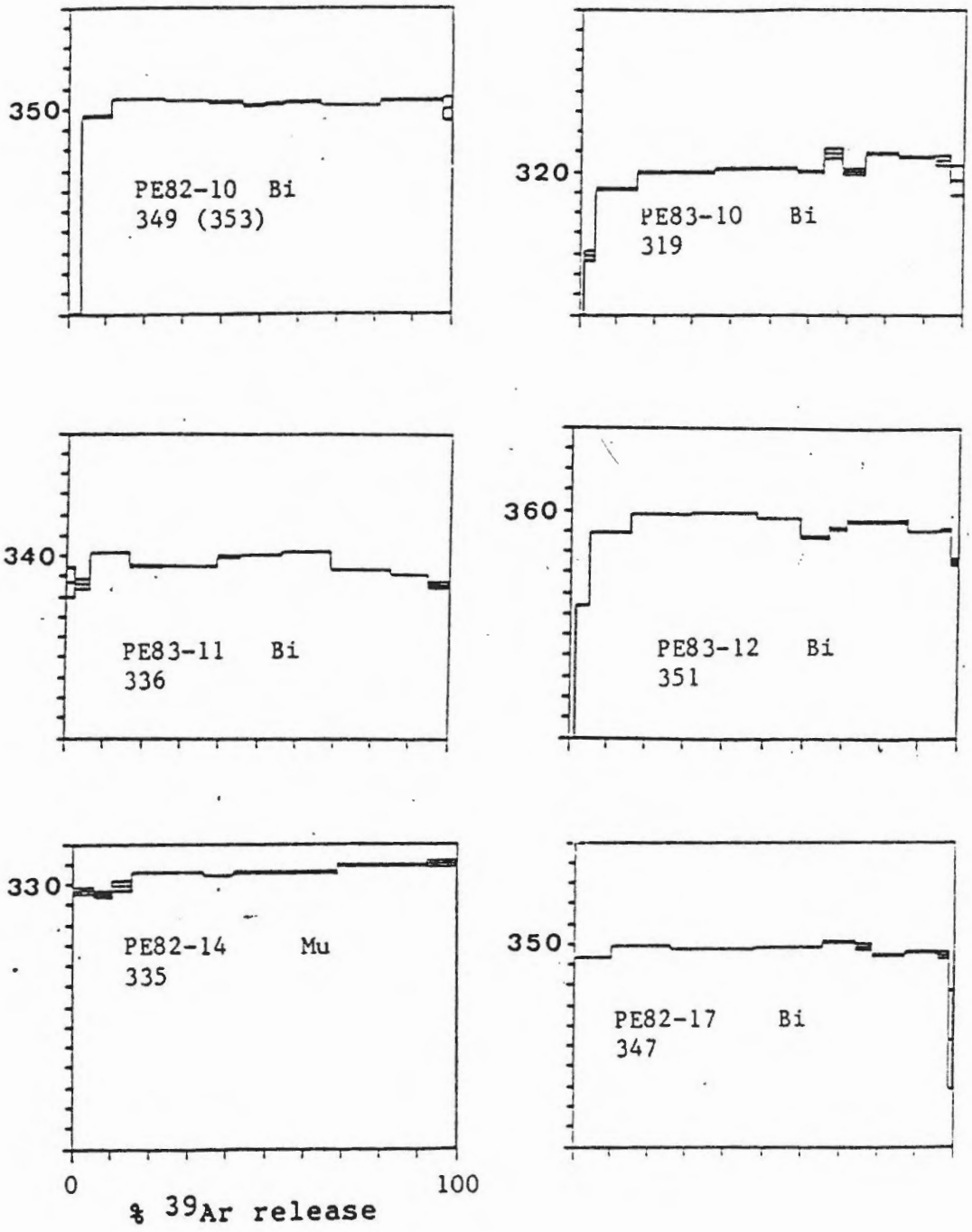
350
PE82-10 Bi
349 (353)
320
PE83-10 Bi
319
340
PE83-11 Bi
336
360
PE83-12 Bi
351
330
PE82-14 Mu
335
350
PE82-17 Bi
347
0
100
% 39Ar release

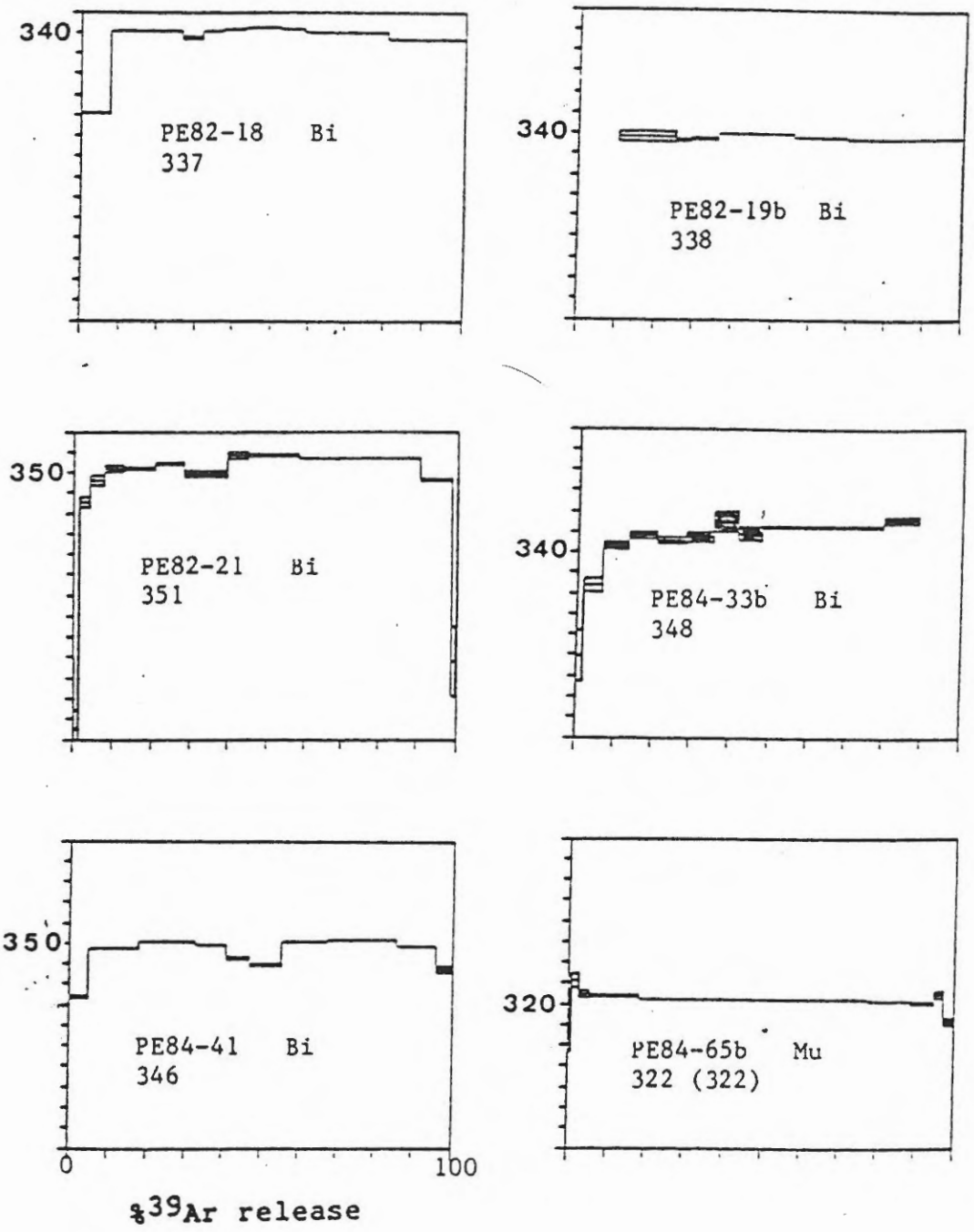
340
PE82-18 Bi
337
340
PE82-19b Bi
338
350
PE82-21 Bi
351
340
PE84-33b Bi
348
350
PE84-41 Bi
346
320
PE84-65b Mu
322 (322)
0
100
%39Ar release

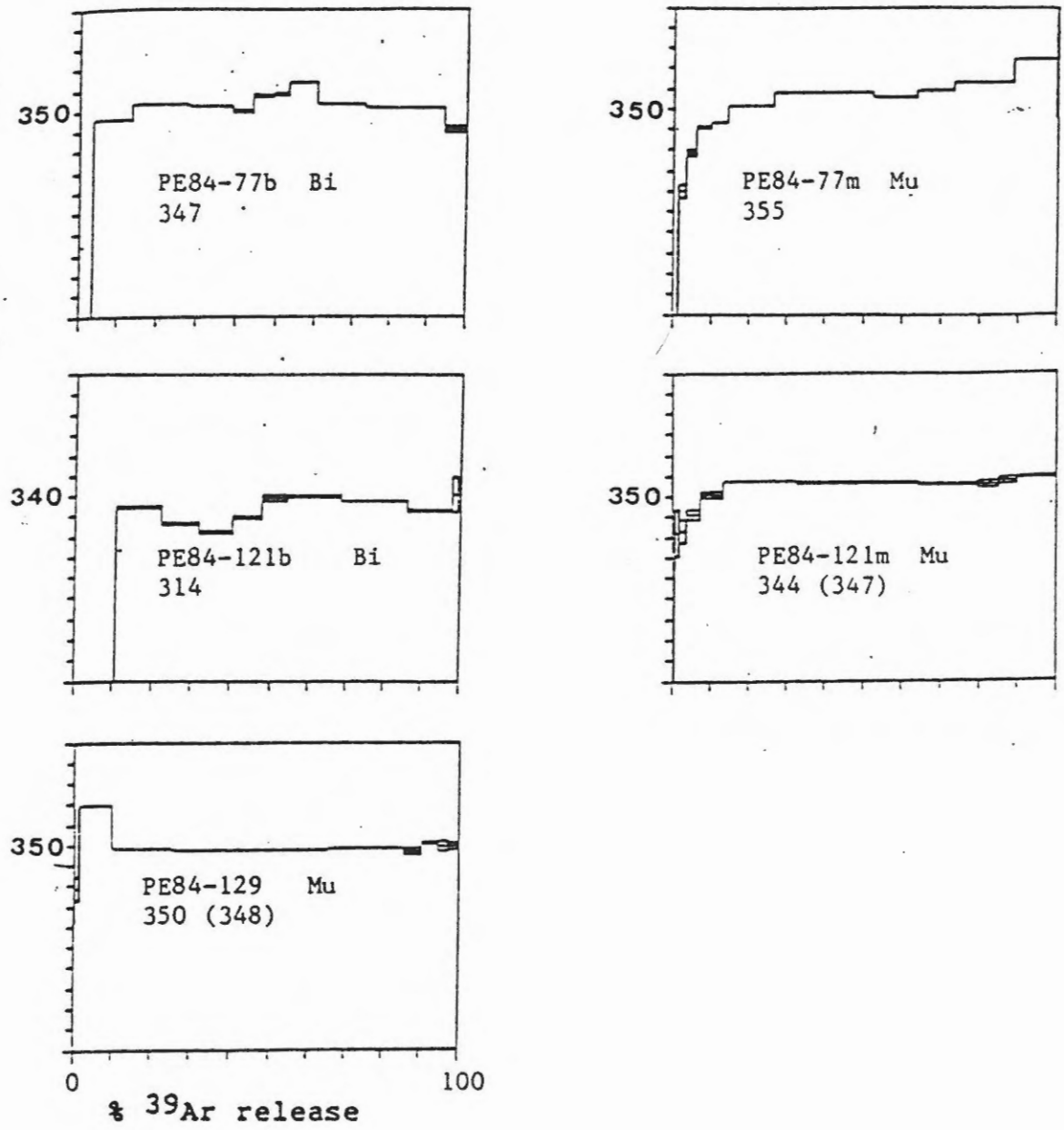
350
PE84-77b Bi
347
350
PE84-77m Mu
355
340
PE84-121b Bi
314
350
PE84-121m Mu
344 (347)
350
PE84-129 Mu
350 (348)
0
100
% 39Ar release

Table 4.2-10.

Ages and discordance factors for 'younger' micas.

SAMPLE	PHASE	AGE (Ma)	IDF	CS Ma	%
MC1	Bi	334	8.49	1.6	0.5
PE82-2	Bi	355	0.54	0.7	0.2
PE83-5	Bi	329	3.51	1.3	0.4
PE83-7	Bi	294	1.92	1.1	0.4
PE82-8	Bi	343	1.54	1.8	0.5
PE82-9	BI	346	2.97	4.3	0.7
PE82-10	Bi	349	2.12	1.9	0.5
PE83-10	Bi	319	2.02	3.5	1.1
PE83-11	Bi	336	1.31	2.1	0.6
PE83-12	Bi	351	1.96	1.3	0.4
PE82-14	Mu	335	0.95	2.7	0.8
PE82-17	Bi	347	0.68	1.9	0.6
PE82-18	BI	337	1.62	0.9	0.3
PE82-19B	Bi	338	0.38	2.4	0.7
PE82-21	Bi	351	2.23	3.0	0.8
PE84-33B	Bi	348	1.81	8.3	2.4
PE84-41	Bi	346	1.68	1.8	0.5
PE84-65B	Mu	322	0.42	1.9	0.6
PE84-77B	Bi	347	3.03	1.3	0.4
PE84-77M	Mu	355	2.76	1.6	0.4
PE84-121B	Bi	314	11.57	2.2	0.7
PE84-121M	Mu	344	1.27	3.3	1.0
PE84-129	Mu	350	0.99	1.8	0.5

Fig. 4.2-19. Photomicrograph of sheared and altered metapelite from the 'Complex Domain.' Note well-developed C-S fabric, with biotite partly replaced by oriented muscovite. Sericite aggregates define the C-plane. Overprinted biotite from this sample produced the lowest mica age in this study. (Sample PE83-7B).

Fig. 4.2-20. Photomicrograph of metapelite from the 'Complex Domain.' Muscovite has replaced biotite and staurolite. Note finer muscovite intergrown with quartz in the groundmass. (Sample PE84-121).

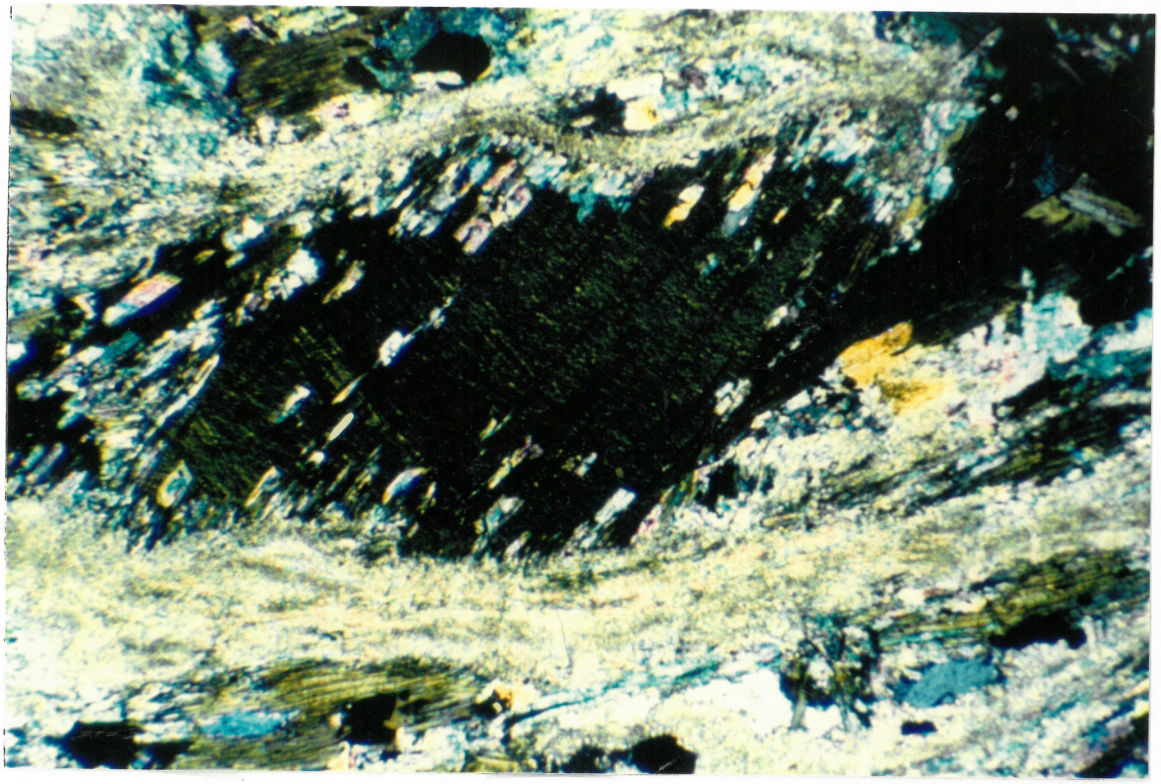

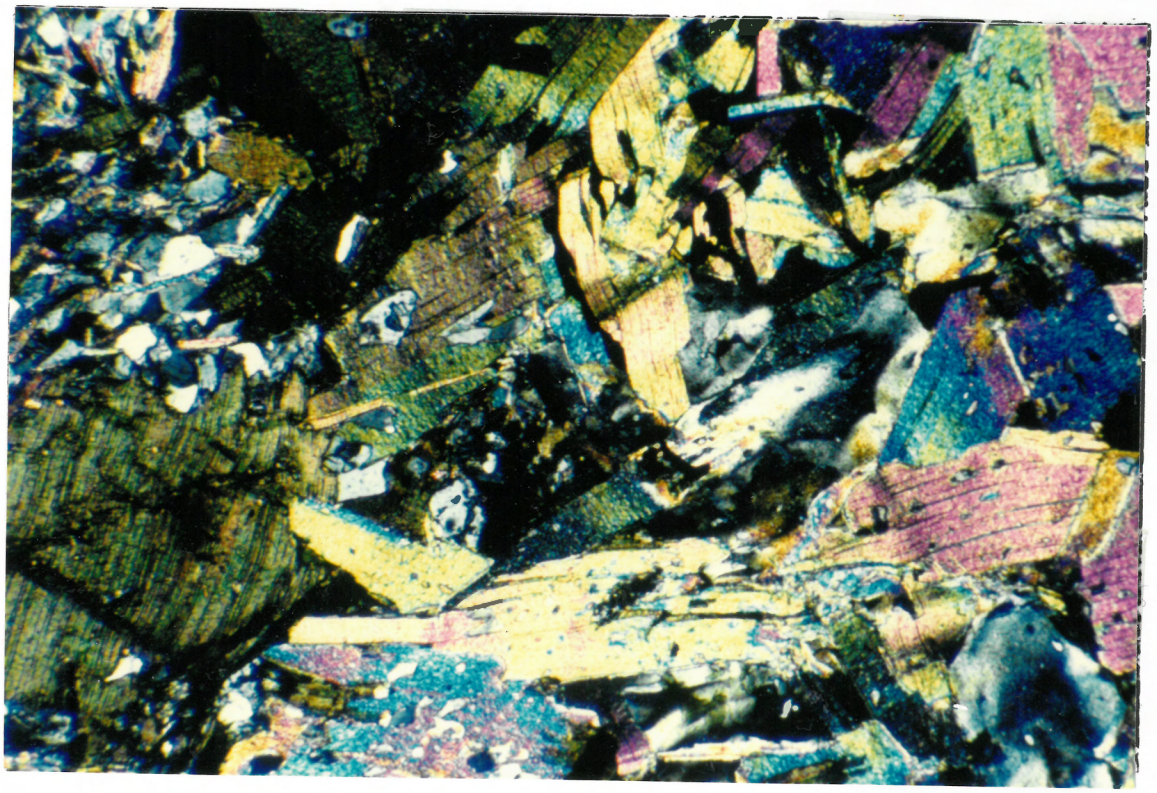

0.5 mm

Fig. 4.2-21. Photomicrograph of metapelite showing muscovite and chlorite (c) replacing staurolite (st). Note weak foliation defined by fine muscovite and quartz in the groundmass.

(Sample PE82-19)

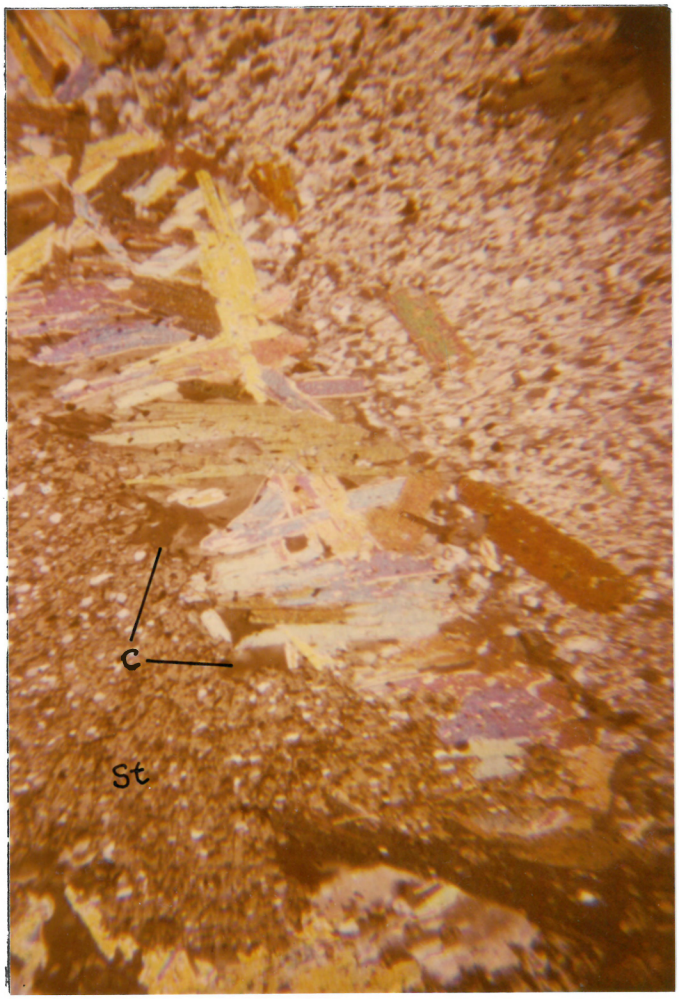
S2
C
St
0.5 mm

Distinct saddles occur in the spectra of seven biotite samples, suggesting at least one overprinting event. A pronounced 'staircase' pattern can be observed in the spectrum of muscovite sample PE84-77m, suggesting ^{40}Ar loss. The age maximum is 374 Ma, but the minimum is poorly defined. The age maximum is a reasonable estimate of the time when this sample first cooled below ca. 350° C.

Biotite apparent ages (t_T) range from 356 Ma to 294 Ma. (fig. 4.2-17). Of these, one sample (PE82-10) gave an eight step (75%) plateau age of 353 Ma. In this sample, biotite has grown parallel to a weakly-defined S_2, but shows little sign of strain (table 4.2-4). It is uncertain whether this plateau age reflects prolonged post-metamorphic cooling, or a later overprinting event, which caused recrystallization of biotite under a mild stress regime. The biotite sample with the lowest age is an excellent example of the extremes of overprinting in the Meguma terrane. Sample PE83-7b was obtained from strongly sheared metapelites of the sillimanite zone south of the Barrington Passage pluton (the complex domain, section 4.2.2). Biotite has been sheared into fish structures, and is largely replaced by chlorite and muscovite (fig. 4.2-19). The spectrum displays a wide shallow saddle, is moderately discordant (IDF=1.92), and yields a t_T age of 294 Ma. This age is remarkably similar to those obtained for dynamically recrystallized micas from the nearby Barrington shear zone (Dallmeyer and Keppie, 1986).

Muscovite apparent ages (t_T) range from 354-335 Ma. Samples PE84-121m and PE84-129 give plateau ages (67%, 90% ^{39}Ar) of 347 Ma and 348 Ma respectively. Corresponding IDF values are 2.76 and 0.99. Both of these samples are from the sillimanite zone, which is intruded by SSP plutons. Both samples have been strongly sheared (Appendix C). In sample PE84-121, coarse muscovite has partly replaced staurolite and biotite (fig. 4.2-20). It is possible that the age represents a mixture of this secondary muscovite and an older generation in the matrix. The age of 314 Ma for the partly chloritized biotite sample PE84-121B supports this interpretation. Alternatively, the plateau age of 347 Ma may be a minimum estimate of the time of retrograde metamorphism. In this case, the biotite age would represent a later event. The high discordance in the spectrum of sample PE84-121B (IDF = 11.57) is probably a reflection of the tectonothermal complexity of the domain from which it was derived (cf. Hwang and Williams, 1985). Sample PE84-129 was obtained from an area of intense shearing west of the Barrington Passage pluton. Muscovite is severely crenulated by a secondary fabric (Appendix C). A neighboring sample 100m away (PE84-41) is also strongly sheared, but free of alteration. Its spectrum is moderately discordant (IDF=1.68) and has a prominent saddle, with a t_T age of 346 Ma. The results from these two biotite-muscovite pairs suggest that biotite is more susceptible to the effects of tectonothermal events than muscovite. Even

though both minerals may have been subject to argon loss, the muscovite sample gives the less discordant spectrum. This is consistent with the higher closure temperature for muscovite. It is likely that the greater susceptibility of biotite to alteration causes redistribution of K as well as ^{40}Ar loss, leading to discordant spectra. The occurrence of well-defined plateaus in overprinted muscovite is not readily explained.

As Fig. 4.2-16 illustrates, these younger mica ages are spread throughout the RMT without regard for metamorphic zone boundaries. These young ages also occur in plutons, clearly illustrating that the controlling factor was post-metamorphic and probably post-plutonic.

4.2.5.6. SUMMARY OF MICA DATA FROM THE RMT

As figs. 4.2-14 and 4.2-17 illustrate, there is no clear gap between the ages of the 'younger micas' and those arbitrarily called the 'older micas'. Instead there is a gradation of ages from 401 Ma to 294 Ma, without any relationship to metamorphic facies. This distribution of apparent ages can be explained by :(1)diachronous cooling; (2) secondary overprinting; or (3) a combination of (1) and (2). Field and petrographic observations suggest that the ages are best explained by a complex tectonothermal history. The range of apparent ages among the younger micas is interpreted as a reflection of varying effects of an

overprinting event. Previous work (Chapter 1) in the Meguma terrane indicate that the overprinting event occurred about 290-320 Ma ago (e.g Zentilli and Reynolds, 1985; Dallmeyer and Keppie, 1986). The three samples with the lowest ages (294-318 Ma) are interpreted as representing those which suffered almost total ^{40}Ar loss. If allowance is made for diachronous cooling in the RMT, the mica dates, along with their inferred pre-SMB relative ages, suggest that regional metamorphism occurred approximately between 400 and 370 Ma ago. This is consistent with stratigraphic constraints, when uncertainties are taken into consideration.

4.2.6. FISSION TRACK DATA

One apatite sample was extracted from metawacke of the Goldenville Formation. The sample (PE82-10) is from the biotite zone. The coexisting biotite gave an eight step (74.9% ^{39}Ar) plateau age of 353 Ma. The apatite fission track age is 278 +/- 29 Ma. Details are listed in table 4.4-3. This age suggests that at least some parts of the RMT cooled to temperatures less than 100 degrees C soon after the overprinting event 320-290 Ma ago (section 4.2.6).

4.3. DATA BASE AND INTERPRETATION FROM THE SOUTHERN SATELLITE PLUTONS

4.3.1. INTRODUCTION

The SSP consist of eight medium- to small-sized bodies outcropping in southwestern Nova Scotia (map 2). Field mapping and petrographic studies suggest that the plutons intruded during or after regional metamorphism (De Albuquerque, 1977; Chu, 1978; White et al., 1985; Hope and Woodend, 1986; Rogers, 1986). On the basis of normative quartz, albite and orthoclase, De Albuquerque (1977) estimated that most of the SSP were intruded at pressures of 3.5-6.5 kbars (10-20 km depth). Composition of the SSP range from hornblende-biotite tonalite to two mica monzogranite, and are of calc-alkaline affinities (Rogers, 1986).

Ductile shear zones have been recognized in most of the SSP. Although these shear zones have not yet been mapped in detail, the effects can be seen in outcrop and in thin section. Quartz is stretched into elongate polycrystalline ribbons, feldspars are mechanically twinned, micas are kinked and sheared, and secondary minerals partly replace the original granitoid mineralogy. Plagioclase and biotite are partly replaced by an assemblage which includes muscovite (sericite), epidote, sphene, carbonate, and chlorite. This implies greenschist facies conditions (e.g.

Ferry, 1979). Shearing is not always associated with low ages (e.g. the Bald Mountain pluton, see below). This may mean that shearing was multiphase or that it was not always accompanied by loss of ^{40}Ar.

The best example of shearing in the SSP is the Brenton pluton to the extreme west in the Meguma terrane. Partly recrystallized porphyroclasts of plagioclase and microcline form augen in a matrix of recrystallized quartz ribbons, biotite and muscovite. Dynamically recrystallized biotite and muscovite from three samples were dated by the ^{40}Ar-^{39}Ar method (O'Reilly, 1976; Reynolds et al., 1981). Three biotite samples yielded total fusion ages of 316, 318, and 328 Ma. Coexisting muscovite yielded ages of 314, 323 and 318 Ma respectively. The average is 319.5 Ma. Ductile shear zones have also been recognized in the Seal Island pluton, 30 km west of Cape Sable Island (Rogers, 1986). Slightly deformed monzogranite grades into mylonite zones 20 cm wide. Quartz ribbons define excellent C-S fabrics (fig. 4.3-1), and micas have been dynamically recrystallized (fig. 4.3-2). Narrow (1m) ductile shear zones occur within the Port Mouton pluton (Woodend, 1986, personal comm.) The author has observed evidence for local shearing within the Shelburne, Barrington Pasage and Bald Mountain plutons.

The overprinting associated with the shearing is reflected in varying degrees of discordance in the age spectra from the SSP (table 4.3-1). Although there is no simple correlation between discordance and age (cf. section

Fig. 4.3-1. Photomicrograph of mylonitized monzogranite from the Seal Island pluton. Note granulation of feldspars and definition of C-S fabric by quartz ribbon aggregates (Sample 756; courtesy, Dean Rogers).

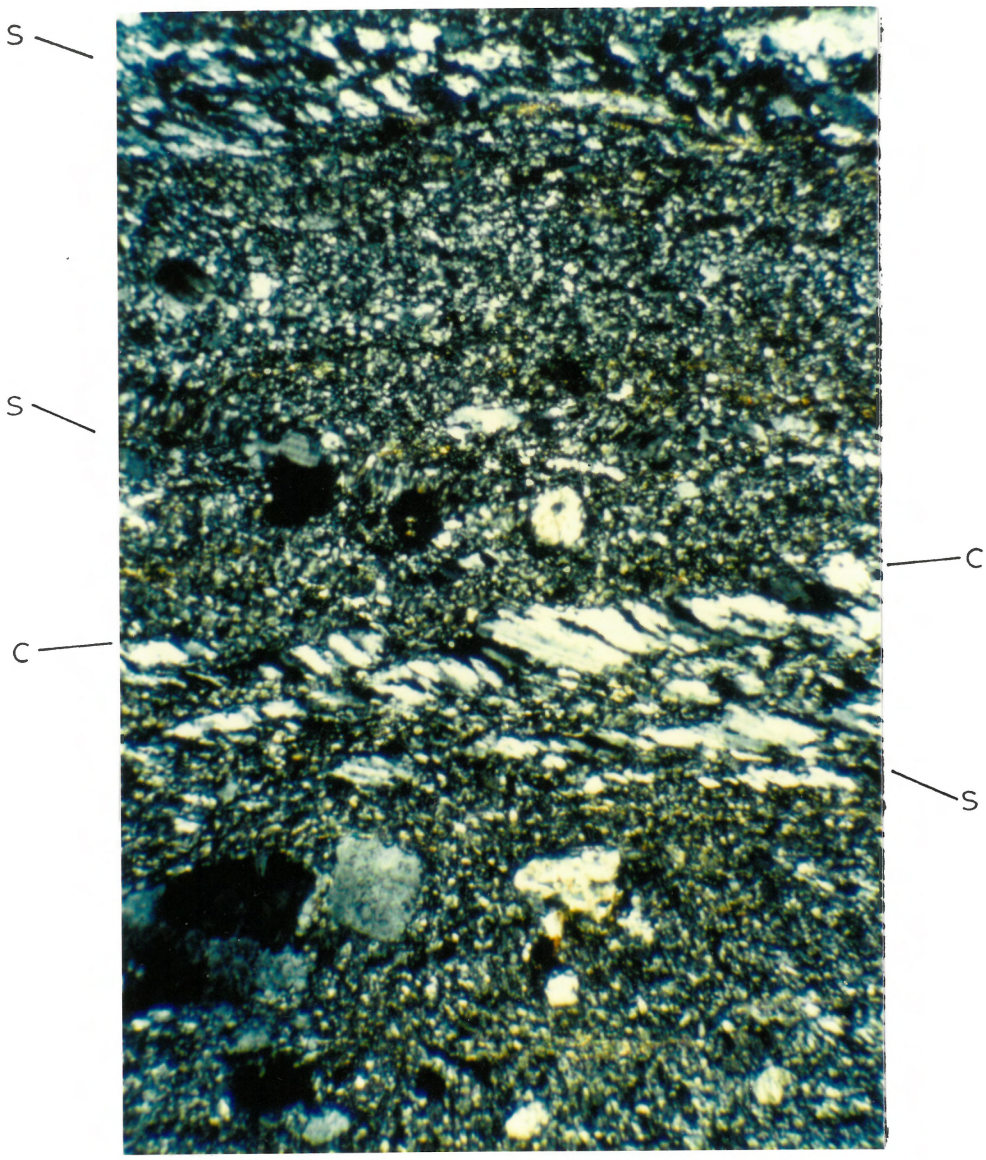
S
S
C
C
S
0.5 mm

Fig. 4.3-2. Photomicrograph of mylonitic monzogranite from the Seal Island pluton. Note mortar texture around microcline, and dynamically recrystallized muscovite, biotite, and quartz. (Sample 576; courtesy, Dean Rogers).

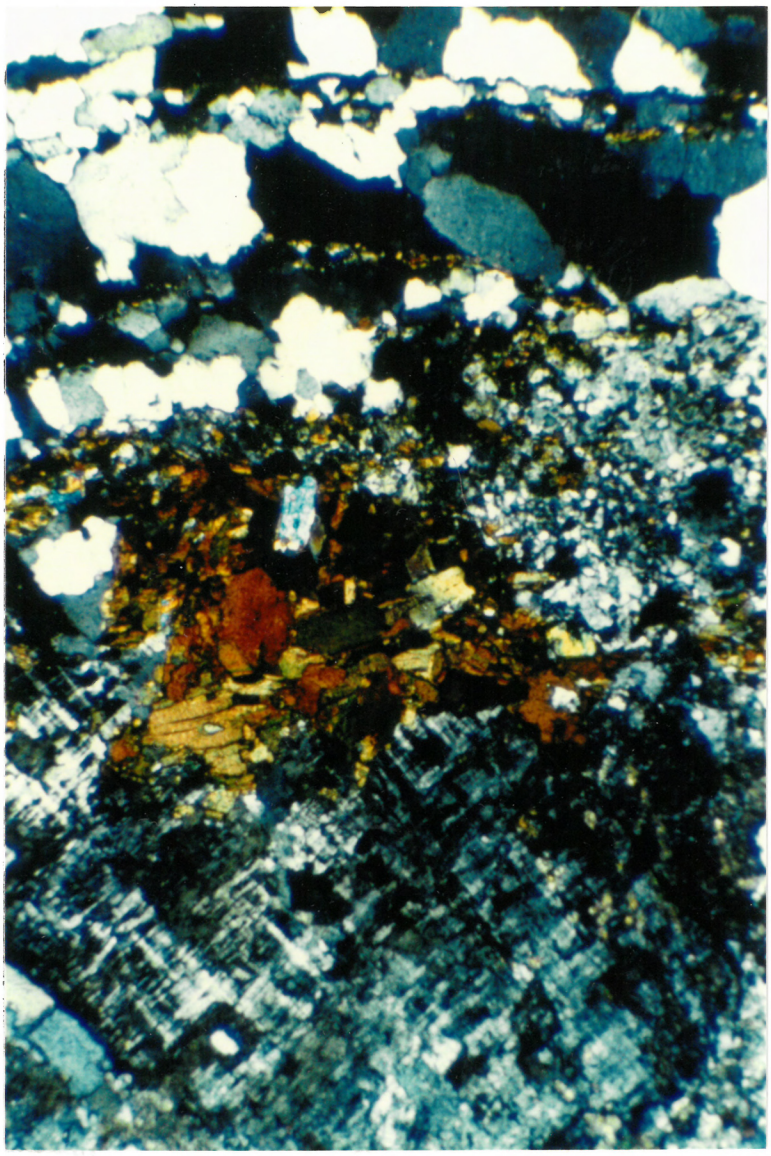

0.5 mm

4.2.5.1), the presence of saddles and staircase patterns in some spectra provides an overall link between the geological setting and the ^{40}Ar-^{39}Ar step-heating technique in explaining the low ages of the SSP (average = 312 Ma, see below). Since the SSP were apparently intruded during or after regional metamorphism, the ages can be constrained between 385 Ma (the approximate average age of regional metamorphism), and the highest apparent ages obtained from ^{40}Ar-^{39}Ar spectra. This approach depends on the assumption that excess argon is not a major factor (section 4.1.2). Data from each pluton are examined to determine the extent to which 'original' cooling ages can be deduced.

As stated in section 1.3, Reynolds et al., (1981), obtained $^{40}Ar/^{39}Ar$ ages for the SSP ranging from 353-297 Ma, with a mean of 312+/-22 Ma. To explain these data, they proposed three alternative hypotheses. They are:

Hypothesis (1): The SSP are much younger (by~70 Ma) than the SMB.

Hypothesis (2): The SSP are the same age as the SMB, but cooled much more slowly to their lower apparent ages.

Hypothesis (3): The SSP are the same age as the SMB, but were overprinted by later event(s).

These alternatives are reexamined in the light of new data obtained in this study. Hypotheses (2) and (3) are not mutually exclusive, but will be treated separately to simplify interpretation.

Several samples (fig. 4.3-3) were dated from the

following plutons: Bald Mountain, Barrington Passage, Port Mouton, Quinan and Shelburne. One sample from a pegmatite intruding RMT schists was also dated. Brief petrographic descriptions are given for each pluton. Detailed descriptions are included in Appendix C. The results, listed in Table 4.3-1, are discussed below.

4.3.2. BARRINGTON PASSAGE PLUTON

The Barrington Passage pluton is an irregularly shaped body about 475 km^2 in area, which intrudes the Halifax and Goldenville Formations in the region of upper amphibolite grade metamorphism (Rogers, 1985). It consists mainly of equigranular, medium-grained tonalite with minor diorite and granodiorite. A strong foliation defined mainly by parallel alignment of biotite is generally parallel to the main axial plane foliation in the surrounding country rocks, which suggests that intrusion may have been syntectonic with respect to folding in the country rocks (Rogers, 1986) The rock is generally fresh in appearance. Biotite is only very mildly chloritized, but it is replaced locally by epidote, sphene, carbonate, and minor muscovite. This greenschist assemblage suggests that the pluton was subjected to an overprinting event at moderate temperatures, during which biotite remained stable. Analysed samples consist of two hornblendes, four biotites, and one muscovite. Spectra are displayed in fig. 4.3-4.

Table 4.3-1. APPARENT AGES AND DISCORDANCE FACTORS FOR SAMPLES FROM THE SOUTHERN SATELLITE PLUTONS

SAMPLE	PLUTON	PHASE	AGE (Ma)	IDF	CS Ma	%
PE84-27	BM	Mu	336	1.53	1.2	0.4
PE84-28	BM	Mu	369	1.01	3.8	1.0
PE84-29	BM	Mu	365	0.65	1.7	0.5
PE84-30	BM	Mu	370	0.73	5.0	1.4
PE83-9	BP	Hb	371	7.62	8.4	2.3
PE83-9	BP	Bi	325	1.25	2.6	0.8
PE84-39	BP	Bi	316	1.60	2.5	0.8
PE84-39	BP	Ksp	271	5.42	2.0	0.8
PE84-114	BP	HB	372	2.65	4.3	1.2
PE84-114	BP	Bi	344	1.32	2.7	0.8
PE84-118	BP	Bi	318	0.72	2.0	0.6
PE84-118	BP	Plag	280	12.99	12.8	4.6
PE84-119	BP	Mu	347	0.64	3.8	1.1
PE84-127A	PM	Mu	318	2.57	3.8	1.2
PE84-127A	PM	Ksp	255	4.05	2.1	0.8
PE84-125	PM	Mu	343	2.50	1.5	0.4
S456	PM	Bi	321	0.74	2.25	0.7
PE84-43B	Q	Bi	348	1.34	1.7	0.5
BQ-1	Sh	Bi	370	2.43	1.8	0.5
BQ2	Sh	Bi	371	0.62	3.1	0.8
PE84-34	Sh	Mu	337	2.96	2.1	0.6
PE84-45	Sh	Mu	341	0.36	2.9	0.8
PE84-46	Sh	Mu	361	0.52	2.3	0.6
PE84-46	Sh	KSp	261	5.70	2.4	0.9
PE84-53	Sh	Mu	342	1.01	1.8	0.5
PE84-53	Sh	Bi	309	2.26	2.1	0.7
PE84-54	Sh	Mu	348	2.12	8.0	2.3
PE84-54	Sh	Ksp	260	6.44	1.4	0.5
PE92-20P	UC	Mu	351	0.45	1.2	0.5

Fig. 4.3-3. Sample locations for the SSP.

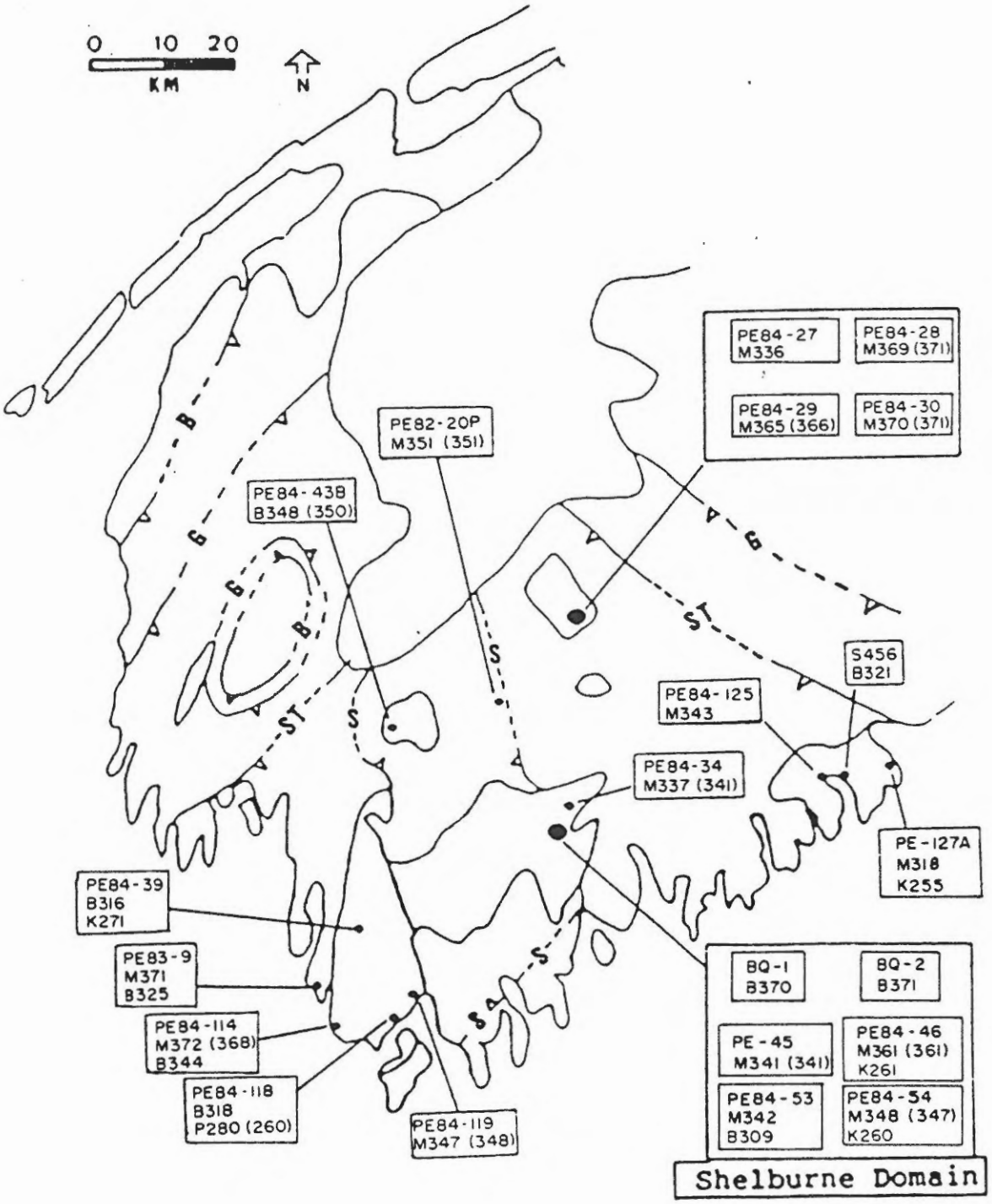
0 10 20
KM
N
PE84-27
M336
PE84-28
M369 (371)
PE84-29
M365 (366)
PE84-30
M370 (371)
PE82-20P
M351 (351)
PE84-438
B348 (350)
S456
B321
PE84-125
M343
PE84-34
M337 (341)
PE-127A
M318
K255
PE84-39
B316
K271
PE83-9
M371
B325
PE84-114
M372 (368)
B344
PE84-118
B318
P280 (260)
PE84-119
M347 (348)
BQ-1
B370
BQ-2
B371
PE-45
M341 (341)
PE84-46
M361 (361)
K261
PE84-53
M342
B309
PE84-54
M348 (347)
K260
Shelburne Domain

Sample PE83-9 is from a hornblende-biotite tonalite (Lyons Bay pluton of Rogers, 1986). A weak to moderate foliation is defined by parallel alignment of biotite and hornblende, but no sign of shearing is apparent. Its location, texture and mineralogy suggest affinities with marginal phases of the Barrington Passage pluton (see below). The spectrum of hornblende sample PE83-9 is highly discordant (IDF=7.62) and displays a staircase pattern typical of samples which have experienced ^{40}Ar loss. The age minimum (time of overprinting) is poorly defined but the age maximum suggests an apparent cooling age of 386 Ma. This apparent cooling age is slightly higher than that of the SMB. It is uncertain whether this represents minor contamination by excess argon, as suggested by the first step, or cooling below 500 degrees C very soon after regional metamorphism, as suggested by the field relationships (Rogers, 1986). Sample PE84-114 is a hornblende-biotite tonalite from the western margin of the Barrington Passage pluton. A moderate foliation is defined by parallel alignment of biotite and hornblende. Biotite shows minor peripheral chloritization and is partly recrystallized around the edges. Quartz is partly recrystallized (Appendix C). It is mineralogically similar to sample PE83-9, obtained 4.5 km to the west. The spectrum for hornblende sample PE84-114 is internally discordant (IDF = 2.65), but defines a three-step (57% ^{39}Ar) plateau age of 368 Ma. This is very similar to its t_T age (371 Ma), and

Fig. 4.3-4. Age spectra of samples from the Barrington Passage pluton.

Bars on vertical axes represent 10 Ma.

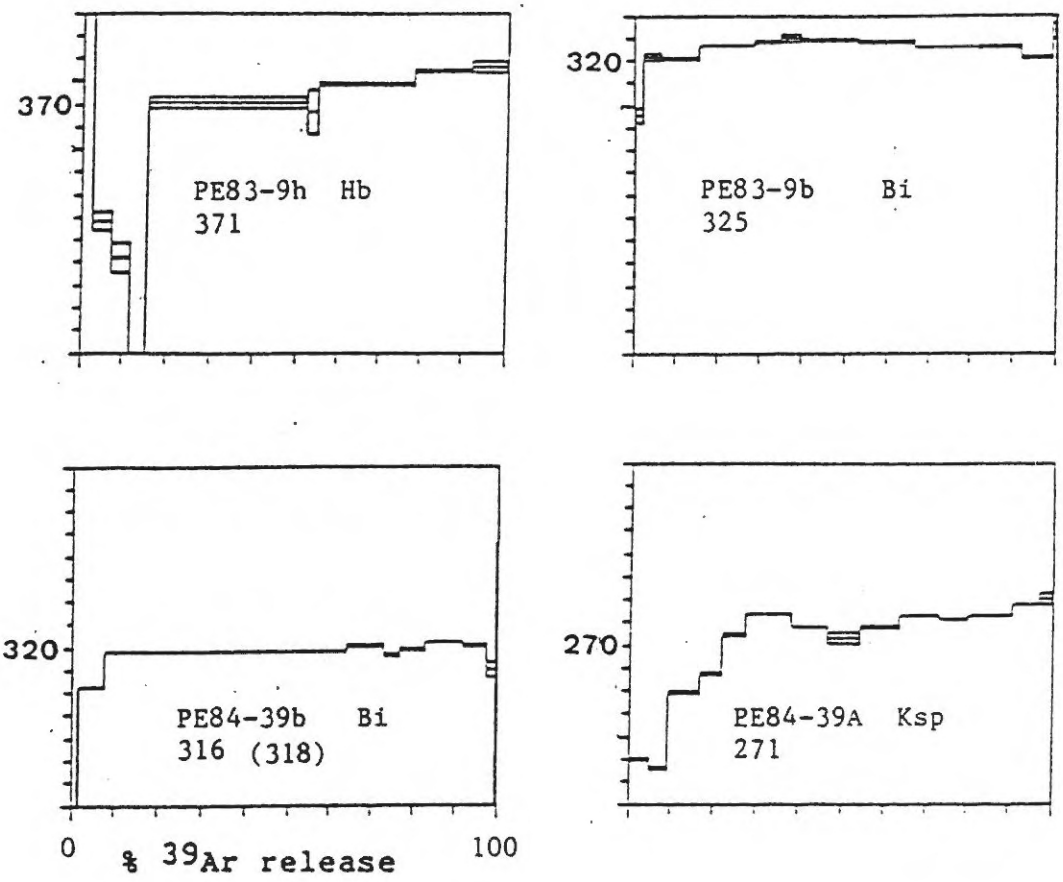
370
PE83-9h Hb
371
320
PE83-9b Bi
325
320
PE84-39b Bi
316 (318)
270
PE84-39A Ksp
271
0
% 39Ar release
100

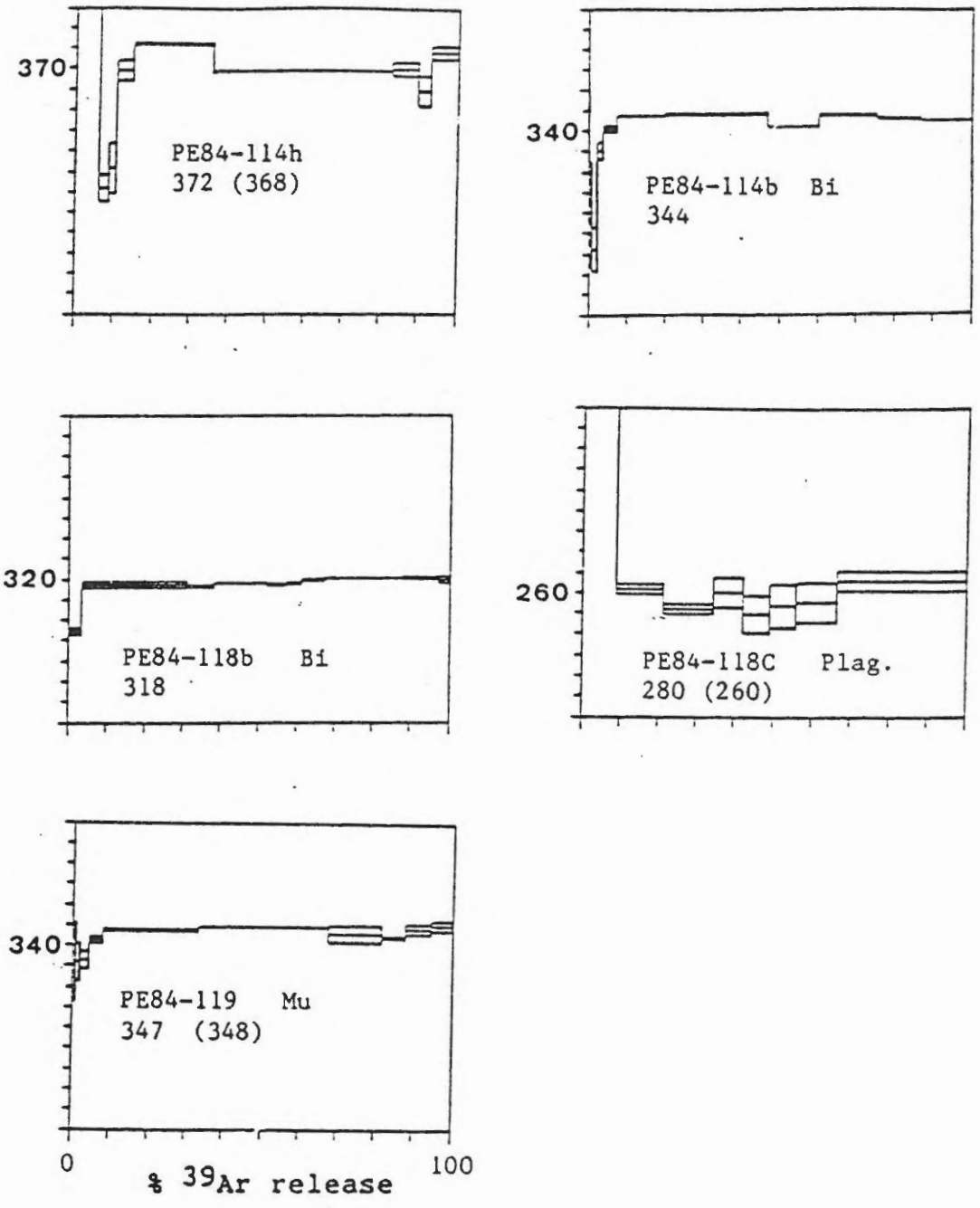
370
PE84-114h
372 (368)
340
PE84-114b Bi
344
320
PE84-118b Bi
318
260
PE84-118C Plag.
280 (260)
340
PE84-119 Mu
347 (348)
0
100
% 39Ar release

the age of the major plutonic event in the Meguma terrane (SMB). The high-temperature part of the spectrum gives an age maximum of 378 Ma. This suggests the possibility that the margin of the pluton may have cooled prior to 370 Ma ago, that is, the Barrington Passage pluton is slightly older than the SMB. The spectra of coexisting biotite samples PE83-9 and PE84-114 show slightly contrasting features. The spectrum of sample PE83-9 displays no saddle and is fairly concordant (IDF=1.25). There is no plateau: apparent ages increase slightly towards the intermediate steps, after which a steady decrease is seen - a 'double staircase' pattern. A moderate saddle occurs in the spectrum of sample PE84-114, suggesting an overprinting event. The t_T ages are 325 Ma and 344 Ma suggesting that sample PE83-9 has suffered greater ^{40}Ar loss. Thus the sample which displays the saddle has apparently suffered the lesser argon loss. It is conceivable that biotite sample PE83-9 was completely outgassed about 325 Ma ago by the same event that produced the apparent ^{40}Ar loss in the coexisting hornblende. The age difference between biotite and hornblende for samples PE83-9 and PE84-114 are 61 Ma and 21 Ma respectively. If these ages were taken to represent simple post-intrusive cooling, the implication would be that cooling in the margin of of the pluton from 500 to 300 degrees C lasted 28-61 Ma. This unlikely scenario (cf. Shepherd et al., 1985) is additional evidence of a substantial post-intrusive overprint.

Sample PE84-39 is a medium-grained equigranular tonalite. Biotite, which defines a weak foliation, is slightly chloritized, and is overgrown by minor muscovite. Plagioclase is moderately saussuritized. The spectrum of biotite sample PE84-39 is fairly concordant (IDF = 1.60), but a small saddle is present. A three-step plateau (56 % ^{39}Ar) defines an age of 318 Ma, which is similar to the t_T age of 316 Ma. The age of this sample is interpreted to reflect near complete outgassing of biotite about 318 Ma ago.

Sample PE84-118 is a biotite tonalite in which a weak foliation is defined by parallel alignment of biotite. Minor alteration of biotite and plagioclase produced an assemblage of sphene, epidote, carbonate, and muscovite (mainly sericite). The spectrum of biotite sample PE84-118 is highly concordant (IDF=0.72), but displays no plateau because of high precision (CS = 0.6%). Although this sample apparently suffered the greatest ^{40}Ar loss (t_T=318 Ma), there is no saddle in the spectrum. This age is interpreted to represent near complete outgassing of biotite about 318 Ma ago.

Sample PE84-119 is from a coarse pegmatitic two mica monzogranite which intruded the tonalite phase of the Barrington Passage pluton. It is strongly sheared, with muscovite partly overgrowing biotite (Appendix C). The spectrum of muscovite sample PE84-119 gives a three-step plateau (73.4% of the gas) with an apparent age of 348 Ma.

As for the Shelburne pluton, the pegmatite which is the latest intrusive phase, gives the older mica age. This may be partly explained by the fact that muscovite has a higher closure temperature than biotite (e.g. Wagner et al., 1977), or that the pegmatite contained minor excess argon. This may also be due to greater resistance of the (coarser) pegmatite micas to post-intrusive ^{40}Ar loss.

In summary, the Barrington Passage pluton records a hornblende cooling age of 386-372 Ma. The mica ages have been variably reset, but the amphiboles have apparently lost little or no ^{40}Ar. The age of this pluton is constrained between 386 and 372 Ma. The latest major overprinting occurred about 318 Ma ago, as suggested by the spectra of biotite samples PE84-39 and PE84-118. This time is remarkably similar to the inferred time of dynamic recrystallization in the Brenton pluton (section 4.3.1).

4.3.3. BALD MOUNTAIN PLUTON

The Bald Mountain pluton (~60 km^2) is a rectangular body intruding the Goldenville formation (amphibolite facies) in Shelburne County (Rogers, 1986). It consists of medium-grained equigranular biotite-muscovite monzogranite. A strong anastomosing penetrative fabric can be observed in outcrop. The foliation is defined by alignment of muscovite, feldspar, and lenticular quartz. This steep NE trending foliation is nearly parallel to the axial plane

foliation in the country rocks (Rogers, 1986). This implies that intrusion of this pluton could be pre- to syn-tectonic with respect to deformation in the Meguma terrane. Alternatively, the near coincidence of the two structures may represent reactivation of older plane of weakness in the country rocks during later shearing of the pluton. Muscovite is moderately kinked, feldspars are strongly sheared, and saussuritized, and biotite is almost completely chloritized. Plagioclase is apparently albitized (An=1.2-5.3). The pluton was sampled in 4 approximately evenly spaced locations along a 3.5 km transect. From west to east, the samples are: PE84-27, PE84-28, PE84-29, and PE84-30 (fig. 4.3-3). Sample PE84-27 is more intensely stained (hematitic), reflecting probable local variation in fluid content. Microprobe analyses reveal very little chemical differences among the muscovite samples (table 4.3-2).

All of the spectra (fig. 4.3.5) show some discordance, with low ages in the initial steps, suggestive of ^{40}Ar loss. The most discordant spectrum is that of sample PE84-27 (IDF=1.53, table 4.3-1). There is a small but distinct saddle in this spectrum, which, as shown in Section 4.2.5, is often associated with overprinting. The t_T age of this sample is 336 Ma, the lowest of the four. Spectra from the other three samples are quite similar. The spectrum for sample PE84-28 displays a seven step plateau of 371 Ma, representing 84% of the gas. There is a four step plateau

Table 4.3-2. Chemical data for Bald Mountain Muscovites

Sample	K/Al	K/(K+Na)	F/FM	Si/Al
PE84-27	.307	.919	.529	3.43
PE84-28	.344	.949	.509	3.39
PE84-29	.328	.927	.507	3.41
PE84-30	.284	.945	.494	3.41

(atomic ratios).

Fig. 4.3-5. Age spectra of samples from the Bald Mountain pluton.
Bars on vertical axes represent 10 Ma

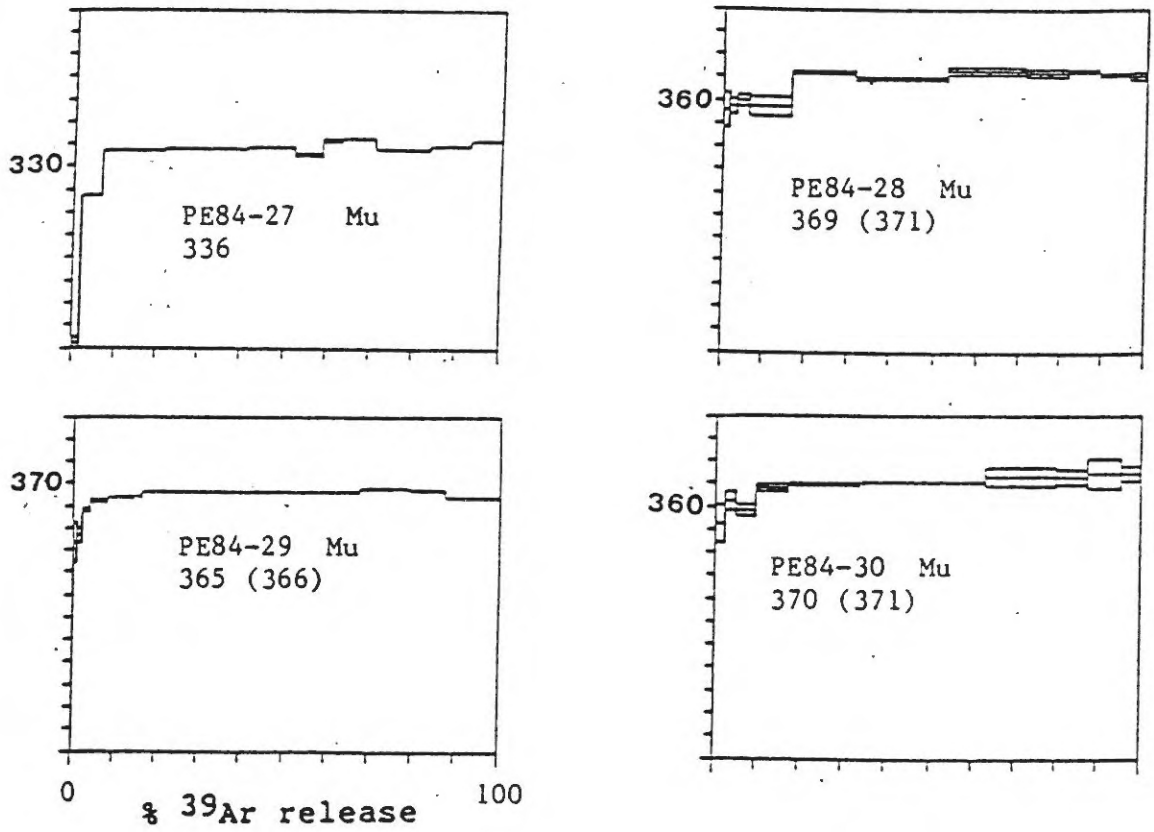
330
PE84-27 Mu
336
360
PE84-28 Mu
369 (371)
370
PE84-29 Mu
365 (366)
360
PE84-30 Mu
370 (371)
0
100
% 39Ar release

in the spectrum of sample PE84-29, representing 70.8% of the gas, giving an age of 366 Ma. A plateau age of 371 Ma is given by sample PE84-30. The plateau is represented by seven steps, constituting 90.3% of the gas.

The plateau ages are similar to that of the SMB, indicating that the Bald Mountain pluton cooled to ca. 350° C. at about the same time as the SMB. The lower age of sample PE84-27 (336 Ma), along with its discordant spectrum, further illustrates that the overprinting event described above was of varying intensity within the Meguma terrane.

4.3.4. THE SHELBURNE PLUTON

The Shelburne pluton is a lobate body outcropping over an area of about 285 km^2 (Rogers, 1985). It intrudes the Goldenville and Halifax Formations at upper amphibolite grade. The pluton consists of medium-grained equigranular monzogranite, with minor amounts of tonalite, and granodiorite. Pegmatite and aplite dykes are common. The pluton is generally undeformed (Muecke, 1986, personal comm.), but is sheared locally. This suggests that intrusion post-dated regional deformation. Both biotite and muscovite occur as minor phases. Except for minor saussuritization of feldspars and chloritization of biotite, these rocks show little evidence of alteration. Eight samples were analysed (fig. 4.3-6). Seven of them were

Fig. 4.3-6.

Map of domain within the Shelburne pluton.
BQ = Birchtown Quarry.
For location, see fig. 4.3-3.

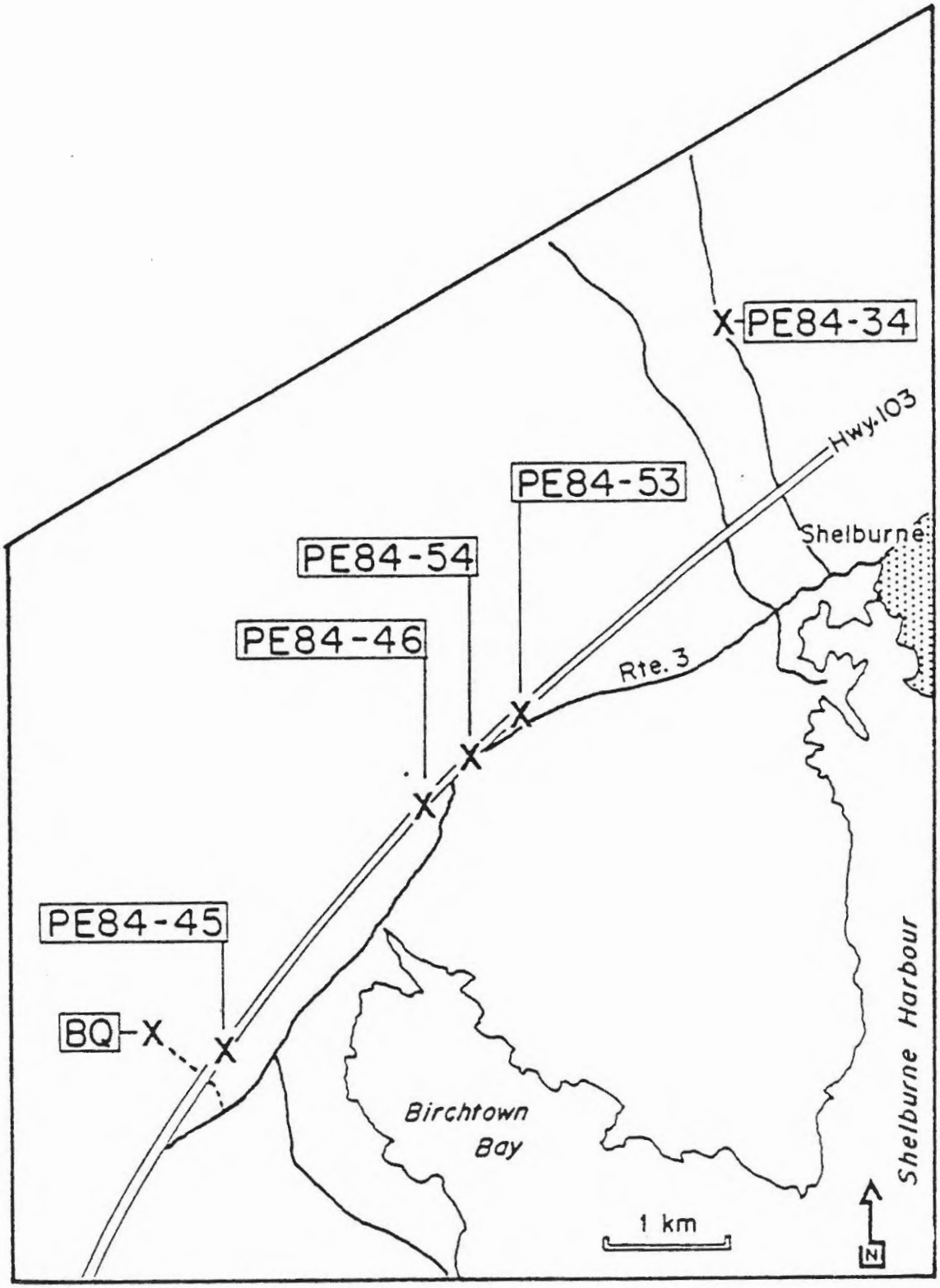
PE84-34
Hwy.103
PE84-53
Shelburne
PE84-54
PE84-46
Rte. 3
PE84-45
BQ
Birchtown
Bay
Shelburne Harbour
1 km
N

Fig. 4.3-7. Age spectra of samples from the Shelburne pluton.

Bars on vertical axes represent 10 Ma.

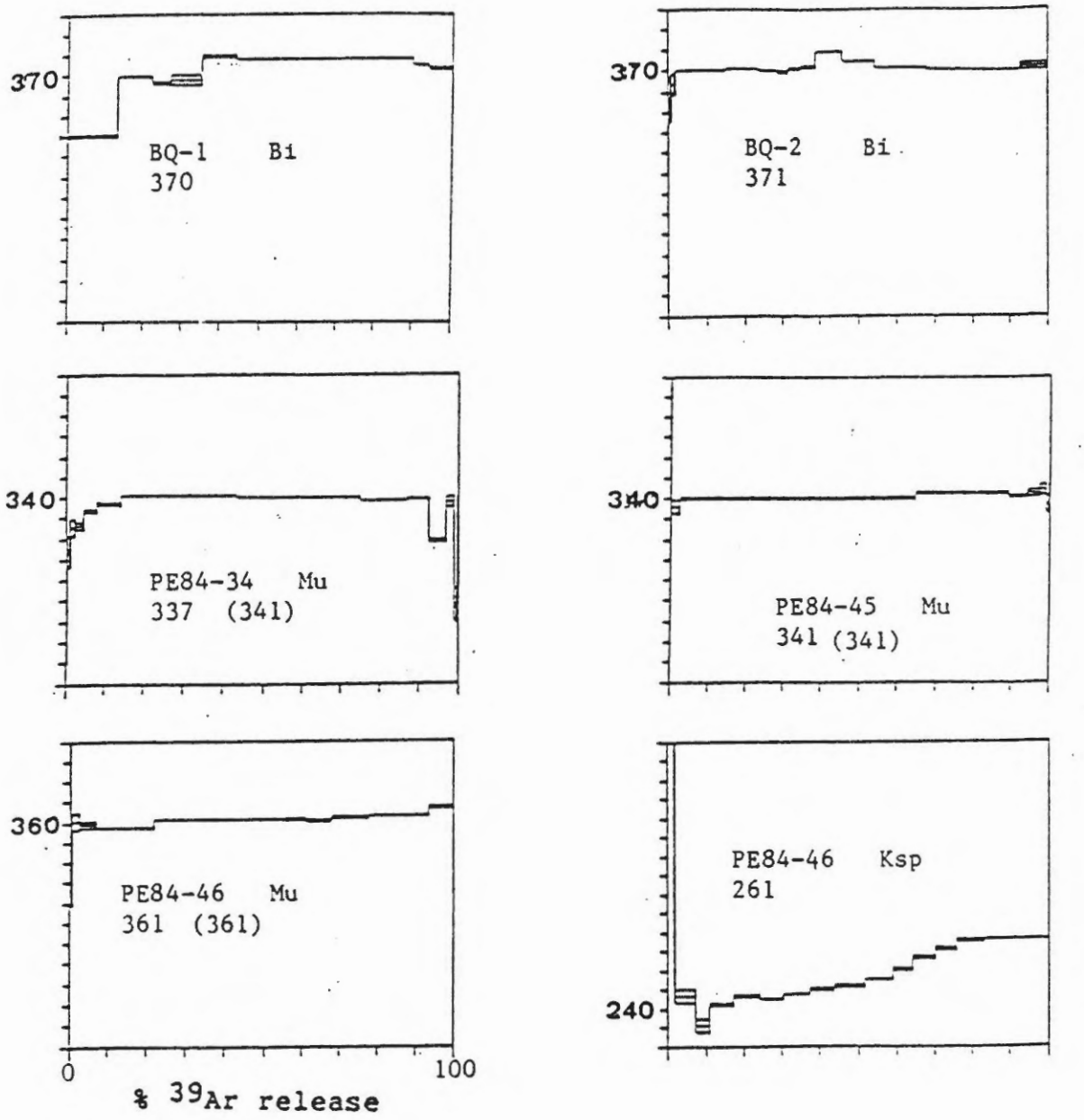
370
BQ-1 Bi
370
370
BQ-2 Bi
371
340
PE84-34 Mu
337 (341)
340
PE84-45 Mu
341 (341)
360
PE84-46 Mu
361 (361)
PE84-46 Ksp
261
240
0
100
% 39Ar release

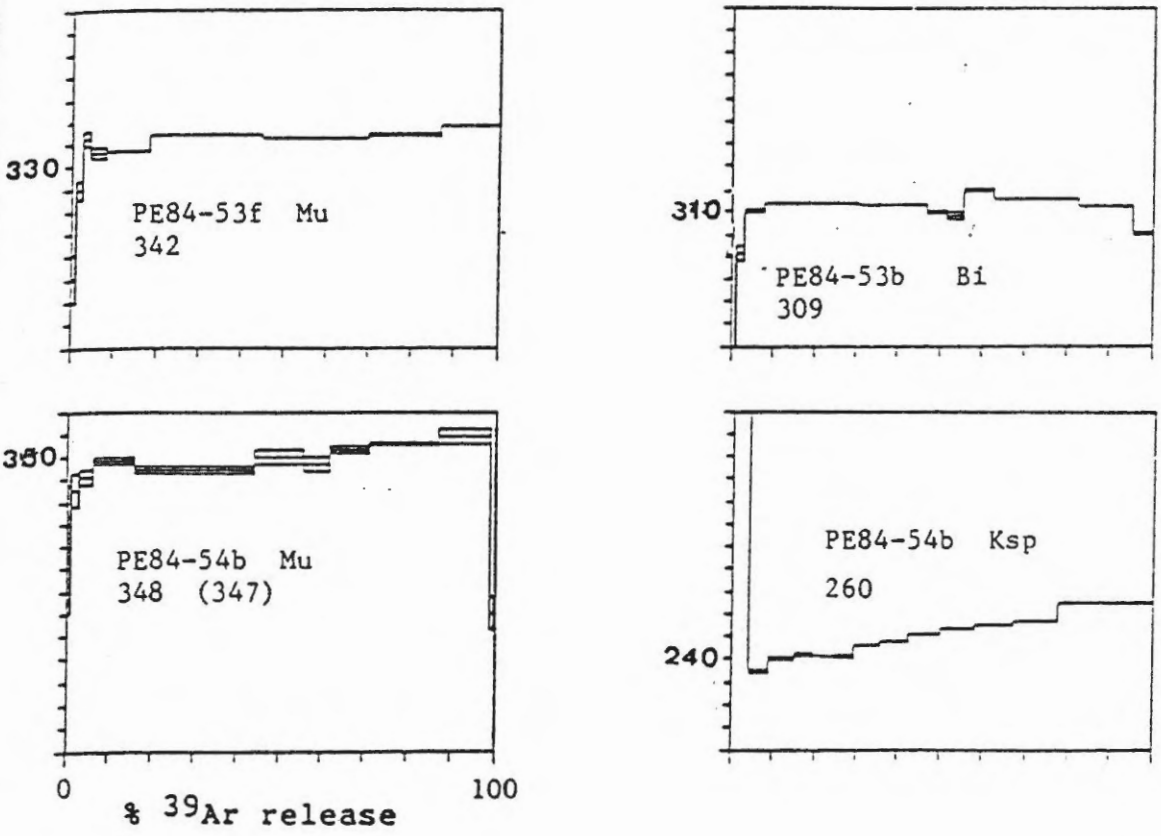
330
PE84-53f Mu
342
310
PE84-53b Bi
309
350
PE84-54b Mu
348 (347)
PE84-54b Ksp
260
240
0
100
% 39Ar release

taken over a distance of 4 km. They are discussed in detail to illustrate the complex tectonothermal history to which the SSP were subjected. The samples are described in order from west to east. Spectra are displayed in fig. 4.3-7.

The Birchtown Quarry quartz diorite is massive and intruded by the Shelburne monzogranite (Rogers, 1984, pers.comm); it is probably an early precursor of the main intrusive phase of that pluton. Two samples were collected 10 m apart. Except for minor peripheral replacement of biotite by sphene and rutile, neither sample shows any sign of significant alteration. Biotite, which partly overgrows hornblende, was extracted and analysed. The biotite samples are chemically similar (K/(K+Na) = .97, .96; F/(FM) = .30, .33, Appendix B). Both spectra are discordant, suggesting thermal overprinting. They differ in detail. The spectrum of sample BQ-1 displays a staircase profile, with moderate discordance (IDF = 2.43). A two-step plateau age (54.7 % ^{39}Ar) of 378 Ma is defined. In contrast, the spectrum of sample BQ-2 displays an 'inverted saddle', is less discordant (IDF = .62), and does not show a plateau (as defined by Fleck et al., 1975). Their t_T ages are indistinguishable (370, 371 Ma). This suggests either that these samples suffered no loss of ^{40}Ar, or that the loss was the same for both. Hence, over a distance of 10 m, a post-intrusive event appears to have had similar effects on the t_T ages, but contrasting effects on the details of the spectra.

Slightly kinked unaltered muscovite (PE84-45B) was extracted from the fault gouge of a narrow (.5 m) brittle fault within the Shelburne monzogranite, 0.6 km southeast of the Birchtown Quarry. The spectrum defined a plateau age of 341 Ma (99 % ^{39}Ar). This spectrum is very well-defined (IDF = 0.36, CS = 0.8 %).

Sample PE84-46 is from a muscovite pegmatite, which intrudes the Shelburne monzogranite 2.4 km east of PE84-45B. The pegmatite is about 1 m thick and consists of microcline, quartz and muscovite. It is slightly sheared, but large domains of apparently undeformed rock remain, from which the sample was taken. The spectrum is quite concordant (IDF = 0.52), but because of high precision (CS = 0.6%), the plateau age of 361 Ma, is defined by only four steps (55.4% ^{39}Ar). The t_T age is also 361 Ma.

Another pegmatite sample PE84-54B was obtained 0.5 km to the east of PE84-46. Its description and geologic setting are similar to that of PE84-46. The spectrum defines a 'staircase' pattern characteristic of ^{40}Ar loss (e.g.Turner 1968). The age maximum is 359 Ma, similar to the youngest phase of the SMB. This spectrum displays a four step plateau (55.1% ^{39}Ar, similar to PE84-46). The plateau age is 347 Ma, the same as the t_T age.

Sample PE84-53F was obtained 0.5 km to the east. It was taken from undeformed, unaltered Shelburne monzogranite. Both biotite and muscovite were analysed. The muscovite spectrum is highly concordant (IDF = 1.0), but because of

the high precision (CS = 0.5%), no plateau was defined. The t_T age is 342 Ma. This is significantly lower than that of the pegmatite (PE84-46) which intrudes the monzogranite 1 km to the west, but overlaps that of pegmatite sample PE84-54B. This apparent age reversal may be explained by minor excess argon in the pegmatite samples. It may be noted that spectra from the pegmatite samples do not display any of the features seen in the spectrum of a muscovite sample thought to contain excess argon (Harrison and McDougall, 1981). Alternatively, the age reversal may reflect differences in ^{40}Ar loss during overprinting.

The spectrum for the coexisting biotite (PE84-53B) is discordant, (IDF = 2.26), with a small but distinct saddle. The t_T age of 309 Ma is the lowest among the mica ages from the SSP. It contrasts sharply with the Birchtown Quarry biotite ages, which are the highest mica ages in the SSP. Chemically, this biotite is slightly different from the Birchtown Quarry samples (F/(FM) = .67, K/(K+Na) = .99, (Appendix B). The slightly higher annite content of biotite sample PE84-53B may be partly responsible for its greater susceptibility to ^{40}Ar loss (e.g. Harrison et al., 1985).

Hence biotite shows a sharp age gradient of 62 Ma over a distance of 4 km in rocks that are apparently undeformed and which show few signs of alteration. The difference in apparent age between muscovite and coexisting biotite may be explained by the difference in their closure temperatures. The following observations may be made.

(1) The sharp age gradients and apparent reversal of ages with respect to intrusive sequence can be explained by overprinting event(s). This is reflected in the discordance in some spectra.

(2) Evidence for overprinting is not always present in the spectra. Muscovite sample PE84-45 produced the best defined plateau, in spite of the fact that the rock was pulverized and weathered (fault gouge). Possibly, muscovite was completely recrystallized about 341 Ma ago during brittle shearing. Details of the age spectra are apparently not reproducible over a distance of 10 m (Birchtown Quarry), although the t_T age is reproducible (cf. section 3.5).

(3) If it is assumed that the entire pluton cooled to mica argon retention temperatures at about the same time, it may be concluded that the apparent ages (t_T) observed are inversely proportional to loss of ^{40}Ar. The inference is that the Birchtown Quarry samples experienced the least ^{40}Ar loss while the biotite sample, PE84-53, suffered the most. The pegmatite samples, which give apparent ages slightly higher than the monzogranites they intrude, were more resistant to argon loss because of their larger grain size. This is what would be expected if ^{40}Ar loss was controlled by a process of thermally driven volume diffusion.

The eighth sample, PE84-34, was collected from the two-mica monzogranite 3.3 km northeast of sample PE84-53, to which it is texturally similar. The spectrum of muscovite sample PE84-34 is moderately discordant (IDF = 2.96) and

displays a staircase profile for the first six steps, after which a two step plateau (50.5% ^{39}Ar) is defined. A small, but distinct, saddle occurs in the high temperature end of the spectrum. These features suggest tectonothermal disturbance. The age (t_T = 337 Ma, t_p = 341 Ma) is very similar to that of muscovite sample PE84-53.

When the Birchtown Quarry samples are included, the Shelburne pluton records mica ages of 371-309 Ma. The age of the pluton is constrained between 371 and 385 Ma (the average age of regional metamorphism). If the Birchtown Quarry samples are excluded, the age of the pluton is constrained between 359 and 385 Ma.

4.3.5. PORT MOUTON PLUTON

The Port Mouton Pluton is an elliptical granitoid complex 20km long by 9km wide. It consists of at least nine phases which show cross cutting relationships (Hope and Woodend, 1986). They include monzogranite, granodiorite, tonalite, minor pegmatites and lamprophyre. Deformation is confined to sporadic shear zones (Woodend, personal comm., 1986). Within a few hundred metres of the pluton, a thermal aureole is superimposed on the regional metamorphic assemblage. This pluton was, therefore, intruded after regional metamorphism. Three samples were analysed: (1) biotite sample S456 from the oldest intrusive phase (slightly sheared tonalite); (2) muscovite sample PE84-125

Fig. 4.3-8. Age spectra of samples from the Port Mouton pluton.

Bars on vertical axes represent 10 Ma.

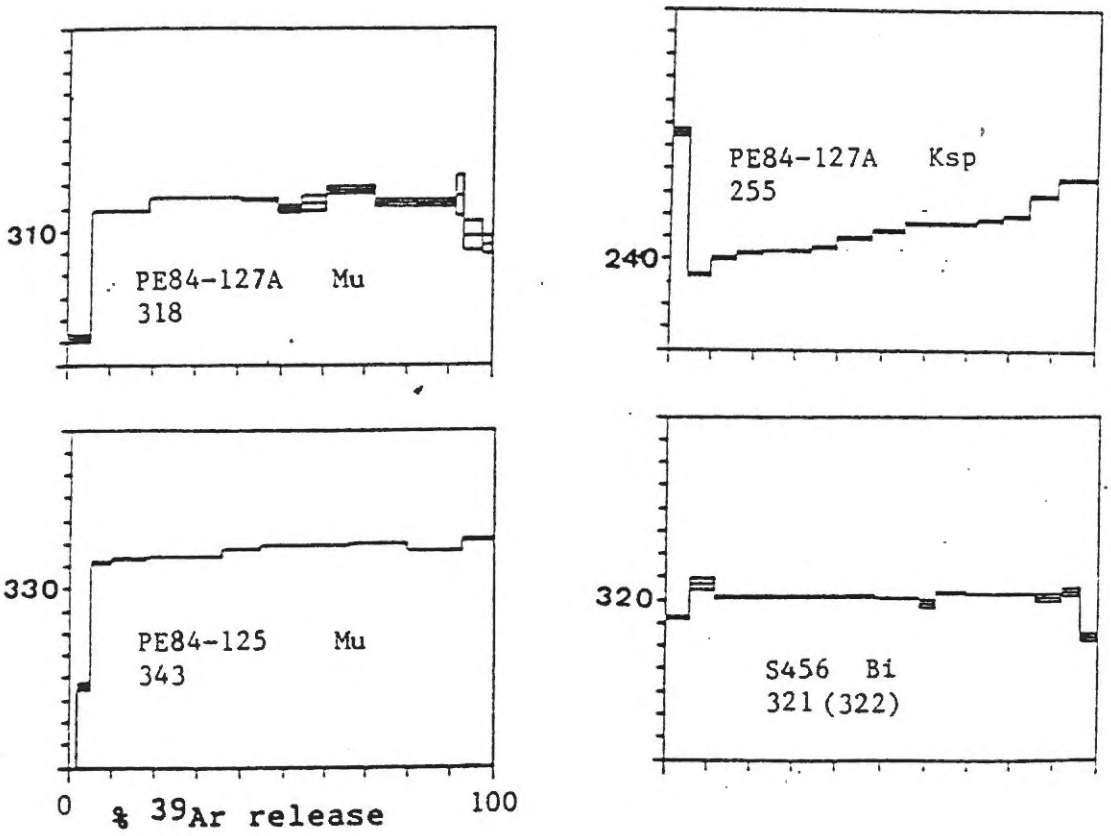
310
PE84-127A Mu
318
240
PE84-127A Ksp
255
330
PE84-125 Mu
343
320
S456 Bi
321 (322)
0
% 39Ar release
100

from a moderately sheared monzogranite intermediate in the intrusive sequence; and (3) muscovite sample PE84-127 from a pegmatite (presumably latest in the intrusive sequence).

All three spectra (fig. 4.3-8) display some discordance, with relatively low apparent ages in the first few steps, which represent a small percentage of the gas. Spectra from the two muscovite samples are more discordant (IDF = 2.50, 2.57) than that of the biotite (IDF = 0.74). A subdued staircase profile can be observed in the spectrum of muscovite sample PE84-125. The age maximum is 352 Ma, but the age minimum (time of overprinting) is poorly defined. Muscovite sample PE84-125 gave a t_T age of 343 Ma while muscovite sample PE84-127 gave a t_T age of 318 Ma, similar to that of biotite sample S456 (the oldest in the intrusive sequence). The biotite spectrum defines a plateau age of 322 Ma, which is similar to that of the Wedgeport pluton (Keppie et al., 1983), and the deformation age of the Brenton pluton (Reynolds et al., 1981). It probably represents the time of near complete resetting of the K-Ar system in this sample. The discrepancy between the intrusive sequence and apparent ages supports the view that the age pattern is controlled by post-intrusive event(s). The age difference of 25 Ma between muscovite samples PE84-125 and PE84-127 is consistent with the inferred sequence of intrusion (Hope and Woodend, 1986), but the internally discordant spectra and evidence for local post-intrusive deformation suggest that the age contrast may

be due to differences in ^{40}Ar loss during a tetonothermal event.

Recently acquired preliminary data (Woodend, 1986, personal comm.), support the above interpretation. Biotite from an undeformed, unaltered domain of the granodiorite unit at the same location as pegmatite sample PE84-127 (fig. 4.3-3), produced a spectrum with a small, but distinct saddle. The t_T age is about 310 Ma, slightly lower than that of the nearby pegmatite muscovite (318 Ma), and substantially lower than that of the other monzogranite sample (muscovite t_T = 343 Ma, age maximum = 352 Ma). Phlogopite from a slightly sheared lamprophyre dike which intrudes the granodiorite, 2.5 km southeast of sample S456, produced a plateau age of about 330 Ma. Although little is known about the closure temperature of phlogopite, diffusion studies suggest that it should be higher than that of biotite (e.g. Harrison et al., 1985). This additional information clearly corroborates the contention that the age pattern in this pluton (and probably all the SSP) is influenced by location (local intensity of overprint) and resistance to ^{40}Ar loss (related to closure temperatures), rather than the intrusive sequence.

In summary, the data from the Port Mouton pluton suggest that this pluton cooled below 350° C before 352 Ma. Subsequent overprinting caused substantial, non-uniform ^{40}Ar loss. Since the pluton intruded after regional metamorphism, its cooling age is constrained between 352 Ma

and about 385 Ma.

4.3.6. THE QUINAN PLUTON

The oval-shaped Quinan pluton underlies an area of 80 km^2. It intrudes the Goldenville Formation (sillimanite grade). The pluton consists of biotite tonalite, similar to the Barrington Passage pluton, of which it is sometimes considered a part (e.g Rogers, 1985). Where exposed, the pluton appears undeformed, but biotite is mildly chloritized and partly replaced by muscovite. One biotite sample (PE84-43B) was analysed. The spectrum (fig. 4.3-9) displays a profile characteristic of ^{40}Ar loss (e.g. Turner, 1968). The age minimum is not precisely determined, but the spectrum attains a three step plateau of 350 Ma comprising 51.8% of ^{39}Ar. Neither the plateau nor the age maximum (352 Ma) corresponds with any known tectonothermal event in the Meguma terrane. The age maximum is interpreted as a lower limit to the cooling age of the Quinan pluton. The alteration described above may be the signature of the overprinting event which is recorded in the nearby Bald Mountain pluton, and other SSP. The age is tentatively constrained between 352 and 385 Ma.

4.3.7. THE UPPER CLYDE RIVER PEGMATITE

A small pegmatite dike, 1 m thick, intrudes Halifax Formation schist in the sillimanite zone in the vicinity of

Fig. 4.3-9.

Age spectra of samples from the Quinan pluton, and Upper Clyde River pegmatite.

Bars on vertical axes represent 10 Ma.

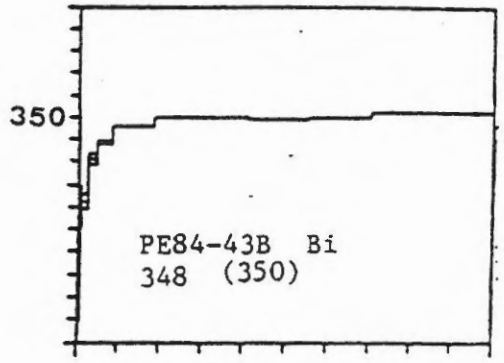
350
PE84-43B Bi
348 (350)

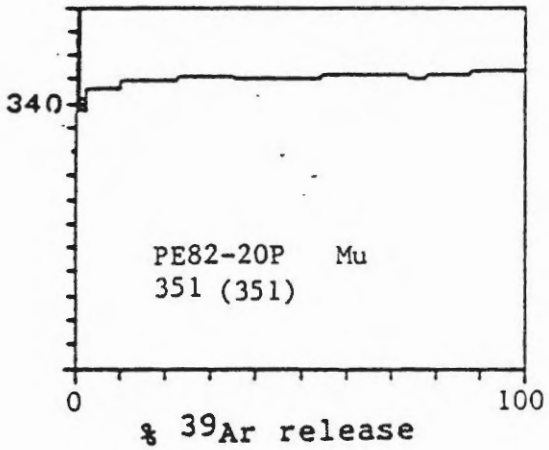
340
PE82-20P Mu
351 (351)
0
100
% 39Ar release

Upper Clyde River, Shelburne County. In thin section, the rock shows evidence of shearing. Muscovite is strongly kinked, plagioclase is bent with deformation twins, and quartz aggregrates have developed highly sutured grain boundaries. There are no obvious signs of alteration. A muscovite sample PE82-20P was dated. The spectrum (fig. 4.3-9) is slightly discordant (IDF = 1.2) and defines a four-step plateau (55 % ^{39}Ar) of 351 Ma, the same as the t_T age. This plateau age is interpreted as a lower limit. The age suggests that the Upper Clyde pegmatite is not substantially younger than the SMB. The age is constrained between 351 and 385 Ma.

4.3.8. SUMMARY OF DATA FROM THE SSP

For two of the plutons, the highest apparent age is about 386-370 Ma. These two plutons (Bald Mountain and Barrington Passage), and probably all the others, were intruded at about the same time as the SMB. The sharp age gradients noted above cannot be explained simply by differential cooling rates. These ages, along with the discordant spectra and clear evidence of tectonothermal disturbance, strongly indicate the effects of a post-intrusive event of varying intensity. Hypothesis (3) of Reynolds et al., (1981) represents the most likely scenario for the southern satellite plutons.

4.4. DATA BASE AND SIGNIFICANCE OF ARGON DATA FROM FELDSPARS AND FISSION TRACK DATA FROM APATITES

4.4.1. INTRODUCTION

In order to elucidate the low temperature (<300 degrees) thermal history of the SSP, one plagioclase and four K-feldspar samples were dated by the ^{40}Ar-^{39}Ar method. Three apatite samples were analysed by the fission track technique. For comparison, four K-feldspar and four apatite samples from the SMB were analysed. The SMB results were reported by Grist (1986) and are shown in Tables 4.4-1 and 4.4-2.

In order to apply the principles of thermochronometry (Chapter 2), certain assumptions must be made about the closure temperatures of the minerals dated. This involves choosing parameters which describe the diffusion behaviour of argon in K-feldspar and annealing of fission tracks in apatite. Since the K-feldspars range from maximum microcline to intermediate microcline (see below), the appropriate parameters for microcline are adopted. For argon diffusion in microcline, estimates of the activation energy, E, vary considerably (e.g. 23 kcal/mol, Evernden et al., 1960; 32, 46 kcal/mol, Gerling et al., 1963; 28.8 kcal/mol, Harrison and McDougall, 1982). This is probably

due to variation in experimental conditions and variation in the structural state of alkali feldspars, which are frequently not adequately documented. Partial or complete homogenization of perthitic alkali feldspars, as well as modification of the structural state during overprinting and vacuum heating may lead to complex kinetic behaviour (eg Foland, 1974). This may impose limitations on geometric models used to describe diffusion behaviour. For the purposes of the discussion that follows, the activation energy, E, for argon diffusion in microcline is assumed to be 30 kcal/mol, and the frequency factor, Do/a2, is taken as 6 per second (Harrison and Be, 1983). These values are close to those derived by Harrison and McDougall (1982) for maximum microcline, which produced ^{40}Ar-^{39}Ar spectra similar to those from the SSP in this study (fig. 4.4-3). From these parameters, closure temperatures corresponding to various cooling rates can be calculated. With the assumption of a sheet model for perthitic K-feldspar, and the formula of Dodson (1973), the closure temperatures which correspond to cooling rates of .5, 5, and 50 degrees per Ma are 124, 148, and 175 degrees C respectively. As stated in section 4.1, an annealing temperature of 100 degrees C is assumed for apatite.

4.4.2. THE SOUTH MOUNTAIN BATHOLITH

The geologic setting of the SMB has been outlined in Chapter 1. The batholith post-tectonically intruded metasedimentary rocks of the Meguma terrane at a depth of 1.5 - 3 km (Clarke and Muecke, 1985). The youngest sedimentary unit cut by the batholith is Siegenian to Emsian in age (ca. 395 Ma, Clarke and Halliday, 1980). The SMB is locally overlain by Horton Group clastic sediments. Deposition of the Horton Group sediments is considered diachronous (P.Schenk, 1986, personal comm.), but the age is thought to be Tournaisian (ca. 358 Ma) at the SMB contact, about 15 km from the area selected for study (e.g. Clarke and Muecke, 1985). Overlying the Horton Group are carbonates and evaporites of the Windsor Group, which have a maximum age of Arundian (ca. 348 Ma, Giles, 1981). The general stratigraphy and areal distribution of the units are outlined in map 2. The age of intrusion of the SMB has been constrained by Rb-Sr mineral-whole-rock isochron dating at 372+/-2 to 361+/-1 Ma (Clarke and Halliday, 1980). These stratigraphic and isotopic data suggest that the SMB was unroofed by erosion within a period of 13-24 Ma. The present erosional surface of the batholith (at least near the Windsor nonconformity) must have been within 1 km of the paleosurface. Prevailing temperatures at that depth would have been about 50 degrees C, assuming a slightly elevated geothermal gradient of 50 degrees/km. Biotite from the

batholith yield an average ^{40}Ar-^{39}Ar apparent age of 367 Ma (Reynolds et al., 1981). If the closure temperature of biotite is assumed to be 300 degrees C, limits can be placed on the cooling rate. If the temperature of the batholith during deposition of the Windsor is assumed to have been about 50 degrees C, this would imply cooling through a 250 degree interval in 13-24 Ma. This corresponds to an average cooling rate of 10-19 degrees/Ma. In this case the closure temperature for microcline would be 155-163 degrees C.

With these stratigraphic and isotopic constraints, the low temperature thermal history of the SMB can be discussed with respect to the data from K-feldspars and apatites. The same principles can be applied to the SSP, where constraints are less well established.

A small area (~2500 km^2) in the eastern part of the batholith was sampled (fig. 4.4-1) This area includes sample locations of biotite standard NS-231 which was previously dated (368 Ma, Reynolds et al., 1981). Alteration of the SMB, including fluorite mineralization, has been observed by the author at several locations within a few km of the samples. Altered mineralized domains within the SMB 20-80 km from these samples produced Rb-Sr isochron ages ranging from 270 to 332 Ma (O'Reilly et al., 1985). Similar ages were obtained for domains of shearing and mineralization elsewhere in the SMB (eg Reynolds and Zentilli, 1985; Dallmeyer and Keppie, 1986). The four samples are PE85-142 (monzogranite), PE85-143

Fig. 4.4-1.

Sample locations for K-feldspars and apatites. (Location for standard NS-231 also shown).

Part of Windsor-SMB nonconformity shown by thick line (see map 2 for details).

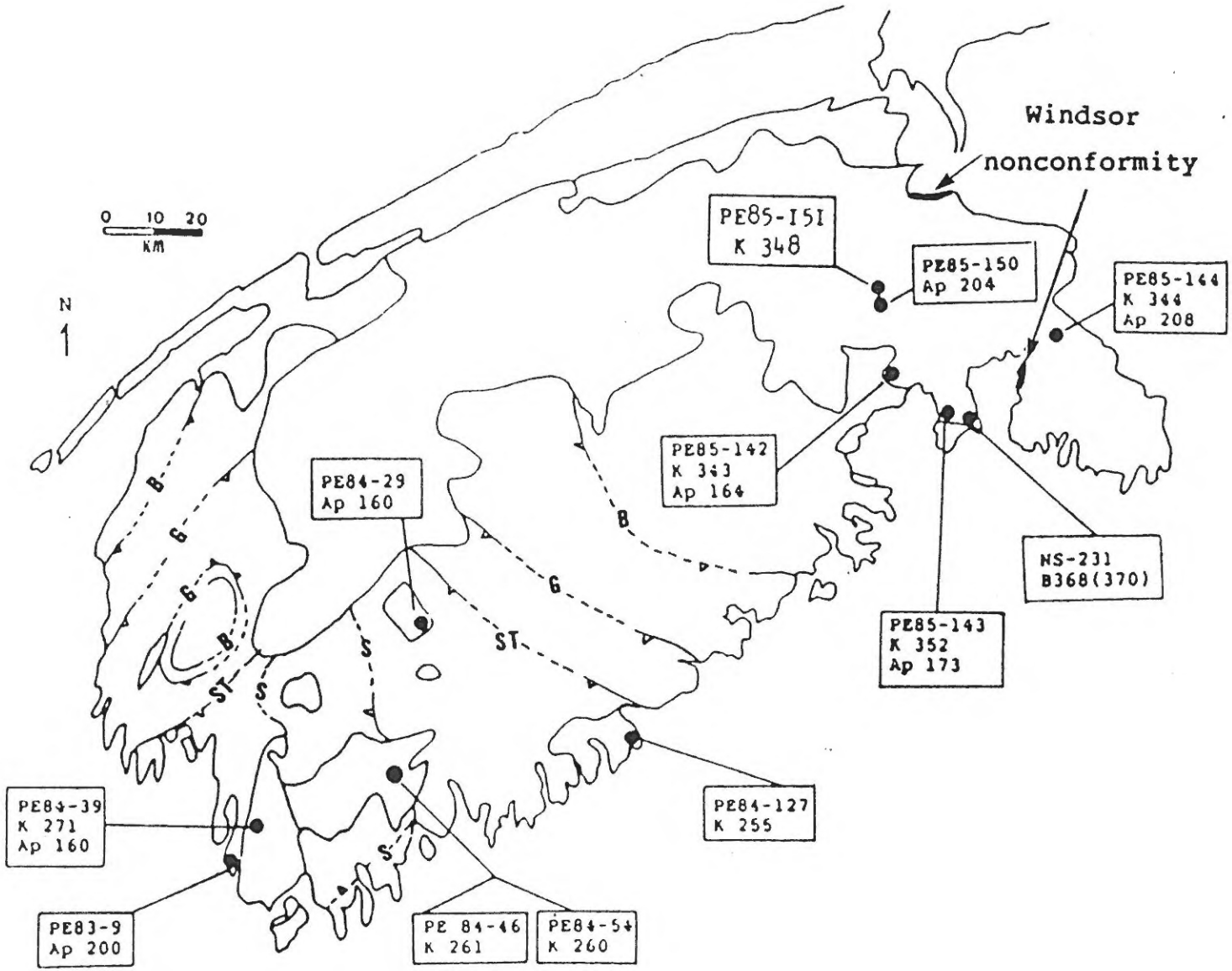
Windsor
nonconformity
0 10 20
KM
N
1
PE85-151
K 348
PE85-150
Ap 204
PE85-144
K 344
Ap 208
PE85-142
K 343
Ap 164
PE84-29
Ap 160
NS-231
B368(370)
PE85-143
K 352
Ap 173
PE84-127
K 255
PE84-39
K 271
Ap 160
PE83-9
Ap 200
PE 84-46
K 261
PE84-54
K 260
B
G
ST
S

(granodiorite), PE85-144 (monzogranite) and PE85-151 (monzogranite). All four samples show evidence of moderate alteration. Biotite is partly replaced by chlorite and sphene, plagioclase is extensively saussuritized, and microcline is partly overgrown by sericite (5-10 %), and coarse muscovite. X-ray analysis by the method of Wright (1968) determined that the four samples are intermediate microcline with 89-93 % $KAlSi_3O_8$. Details are shown in Appendix C. X-ray analysis also reveals that three of the separates contain minor amounts of sericite. In the fourth sample, PE85-143, sericite content was below the the detection limit of XRD. Petrographic examination and electron backscatter images indicate abundant perthite lamellae less than 20 um wide.

Apatite was extracted from samples PE85-142, PE85-143, and PE85-144 for dating by the fission track technique. A fourth apatite sample was extracted from monzogranite collected 500m south of sample PE85-151. The apparent ages are listed in tables 4.4-1 and 4.4-2. The average fission track age is 187 +/- 17 Ma.

Spectra from the K-feldspar samples are shown in fig. 4.4-2. Spectra from the three samples which show sericite contamination are quite complex, with anomalously high ages in steps representing the first 20% of the gas released. These high ages represent temperature steps 500-800 degrees C. This is the same temperature range where fine-grained white micas have been shown to release most of their argon

Table 4.4-1(a). Data for glass dosimeter used with SMB samples.

GLASS	CAPLULE POSITION(MM)	TOTAL FIELDS	TOTAL TRACKS	ρ_0 (PER CM2)
T	2.05	300	819	(1.72±.08) EXP4
MT	8.95	300	833	(1.75±.07) EXP4
MB	18.35	600	1583	(1.69±.06) EXP4
B	28.00	300	771	(1.62±.06) EXP4

Table 4.4-1(b). Data for standards and unknowns used in fission track dating of SMB.

STANDARD/ SAMPLE	FIELDS COUNTED	TRACKS GRAIN/MICA	ρ_s/ρ_i	ρ_s (PER CM2) EXP4	AGE OR ZETA*
FCN 4	37	194/733	.265±.021	1.72±.07	122.1±11.4
FCN 7	50	274/962	.285±.02	1.67±.07	116.5±9.3
FCN 8	50	339/477	.387±.025	1.71±.07	84.1±6.3
PE84-142	12	1271/728	1.775±.126	1.65±.07	163.8±15.9
PE85-143	15	1693/896	1.89±.078	1.64±.07	173.4±13.6
PE85-144	11	1386/716	2.135±.191	1.74±.07	207.9±23.0
PE85-150	15	1655/784	2.111±.092	1.73±.07	204.3±16

(Ma) $\times 10^{-4}$

Zeta after 4 irradiation cans = (111.9 +/- 5.7) x 10^{-4}

Standard: Fish Canyon Tuff apatite with accepted age of 27.79 +/- .7 Ma. Standard calibrated against MMhb-1 (519.4 Ma), (Kunk et al., 1985).

Table 4.4-2.

Ages and discordance factors for samples from the SMB.

SAMPLE	PHASE	Age (Ma)		IDF	CS Ma	%
PE85-142	Ksp	343		4.33	4.3	.5
PE85-143	Ksp	352		4.27	1.5	1.2
PE85-144	Ksp	344		2.83	2.0	.8
PE85-151	Ksp	348		3.37	2.5	1.0
NS-231	Bi	368		1.12	5.7	1.6

Fig. 4.4-2. Age spectra of samples from the SMB. Bars on vertical axes represent 10 Ma

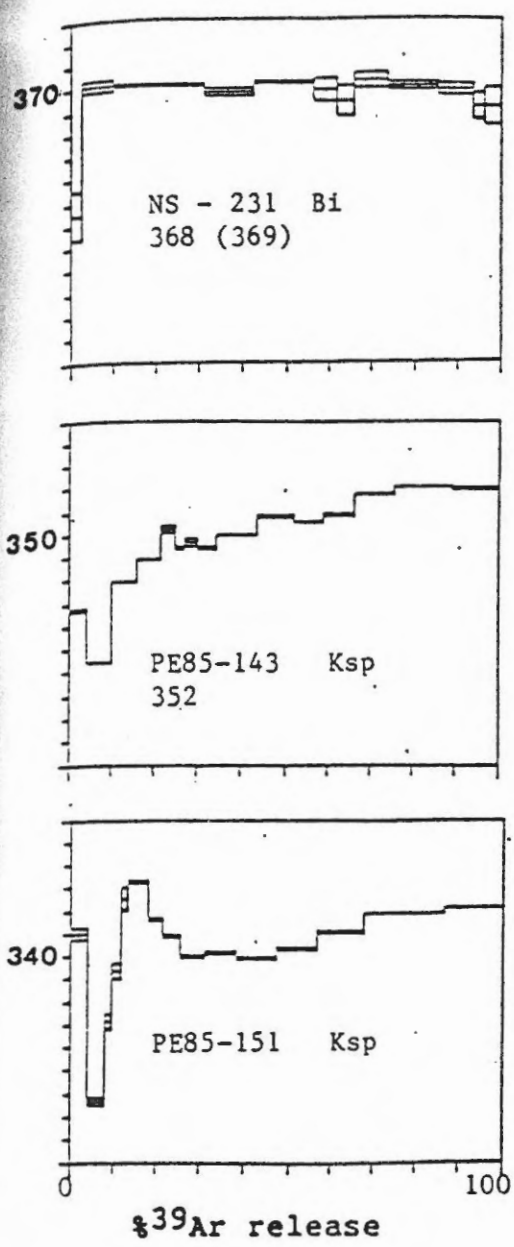
370
NS - 231 Bi
368 (369)
350
PE85-143 Ksp
352
340
PE85-151 Ksp
0
100
%39Ar release

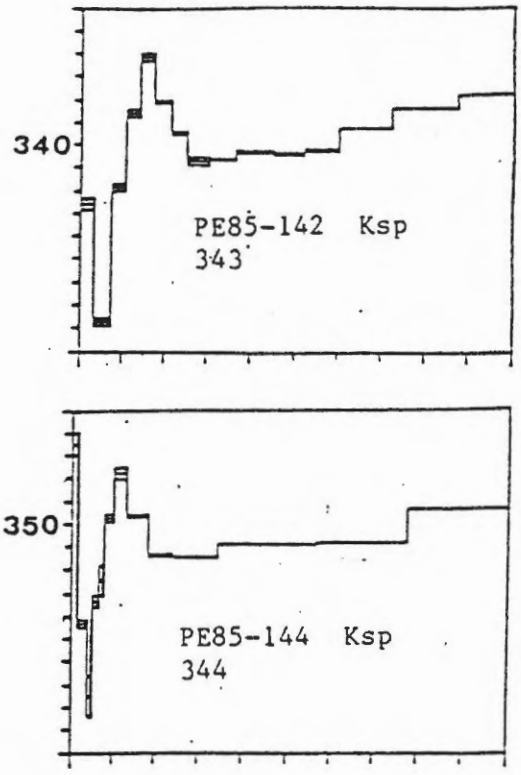
340
PE85-142 Ksp
343
350
PE85-144 Ksp
344

(section 3.6). The anomalous ages in the low temperature part of the spectra approach or slightly exceed that of the SMB (ca. 370 Ma). Although it is recognized that some of these high ages may be partly due to recoil, the argon contribution of the sericite can be estimated from a simple mixing calculation. If the sericite is a product of deuteric alteration, it can be assumed that the sericite age is about 370 Ma. The mean K-feldspar ages in the temperature range 500-800 degrees C are 325, 330, and 335 Ma respectively for samples PE85-142, 144, and 151 respectively (by extrapolation through the normal staircase profile). This corresponds to an argon contribution of 10.4, 7.2 and 10.0 % for samples PE85-142, 144 and 151 respectively. This is consistent with the petrographically estimated sericite content of 5-10 %. The spectrum of sample PE85-143 displays a simple 'staircase' pattern, except for a minor anomaly at 700 degrees, which is probably due to sericite. This pattern is explained either by slow cooling, or episodic argon loss by diffusion (e.g. Harrison and McDougall, 1982). An episodic loss model is preferred for the following reasons:

(1) The stratigraphic and isotopic evidence outlined above suggests rapid uplift and erosion. This implies a relatively fast cooling rate.

(2) The coexisting apatite gave an average fission track age about 160 Ma younger than the overlying sediments (table 4.4.1). Since the closure temperature of apatite is

about 100 degrees C, the batholith must have initially cooled through this temperature by 348 Ma ago. The younger fission track age must have been caused by a later event.

(3) If the slow cooling model is adopted, the meaningful age for the K-feldspars would be the average t_T age, which is 347 Ma. This would imply a cooling rate of 5-10 degrees/Ma, with corresponding closure temperatures of about 148-155 degrees C. This would require unlikely batholith temperatures of 148-155 degrees C (at least locally), when the SMB should have been close to the surface, as required by the stratigraphic constraints.

The spectrum of sample PE85-143 shows a profile which indicates a cooling age of 370 Ma from its age maximum. Corresponding cooling ages for samples PE85-142, PE85-144, and PE85-151 are 362, 356, and 361 Ma respectively. This is consistent with the slightly younger Rb-Sr ages for monzogranites (Clarke and Halliday, 1980). According to the model of Turner (1968) for episodic loss, ^{40}Ar loss occurred about 300 Ma ago (defined by the first few steps of the spectrum of sample PE85-143). Because of poor resolution in the low temperature gas release, this point is not well constrained. It may be noted, however, that there is considerable evidence for tectonothermal activity in the Meguma terrane about 300 Ma ago. (see sections 4.2.2, 4.3.1 and table 1-2). Age minima are poorly defined in the spectra of the other three samples. The average fission track age is 187+/-17 Ma, which coincides with the time of

rifting and mafic magmatism associated with opening of the present Atlantic Ocean (e.g. Keen and Cordsen, 1981). The most abundant evidence of mafic magmatism in the Meguma terrane is the North Mountain basalt. This unit is underlain by the Blomidon Formation, which on fossil evidence is Rhaetian (213-219 Ma). The overlying Scots Bay Formation is similarly dated as Hettangian (213-206 Ma). Within these stratigraphic brackets, the age of the North Mountain basalt is taken as 210 Ma. The K-Ar age of the North Mountain basalt is 200 Ma (Wark and Clarke, 1980). It is possible that episodic loss of ^{40}Ar in K-feldspar could have occurred at 300 Ma, or 210 Ma, or 187 Ma ago (average fission track age). There may have been some loss all three times. If the ^{40}Ar loss is assumed to have occurred at 300 Ma, the amount lost is about 31%. The corresponding amount for a possible event 210 Ma ago is 13.3%. For a possible event 187 Ma ago, the loss would have been 11.6%. These calculations are based on sample PE85-143, with the reservations listed in section 3.5.

4.4.3. THE SOUTHERN SATELLITE PLUTONS

Four K-feldspar samples were extracted from pegmatites intruding the SSP described in section 4.3. Two of these (PE84-46 and PE84-54) are from the Shelburne pluton. Sample PE84-39 is from the Barrington Passage pluton and sample PE84-127 from the Port Mouton pluton. In all four samples

K-feldspar shows very minor sericite alteration, which was not detectable by XRD. The samples all contain perthitic microcline. X-ray analysis indicates that they are maximum microcline with 89-95% $KAlSi_3O_8$ (Appendix C). Three apatite samples were dated by the fission track method. Two were collected from the Barrington Passage tonalite (PE83-9 and PE84-39). The other sample was extracted from the Bald Mountain monzogranite. The fission track ages range from 160 to 200 Ma, with an average of 173 +/- 16 Ma (table 4.4.3).

As outlined in this chapter, the thermal history of the southern satellite plutons (and the rest of southwest Nova Scotia) is much more complex than that of the South Mountain Batholith. Specifically, the overprinting event about 300 Ma ago was much more intense. At this time micas were almost completely outgassed where the effect was strongest (section 4.3). It is, therefore, likely that the K-feldspars from the SSP (Barrington Passage, Port Mouton, Shelburne) were completely reset at about 300 Ma ago. All four spectra (fig. 4.4-3) display relatively simple staircase patterns.

The age maxima in these spectra range from 264 Ma to 290 Ma. This is what would be expected if the feldspars were completely reset about 300 Ma ago. The anomalously high ages from the first steps of samples PE84-46, 54 and 127 (representing less than 5% of the total ^{39}Ar), may be explained by minor recoil loss of ^{39}Ar, or minor peripheral

Table 4.4-3.a. Data for neutron dosimeter used with SSP apatite samples.

GLASS	CAPSULE POSITION (mm)	TOTAL FIELDS	TOTAL TRACKS	ρ_D (10E4 per cm2)	FLUENCE (10E15 per cm2)
T	2	399	1345	2.55+/-.10	5.05+/-.50
MT	7.7	368	1340	2.36+/-.10	4.67+/-.57
MB	15.2	376	1356	2.26+/-.10	4.48+/-.45
B	22.7	326	1004	2.08+/-.10	4.12+/-.51

Table 4.4-3.b. Fission track data for Standards and Unknowns.

STANDARD/ SAMPLE	FIELDS COUNTED	TRACKS Grain/mica	ρ_S/ρ_L	ρ_S 10E4 per cm2	AGE or ZETA
FCP1	12	66/273	.242+/-.033	2.33+/-.1	(98.7+/-14.2) x10-4
FCN2	60	329/1208	.272+/-.017	2.55+/-.1	(80+/-5.9) x10-4
FCN4	54	279/1122	.249+/-.017	2.12+/-.1	(103.4+/-8.4) x10-4
PE83-9	7	1012/691	1.507+/-.107	2.38+/-.1	200+/-18
PE84-29	5	513/452	1.174+/-.088	2.43+/-.1	160+/-16
PE84-39B	12	479/421	1.150+/-.073	2.48+/-.1	160+/-15
PE82-10	5	392/179	2.159+/-.176	2.30+/-.1	276+/-29

Ma

Zeta after 4 irradiation cans = (111.9 +/- 5.7) x 10^{-4}

Standard: Fish Canyon Tuff apatite with accepted age of 27.79 +/- .7 Ma. Standard calibrated against MMhb-1 (519.4 Ma), (Kunk et al., 1985).

Fig. 4.4-3. Spectra for SSP K-feldspars.
Bars on vertical axes represent 10 Ma.

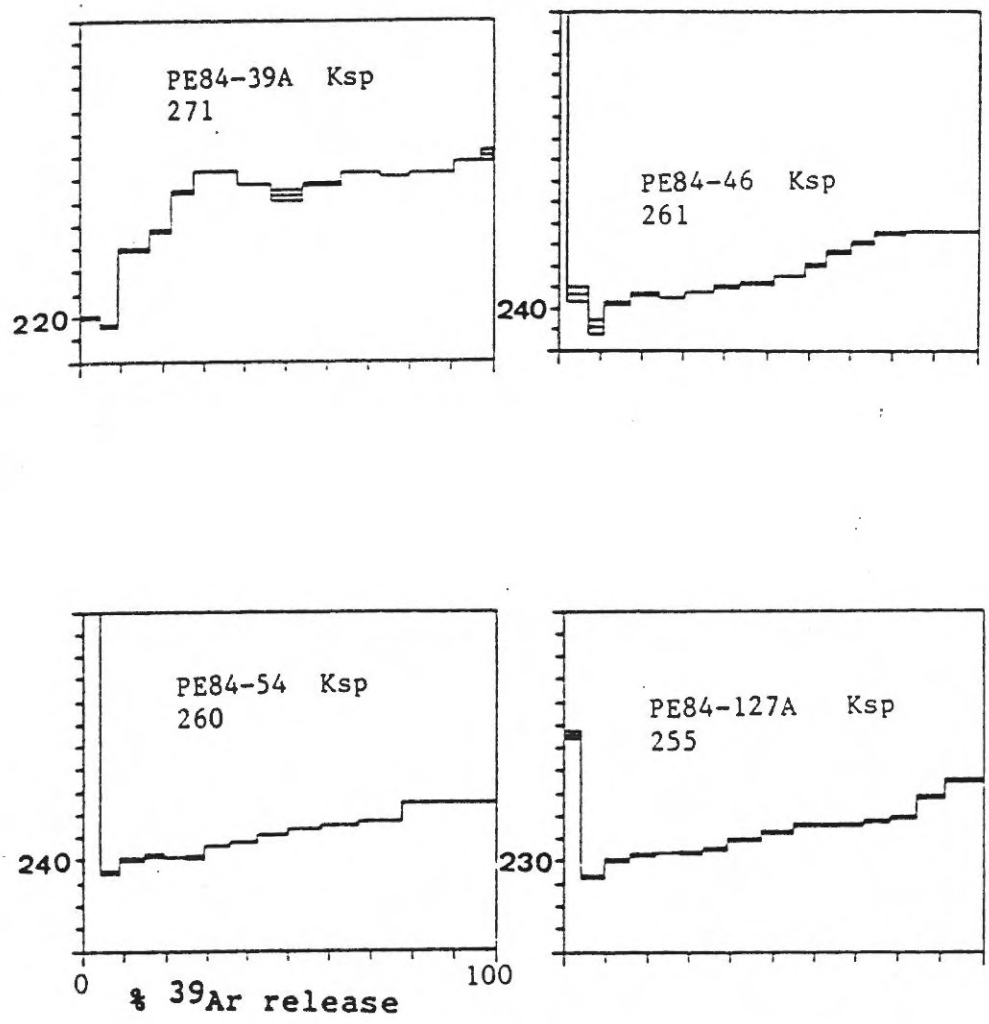
PE84-39A Ksp
271
220
PE84-46 Ksp
261
240
PE84-54 Ksp
260
240
PE84-127A Ksp
255
230
0
100
% 39Ar release

contamination by excess argon. Because of the apparent complex nature of tectonothermal events in the southern Meguma terrane, it is difficult to say whether the staircase profiles on the K-feldspar spectra are due to slow cooling or to episodic loss. From section 4.4.1, if these profiles are due to slow cooling, (ca. 0.5 degrees/Ma), they indicate that the plutons reached 124 degrees C at 262 Ma (average t_T age). If the staircase pattern is due to episodic loss, according to Turner's (1968) model, the spectra suggest that the time of loss is 220-230 Ma. As for the SMB samples, this time is not well constrained. A possible alternative is 210 Ma (major basalt extrusion).

The estimated time of possible argon loss in the K-feldspars (220-230 Ma) coincides with cooling ages of biotite from mafic dikes which intrude the Wedgeport pluton 40km west of the Shelburne pluton. The mafic dikes occur in swarms (Wolfson, 1984) and gave a biotite conventional K-Ar apparent age age of 232 +/- 6 Ma, and an ^{40}Ar-^{39}Ar plateau age of ca. 225 Ma (Reynolds, 1986 written comm.). Mafic dikes have been observed cutting the SSP in several other locations (e.g. Rogers 1985), but most are not yet dated radiometrically. These dikes may be related to the slightly younger North Mountain basalt and Shelburne dike (200-210 Ma, section 1.3.3). This episode of magmatism is associated temporally with the opening of the Fundy rift, and is possibly a precursor to the opening of the present North Atlantic Ocean (e.g. Keen and Cordsen, 1981). From the

spectrum of sample PE84-39 (taken to represent SSP samples), constraints can be placed on any thermal event which occurred about 230-210 Ma ago, causing ^{40}Ar loss. For an event 230 Ma ago, the estimated loss is 47%, while an event 210 Ma ago would have produced a loss of about 36.4%.

4.4.4. SUMMARY OF K-FELDSPAR/FISSION TRACK DATA

K-feldspars record contrasting thermal histories for the SMB and SSP. The original cooling age (~370 Ma) can be deduced from the SMB age spectra. This cannot be done with spectra from SSP samples. Although age minima are not well-defined, the spectra suggest that the SMB samples were partially outgassed about 300 Ma, while their SSP counterparts were being completely reset (section 4.3). Age minima in the SSP K-feldspar spectra also indicate episodic loss of ^{40}Ar about 230-220 Ma ago. The contrast may be due to the differences in structural state. The SMB samples are intermediate microcline, which are likely to be more retentive of argon than the maximum microcline samples of the SSP (e.g. Foland, 1974; Berger and York, 1981). It is also likely that the SMB was subjected to a milder overprinting event than the SSP. This is evidenced by the preservation of mica ages close to 370 Ma in the SMB, and the rare occurrence of such ages in the SSP. Apatite from the SSP as well as the SMB record cooling ages of about 160-200 Ma ago. This indicates a broad convergence of the

low temperature (below 100 degrees C) cooling pattern across the Meguma terrane, although the one sample from the RMT (section 4-2) suggests some local variation.

The age difference between K-feldspar and apatite is larger for the SMB than for the SSP (160, 89 Ma respectively). If, as argued in section 4.3, the SSP are about the same age as the SMB (or slightly older), the difference in K-feldspar-apatite behaviour in the two plutonic settings may reflect differences in closure temperatures under contrasting thermal regimes. It may be noted that the difference between microcline closure temperature and apatite fission track annealing temperature increases with cooling rate. For instance a cooling rate of 3 degrees/Ma produces a difference of 52 degrees, whereas the difference is 64 degrees for a cooling rate of 30 degrees/Ma. (cf. Dodson, 1979). The difference is larger for intermediate microcline. The SMB initially cooled rapidly (section 4.4.2), and the K-feldspars are intermediate microcline. Initial cooling rates for the SSP are not well-constrained; SSP K-feldspar is maximum microcline. The interplay of cooling rate and structural state can account for the differences observed.

4.4.5. INFERENCE FROM PLAGIOCLASE

One plagioclase sample (% an=25) was analysed. It was extracted from the Barrington Passage tonalite (sample

PE84-118, section 4.3). Plagioclase in this sample shows only minor saussuritization and the rock is slightly deformed. The plagioclase sample produced a spectrum (fig. 4.3-4) which displays a five-step plateau (65% of ^{39}Ar) of about 260 Ma. This plateau is not very well defined (CS=4.6%). Little is known about the closure temperature of plagioclase. However, Berger and York (1981) derived a value of 200 degrees C by the vacuum step heating technique. Since the plateau age is similar to the estimated cooling ages of the SSP microcline samples, it is quite likely that these two minerals have similar closure temperatures. Until further work is done to better define the closure temperatures of plagioclase and microcline, they will be regarded as similar. If this interpretation is correct, it would imply that the SSP were cooled through the appropriate K-feldspar closure temperature (125-200 degrees) close to 260 Ma ago. The poor definition of the plagioclase spectrum requires some caution in the above interpretation.

4.5. THERMAL MODELS FOR THE MEGUMA TERRANE

The thermal history of the Meguma terrane can be summarized by schematic models, which are constrained by conclusions reached in this chapter. On the basis of assumed closure temperatures for hornblende, biotite, K-feldspar, and apatite, time-temperature points can be established. The time-temperature estimates with reference

to the relevant sections of the preceding text are listed in table 4.4-4. Since most muscovite samples apparently show evidence of overprinting, no t-T points can be generated from them. Three muscovite samples from the Bald Mountain pluton are exceptional in that they give plateau ages of about 370 Ma. These ages are assumed to represent cooling through temperatures of 350 degrees C (e.g. Purdy and Jager, 1976). The thermal history of the SMB (at least the eastern section) is apparently the least complex, and is described first. Deductions are then made for the SSP and RMT.

From the above data, the thermal history of the SMB can be described in terms of three models. They are as follows:

4.5.1. SMB MODEL 1

This model (fig. 4.4-4) assumes rapid cooling between 372 and 350 Ma, followed by two later thermal pulses. The first pulse occurred about 300 Ma ago, resulting in partial ^{40}Ar loss from K-feldspar and complete annealing of apatite fission tracks. During a possible 210-200 Ma event, apatite fission tracks were completely reset, but ^{40}Ar loss from K-feldspar was small.

Table 4.4-4.

Time-temperature constraints for thermal models for the SMB, the SSP and the RMT.

	TIME (Ma)	TEMPERATURE (degrees C)	REMARKS
SMB	367	300-350	Average muscovite-biotite age, (Reynolds et al., 1981).
	370-356	159	Inferred K-feldspar cooling age (section 4.4.2).
	348	~50	Estimated batholith temperature at/near nonconformity (section 4.4.2).
	~300	>150	Partial degassing of K-feldspar (sections 4.4.2, 4.5.4.2).
	~210	>100	Fission tracks annealed, major mafic magmatism (sections 4.4.2, 4.5.4.2).
	187	100	Average fission track age, (section 4.4.2).
SSP	386-370	500	Hornblende ages (section 4.3.2)
	370	350-300	Muscovite-biotite ages, (section 4.3).
	~300	>300	Some biotites completely reset (sections 4.2, 4.3).
	~210	>100	Fission tracks annealed, major mafic magmatism (sections 4.4.2, 4.5.4.2).
	173	100	Average fission track age (section 4.4.3).
RMT	400	500	Hornblende age (section 4.2.4).
	400-370	300	Older mica ages (section 4.2.5.4).
	280	100	Fission track age (section 4.2.6).

Fig. 4.4-4. SMB Model 1.

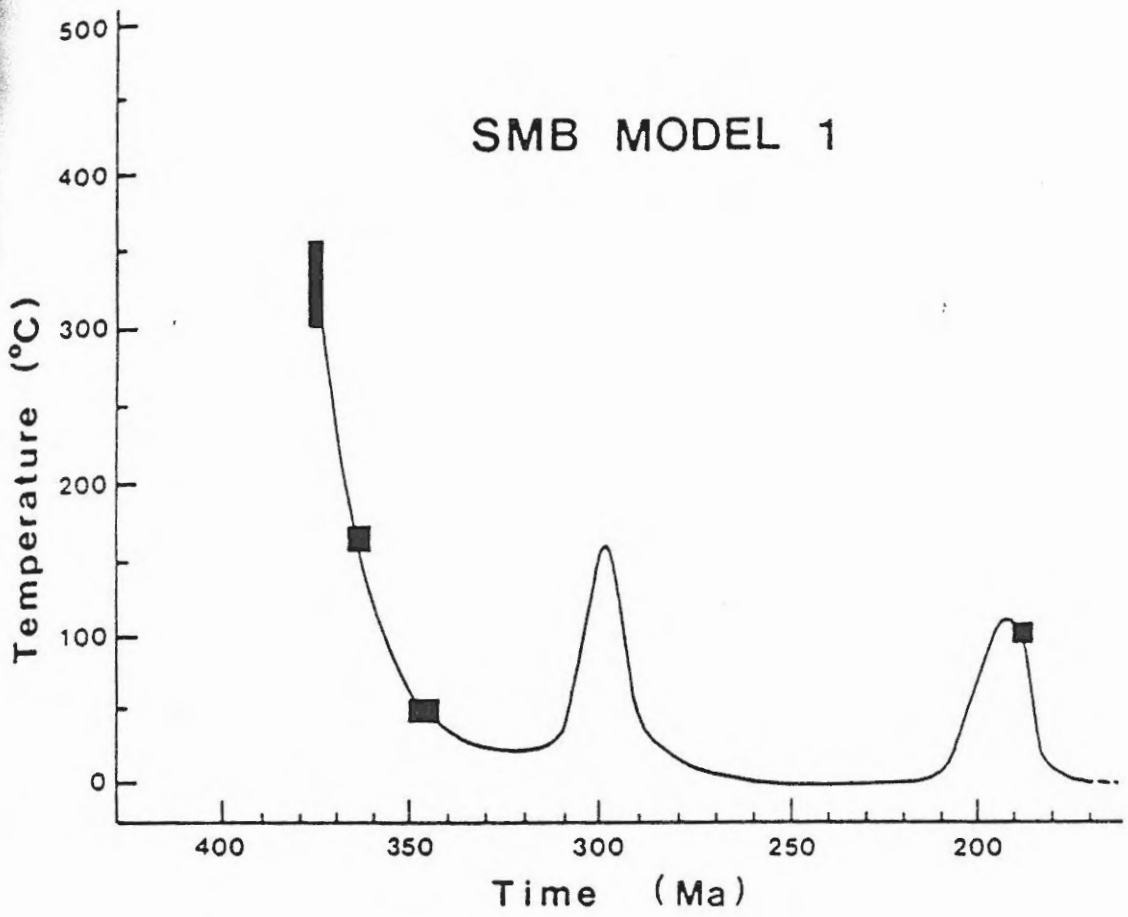
SMB MODEL 1
Temperature (°C)
500
400
300
200
100
0
400
350
300
250
200
Time (Ma)

Fig. 4.4-5. SMB Model 2.

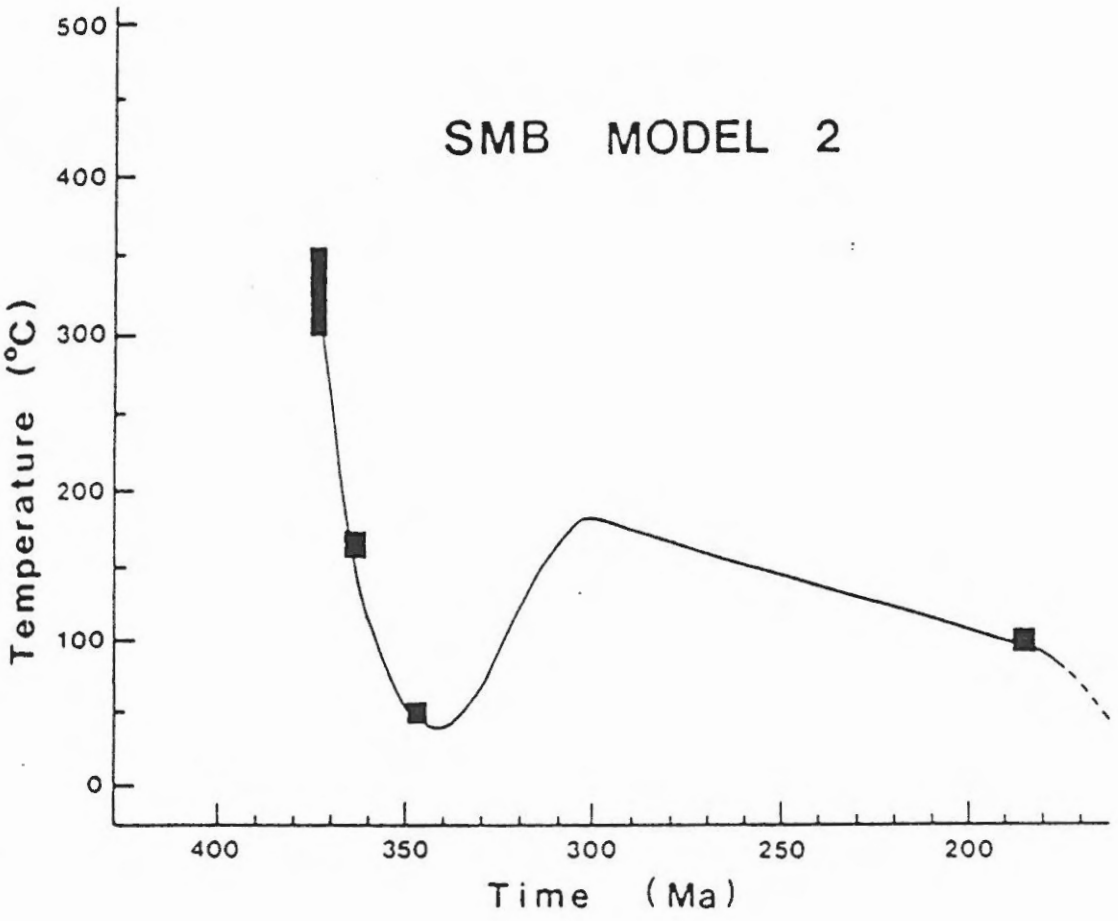
SMB MODEL 2
Temperature (°C)
500
400
300
200
100
0
400
350
300
250
200
Time (Ma)

Fig. 4.4-6. SMB Model 3.

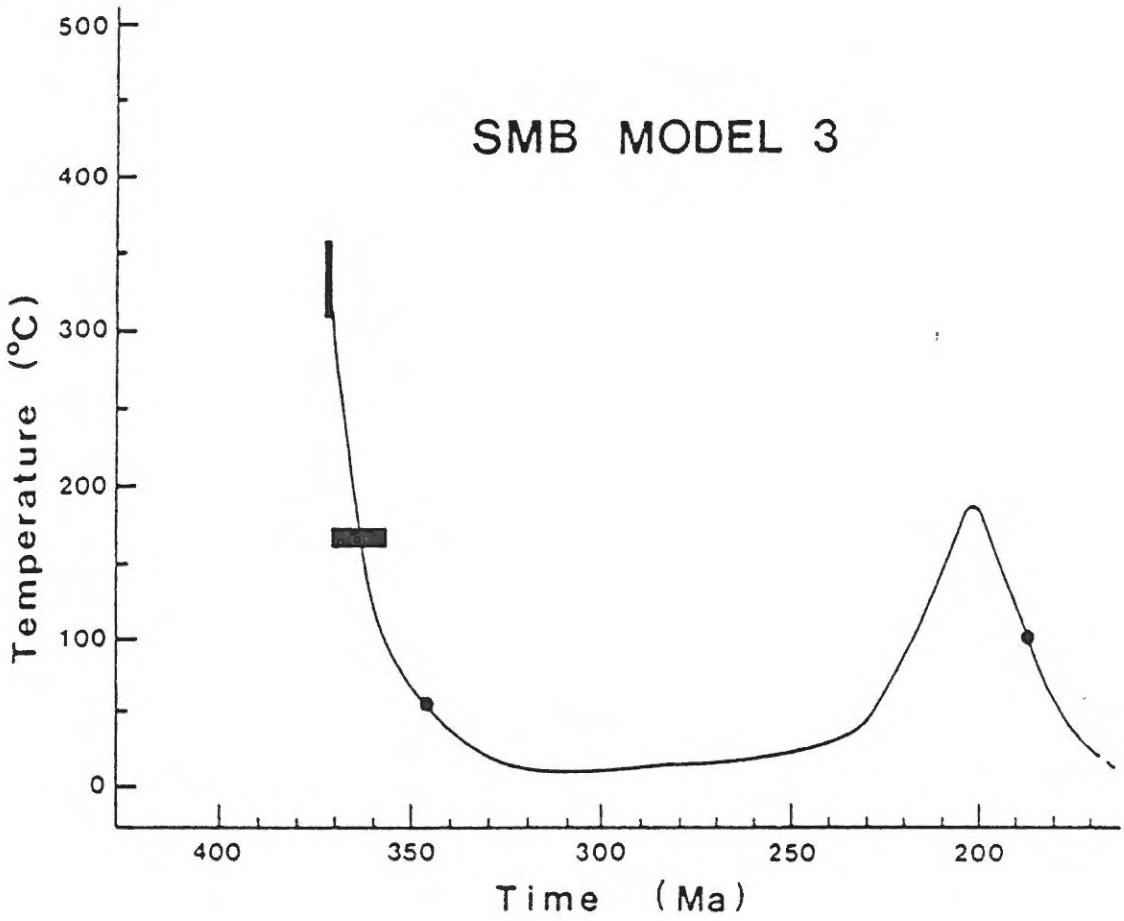
SMB MODEL 3
Temperature (°C)
500
400
300
200
100
0
400
350
300
250
200
Time (Ma)

4.5.2. SMB MODEL 2.

Model 2 (fig. 4.4-5) assumes rapid cooling between 372 and 350 Ma followed by a thermal pulse about 300 Ma. K-feldspar was partially outgassed and apatite fission tracks were completely annealed. The batholith cooled slowly, reaching 100 degrees C at about 187 Ma ago.

4.5.3. SMB MODEL 3

The third model proposes rapid cooling between 372 and 350 Ma followed by a thermal pulse approximately 210-200 Ma ago. In this possible event, apatite fission tracks were completely annealed and K-feldspar was partly outgassed.

4.5.4. DISCUSSION OF SMB MODELS

The first two models indicate that the major overprinting event occurred about 300 Ma ago. This interpretation is supported by several previous studies in the Meguma terrane (e.g. Reynolds et al., 1981; O'Reilly et al., 1985; Zentilli and Reynolds, 1985; Dallmeyer and Keppie, 1986).

The second model suggests that the temperature of the surface now exposed was maintained above 100 degrees between 300 and 200 Ma ago. With 'normal'geothermal gradients (30 degrees/km), this would imply burial to about 3.5 km.

It is difficult to choose between the first and second

models on the basis of the available age data. However, model 2 is less plausible because it requires about 100 Ma for relaxation of the thermal pulse which occurred about 300 Ma ago. Although deep burial and/or elevated geothermal gradients between 300 Ma and 200 Ma could account for model 2, the more realistic brief thermal pulses of model 1 make it more attractive.

The third model suggests that major overprinting occurred about 210-187 Ma ago. This is the inferred time of rifting and basaltic magmatism associated with opening of the present North Atlantic Ocean (e.g. Wark and Clarke, 1980; Keen and Cordsen, 1981). Although the apatite fission track ages indicate final cooling below 100 degrees about 187 Ma ago, there is little independent data to facilitate assessment of the intensity, or areal extent of a possible 210-187 Ma tectonothermal event. For instance, there are no known mica dates of this age from the RMT. Rocks of this age from the Meguma Terrane are only slightly deformed (M. Gibling, 1986, personal comm.). However, if this model was applicable, (perhaps locally), constraints can be placed on both the duration and intensity (temperature) of the overprinting event. The method is based on the kinetics of argon diffusion in K-feldspar and fission track annealing in apatite. It permits direct comparison of the kinetic parameters governing argon loss in K-feldspar and fission track annealing in apatite for the SMB, or at least for sample PE85-143. The procedure is described below.

4.5.4.1. ARGON DIFFUSION CURVES FOR K-FELDSPAR

Diffusion in perthitic K-feldspar is usually described by the sheet model (section 2.4, Harrison and McDougall, 1982). For small losses, the fraction of argon lost (f) can be related to the duration of the heating event (t), by the following equation:

$f^2 = (4Dt)/(..a^2)$ ..... (1) (Mussett, 1969, section 2.4).

D = diffusion coefficient

a = grain size parameter

When equation (1) is substituted into the Arrenhius relationship,

D = Do exp (-E/RT) (section 2.4), the following result is derived:

$T = (E/R)/[\ln\{(4tDo/a^2)/(f^2..)\}]$..... (2)

(Terms defined in section 2.4).

Three variables emerge from equation (2). During an overprinting event, the fraction of ^{40}Ar lost (f) depends on the duration of heating (t) and the temperature applied, T, (e.g. Harrison and Be, 1983). If values are assumed for E and Do/a2, (taken as constants for a given mineral), t-T pairs can be calculated for fixed values of f. For a given f, log t can be plotted against 1/T, producing a straight line whose slope is proportional to E. Several curves can

be drawn, corresponding to various values of f (fig. 4.3-4). Constraints can be placed on the temperature of an event which caused ^{40}Ar loss if reasonable estimates are made of the duration of that event (see below).

4.5.4.2. COMBINATION OF KINETIC DATA FROM K-FELDSPAR AND APATITE

Experimental curves have been drawn which describe fission track annealing in apatite (e.g. Naeser 1979; Gleadow and Duddy, 1981). The curves (fig. 4.4-7), are analogous to those described for argon loss in K-feldspar. The apatite fission track age is assumed to represent the minimum age for 100% annealing. If, as suggested in section 4.4.2, 11.6% argon loss occurred at the same time as 100% annealing of fission tracks (187 Ma ago), a unique point can be defined by the intersection of the corresponding curves (fig. 4.4-7). The point of intersection indicates a temperature of about 123 degrees C during an event lasting about 3 Ma. Alternatively, the argon loss may have occurred at a temperature greater than that required for 100% annealing of fission tracks in apatite. Timing of such an event would have been earlier than that suggested by the fission track ages (perhaps 210 Ma ago). The average fission track age would then represent cooling to about 100 degrees C after the thermal event. In this case, the loss is 13.3%, but the duration of the event cannot be precisely

Fig. 4.4-7. Time-temperature curves for argon loss from K-feldspars and fission track annealing of apatite (SMB).

(a) Argon loss — 187, 210 Ma ago.

(b) Argon loss — 300 Ma ago.

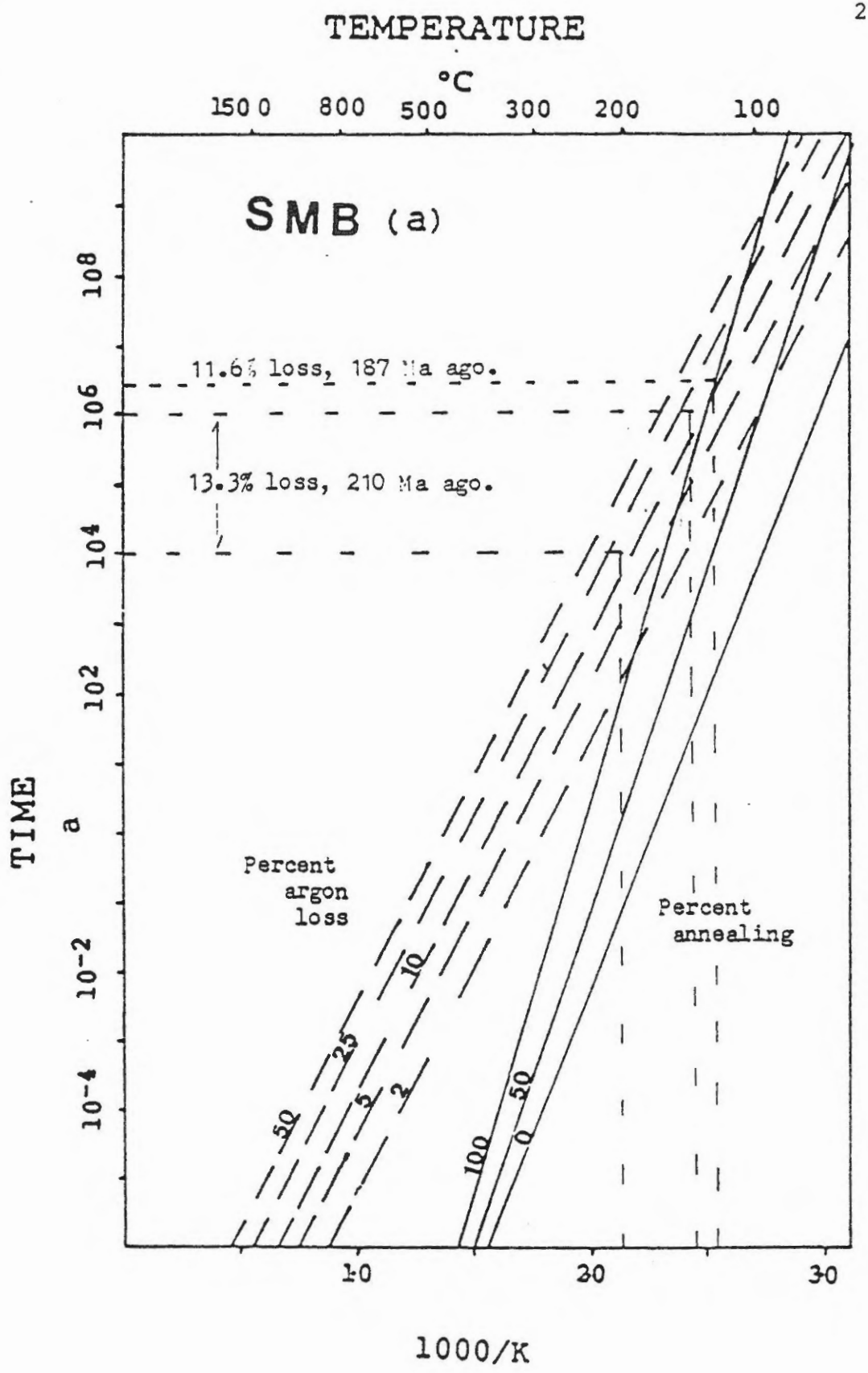
TEMPERATURE
°C
150 0
800
500
300
200
100
SMB (a)
11.6% loss, 187 Ma ago.
13.3% loss, 210 Ma ago.
TIME
a
10^8
10^6
10^4
10^2
10^-2
10^-4
Percent argon loss
Percent annealing
50
25
10
5
2
100
50
0
1·0
2·0
3·0
1000/K

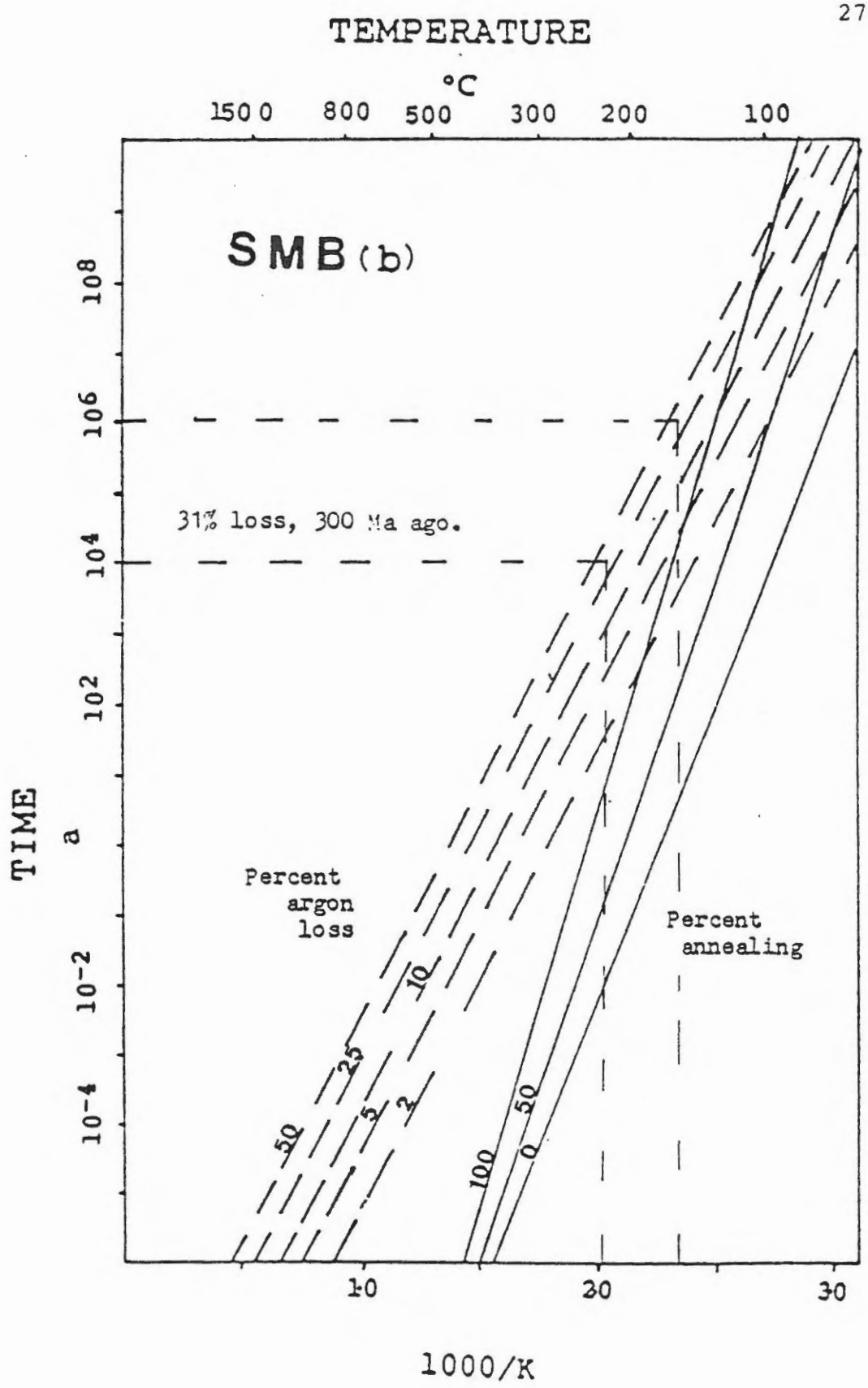
TEMPERATURE
°C
150 0
800
500
300
200
100
SMB (b)
31% loss, 300 Ma ago.
TIME
a
10⁸
10⁶
10⁴
10²
10⁻²
10⁻⁴
Percent argon loss
Percent annealing
50
25
10
5
2
100
50
0
10
20
30
1000/K

specified from fig. 4.4-7. By analogy with published estimates on the persistence of hydrothermal events, limits can be placed on the intensity of the SMB overprint. A reasonable minimum is 10, 000 years, as deduced from modern geothermal fields (e.g. Ellis and Mahon, 1977). For an event about 210 Ma ago, lasting 1 million to 10, 000 years, the temperatures required for 13.3% loss in K-feldspar are 136-194 degrees C. Corresponding temperatures for an event 300 Ma ago (31% loss), are 156-225 degrees C. The fission track annealing curves have been adopted from Gleadow and Duddy (1981), with modifications suggested by Harrison (1984), who contended that they were too steep. The effect of the modification is a tenfold increase in the estimated heating time, with a corresponding 30% lowering of the estimated temperature. This uncertainty must be considered when comparisons are made with other estimates.

4.5.5. SSP MODEL 1 (ONE OVERPRINT).

As shown in fig. 4.4-8, initial post-crystallization cooling was rapid. The temperature was 500 degrees C 386-370 Ma ago. This is based in the available hornblende data. The maximum age obtained from muscovite and biotite also suggests that temperatures of 350-300 degrees C were reached about 370 Ma ago. This indicates rapid initial cooling through 300 degrees C, approximately 370 Ma ago

Fig. 4.4-8. SSP Model 1.

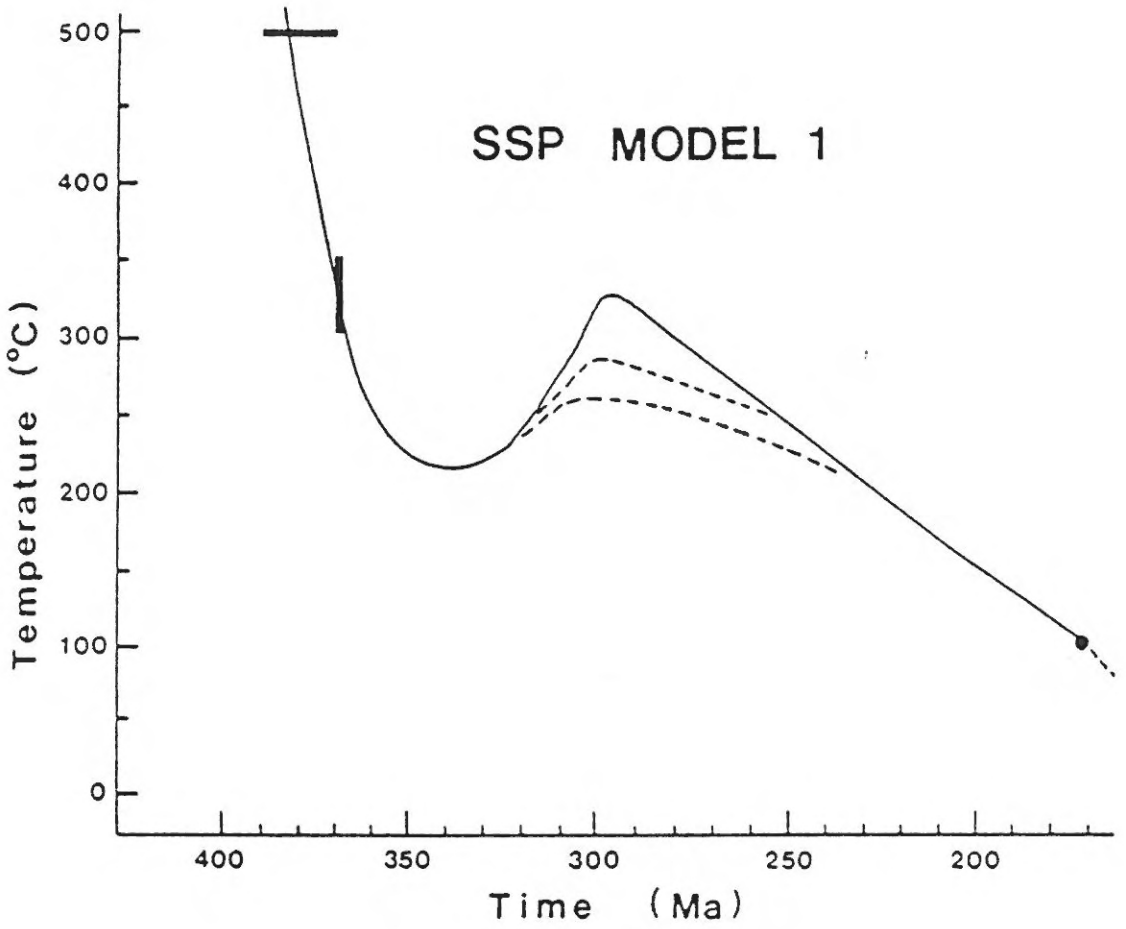
SSP MODEL 1
Temperature (°C)
500
400
300
200
100
0
400
350
300
250
200
Time (Ma)

Fig. 4.4-9. SSP Model 2.

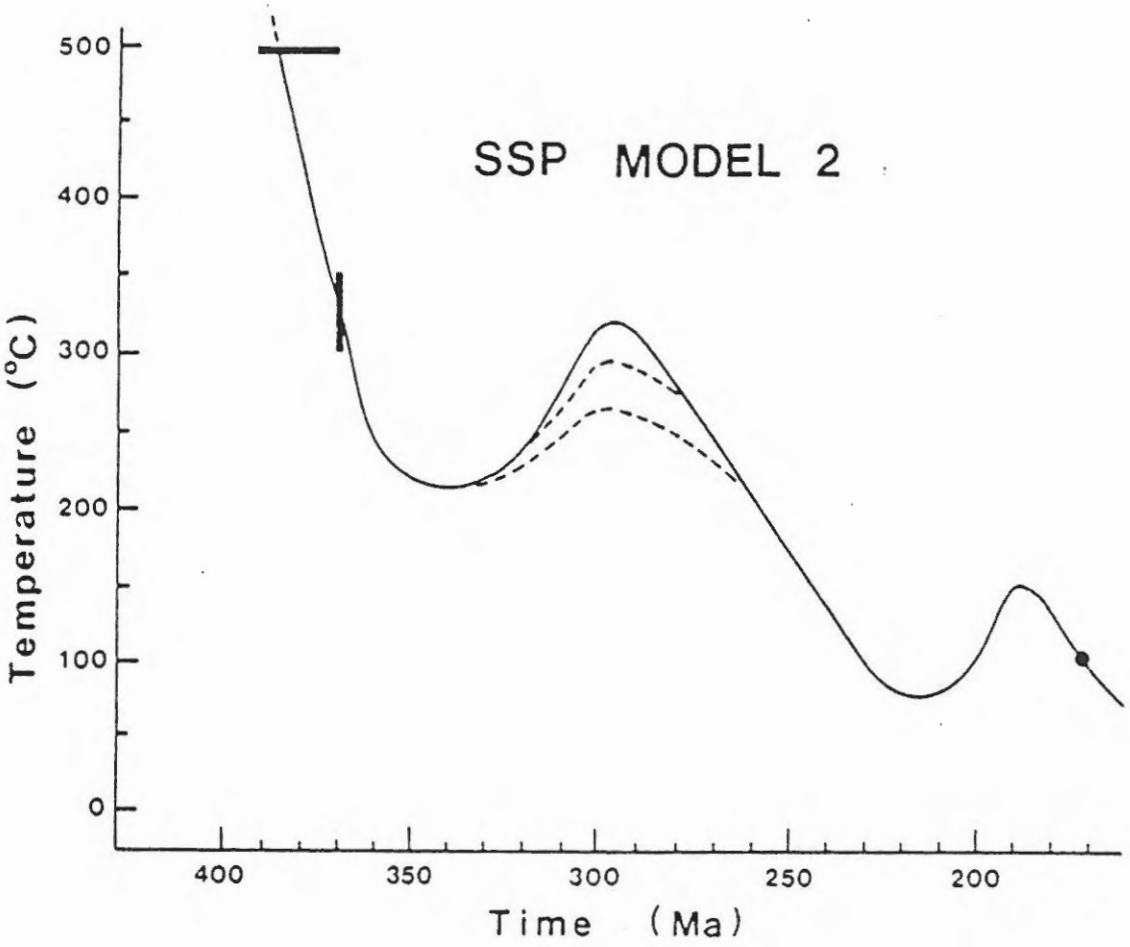
SSP MODEL 2
Temperature (°C)
500
400
300
200
100
0
400
350
300
250
200
Time (Ma)

(biotite Tc). The cooling rate below 300 degrees immediately after 370 Ma is poorly constrained. The overprinting event at about 300 Ma was of varying intensity, but sufficient to partly or completely outgas biotite, and completely reset K-feldspar. Subsequent cooling is constrained by the average K-feldspar age (Tt) and the observed fission track age (about 173 Ma). In this model, the age gradients in K-feldspar spectra are assumed to be due to slow cooling after about 300 Ma ago. Turner (1968) suggested that the age spread in the spectrum of a sample that cooled very slowly should approximately correspond to a cooling interval of 10-20 degrees C. With the assumed closure temperatures for apatite and microcline, (100, 130 degrees C respectively), the age spread on the SSP K-feldspar samples correspond to a cooling interval of 10 to 23 degrees C, which is close to the prediction.

4.5.6. SSP MODEL 2 (TWO OVERPRINTS)

As for model 1, initial cooling to about 300 degrees C was rapid (fig. 4.4-9). The 300 Ma event was similar to Model 1. A thermal pulse at about 230-200 Ma is responsible for loss of ^{40}Ar in K-feldspar and complete annealing of apatite fission tracks. The age gradients in K-feldspar spectra are assumed to be due to episodic loss of ^{40}Ar. From the estimated ^{40}Ar loss (section 4.4-3), limits can be placed on the temperature and duration of such an event.

Fig. 4.4-10. Time-temperature curves for argon loss from K-feldspars and fission track annealing of apatite (SSP).

(a) Argon loss - 230 Ma ago.

(b) Argon loss - 210 Ma ago.

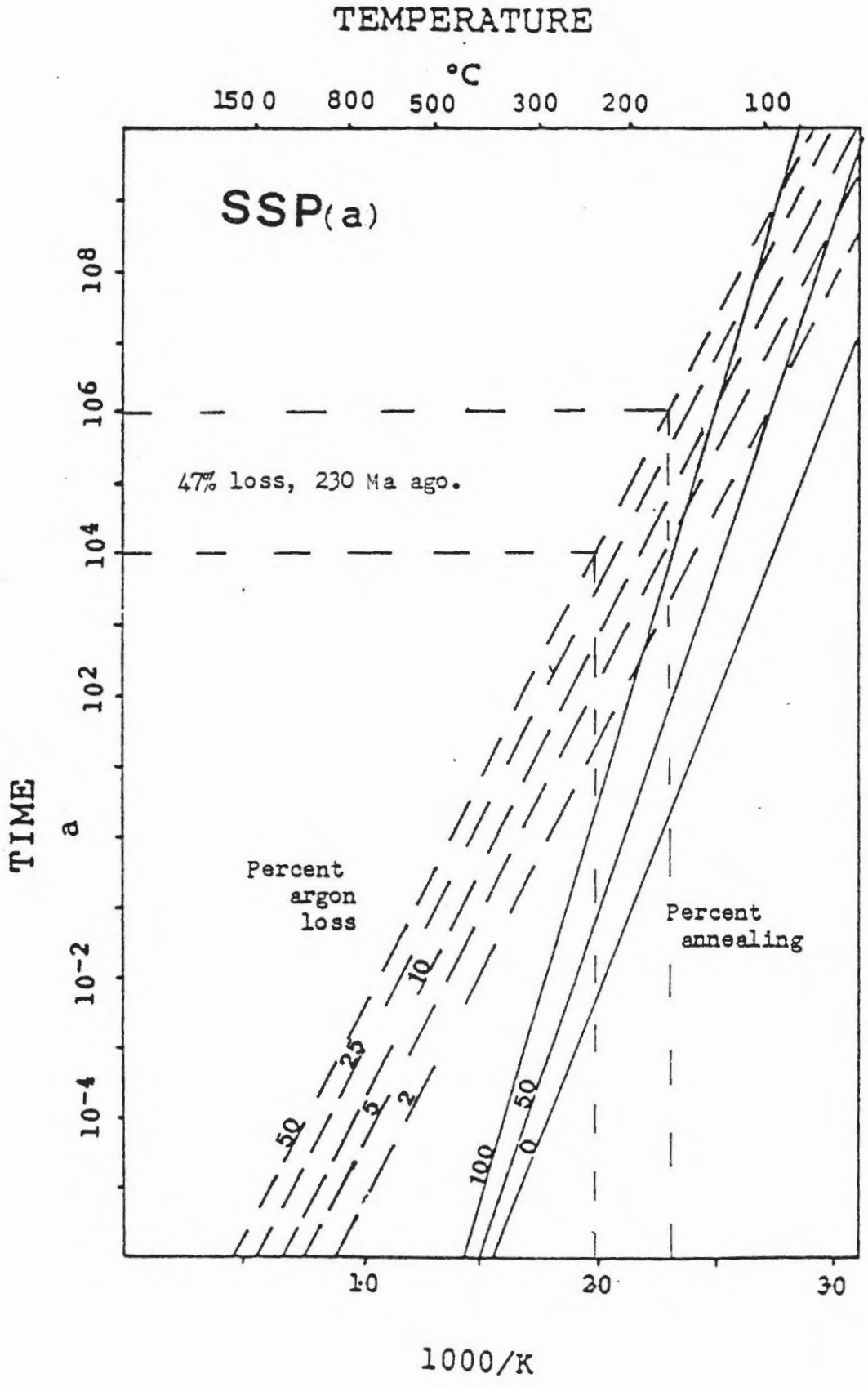
TEMPERATURE
°C
150 0
800
500
300
200
100
SSP(a)
47% loss, 230 Ma ago.
TIME
a
10⁸
10⁶
10⁴
10²
10⁻²
10⁻⁴
Percent argon loss
50
25
10
5
2
Percent annealing
100
50
0
1·0
2·0
3·0
1000/K

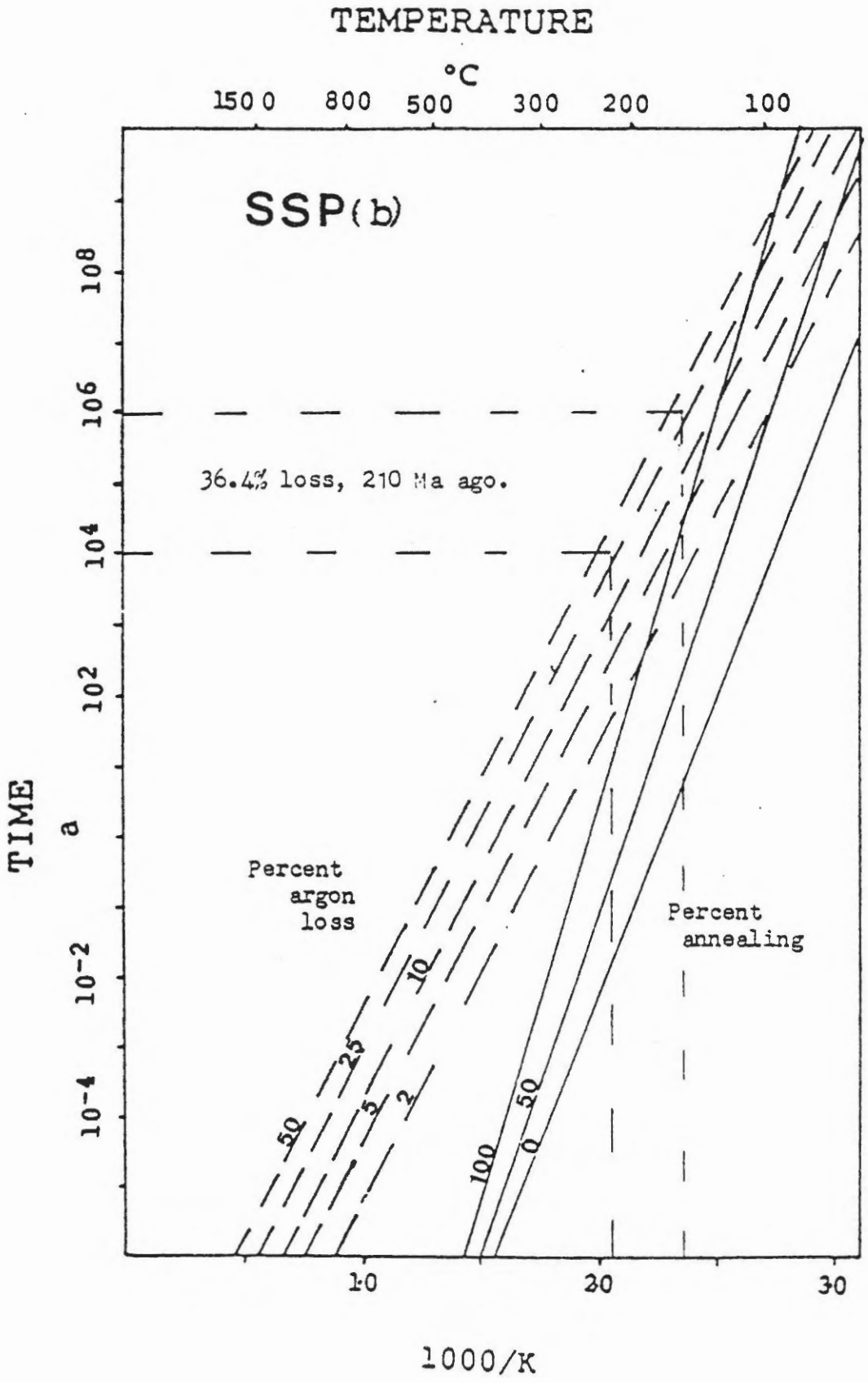
TEMPERATURE
°C
150 0
800
500
300
200
100
SSP(b)
36.4% loss, 210 Ma ago.
TIME
a
10⁸
10⁶
10⁴
10²
10⁻²
10⁻⁴
Percent argon loss
50
25
10
5
2
Percent annealing
100
50
0
10
20
30
1000/K

From fig. 4.4-10, a thermal event about 230 Ma ago (47% loss), lasting 1 million to 10, 000 years would require temperatures of 161-230 degrees C. The corresponding temperatures for an event 210 Ma ago (36.4% loss), are 153-203 degrees C.

4.5.7. DISCUSSION OF SSP MODELS

The two models require an overprinting event about 300 Ma ago. Abundant evidence for this event has been cited above. Circumstantial evidence for a significant tectonothermal event about 230-200 Ma is more equivocal. Mafic magmatism around this time (Chapter 1) could have caused substantial overprinting, if it was sufficiently widespread. Except for sporadic occurrence of small mafic dikes throughout the Meguma terrane (eg.Taylor, 1967, 1969), surface exposure of mafic rocks about 200 Ma old, is confined to the northwestern and southeastern flanks of the study area. There is no evidence of sharp decreases in mica ages close to the flanks. As stated in section 1.3.3, there is apparently little deformation in rocks of this age. Apparently the event (ca. 230-200 Ma ago) had no widespread severe overprinting effect among the SSP. Model 2 is plausible only if the 230-200 Ma event was very mild. With these reservations, the evidence from the Wedgeport mafic dikes, and the K-feldspar age minima (section 4.4.3), model 2 is preferred.

4.5.8. RMT COMPOSITE MODEL 1

This model (fig. 4.4-11) is constrained by three points. The 500 degree point is defined by the hornblende cooling age of about 404 Ma. The 300 degree point is defined by the 'older micas'. Biotite apparent ages range from 401 Ma to 360 Ma. Some of these micas may have been partially reset during intrusion of the plutons about 370 Ma ago. The range in age may also reflect diachronous cooling, a common feature in regional metamorphic terranes (eg Dallmeyer and VanBreeman, 1981).

The 300 Ma event is interpreted as for the SSP. Cooling through 100 degrees C is constrained by only one point: the apatite fission track age of about 280 Ma contrasts sharply with those from the plutons. This suggests that there was considerable variation in the late stage cooling of the Meguma Terrane. More data are required to constrain this aspect of the thermal history.

4.5.9. RMT COMPOSITE MODEL 2

This model (fig. 4.4-12) applies to the thermal aureole of the plutons. Since much of the RMT was strongly overprinted about 300 Ma ago, the effects of a 370 Ma event on the RMT are obscured. Except for the thermal pulse at 370 Ma, details of this model are similar to those of model 1.

Fig. 4.4-11. RMT Composite model 1.

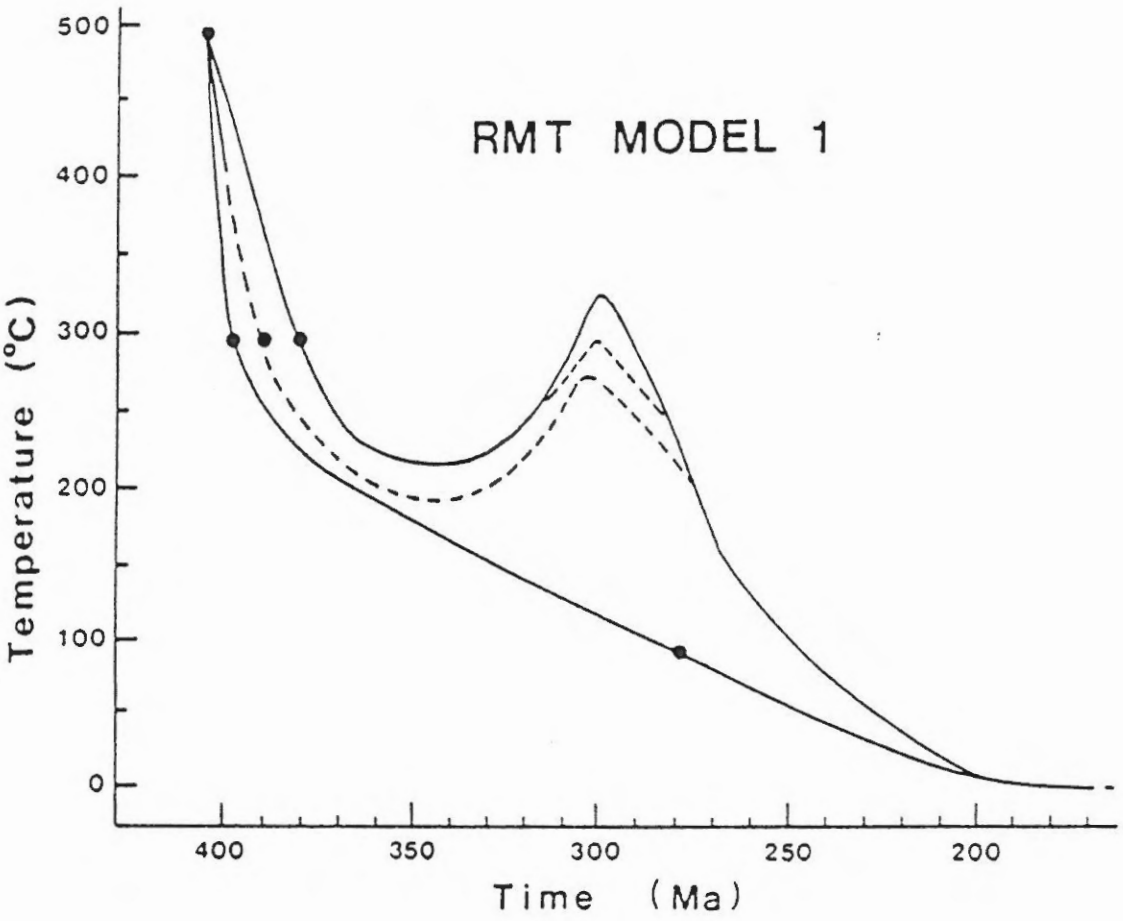
RMT MODEL 1
Temperature (°C)
500
400
300
200
100
0
400
350
300
250
200
Time (Ma)

Fig. 4.4-12. RMT Composite model 2.

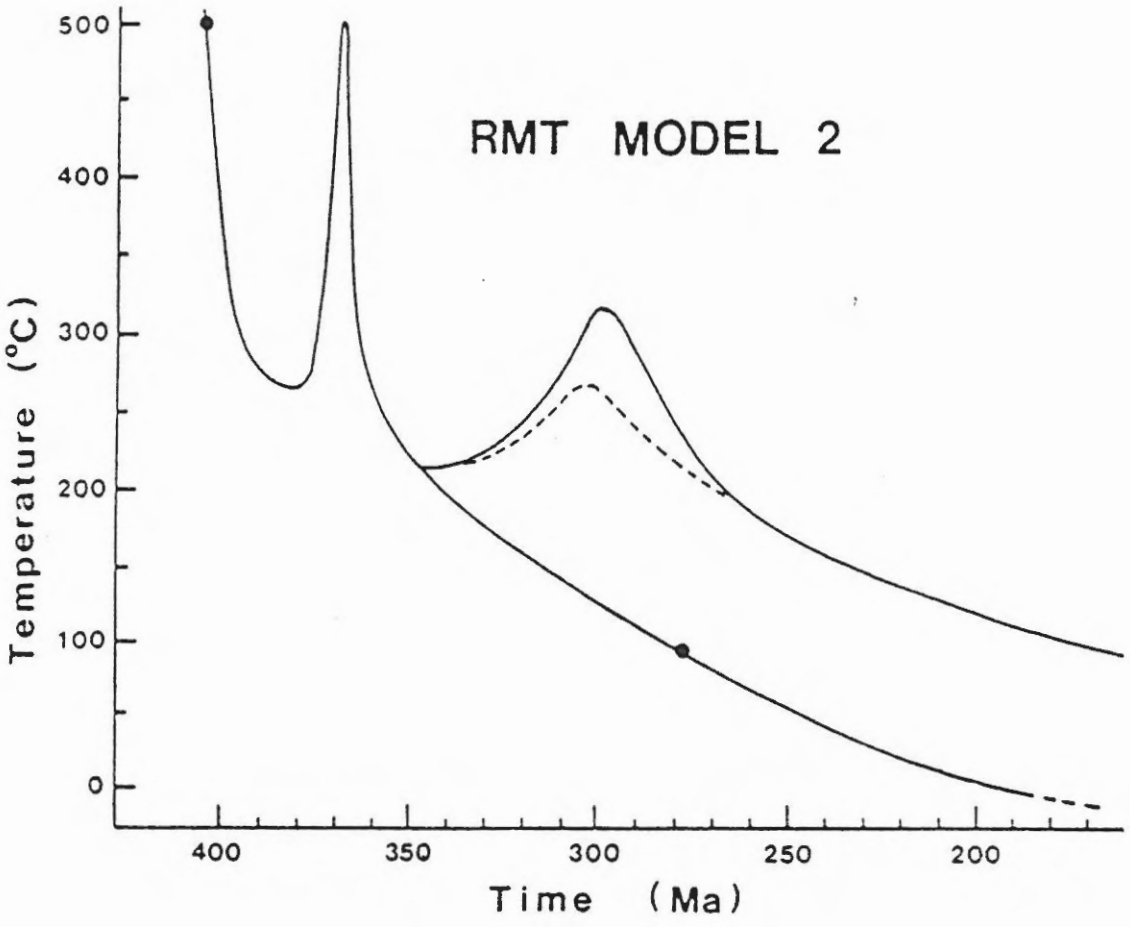
RMT MODEL 2
Temperature (°C)
500
400
300
200
100
0
400
350
300
250
200
Time (Ma)

4.5.10. DISCUSSION OF RMT MODELS

The RMT models are poorly constrained by the available data. Since regional metamorphism preceded most of the plutonism in the Meguma terrane, it can be expected that at least some aspects of the post-intrusive thermal history would be similar for both plutons and the RMT. This prediction is generally confirmed by observation. In the extreme northeastern part of the Meguma terrane, plutons do not appear to be disturbed by any major post-intrusive event. Both plutons and the RMT reflect a simple thermal history in plateau ages in their mica age spectra (Dallmeyer and Keppie, 1984). In contrast, the major resetting event which affected the SSP is reflected in low ages and discordant age spectra for micas from both the SSP and the RMT in the immediate vicinity (section 4.2.5.5). Although correlations can be made between the RMT and the plutons with respect to mica age data (> 300 ^{o}C), the low-temperature aspects of the thermal history of the RMT can be clarified only when more data from K-feldspar and apatite fission track become available.

CHAPTER 5 SUMMARY

5.1. INTRODUCTION

In this chapter, the main conclusions of the study are summarized. The implications of the inferences from thermochronometry are discussed, with special emphasis on the Late Carboniferous overprinting event described in Chapter 4. An attempt is made to interpret the data in the larger context of major tectonothermal events in the Appalachians and elsewhere. The main geologic events in the Meguma terrane, as presently understood, are summarized in fig. 5-1.

5.2. MAIN CONCLUSIONS

1. Regional metamorphism in the Meguma terrane was initiated about 400 Ma ago. The database from which previous estimates (e.g. Reynolds and Muecke, 1978) were made, has been considerably extended and refined. The present estimate is based on detailed ^{40}Ar-^{39}Ar age spectra from slates, amphiboles, and micas throughout most of the RMT. If this new estimate is correct, it would mean that regional metamorphism was initiated in the Meguma terrane

Fig. 5-1. Summary of geologic events in the Meguma terrane.

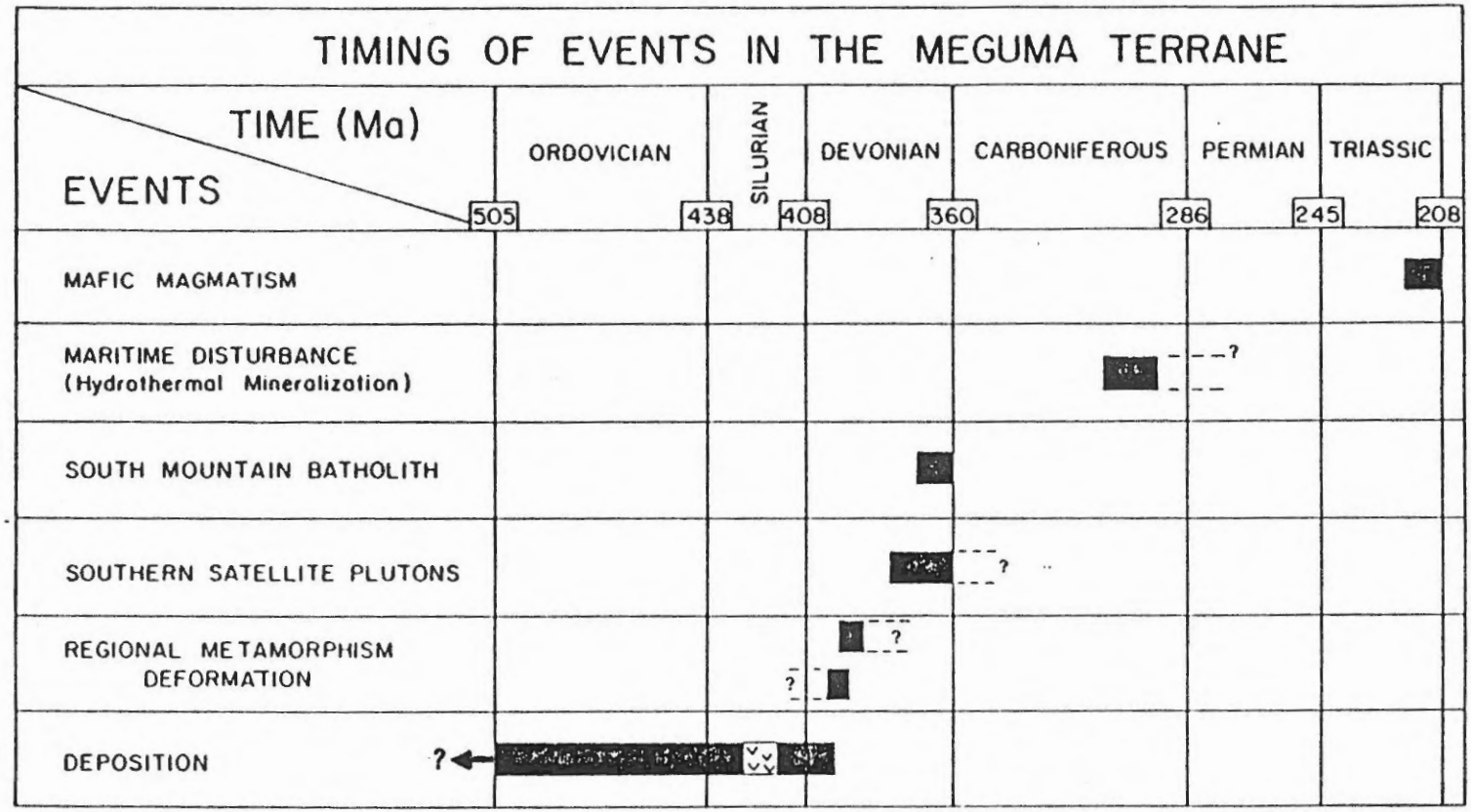
TIMING OF EVENTS IN THE MEGUMA TERRANE
TIME (Ma)
EVENTS
ORDOVICIAN
SILURIAN
DEVONIAN
CARBONIFEROUS
PERMIAN
TRIASSIC
505
438
408
360
286
245
208
MAFIC MAGMATISM
MARITIME DISTURBANCE
(Hydrothermal Mineralization)
SOUTH MOUNTAIN BATHOLITH
SOUTHERN SATELLITE PLUTONS
REGIONAL METAMORPHISM
DEFORMATION
DEPOSITION
?

while at least the upper parts of the Torbrook Formation were still being deposited (see Chapter 1). The probable diachronous nature of such thermal events has been recorded in the Alps, a younger orogenic analog (e.g. Bradbury and Nolen-Hoeksema, 1985). Because of complexities in the thermal history of the Meguma terrane, the age pattern which would be expected from simple post-metamorphic cooling (systematic younging towards higher grades, e.g. Adams et al., 1985), is highly distorted. In metamorphic zones higher than biotite grade, only a few mica ages reflect the regional metamorphic event. They are too young (as low as 294 Ma) to be explained by diachronous cooling (see below).

2. Intrusion of granitoid plutons occurred approximately 370-360 Ma ago. This includes the SMB and some or all of the SSP. Parts of the tonalitic Barrington Passage pluton may have intruded as early as 386 Ma ago. Because of overprinting, the original cooling ages of the SSP are preserved in only a few small domains (see below).

3. Timing of regional metamorphism and plutonism indicates that they are part of the Acadian orogeny, which affected most of the Appalachian belt. These events are associated temporally with juxtaposing of the Meguma terrane to the North American craton (e.g. Dallmeyer and Keppie, 1984).

4. A second, less pervasive event, assigned to the Maritime Disturbance, peaked approximately 320-300 Ma ago. It is likely that this event was of longer duration, as

evidenced by radiometric ages derived elsewhere that are slightly older or slightly younger than 320-300 Ma, (see table 1. 2). This event left a strong overprinting signature on the K-Ar system. The overprinting event was less severe in the SMB than in the SSP. Shear zones on various scales occur within the SSP as well as the RMT in the southwestern portion of the Meguma terrane (e.g. Calder and Barr, 1982; Dallmeyer and Keppie, 1986; Rogers, in preparation). Except in the southwestern extremity, very few shear zones have been observed in the SMB. It is very likely that these zones acted as conduits for hydrothermal fluids, through which heat was transmitted for mineralization and overprinting of the K-Ar system. Whereas at least part of the SMB was unroofed by 348 Ma, there is no evidence that this happened to the SSP, although they must have cooled below 300 degrees C by 370 Ma. Probably the combination of greater permeability and greater depth rendered the SSP and the RMT more susceptible to the effects of the Maritime Disturbance. Although local details vary, the 320-300 Ma event can be broadly correlated with the Alleghanian orogeny elsewhere in the Appalachians and the Hercynian-Variscan event in Western Europe and North Africa. This is further discussed below.

5. The combination of data from ^{40}Ar-^{39}Ar dating of K-feldspars and fission track dating of apatite has been successfully employed to deduce the late stage thermal history of the Meguma terrane. Constraints have been placed

on the timing, temperature, and duration of overprinting events. The available data suggest that the SSP, and probably most of the southwestern Meguma terrane, were affected by a mild overprinting event about 230-210 Ma ago. It is uncertain to what extent this event, which is associated with rifting, affected the SMB.

6. Data from fission tracks in apatite show that final cooling of the Meguma terrane through 100 degrees C occurred about 170-190 Ma ago.

7. Quantification of discordance is an aid in evaluating ^{40}Ar-^{39}Ar spectra. It provides a means of testing the effects of tectonothermal disturbance and other factors on the extent of discordance in an age spectrum. The Compound Sigma parameter (CS) provides an estimate of inter-step uncertainty, which indicates how well the spectrum is defined.

8. The step-heating technique appears incapable of yielding consistent values for activation energies and closure temperatures. This may be partly due to the effects of overprinting on the crystalline structures from which diffusion occurs. This is superimposed on the effects of possible phase changes during the vacuum step-heating experiment.

5.3. IMPLICATIONS OF TECTONOTHERMAL EVENTS IN THE MEGUMA TERRANE

5.3.1. THE ACADIAN EVENT

As stated in Chapter 1, the Acadian event in the Meguma terrane resulted in folding, regional metamorphism, and plutonism (e.g. Fyson, 1966; Poole et al., 1970; Schenk, 1978). At this time, the Meguma terrane is thought to have become attached to the eastern flank of the North American craton (the Avalon zone). The relatively straight nature of the Meguma-Avalon boundary has led some workers to suggest convergence by transcurrent motion (e.g. Williams and Hatcher, 1982). Folding is open to isoclinal in the Meguma terrane (e.g. Fyson, 1966), which suggests significant horizontal shortening (compressional component) during convergence. This is equivalent to the transpressional convergence mechanism suggested for accretion of terranes in western North America (e.g. Nur, 1983). The Middle to Late Devonian event is part of the Acadian orogeny that affected most of the Appalachian belt (e.g. Boucot, 1968; Naylor, 1971; Poole, 1976). The arrival of the Meguma terrane was conceivably part of a larger collision between the Euro-African plate and North America (e.g. Bird and Dewey, 1970; Poole, 1976; Schenk, 1978). Metamorphism and plutonism may have resulted from thickening of the crust by

shortening during collision (Poole, 1976), although Keppie (1977) suggested a southeasterly dipping subduction zone beneath the Meguma terrane. When the uncertainties of the ^{40}Ar-^{39}Ar system are considered, (e.g. minor excess argon, argon loss), the estimated duration of Acadian regional metamorphism and plutonism in the Meguma terrane (section 5.2) is consistent with the suggestion of Naylor (1971) that the Acadian orogeny in the Appalachians lasted about 30 Ma during the Devonian. Glover et al., (1983) reported radiometric data which suggest that the Acadian orogeny lasted beyond the Devonian (until 340 Ma) in the southern Appalachians. This discrepancy may reflect diachronous cooling along the Appalachian belt, or complexities associated with later overprinting.

5.3.2. THE ALLEGHANIAN EVENT (MARITIME DISTURBANCE)

The 320-300 Ma thermal pulse (section 4.5) can be correlated with several examples of significant tectonothermal events in Atlantic Canada and elsewhere in the Appalachians. On the basis of strong deformation in Carboniferous sediments in Atlantic Canada, Poole (1967) assigned post-Devonian, pre-Triassic tectonothermal events to the 'Maritime Disturbance.' Complex folding and faulting have been observed in Carboniferous strata older than Westphalian C in the Fundy-Magdalen Basin of Atlantic Canada

(e.g. Fyson, 1967; Belt, 1968; Poole et al., 1970). These stratigraphic constraints set an upper limit on the timing of this event at approximately 300 Ma, which is in good agreement with the estimates from this study. The Late Carboniferous overprint also corresponds in time to a depositional hiatus between 325 Ma and 303 Ma (Late Namurian to Westphalian), which is associated with basement uplift in the Sydney Basin, Cape Breton (Gibling et al., in press). In their review of post-Acadian deformation in Maritime Canada, Mosher and Rast (1984) noted that although some polyphase deformation had been observed within the Meguma terrane, the phenomenon was only partially studied. Recent research has, however, provided more details on post-Acadian deformation. Complex patterns of faulting and folding have been observed in the Stellarton Basin, adjacent to the Minas Geofracture (Fralick and Schenk, 1981; Yeo and Ruixing, 1986). This tectonism is stratigraphically dated as Westphalian (ca. 300 Ma). Yeo and Ruixing (1986) concluded that the observed structures could be explained by a large-scale Riedel shear couple, a similar interpretation to that of Fralick and Schenk (1981). Preliminary studies in the Meguma terrane south of the Shelburne and Barrington Passage plutons, indicate a complex deformational history (Hwang and Williams, 1985; see section 4.2.6.1). ^{40}Ar-^{39}Ar data suggest that at least some of this deformation occurred about 320-290 Ma ago (section 4.2.6.3). The Late Carboniferous deformation is ascribed to complexities due to

strike-slip movement on curved faults (e.g. Bradley, 1982; Nance and Warner, 1986). This event is also interpreted as final closure of the suture between North America and the Afro-Eurasian plate (Schenk, 1976; Fralick and Schenk, 1981). Although much work is still required on the late structures, data from this study indicate that the Maritime Disturbance was more widespread within the Meguma terrane than previously realized. This event, which apparently peaked about 320-300 Ma ago, is recorded in ^{40}Ar-^{39}Ar spectra from the regional metamorphic terrane, the South Mountain batholith, and the southern satellite plutons. Available ^{40}Ar-^{39}Ar data on dynamically recrystallized micas from ductile shear zones in the southwestern part of the Meguma terrane, indicate that major shearing occurred 325-275 Ma ago (see also Dallmeyer and Keppie, 1986). As stated in Chapters 1 and 4, these deformation events coincide temporally with mineralization in widely separated domains within the Meguma terrane (e.g. Chatterjee and Keppie, 1981; Reynolds et al., 1981; O'Reilly et al., 1985; Zentilli and Reynolds, 1985). The implication is that although much of the mineralization is spatially associated with the plutons, deposition of economically important minerals occurred much later than plutonism. This suggests that the controlling factors were largely related to post-magmatic features such as fluid availability as well as shearing (permeability), rather than processes such as magmatic differentiation. This has significant implications

for mineral exploration programs. Similar conclusions have been reached on the timing of mineralization in Hercynian granites in southwest England (Shepherd et al., 1985). Paleomagnetic studies suggest major strike-slip motion by Meguma terrane rocks, constrained stratigraphically between early Carboniferous (348 Ma), and the Triassic (ca. 200 Ma) (Scotese et al., 1984; Spariosu et al., 1984). This is consistent with the ^{40}Ar-^{39}Ar data, although the extent of these transcurrent movements have been disputed (e.g. Irving and Strong, 1984).

Within a larger context, it may be noted that the central and southern parts of the Appalachian System were affected by a major event 330-230 Ma ago (Glover et al., 1983). As summarized by Arthaud and Matte (1977), the Alleghanian events in the Appalachian system included: (1) Dextral strike-slip faulting, accompanied by folding and thrusting. (2) Reactivation of older faults. (3) Retrograde metamorphism (except in the Narragansett Basin, where metamorphism was largely prograde). (4) Compression in a NW-SE direction. A well-documented example of strike-slip faulting in the Appalachians is the Brookneal shear zone in the Virginia Piedmont (Gates et al., 1986). The shear zone is 4 km wide, and imposes a prominent S-C mylonitic fabric on the Melrose granite. Metamorphic conditions were in the albite-epidote facies (about 450 degrees C). A Rb-Sr isochron on dynamically recrystallized biotite and whole rock yielded an age of 300 +/- 5 Ma.

Timing, metamorphic grade, and deformational style are remarkably similar to those of the Brenton pluton in Nova Scotia. Two other examples of Alleghanian deformation in the southern Appalachians, are the Modoc and Nutbush Creek dextral strike-slip faults. Movement on these faults has been radiometrically dated at 285-313 Ma (Gates et al., 1986). More recent work (e.g. Secor et al., 1986a, 1986b), suggests that the Alleghanian orogeny in the southern Appalachians involved large-scale thrusting, regional metamorphism up to amphibolite grade, and granite plutonism. The earliest phase of this event occurred approximately 315-295 Ma ago (Late Carboniferous). Although interpretation of the scale and magnitude of deformation may vary locally, general similarities in the nature and timing, suggest that the 320-300 Ma event in the Meguma terrane was part of the larger Alleghanian event in the Appalachian belt.

Correlations can be made on an even larger scale. The Hercynian-Variscan orogeny in Western Europe and North Africa occurred about 290-250 Ma ago (Arthaud and Matte, 1977). This event involved wrench faulting and major shearing. The similarity in timing between the Alleghanian and Hercynian-Variscan events led Arthaud and Matte (1977) to propose a large-scale Riedel shear system involving the Euro-American, African, and Siberian plates, to account for the observed deformation. Similar models, largely based on geophysical data, were proposed by Morel and Irving (1978),

and Lefort and Van der Voo (1981). Although these models are too general to account for some local details (e.g. slight differences in age), it seems that the Meguma terrane was involved in a major Permo-Carboniferous event on a global scale.

5.3.3. THE MESOZOIC EVENT

Data from biotite and K-feldspar (section 4.4.3) suggest that an additional mild thermal event occurred at about 230-210 Ma, at least in the southwestern part of the Meguma terrane. As stated previously (sections 1.3.3, 4.4.3), this time overlaps that of mafic magmatism. The North Mountain basalts, which represent most of this magmatism in the Meguma terrane, are interbedded with fluvio-lacustrine sediments of the Fundy Group (Klein, 1962). The oldest flows of the North Mountain basalts lie approximately 30 meters above the stratigraphically defined Triassic-Jurassic boundary, and the age of the overlying McCoy Brook Formation is Hettangian (Jellinek, 1986). This suggests an age of approximately 207 Ma for the North Mountain basalts. This stratigraphically constrained age is slightly higher than the K-Ar isochron age of 191 +/- 2 Ma obtained by Hayatsu (1979), and the conventional K-Ar age of 202 Ma reported by Poole et al., (1970, recalculated by Wark and Clarke, 1980). The estimate of 207 Ma is more compatible with the 225 Ma plateau age obtained for biotite

from mafic dykes intruding north of the Wedgeport pluton, in southwestern Nova Scotia. Deposits of similar age and geologic setting occur throughout most of the Appalachians as the Newark Supergroup (e.g. Van Houten, 1977). This Late Triassic event corresponds in time to the 'rift phase' in the development of the passive Atlantic continental margin (Uchupi and Austin, 1979). Similar basins with non-marine sediments interbedded with basalts, have been identified in northwestern Africa (e.g. Van Houten, 1977). This is consistent with the suggestion of Schenk (1971) that the Meguma terrane is of North African origin. Final cooling to below 100 degrees C occurred at 190-170 Ma, as indicated by the fission track ages. This time is coincident with opening of the present Atlantic margin approximately parallel to the Bay of Fundy rift. Although thermal activity apparently ceased in the Meguma terrane in Early Jurassic, it persisted longer elsewhere in the Appalachians. For example, magmatism continued in the White Mountains of New Hampshire and the Monteregian Hills of Quebec well into the Early Cretaceous (e.g. Foland and Faul, 1977; McHone, 1978). Early Cretaceous (125-100 Ma) basaltic magmatism has also been recorded on the Atlantic continental shelf of Canada (Jansa and Pe-Piper, 1985).

APPENDIX A SUMMARY TABLES FROM ARGON ANALYSES.

APPENDIX A-1

SLATES

THIS STUDY

NB71-13Y (CB7) BLATE SUMMARY

TEMP.(DEG.C)	aV Ar39	% Ar39	AGE(Ma)	% ATMOS.	Ar37/Ar39	% I.I.C.
			J = 2.858E-03			
200-500	23	8.1	336.1 +/- 1.3	27.8	0	0
500-570	51.5	18.3	383.5 +/- 1	14.8	0	0
570-630	47.8	17	408.7 +/- .5	7	0	0
630-670	35.4	12.6	407.7 +/- .6	9.8	0	0
670-710	28.8	10.2	412.7 +/- 1.1	12.4	0	0
710-750	25	8.9	419.2 +/- 1.1	17	0	0
750-790	17.8	6.3	435.6 +/- 1.4	19.6	0	0
790-830	14.8	5.2	444.3 +/- 2.5	21.6	0	0
830-900	21.4	7.6	447.3 +/- 1.6	19.9	0	0
900-970	9	3.2	409.6 +/- 3	37.4	0	0
970-1050	6.1	2.1	374.8 +/- 8.6	59.9	0	0

TOTAL GAS AGE = 403.8 MY.

% I.I.C. - INTERFERING ISOTOPES CORRECTION

ERROR ESTIMATES AT ONE SIGMA LEVEL

NB72-31 BLATE SUMMARY

TEMP.(DEG.C)	aV Ar39	% Ar39	AGE(Ma)	% ATMOS.	Ar37/Ar39	% I.I.C.
			J = 1.97E-03			
200-500	14	4.1	290.2 +/- 2.6	41.3	0	0
500-570	28	8.2	342.3 +/- .7	7.7	0	0
570-630	42.7	12.6	404.9 +/- .7	2.5	0	0
630-670	47.5	14	405.2 +/- .5	2.8	0	0
670-710	60.6	17.9	397 +/- .4	2.4	0	0
710-750	48.4	14.3	388.5 +/- .7	3.5	0	0
750-790	24.5	7.2	392.3 +/- 1.4	4.4	0	0
790-830	22	6.5	401.1 +/- 1.5	7.2	0	0
830-900	28.3	8.3	413.4 +/- 1.3	6.2	0	0
900-1150	22.1	6.5	391.4 +/- 1.3	25.3	0	0

TOTAL GAS AGE = 390.1 MY.

% I.I.C. - INTERFERING ISOTOPES CORRECTION

ERROR ESTIMATES AT ONE SIGMA LEVEL

THIS STUDY

NB72-33 BLATE SUMMARY

TEMP. (DEG.C)	mV Ar39	% Ar39	AGE (Ma)	% ATMOS.	Ar37/Ar39	% I.I.C.
			J = 1.9686E-03			
200-500	9.9	5.4	334.9 +/- 1.5	28	0	0
500-570	30.7	16.8	402.1 +/- .8	12.6	0	0
570-630	39.3	21.5	396.5 +/- .7	5.8	0	0
630-670	20.6	11.3	389.4 +/- .8	7.8	0	0
670-710	32.7	17.9	382.2 +/- .7	10.4	0	0
710-750	19.6	10.7	377.2 +/- 1	20.8	0	0
750-790	10.6	5.8	372.9 +/- 2.6	39.5	0	0
790-830	5.5	3	375.7 +/- 6	57	0	0
830-900	8	4.4	364.9 +/- 6	48.2	0	0
900-1150	5	2.7	0 +/- 0	0	0	0

TOTAL GAS AGE = 384.4 MY.

% I.I.C. - INTERFERING ISOTOPES CORRECTION
ERROR ESTIMATES AT ONE SIGMA LEVEL

KB-1 BLATE SUMMARY

TEMP. (DEG.C)	mV Ar39	% Ar39	AGE (Ma)	% ATMOS.	Ar37/Ar39	% I.I.C.
			J = 3.785E-03			
200-500	2.4	.6	330.6 +/- 25.6	41.3	0	0
500-600	23.1	6.4	331.6 +/- 1.2	14.1	0	0
600-675	24.3	6.8	370.5 +/- 1.6	3.5	0	0
675-750	43	12	381.7 +/- .5	2.3	0	0
750-825	90	25.2	378.1 +/- .9	2.8	0	0
825-900	60	16.8	383.5 +/- 1.2	2.4	0	0
900-975	56	15.6	401.2 +/- .5	6.2	0	0
975-1100	58	16.2	391.2 +/- 1	10.6	0	0

TOTAL GAS AGE = 381.4 MY.

% I.I.C. - INTERFERING ISOTOPES CORRECTION
ERROR ESTIMATES AT ONE SIGMA LEVEL

(SILTY SLATE)

KB-3 "SLATE" SUMMARY

TEMP. (DEG.C)	mV Ar39	% Ar39	AGE (Ma)	% ATMOS.	Ar37/Ar39	% I.I.C.
			J = 3.78E-03			
200-500	2	1	241.2 +/- 6.3	76.2	0	0
500-600	8.8	4.5	314.8 +/- 2.7	28.9	0	0
600-675	16.5	8.4	375.2 +/- 2.2	8.8	0	0
675-750	15	7.6	384 +/- 2.4	5.4	0	0
750-825	39	19.9	383.8 +/- 1	4.5	0	0
825-900	43	22	393.8 +/- .3	6.4	0	0
900-975	35	17.9	420.9 +/- 1.4	14.2	0	0
975-1100	36	18.4	411.8 +/- 1.1	19	0	0

TOTAL GAS AGE = 392.7 MY.

% I.I.C. - INTERFERING ISOTOPES CORRECTION

ERROR ESTIMATES AT ONE SIGMA LEVEL

(SILTSTONE)

KB-4 "SLATE" SUMMARY

TEMP. (DEG.C)	mV Ar39	% Ar39	AGE (Ma)	% ATMOS.	Ar37/Ar39	% I.I.C.
			J = 3.765E-03			
200-500	.6	.9	471.1 +/- 82.6	83	0	0
500-600	3.4	4.4	333.2 +/- 4.4	42.4	0	0
600-675	6	8	394.6 +/- 10.6	14.3	0	0
675-750	22.7	29.9	381 +/- 1.1	15.3	0	0
750-825	9.1	12	400.8 +/- 8.4	13	0	0
825-900	7	9.1	395.6 +/- 1.9	20	0	0
900-975	10.9	14.3	411.2 +/- 4.6	34.9	0	0
975-1100	16	21	393 +/- 1.1	42.9	0	0

TOTAL GAS AGE = 391.9 MY.

% I.I.C. - INTERFERING ISOTOPES CORRECTION

ERROR ESTIMATES AT ONE SIGMA LEVEL

PE83-137A SLATE SUMMARY

TEMP.(DEG.C)	aV Ar39	% Ar39	AGE(Ma)	% ATMOS.	Ar37/Ar39	% I.I.C.
			J = 1.967E-03			
200-500	12.1	6.4	232.6 +/- 4.7	48.8	0	0
500-570	38.4	20.3	313.1 +/- .8	26	0	0
570-630	43	22.7	344.9 +/- 1.2	3.2	0	0
630-670	32.5	17.2	381.1 +/- 1.6	4.2	0	0
670-710	20.9	11.1	393.1 +/- 2.4	5.2	0	0
710-750	11.4	6	411.5 +/- 3.3	6.5	0	0
750-800	11.5	6	448.7 +/- 3.3	10.8	0	0
800-900	13	6.8	446.3 +/- 11.2	10.4	0	0
900-1050	5.8	3	412.9 +/- 8.6	27.4	0	0

TOTAL GAS AGE = 367.8 MY.

% I.I.C. - INTERFERING ISOTOPES CORRECTION

ERROR ESTIMATES AT ONE SIGMA LEVEL

PE83-138 SLATE SUMMARY

TEMP.(DEG.C)	aV Ar39	% Ar39	AGE(Ma)	% ATMOS.	Ar37/Ar39	% I.I.C.
			J = 1.965E-03			
200-500	10.2	5.1	263.5 +/- 2.6	21.7	0	0
500-570	33.8	16.8	287.8 +/- 1.1	7.3	0	0
570-630	51.7	25.7	348.7 +/- 1.1	4.1	0	0
630-670	34.2	17	354.5 +/- 1.8	6.9	0	0
670-700	20	9.9	359.5 +/- 2.9	4.7	0	0
700-750	14.7	8.3	356.2 +/- 2.8	5.3	0	0
750-900	15.3	7.6	380.7 +/- 1.9	8.9	0	0
900-900	14.5	7.2	407.3 +/- 2.1	10.2	0	0
900-1150	4.3	2.1	434.3 +/- 8.8	45	0	0

TOTAL GAS AGE = 345.7 MY.

% I.I.C. - INTERFERING ISOTOPES CORRECTION

ERROR ESTIMATES AT ONE SIGMA LEVEL

(REYNOLDS AND MUECKE, 1978)

NB71-139 SLATE SUMMARY

TEMP.(DEG.C)	mV Ar39	% Ar39	AGE(Ma)	% ATMOS.	Ar37/Ar39	% I.I.C.
			J = 4.98E-03			
200-300	34.5	8	332.8 +/- 1.7	52.8	0	0
300-400	37.4	8.7	376.6 +/- 1.3	35.8	0	0
400-700	120	28.1	389 +/- 2.7	58.7	0	0
700-820	167	39.1	401.8 +/- .7	17.5	0	0
820-920	44.5	10.1	404.9 +/- 1.4	35.1	0	0
920-1020	2.2	.5	351 +/- 63	88	0	0
1020-1200	.6	.1	274.9 +/- 86.5	94.6	0	0

TOTAL GAS AGE = 390.5 MY.

% I.I.C. - INTERFERING ISOTOPES CORRECTION

ERROR ESTIMATES AT ONE SIGMA LEVEL

NB 72-31 SLATE SUMMARY

TEMP.(DEG.C)	mV Ar39	% Ar39	AGE(Ma)	% ATMOS.	Ar37/Ar39	% I.I.C.
			J = 5.29E-03			
200-510	40	9.7	294.9 +/- .7	13.3	0	0
510-610	68	16.3	409.6 +/- .8	4.7	0	0
610-720	160	38.8	401.1 +/- .6	2.9	0	0
720-820	88	21.3	413.2 +/- .6	4.4	0	0
820-920	49	11.9	406 +/- .8	12.5	0	0
920-1020	5	1.2	329.9 +/- 7.9	76	0	0
1020-1180	1.3	.3	322.6 +/- 33.2	91.7	0	0

TOTAL GAS AGE = 394.5 MY.

% I.I.C. - INTERFERING ISOTOPES CORRECTION

ERROR ESTIMATES AT ONE SIGMA LEVEL

(REYNOLDS AND MUECKE, 1978)

NB 72-33 SLATE SUMMARY

TEMP.(DEG.C)	aV Ar37	% Ar39	AGE(Ma)	% ATMOS.	Ar37/Ar39	% I.I.C.
			J = 5.29E-03			
100-500	15.3	4.2	292.2 +/- 32.9	94.4	0	0
500-600	55.7	15.2	414.3 +/- .3	10.9	0	0
600-700	140	38.4	404.9 +/- .2	2.1	0	0
700-800	82.8	22.7	396.3 +/- .5	4.2	0	0
800-900	44.9	18.3	401.4 +/- .3	10.9	0	0
900-1000	3.4	.9	388.5 +/- 4.4	73	0	0

TOTAL GAS AGE = 399.3 MY.

% I.I.C. - INTERFERING ISOTOPES CORRECTION

ERROR ESTIMATES AT ONE SIGMA LEVEL

APPENDIX A - 2

REGIONAL METAMORPHIC AMPHIBOLES

PE83-11 HORNBLENDE SUMMARY

TEMP.(DEG.C)	mV Ar39	% Ar39	AGE(Ma)	% ATMOS.	Ar37/Ar39	% I.I.C.
			J = 1.843E-03			
200-650	3.3	6.2	501.7 +/- 20	63.7	4.8	.4
650-750	3.5	6.6	409.1 +/- 24.9	65.6	3.1	.3
750-850	2.5	4.8	397.9 +/- 20.4	56.2	3.1	.6
850-900	2.5	4.8	500.3 +/- 21.7	37.9	4.6	.4
900-950	3.9	7.3	437.9 +/- 4.8	30.1	8.1	.9
950-1000	10.3	19.5	404.2 +/- 3.4	15.4	15.8	1.8
1000-1050	6.2	11.7	371.6 +/- 5.4	27.9	16.8	2.1
1050-1100	3.8	7.3	353.2 +/- 11.2	44.6	18.4	2.3
1100-1130	8.1	15.4	402.7 +/- 3.2	32.9	19.2	2.3
1130-1160	8.4	16	423.1 +/- 4.3	31.6	19.3	2.2

TOTAL GAS AGE = 413.1 MY.

% I.I.C. - INTERFERING ISOTOPES CORRECTION

ERROR ESTIMATES AT ONE SIGMA LEVEL

PE84-64C AMPHIBOLE SUMMARY

TEMP.(DEG.C)	mV Ar39	% Ar39	AGE(Ma)	% ATMOS.	Ar37/Ar39	% I.I.C.
			J = 1.965E-03			
200-750	5.3	4.3	747.1 +/- 10.8	40.4	8.9	.8
750-850	6.1	4.9	356.8 +/- 5	40.9	12	1.5
850-950	16.3	13.1	379.2 +/- 2.2	27.1	13	1.6
950-1000	11.8	9.5	389.4 +/- 3.6	27.9	12.8	1.6
1000-1050	35.5	28.6	366.5 +/- .8	22.3	13.4	1.7
1050-1100	31.5	25.4	399.5 +/- .9	14.5	13.4	1.6
1100-1190	17.2	13.8	404 +/- 1.5	30.4	13	1.6

TOTAL GAS AGE = 401.5 MY.

% I.I.C. - INTERFERING ISOTOPES CORRECTION

ERROR ESTIMATES AT ONE SIGMA LEVEL

PE84-130 HORNBLENDE SUMMARY

TEMP.(DEG.C)	mV Ar39	% Ar39	AGE(Ma)	% ATMOS.	Ar37/Ar39	% I.I.C.
			J = 1.849E-03			
200-650	3.2	4.2	303.4 +/- 34.3	84	4.2	.5
650-750	2.8	3.6	285.7 +/- 19.4	78.6	4.5	.6
750-850	3.1	4.1	300.8 +/- 15.8	75.8	7.9	1.1
850-930	27.2	35.5	341.1 +/- 1	24.6	11.3	1.4
930-1000	6.9	9	335.1 +/- 3.4	31.3	11.3	1.5
1000-1030	15.2	19.8	344.4 +/- 1.4	22.5	11.7	1.5
1030-1100	10.2	13.2	336.1 +/- 3.2	27.1	11.8	1.5
1100-1130	4.8	6.3	346.8 +/- 6.6	43.2	11.8	1.5
1130-1170	2.9	3.8	333.3 +/- 13.3	58.2	11.7	1.5

TOTAL GAS AGE = 338.2 MY.

% I.I.C. - INTERFERING ISOTOPES CORRECTION

ERROR ESTIMATES AT ONE SIGMA LEVEL

APPENDIX A - 3

'OLDER' MICAS

REGIONAL METAMORPHIC TERRANE

PE82-1A SCHIST SUMMARY

TEMP.(DEG.C)	mV Ar39	% Ar39	AGE(Ma)	% ATMOS.	Ar37/Ar39	% I.I.C.
			J = 3.02E-03			
200-500	22.5	3.9	270.2 +/- 1.2	31.1	.2	0
500-600	39	6.7	372.1 +/- .5	4.4	.8	.1
600-700	192	33.4	384.7 +/- 2.2	2.8	.2	0
700-800	98	17	377.6 +/- .3	2.8	.2	0
800-850	78.6	13.7	379.7 +/- .3	2.7	0	0
850-900	39.9	6.9	384.6 +/- .8	5.4	0	0
900-950	60.9	10.6	384.9 +/- .5	3	0	0
950-1000	30.8	5.3	392.8 +/- 1	3.2	0	0
1000-1050	11.8	2	449.3 +/- 2.6	15.8	.9	.1

TOTAL GAS AGE = 380.1 MY.

% I.I.C. - INTERFERING ISOTOPES CORRECTION

ERROR ESTIMATES AT ONE SIGMA LEVEL

PE 82-4 BIOTITE SUMMARY

TEMP.(DEG.C)	mV Ar39	% Ar39	AGE(Ma)	% ATMOS.	Ar37/Ar39	% I.I.C.
			J = 2.927E-03			
200-300	2.3	.7	202.7 +/- 17.7	68.3	0	0
300-350	8.3	2.4	298.7 +/- 4.6	27.2	0	0
350-400	30.6	8.8	362.3 +/- 1.8	9	0	0
400-450	57.4	16.4	376.6 +/- .6	4.8	0	0
450-700	63.1	18.2	378.5 +/- .5	4.8	0	0
700-750	26.6	7.7	376.3 +/- 1.7	13	0	0
750-800	13.8	4	373.1 +/- 1.4	19.8	0	0
800-850	18.3	5.3	377.3 +/- 2	10.6	0	0
850-900	26	7.5	377.8 +/- 1.1	11.7	0	0
900-1000	90.4	26.2	379.6 +/- .2	6.1	0	0
1000-1050	5.7	1.6	396.6 +/- 9.1	36.1	0	0
1050-1100	1.9	.5	439.1 +/- 33	61.6	0	0

TOTAL GAS AGE = 374.2 MY.

% I.I.C. - INTERFERING ISOTOPES CORRECTION

ERROR ESTIMATES AT ONE SIGMA LEVEL

PE82-5 BIOTITE SUMMARY

TEMP.(DEG.C)	mV Ar39	% Ar39	AGE(Ma)	% ATMOS.	Ar37/Ar39	% I.I.C.
			J = 1.948E-03			
200-500	8.4	1.6	163.8 +/- 3.9	64.9	0	0
500-550	25.2	4.9	223.2 +/- .9	18.4	0	0
550-600	38.6	7.6	337.3 +/- .7	5.8	0	0
600-642	35.2	6.9	374.9 +/- .9	4.4	0	0
642-700	33	6.9	368.7 +/- .9	7.4	0	0
700-750	26	5.1	365.2 +/- 1	10.1	0	0
750-800	25.4	5	372.3 +/- 1.6	11.3	0	0
800-850	34.8	6.9	373.2 +/- 1.2	9.9	0	0
850-900	58.2	11.5	378.1 +/- .7	7.2	0	0
900-950	173.7	34.7	378.6 +/- .5	2.9	0	0
950-1000	37	7.3	373.7 +/- 1.2	13.1	0	0
1000-1100	5.6	1.1	330.6 +/- 9.9	55.4	0	0

TOTAL GAS AGE = 362.9 MY.

% I.I.C. = INTERFERING ISOTOPES CORRECTION

ERROR ESTIMATES AT ONE SIGMA LEVEL

PE82-20N BIOTITE SUMMARY

TEMP.(DEG.C)	mV Ar39	% Ar39	AGE(Ma)	% ATMOS.	Ar37/Ar39	% I.I.C.
			J = 2.973E-03			
200-630	18	7.3	311.9 +/- 2.8	41.7	0	0
630-730	37	15.4	368.8 +/- 2.7	22	0	0
730-850	13	5.4	367.7 +/- 5.9	23.4	0	0
850-900	36	15.1	365.3 +/- 3.3	25.5	0	0
900-950	12	5	371.2 +/- 4	21.4	0	0
950-1000	14	5.9	369.4 +/- 5.7	20.4	0	0
1000-1050	38	16	367.7 +/- 4	17.4	0	0
1050-1100	41.9	17.7	372.6 +/- 6.3	23.4	0	0
1100-1150	27	11.3	362.5 +/- 2.4	35.4	0	0

TOTAL GAS AGE = 363.9 MY.

% I.I.C. = INTERFERING ISOTOPES CORRECTION

ERROR ESTIMATES AT ONE SIGMA LEVEL

PE 82-22M MUSCOVITE SUMMARY

TEMP.(DEG.C)	mV Ar39	% Ar39	AGE(Ma)	% ATMOS.	Ar37/Ar39	% I.I.C.
			J = 1.859E-03			
200-500	3.8	.9	253 +/- 5	41.3	0	0
500-550	4	.9	357.4 +/- 4.7	15.2	0	0
550-600	8.1	1.9	358.1 +/- 2.4	10.6	0	0
600-650	13.8	3.3	361.7 +/- 1.1	7.5	0	0
650-700	27.9	6.7	358.9 +/- .9	5.8	0	0
700-750	34.8	8.4	358.8 +/- .6	4.5	0	0
750-800	129.3	31.3	361.5 +/- .7	2.1	0	0
800-850	106	25.6	360.8 +/- .4	3.8	0	0
850-900	28	6.7	363.2 +/- .8	14	0	0
900-950	18.7	4.5	358.3 +/- .8	17.9	0	0
950-1140	38	9.2	358 +/- .8	31.5	0	0

TOTAL GAS AGE = 359.5 MY.

% I.I.C. - INTERFERING ISOTOPES CORRECTION

ERROR ESTIMATES AT ONE SIGMA LEVEL

PE83-2 BIOTITE SUMMARY

TEMP.(DEG.C)	mV Ar39	% Ar39	AGE(Ma)	% ATMOS.	Ar37/Ar39	% I.I.C.
			J = 1.875E-03			
200-500	7.5	2.8	293 +/- 2.8	31.8	0	0
500-550	4.5	1.7	310.3 +/- 3	18.5	0	0
550-600	9.6	3.6	348.8 +/- 2.3	9.2	0	0
600-650	20.2	7.6	366.5 +/- 1.1	3.3	0	0
650-700	33	12.3	368.2 +/- .8	3.5	0	0
700-750	35	13.1	364.9 +/- .8	4.8	0	0
750-800	28.3	10.6	365.1 +/- .8	4.7	0	0
800-850	25	9.3	366.8 +/- .8	9.1	0	0
850-900	48	17.9	368.5 +/- .5	6.3	0	0
900-950	33.4	12.5	365.3 +/- .8	9.3	0	0
950-1000	14.7	5.5	354.4 +/- 1.6	17.2	0	0
1000-1140	7.1	2.6	374.2 +/- 4.7	44.1	0	0

TOTAL GAS AGE = 362.6 MY.

% I.I.C. - INTERFERING ISOTOPES CORRECTION

ERROR ESTIMATES AT ONE SIGMA LEVEL

PE83-48 BIOTITE SUMMARY

TEMP. (DEG.C)	mV Ar39	% Ar39	AGE (Ma)	% ATMOS.	Ar37/Ar39	% I.I.C.
			J = 3.026E-03			
200-500	6	1.9	242.8 +/- 7	73.2	0	0
500-550	14.1	4.6	373.7 +/- 2.6	21.8	0	0
550-600	33.8	11.1	392.6 +/- .7	12.3	0	0
600-650	80.1	26.3	393.4 +/- .5	7.3	0	0
650-700	26.9	8.8	385 +/- 1.9	22.2	0	0
700-750	9.5	3.1	375.4 +/- 4.9	49.4	0	0
750-800	50.1	16.4	389.4 +/- .8	14.2	0	0
800-825	34.8	11.4	390.1 +/- 1.3	16.9	0	0
825-850	19.1	6.2	391.7 +/- 2.7	27.8	0	0
850-900	20	6.5	390.2 +/- 3.6	30.6	0	0
900-950	6.6	2.1	368.2 +/- 14.3	62	0	0
950-1000	2.8	.9	294.6 +/- 58.9	85.5	0	0

TOTAL GAS AGE = 385.9 MY.

% I.I.C. - INTERFERING ISOTOPES CORRECTION

ERROR ESTIMATES AT ONE SIGMA LEVEL

PE84-44D BIOTITE SUMMARY

TEMP. (DEG.C)	mV Ar39	% Ar39	AGE (Ma)	% ATMOS.	Ar37/Ar39	% I.I.C.
			J = 1.874E-03			
200-500	1.5	.6	140.7 +/- 50.8	90.2	0	0
500-550	4.6	1.8	292.1 +/- 4.9	50.5	0	0
550-600	12.2	4.9	372.9 +/- 1.3	18.9	0	0
600-650	26.9	10.9	379.2 +/- .8	13.2	0	0
650-700	31.3	12.7	378.3 +/- .6	11.8	0	0
700-750	16.6	6.7	375.4 +/- 1.3	17.5	0	0
750-800	12	4.8	371.1 +/- 1.7	24.6	0	0
800-850	22.7	9.2	371.6 +/- 1	13.2	0	0
850-900	33	13.4	379.4 +/- .5	5.2	0	0
900-950	54.6	22.2	379.5 +/- .4	5.3	0	0
950-1000	16	6.5	377.2 +/- 1.5	15.4	0	0
1000-1050	6.8	2.7	358.1 +/- 3.6	40.7	0	0
1050-1100	4	1.6	372.6 +/- 6.2	44.5	0	0
1100-1140	2.9	1.2	357 +/- 11	55.8	0	0

TOTAL GAS AGE = 373.4 MY.

% I.I.C. - INTERFERING ISOTOPES CORRECTION

ERROR ESTIMATES AT ONE SIGMA LEVEL

PE84-72 BIOTITE SUMMARY

TEMP.(DEG.C)	aV Ac39	% Ac39	AGE(Ma)	% Atm80.	Ac37/Ac39	% I.I.C.
			J = 1.875E-03			
200-300	4.3	1.9	311.3 +/- 7.4	53.8	0	0
300-350	10.9	4.9	320.2 +/- 1.3	13.1	0	0
350-400	26	11.8	376.5 +/- .7	6.2	0	0
400-450	34.3	15.6	372.3 +/- .6	3.4	0	0
450-700	25.9	11.8	361.4 +/- .6	5.9	0	0
700-750	6.3	2.8	332.3 +/- 3.6	22.9	0	0
750-800	4	1.8	371.4 +/- 3.1	23	0	0
800-850	9.6	4.3	383.4 +/- 2.1	14.8	0	0
850-900	26.8	12.2	384 +/- .7	9.3	0	0
900-950	45	20.4	377.3 +/- .6	3.9	0	0
950-1000	22	10	366.3 +/- .8	11	0	0
1000-1050	2.6	1.2	358.1 +/- 11.3	54.6	0	0
1050-1150	1.5	.6	351.3 +/- 27.1	77.7	0	0

TOTAL GAS AGE = 369.6 MY.

% I.I.C. - INTERFERING ISOTOPES CORRECTION

ERROR ESTIMATES AT ONE SIGMA LEVEL

PE 84-74A BIOTITE SUMMARY

TEMP.(DEG.C)	aV Ac39	% Ac39	AGE(Ma)	% Atm05.	Ac37/Ac39	% I.I.C.
			J = 1.877E-03			
200-300	1.9	.4	198.8 +/- 49.5	93.2	0	0
300-350	1.7	.3	231.4 +/- 19.9	89.8	0	0
350-400	3.4	.7	310.1 +/- 14.1	80.5	0	0
400-450	5.9	1.2	328.6 +/- 8.9	69.2	0	0
450-700	10.6	2.2	344 +/- 2.8	32.9	0	0
700-750	19.8	4.2	350.9 +/- 1.2	33.4	0	0
750-800	88.6	19	360.1 +/- .6	13.8	0	0
800-850	177.1	38	363.9 +/- .4	5.8	0	0
850-900	66	14.1	360 +/- .5	13.8	0	0
900-950	32	6.8	344.7 +/- .7	9.1	0	0
950-1000	36	7.7	344.6 +/- .8	11.6	0	0
1000-1150	22	4.7	377.9 +/- 1.5	46.3	0	0

TOTAL GAS AGE = 360.3 MY.

% I.I.C. - INTERFERING ISOTOPES CORRECTION

ERROR ESTIMATES AT ONE SIGMA LEVEL

PE84-78 BIOTITE SUMMARY

TEMP.(DEG.C)	mV Ar39	% Ar39	AGE(Ma)	% ATMOS.	Ar37/Ar39	% I.I.C.
			J = 1.974E-03			
200-500	7	2.8	173.1 +/- 5.4	48.4	0	0
500-550	12.1	4.3	315.3 +/- 3.1	18.6	0	0
550-600	22.9	8.2	369.3 +/- 1.4	9	0	0
600-650	19.8	7.1	369.2 +/- 2.4	9.4	0	0
650-700	36	12.9	375.6 +/- .6	9.3	0	0
700-750	11.7	4.2	367.2 +/- 3.5	24.6	0	0
750-800	20.6	7.4	378.1 +/- 2.7	12.8	0	0
800-850	49	17.5	380.1 +/- 1.3	7.4	0	0
850-900	64	22.9	380.3 +/- .5	8.7	0	0
900-950	33.7	12.1	380.9 +/- .7	9.6	0	0
1000-1100	1.7	.6	402.9 +/- 90.1	87.1	0	0

TOTAL GAS AGE = 369.8 MY.

% I.I.C. - INTERFERING ISOTOPES CORRECTION

ERROR ESTIMATES AT ONE SIGMA LEVEL

PE84-97 PHLOGOPITE SUMMARY

TEMP.(DEG.C)	mV Ar39	% Ar39	AGE(Ma)	% ATMOS.	Ar37/Ar39	% I.I.C.
			J = 1.995E-03			
200-350	3.5	.5	189.7 +/- 12.4	68	0	0
390-430	2.4	.3	349.9 +/- 12	37.5	0	0
430-700	8.8	1.4	368 +/- 2.5	25.3	0	0
700-800	97.7	15.4	371.6 +/- .4	6.2	0	0
800-850	121.9	19.2	370.4 +/- .4	3.9	0	0
850-900	126.9	20	368.7 +/- .5	6	0	0
900-950	119	18.8	366.7 +/- .5	10.2	0	0
950-1000	56	8.8	365.5 +/- .7	16.3	0	0
1000-1050	59	9.3	361.3 +/- .6	20	0	0
1050-1150	37	5.8	359.3 +/- 1	40.3	0	0

TOTAL GAS AGE = 366.6 MY.

% I.I.C. - INTERFERING ISOTOPES CORRECTION

ERROR ESTIMATES AT ONE SIGMA LEVEL

PE84-100 BIOTITE SUMMARY

TEMP.(DEG.C)	mV Ar39	% Ar39	AGE(Ma)	% ATMOS.	Ar37/Ar39	% I.I
			J = 1.877E-03			
200-500	7.1	2.6	43.1 +/- 12.2	92	0	.1
500-550	8.9	3.2	337.6 +/- 2.8	23.1	0	0
550-600	36.1	13.1	377.9 +/- 1.6	3.8	0	0
600-650	66.4	24.1	376.2 +/- 1.3	4.4	0	0
650-700	69.4	25.2	375.3 +/- 1.3	4.8	0	0
700-750	40	14.5	378.4 +/- 1.6	8.5	0	0
750-800	1.5	.5	375.5 +/- 1.8	12.5	0	0
800-850	14.5	5.3	371.1 +/- 2.1	10.3	0	0
850-900	13.1	4.7	349.9 +/- 2.1	16.4	0	0
900-950	9.9	3.6	371.9 +/- 3.1	22.7	0	0
950-1150	7.3	2.6	342.3 +/- 6.3	53.7	0	0

TOTAL GAS AGE = 344.9 MY.

% I.I.C. - INTERFERING ISOTOPES CORRECTION

ERROR ESTIMATES AT ONE SIGMA LEVEL

PE84-108 BIOTITE SUMMARY

TEMP.(DEG.C)	mV Ar39	% Ar39	AGE(Ma)	% ATMOS.	Ar37/Ar39	% I.I.C.
			J = 1.876E-03			
200-500	3.2	1.2	224.9 +/- 40.7	89.9	0	0
500-550	6.1	2.3	314.8 +/- 5	52.9	0	0
550-600	24.5	9.3	351.9 +/- .9	20.8	0	0
600-650	45.6	17.2	364 +/- 1.1	5.7	0	0
650-700	52	19.7	362.8 +/- .4	6.3	0	0
700-750	26.4	10	360.3 +/- .8	7.8	0	0
750-800	17.3	6.5	361.5 +/- 1.1	10	0	0
800-850	22.9	8.7	359.3 +/- .8	10.2	0	0
850-900	32	12.1	361.4 +/- .7	13.1	0	0
900-950	19	7.2	364 +/- .9	17.4	0	0
950-1000	8.9	3.4	354.7 +/- 2.9	43.1	0	0
1000-1150	5.3	2	344.7 +/- 6.3	66.6	0	0

TOTAL GAS AGE = 357.9 MY.

% I.I.C. - INTERFERING ISOTOPES CORRECTION

ERROR ESTIMATES AT ONE SIGMA LEVEL

PE85-141 BIOTITE SUMMARY

TEMP. (DEG.C)	mV Ar39	% Ar39	AGE (Ma)	% Atmos.	Ar37/Ar39	% I.I.C.
			J = 2.815E-03			
200-600	60.2	14.7	393.9 +/- .8	16	0	0
600-650	42.6	11.8	404.6 +/- .8	6.3	0	0
650-700	47.2	13.1	401.3 +/- .5	6.9	0	0
700-750	16.5	4.5	395.4 +/- 2	18.2	0	0
750-800	22.2	6.1	402.1 +/- 1.2	17.1	0	0
800-850	33.5	9.3	407.6 +/- .8	10	0	0
850-900	48.8	13.5	408.9 +/- .7	5.9	0	0
900-950	54.9	15.2	402.7 +/- .9	6.1	0	0
950-1000	26	7.2	398.4 +/- 1.3	14.7	0	0
1000-1050	5.4	1.5	393 +/- 6.1	43.8	0	0
1050-1150	2.5	.7	405.8 +/- 16.6	54.4	0	0

TOTAL GAS AGE = 393.8 MY.

% I.I.C. - INTERFERING ISOTOPES CORRECTION

ERROR ESTIMATES AT ONE SIGMA LEVEL

PE85-142 BIOTITE SUMMARY

TEMP. (DEG.C)	mV Ar39	% Ar39	AGE (Ma)	% Atmos.	Ar37/Ar39	% I.I.C.
			J = 2.767E-03			
200-600	33.7	10.2	373.6 +/- .8	20.8	0	0
600-650	50.4	14.4	403.2 +/- .6	7.6	0	0
650-700	70.8	20.2	402.8 +/- .6	7.2	0	0
700-750	17.8	5	390.2 +/- 1.8	26.4	0	0
750-800	16	4.6	396.7 +/- 2	20.9	0	0
800-850	30	8.5	403.5 +/- 1	13	0	0
850-900	71.4	20.4	410 +/- .5	3.1	0	0
900-950	44	12.5	407.2 +/- .6	7	0	0
950-1000	8.2	2.3	395.5 +/- 3.4	30.6	0	0
1000-1050	5	1.4	395.8 +/- 7	50.4	0	0

TOTAL GAS AGE = 401.5 MY.

% I.I.C. - INTERFERING ISOTOPES CORRECTION

ERROR ESTIMATES AT ONE SIGMA LEVEL

APPENDIX A - 4

'YOUNGER' MICAS

REGIONAL METAMORPHIC TERRANE

MC-1 BIOTITE SUMMARY

TEMP.(DEG.C)	eV Ar39	% Ar39	AGE(Ma)	% ATMOS.	Ar37/Ar39	% I.I.C.
			J = 3.305E-03			
200-450	103	5.7	78.5 +/- .4	77.8	0	.1
450-750	228.3	12.7	344.7 +/- 1.4	56.3	0	0
750-850	94.4	5.2	353.5 +/- 1.1	37.8	0	0
850-900	84	4.8	337.3 +/- 1.1	25.4	0	0
900-950	40.4	2.2	355.7 +/- 1.1	29.2	0	0
950-1000	63.5	3.5	361.4 +/- .8	27.5	0	0
1000-1050	166.1	9.2	349.5 +/- 1.3	54.3	0	0
1050-1100	244.7	13.6	353 +/- .4	13.8	0	0
1100-1150	641.6	35.8	340.8 +/- .6	21.9	0	0
1150-1200	121	6.7	341.6 +/- 1	51.6	0	0

TOTAL GAS AGE = 334.2 MY.

% I.I.C. - INTERFERING ISOTOPES CORRECTION

ERROR ESTIMATES AT ONE SIGMA LEVEL

PEG2-2 BIOTITE SUMMARY

TEMP.(DEG.C)	eV Ar39	% Ar39	AGE(Ma)	% ATMOS.	Ar37/Ar39	% I.I.C.
			J = 2.955E-03			
200-300	32	1.5	309.6 +/- .9	35.1	0	0
300-350	90.1	4.4	331.2 +/- .4	5.5	0	0
350-400	203.2	9.9	335 +/- .4	2.7	0	0
400-450	364.5	17.8	337.1 +/- .3	1.7	0	0
450-700	252.3	12.3	336.2 +/- .4	2.4	0	0
700-750	89.5	4.3	333.4 +/- .4	6.3	0	0
750-800	81.9	4	333.5 +/- .5	7	0	0
800-850	86.1	4.2	334.8 +/- .4	8	0	0
850-900	146	7.1	333.4 +/- .3	3.8	0	0
900-950	239.6	11.7	333.9 +/- .3	4	0	0
950-1000	169	8.2	336.1 +/- .3	4.4	0	0
1000 -1050	251.6	12.3	337.8 +/- .3	3.5	0	0
1050-1150	33.7	1.6	340.4 +/- .8	19.1	0	0

TOTAL GAS AGE = 333.4 MY.

% I.I.C. - INTERFERING ISOTOPES CORRECTION

ERROR ESTIMATES AT ONE SIGMA LEVEL

PEG3-6 BIOTITE SUMMARY

TEMP.(DEG.C)	aV Ar39	% Ar39	AGE(Ma)	% ATMOS.	Ar37/Ar39	% I.I.C.
			J = 1.993E-03			
150-300	4.1	.7	224.9 +/- 7.7	40.8	0	0
300-350	13.1	2.8	191.4 +/- 1.4	14.5	0	0
350-400	22	4.2	309.4 +/- .8	4.5	0	0
400-450	44.2	8.4	326.1 +/- .4	2	0	0
450-700	39.5	7.5	334.5 +/- .5	2	0	0
700-780	36.6	7	337.8 +/- .7	3.5	0	0
750-800	27	5.1	338.6 +/- 1.1	5.9	0	0
800-850	24	4.9	339.8 +/- .6	9.2	0	0
850-900	50	9.5	339.9 +/- .6	9.8	0	0
900-950	93	17.8	336.5 +/- .3	10	0	0
950-1000	75	14.3	331.4 +/- .4	14	0	0
1000-1050	69	13.2	330 +/- .3	21.5	0	0
1050-1150	20	3.8	343.3 +/- 2.9	43.1	0	0

TOTAL GAS AGE = 328.8 MY.

% I.I.C. - INTERFERING ISOTOPES CORRECTION

ERROR ESTIMATES AT ONE SIGMA LEVEL

PEG3-7B BIOTITE SUMMARY

TEMP.(DEG.C)	aV Ar39	% Ar39	AGE(Ma)	% ATMOS.	Ar37/Ar39	% I.I.C.
			J = 3.024E-03			
200-300	13.3	1	193.1 +/- 5.6	69.7	0	0
300-350	34.7	2.7	244.7 +/- 1.1	18.3	0	0
350-400	60.2	4.8	293.2 +/- .6	8	0	0
400-450	131.6	10.3	294.5 +/- .3	4.7	0	0
450-700	228.4	18.3	291.1 +/- .2	2.9	0	0
700-750	90.8	7.3	291.8 +/- .4	6.4	0	0
750-800	62.2	5	292.3 +/- .8	10.4	0	0
800-850	100.6	8.1	290.4 +/- .3	7.3	0	0
850-900	148	11.9	297.3 +/- .3	4.7	0	0
900-950	144	11.5	296.2 +/- .7	5.9	0	0
950-1000	107	8.6	299.4 +/- 1.4	8.8	0	0
1000-1050	87	7	309.2 +/- .5	18.1	0	0
1050-1100	33.6	2.7	307 +/- .8	41.4	0	0

TOTAL GAS AGE = 293.7 MY.

% I.I.C. - INTERFERING ISOTOPES CORRECTION

ERROR ESTIMATES AT ONE SIGMA LEVEL

PE82-8 BIOTITE SUMMARY

TEMP.(DEG.C)	mV Ar39	% Ar39	AGE(Ma)	% ATMOS.	Ar37/Ar39	% I.I.C.
			J = 1.934E-03			
150-500	6.3	1.3	0 +/- 0	0	0	0
500-550	12.2	2.5	305 +/- 2.4	35.6	0	0
550-600	49.7	10.3	343.8 +/- .5	11	0	0
600-650	71	14.7	349.1 +/- .5	4.1	0	0
650-700	102.3	21.2	350.1 +/- .9	4.4	0	0
700-750	49.3	10.2	346.9 +/- .7	5.8	0	0
750-800	34.6	7.6	348.5 +/- .8	12.1	0	0
800-930	31	6.4	351.1 +/- .9	30.9	0	0
930-960	49	10.1	346.9 +/- .7	14.6	0	0
960-1000	36	7.4	351.6 +/- .8	23.5	0	0
1000-1050	15	3.1	340.2 +/- 3.2	23	0	0
1050-1100	22	4.5	347.8 +/- 1.5	27.6	0	0

TOTAL GAS AGE = 343.1 MY.

% I.I.C. - INTERFERING ISOTOPES CORRECTION

ERROR ESTIMATES AT ONE SIGMA LEVEL

PE82-9 BIOTITE SUMMARY

TEMP.(DEG.C)	mV Ar39	% Ar39	AGE(Ma)	% ATMOS.	Ar37/Ar39	% I.I.C.
			J = 1.872E-03			
200-500	3.5	1.3	202.9 +/- 92.1	84	0	0
500-550	5.4	2	283.5 +/- 4.7	27.8	0	0
550-600	18.5	6.9	318.5 +/- 1.3	12.8	0	0
600-650	35.6	13.3	348.2 +/- 1.1	5.3	0	0
650-700	46.1	17.2	351 +/- .4	5.4	0	0
700-750	35.1	13.1	354.6 +/- .5	4.9	0	0
750-800	18.2	6.8	349.7 +/- .9	13.4	0	0
800-850	17.3	6.4	352.1 +/- 1.5	12.7	0	0
850-900	17.4	6.5	355.3 +/- 1.1	18.2	0	0
900-950	32.6	12.1	355.3 +/- .6	10.7	0	0
950-1000	26.9	10	353.3 +/- .9	8.6	0	0
1000-1150	10.6	3.9	343.1 +/- 2.3	37.6	0	0

TOTAL GAS AGE = 344.4 MY.

% I.I.C. - INTERFERING ISOTOPES CORRECTION

ERROR ESTIMATES AT ONE SIGMA LEVEL

PE82-10 BIOTITE SUMMARY

TEMP.(DEG.C)	mV Ar39	% Ar39	AGE(Ma)	% ATMOS.	Ar37/Ar39	% I.I.C.
			J = 1.992E-03			
150-550	14.5	3.5	248.4 +/- 1.9	31.1	0	0
550-600	37.4	8	344.9 +/- .9	5.7	0	0
600-650	60.3	12.9	354.8 +/- .6	3.9	0	0
650-700	54.2	11.6	353.8 +/- .7	4.5	0	0
700-750	42.7	9.2	353.3 +/- 1	6.4	0	0
750-800	25.7	5.5	351.6 +/- .9	13.2	0	0
800-850	23	4.9	352.5 +/- 1.1	15.9	0	0
850-900	44.2	9.5	353 +/- .8	11.7	0	0
900-950	72	15.4	351.8 +/- .6	8.1	0	0
950-1050	77	16.5	353.7 +/- .8	15.5	0	0
1050-1150	11	2.3	350 +/- 6.4	71.4	0	0

TOTAL GAS AGE = 349 MY.

% I.I.C. - INTERFERING ISOTOPES CORRECTION

ERROR ESTIMATES AT ONE SIGMA LEVEL

PE83-10 BIOTITE SUMMARY

TEMP.(DEG.C)	mV Ar39	% Ar39	AGE(Ma)	% ATMOS.	Ar37/Ar39	% I.I.C.
			J = 1.876E-03			
200-500	2.9	1.3	233.4 +/- 11.9	70.5	0	0
500-550	6.5	2.9	278.8 +/- 3	25.4	0	0
550-600	24.3	11	311.1 +/- 1.3	9.1	0	0
600-650	44	20	319.8 +/- .8	3.3	0	0
650-700	46.9	21.3	321.1 +/- .8	7.5	0	0
700-750	15.5	7	319.8 +/- 1.5	15.5	0	0
750-800	10.7	4.8	328.2 +/- 2.8	18.8	0	0
800-850	13	5.9	319.9 +/- 2.4	21.7	0	0
850-900	18	8.1	329 +/- 1.3	17.3	0	0
900-950	20.9	9.5	326.8 +/- 1.5	19.6	0	0
950-1000	9.5	4.3	323.7 +/- 3.1	32.6	0	0
1000-1150	7.3	3.3	313.9 +/- 7.4	44.7	0	0

TOTAL GAS AGE = 318.8 MY.

% I.I.C. - INTERFERING ISOTOPES CORRECTION

ERROR ESTIMATES AT ONE SIGMA LEVEL

PE83-11 BIOTITE SUMMARY

TEMP. (DEG.C)	mV Ar39	% Ar39	AGE(Ma)	% ATMOS.	Ar37/Ar39	% I.I.C.
			J = 1.99E-03			
150-350	6.7	2.3	327.3 +/- 8.1	78.6	0	0
350-600	11.7	3.9	326.6 +/- 2.6	32.6	0	0
600-650	29.5	10	341.3 +/- .7	10.7	0	0
650-700	23.1	8.5	335.5 +/- 1.1	9.8	0	0
700-750	42.4	14.4	335 +/- .5	13.6	0	0
750-800	17	5.7	339.9 +/- 1.5	27.5	0	0
800-850	32.2	10.9	341.2 +/- .6	18.3	0	0
850-900	38	12.9	342.7 +/- .7	17.3	0	0
900-950	46.2	15.7	333.6 +/- .6	15.2	0	0
950-1000	28	9.5	330.9 +/- .7	18.5	0	0
1000-1100	17	5.7	323.9 +/- 2.4	51.8	0	0

TOTAL GAS AGE = 334 MY.

% I.I.C. - INTERFERING ISOTOPES CORRECTION

ERROR ESTIMATES AT ONE SIGMA LEVEL

PE83-12 BIOTITE SUMMARY

TEMP.(DEG.C)	mV Ar39	% Ar39	AGE(Ma)	% ATMOS.	Ar37/Ar39	% I.I.C.	Ar37/Ar39	% I.I.C.
			J = 1.991E-03					
150-500	8.6	1.5	241.1 +/- 2.9	33.7	0	0	0	0
500-650	21.9	3.8	313.4 +/- .7	12.9	0	0	0	0
650-600	61.9	10.8	349.2 +/- .4	4.2	0	0	0	0
600-650	87.2	15.2	350.1 +/- .3	2.4	0	0	0	0
650-700	94.7	16.5	350.8 +/- .3	2.2	0	0	0	0
700-730	63.1	11	336 +/- .4	3.6	0	0	0	0
730-760	20.9	3.6	347.6 +/- 1.1	10.3	0	0	0	0
760-800	21.3	3.7	347.7 +/- 1	11.9	0	0	0	0
800-850	24.9	4.3	351.8 +/- .9	12.1	0	0	0	0
850-900	91	15.8	354.7 +/- .8	38.4	0	0	0	0
900-950	47.7	8.3	330.1 +/- .6	19.9	0	0	0	0
950-1000	17.2	3	350.4 +/- 1.5	34.9	0	0	0	0
1000-1100	11.9	2	333 +/- 2.2	59.1	0	0	0	0

TOTAL GAS AGE = 350.7 MY.

% I.I.C. - INTERFERING ISOTOPES CORRECTION
ERROR ESTIMATES AT ONE SIGMA LEVEL

PE82-14 MUSCOVITE SUMMARY

TEMP.(DEG.C)	mV Ar39	% Ar39	AGE(Ma)	% ATMOS.	Ar37/Ar39	% I.I.C.
			J = 2.767E-03			
200-630	14.6	5.7	327.1 +/- 2.2	30.1	0	0
630-750	11.8	4.6	325.2 +/- 2.1	10.3	0	0
750-830	13.1	5.2	329 +/- 3.2	5.1	0	0
830-900	46.9	18.3	336 +/- .7	.7	0	0
900-1000	19.4	7.6	334.4 +/- .6	.2	0	0
1000-1050	68.8	27.1	335.3 +/- .9	1.4	0	0
1050-1100	58.4	23	339.1 +/- .9	3.2	0	0
1100-1160	19.4	7.6	339.7 +/- 1.7	4.4	0	0
1160-1200	.9	.3	234.9 +/- 36.1	33.4	0	0

TOTAL GAS AGE = 333 MY.

% I.I.C. - INTERFERING ISOTOPES CORRECTION
ERROR ESTIMATES AT ONE SIGMA LEVEL

PE 82-17 BIOTITE SUMMARY

TEMP.(DEG.C)	mV Ar39	% Ar39	AGE(Ma)	% ATMOS.	Ar37/Ar39	% I.I.C.
			J = 1.868E-03			
200-550	33	10.6	343.3 +/- .6	21	0	0
550-600	47	15.1	348.8 +/- .4	3.3	0	0
600-650	68	21.9	347 +/- .3	2.7	0	0
650-700	55	17.7	348.5 +/- .4	3.7	0	0
700-750	26.6	8.5	350.7 +/- 1.4	7.2	0	0
750-800	14	4.5	347.9 +/- 2.2	12.8	0	0
800-850	26	8.3	344.4 +/- .8	11.5	0	0
850-900	26	8.3	345.9 +/- .8	13.1	0	0
900-950	11	3.5	344.4 +/- 2	31.3	0	0
950-1050	3.5	1.1	302.4 +/- 25.1	79.5	0	0

TOTAL GAS AGE = 346.6 MY.

% I.I.C. - INTERFERING ISOTOPES CORRECTION

ERROR ESTIMATES AT ONE SIGMA LEVEL

PE-18-B BIOTITE SUMMARY

TEMP.(DEG.C)	mV Ar39	% Ar39	AGE(Ma)	% ATMOS.	Ar37/Ar39	% I.I.C.
			J = 2.803E-03			
200-630	55.3	7.6	300.8 +/- .6	56.8	0	0
630-730	132.4	18.3	340.2 +/- .4	19	0	0
730-830	38	5.2	337 +/- 1	19.9	0	0
830-900	37.2	5.1	340.3 +/- .7	11.8	0	0
900-950	46.3	6.4	341.2 +/- .7	17.1	0	0
950-1000	65.1	9	342 +/- .4	15.4	0	0
1000-1050	45	6.2	341.6 +/- .4	11	0	0
1050-1100	160.8	22.2	339.8 +/- .2	9.6	0	0
1100-1150	71.8	9.9	334.5 +/- .5	13.1	0	0
1150-1200	69.8	9.6	336.4 +/- .3	23.4	0	0

TOTAL GAS AGE = 336.6 MY.

% I.I.C. - INTERFERING ISOTOPES CORRECTION

ERROR ESTIMATES AT ONE SIGMA LEVEL

PE-19-B BIOTITE SUMMARY

TEMP.(DEG.C)	mV Ar39	% Ar39	AGE(Ma)	% ATMOS.	Ar37/Ar39	% I.I.C.
			J = 2.764E-03			
750-800	90	16.6	338.7 +/- 2.5	56.4	0	0
850-900	22.1	4	336.6 +/- 1.2	19	0	0
900-950	41	7.5	337.8 +/- .9	7.6	0	0
950-1000	118.2	21.8	339.9 +/- .2	0.2	0	0
1000-1050	82.7	15.3	338.3 +/- .4	6	0	0
1050-1100	75.9	14	337.3 +/- .4	22.3	0	0
1100-1150	109.3	20.2	337.3 +/- .4	19.6	0	0
1150-1200	.8	.1	72.8 +/- 299.4	98.3	0	.1

TOTAL GAS AGE = 337.9 MY.

% I.I.C. - INTERFERING ISOTOPES CORRECTION

ERROR ESTIMATES AT ONE SIGMA LEVEL

PE82-21 BIOTITE SUMMARY

TEMP.(DEG.C)	mV Ar39	% Ar39	AGE(Ma)	% ATMOS.	Ar37/Ar39	% I.I.C.
			J = 2.697E-03			
200-300	3.3	.6	230 +/- 29.8	82	0	0
300-350	4.4	.8	225.4 +/- 9.1	56.2	0	0
350-400	14.5	2.7	335.7 +/- 2.7	22.8	0	0
400-430	18.4	3.5	345.8 +/- 2.4	18.2	0	0
430-460	26.2	5	331.4 +/- 1.7	14.2	0	0
460-700	41.2	7.9	352 +/- 1.2	14.7	0	0
700-745	38.8	7.4	334.4 +/- .9	13.8	0	0
745-800	22.7	4.3	349.4 +/- 2.2	20.1	0	0
800-850	36.6	7	349.4 +/- 1.6	21.1	0	0
850-900	28.2	5.4	350.3 +/- 2	18.9	0	0
900-950	69.5	13.3	350.1 +/- 1	8.9	0	0
950-1000	169	32.4	336.6 +/- .3	9.3	0	0
1000-1100	42.3	8.1	345.5 +/- .9	26.2	0	0
1100-1150	5.7	1.1	237.7 +/- 17.3	79.8	0	0

TOTAL GAS AGE = 330.5 MY.

% I.I.C. - INTERFERING ISOTOPES CORRECTION

ERROR ESTIMATES AT ONE SIGMA LEVEL

PE84-33B BIOTITE SUMMARY

TEMP.(DEG.C)	aV Ar39	% Ar39	AGE(Ma)	% ATMOS.	Ar37/Ar39	% I.I.C.
			J = 1.876E-03			
200-500	.6	.4	260.3 +/- 357.1	92.6	0	0
500-550	1.9	1.4	289.7 +/- 12.3	42.4	0	0
550-600	6.5	4.7	323.5 +/- 3.2	17.2	0	0
600-650	9.4	6.9	343.2 +/- 2.1	8.3	0	0
650-700	9.9	7.3	348.2 +/- 2.1	6.9	0	0
700-750	10.4	7.6	346.1 +/- 2.1	9.2	0	0
750-800	9.6	7	347.8 +/- 2.4	9	0	0
800-850	8.3	6.1	354.5 +/- 5.6	7.6	0	0
850-900	8.5	6.3	348.9 +/- 3.2	7.4	0	0
900-950	43	31.6	352.8 +/- 1.4	3.9	0	0
950-1000	12.5	9.1	353.6 +/- 2	10.2	0	0
1000-1140	15	11	0 +/- 0	0	0	0

TOTAL GAS AGE = 347.7 MY.

% I.I.C. - INTERFERING ISOTOPES CORRECTION

ERROR ESTIMATES AT ONE SIGMA LEVEL

PE84-41 BIOTITE SUMMARY

TEMP.(DEG.C)	aV Ar39	% Ar39	AGE(Ma)	% ATMOS.	Ar37/Ar39	% I.I.C.
			J = 1.973E-03			
200-500	.8	.2	5.3 +/- 105.7	99.6	0	1
500-600	21.5	4.8	323.4 +/- 1.3	17.4	0	0
600-650	56	12.7	347.7 +/- .4	10	0	0
650-700	62.9	14.2	350.7 +/- .6	5.3	0	0
700-750	37.5	8.5	348.9 +/- .8	9.2	0	0
750-800	28.2	6.4	342.5 +/- 1	10.6	0	0
800-850	36.4	8.2	338.9 +/- 1	21.9	0	0
850-900	51.3	11.6	350.2 +/- .6	10.5	0	0
900-950	82.4	18.7	351.3 +/- .4	5.2	0	0
950-1000	44.7	10.1	348.1 +/- .5	12.1	0	0
1000-1140	18.6	4.2	337 +/- 2.1	30.6	0	0

TOTAL GAS AGE = 345.9 MY.

% I.I.C. - INTERFERING ISOTOPES CORRECTION

ERROR ESTIMATES AT ONE SIGMA LEVEL

PE84-659 MUSCOVITE SUMMARY

TEMP.(DEG.C)	mV Ar39	% Ar39	AGE(Ma)	% ATMOS.	Ar37/Ar39	% I.I.C.
			J = 1.875E-03			
200-500	3.9	.8	304.4 +/- 8	52.4	0	0
500-600	9.1	1.9	331.1 +/- 3.8	28.5	0	0
600-700	12	2.5	324.7 +/- 2.1	24.8	0	0
700-750	59.5	12.7	323.9 +/- .8	4.6	0	0
750-800	158.5	33.9	321.9 +/- .7	3.1	0	0
800-850	119.1	25.4	322.8 +/- .7	3.7	0	0
850-900	51.1	10.9	320.9 +/- .7	7.1	0	0
900-950	29	4.2	320.5 +/- .8	10.3	0	0
950-1000	12.4	2.6	324.4 +/- 1.9	15.3	0	0
1000-1150	12.6	2.6	311.4 +/- 2.2	38.7	0	0

TOTAL GAS AGE = 322 MY.

% I.I.C. - INTERFERING ISOTOPES CORRECTION

ERROR ESTIMATES AT ONE SIGMA LEVEL

PE84-779 BIOTITE SUMMARY

TEMP.(DEG.C)	mV Ar39	% Ar39	AGE(Ma)	% ATMOS.	Ar37/Ar39	% I.I.C.
			J = 1.980E-03			
200-550	20.6	3.6	213.5 +/- 1.3	32.3	0	0
550-600	54.6	10	345.8 +/- .6	6.3	0	0
600-650	79.7	14	353.2 +/- .5	3.5	0	0
650-700	63.5	11.2	352.1 +/- .5	4.3	0	0
700-750	28	4.9	349.7 +/- .9	10.7	0	0
750-800	28.9	5.1	357.3 +/- .9	13.7	0	0
800-850	22.4	3.9	357.9 +/- .9	14.8	0	0
850-900	41.5	7.3	363.9 +/- .7	10.2	0	0
900-950	72.2	12.7	352.9 +/- .5	6.5	0	0
950-1050	120.3	21.2	351.1 +/- .5	7.6	0	0
1050-1150	31.8	5.6	341.2 +/- 1.6	47	0	0

TOTAL GAS AGE = 347.3 MY.

% I.I.C. - INTERFERING ISOTOPES CORRECTION

ERROR ESTIMATES AT ONE SIGMA LEVEL

PE84-77M MUSCOVITE SUMMARY

TEMP.(DEG.C)	aV Ar39	% Ar39	AGE(Ma)	% ATMOS.	Ar37/Ar39	% I.I.C.
			J = 1.983E-03			
150-350	10.1	1.6	229.3 +/- 5.1	78	0	0
350-600	10.8	1.7	309.7 +/- 3.8	62.3	0	0
600-650	15.8	2.5	328.2 +/- 1.7	46.6	0	0
650-700	24.1	3.8	341.1 +/- 1.2	32.6	0	0
700-750	28	4.5	343.3 +/- .7	19.8	0	0
750-800	75	12	351.1 +/- .4	10.3	0	0
800-850	160	25.6	358.2 +/- .5	9.1	0	0
850-900	72	11.5	355.4 +/- .4	13.2	0	0
900-950	58	9.3	358.4 +/- .4	13	0	0
950-1050	96	15.4	362.8 +/- .4	12.1	0	0
1050-1100	70	11.2	374.1 +/- .5	10.5	0	0
1100-1150	2.7	.4	374 +/- 30	74.7	0	0

TOTAL GAS AGE = 354.7 MY.

% I.I.C. - INTERFERING ISOTOPES CORRECTION

ERROR ESTIMATES AT ONE SIGMA LEVEL

PE 84-121B BIOTITE SUMMARY

TEMP.(DEG.C)	aV Ar39	% Ar39	AGE(Ma)	% ATMOS.	Ar37/Ar39	% I.I.C.
			J = 1.964E-03			
200-600	29.2	10.9	145.2 +/- 1	37.1	0	0
600-650	30.1	11.3	334 +/- .9	5.1	0	0
650-700	25.5	9.6	325.8 +/- 1.1	7.2	0	0
700-750	22.4	8.4	322.1 +/- 1	8.2	0	0
750-800	19	7.1	329.4 +/- 1.2	8.6	0	0
800-850	17.5	6.6	339.6 +/- 1.8	5.6	0	0
850-900	37	13.9	339.7 +/- 1	4	0	0
900-950	47.3	17.7	337.8 +/- .6	2.4	0	0
950-1000	32	12	333.1 +/- .8	7.3	0	0
1000-1050	4.6	1.7	340.8 +/- 9.2	30.7	0	0
1050-1150	1	.3	0 +/- 0	0	0	0

TOTAL GAS AGE = 313.8 MY.

% I.I.C. - INTERFERING ISOTOPES CORRECTION

ERROR ESTIMATES AT ONE SIGMA LEVEL

PE84-121M MUSCOVITE SUMMARY

TEMP.(DEG.C)	mV Ar39	% Ar39	AGE(Ma)	% ATMOS.	Ar37/Ar39	% I.I.C.
			J = 1.965E-03			
200-500	.8	.4	219.7 +/- 63.6	76	0	0
500-550	.9	.5	277.9 +/- 27.5	50.1	0	0
550-600	1.6	.9	322 +/- 11.6	35.6	0	0
600-650	3.4	1.8	322.6 +/- 5.8	19.9	0	0
650-700	7	3.7	331.2 +/- 3.1	14.6	0	0
700-750	11.1	5.9	340.7 +/- 2.2	8.9	0	0
750-800	33.5	19	347.6 +/- .5	4.5	0	0
800-850	59	31.5	346.6 +/- .8	3.6	0	0
850-900	28.1	15	345.5 +/- .8	4.3	0	0
900-950	11.3	6	345.7 +/- 2.1	12.5	0	0
950-1000	8.8	4.7	347.8 +/- 2	13.9	0	0
1000-1150	18.6	9.9	349.3 +/- 1.2	16.5	0	0

TOTAL GAS AGE = 344.4 MY.

% I.I.C. - INTERFERING ISOTOPES CORRECTION,
ERROR ESTIMATES AT ONE SIGMA LEVEL

PE84-129 MUSCOVITE SUMMARY

TEMP.(DEG.C)	mV Ar39	% Ar39	AGE(Ma)	% ATMOS.	Ar37/Ar39	% I.I.C.
			J = 1.965E-03			
200-600	2.1	.5	340.3 +/- 28.2	66.2	0	0
600-650	4	1.1	328.9 +/- 5.7	38.4	0	0
650-700	31	8.5	349.7 +/- .6	7	0	0
700-750	53.6	15.2	348.3 +/- .4	3	0	0
750-800	145.4	39.8	347.7 +/- .3	2.4	0	0
800-850	74	20.2	348.5 +/- .3	2.3	0	0
850-900	17.4	4.7	346.5 +/- 1.8	6.1	0	0
900-950	15.6	4.2	350.8 +/- 1.2	9.4	0	0
950-1000	9	2.4	349.1 +/- 3	32.6	0	0
1000-1150	10.6	2.9	348.9 +/- 2.2	20.6	0	0

TOTAL GAS AGE = 349.7 MY.

% I.I.C. - INTERFERING ISOTOPES CORRECTION
ERROR ESTIMATES AT ONE SIGMA LEVEL

APPENDIX A - 5

MICAS, AMPHIBOLES, AND FELDSPARS FROM THE SOUTHERN SATELLITE PLUTONS

PE83-9H HORNBLENDE SUMMARY

TEMP.(DEG.C)	mV Ar39	% Ar39	AGE(Ma)	% AlNO3	Ar37/Ar39	% I.I.C.
			J = 2.34E-03			
150-650	7.1	2.9	670.8 +/- 20	43.3	1.6	.1
650-750	11.1	4.6	318 +/- 4.2	84.8	.6	0
750-850	10.6	4.3	302.3 +/- 6.9	63	1.5	.2
850-900	8.7	3.6	123.6 +/- 31.4	96.8	2.1	.6
900-1000	89.2	36.8	370.2 +/- 3.1	69.9	10.8	1.3
1075-1100	6.4	2.6	344.3 +/- 9.9	87.9	14	2
1100-1150	54.2	23.2	378.4 +/- .8	22.2	11.9	1.7
1150-1175	32.3	13.3	384 +/- 1.3	23.9	10.3	1.8
1175-1200	20.3	8.4	386.1 +/- 2.3	33.3	10.4	1.3

TOTAL GAS AGE = 371.2 MY.

% I.I.C. = INTERFERING ISOTOPES CORRECTION

ERROR ESTIMATES AT ONE SIGMA LEVEL

PE83-9B BIOTITE SUMMARY

TEMP.(DEG.C)	mV Ar39	% Ar39	AGE(Ma)	% AlNO8	Ar37/Ar39	% I.)
			J = 3.02E-03			
200-300	2.3	.6	202.6 +/- 24.7	76.8	0	0
300-350	6.7	1.7	293.7 +/- 3.8	23.1	0	0
350-400	16.1	4	321.8 +/- 1.7	7.2	0	0
400-450	36.7	9.2	320.7 +/- .9	4.3	0	0
450-700	50.7	12.8	326.3 +/- .5	2.2	0	0
700-750	23	6.3	327.8 +/- 1.5	4.8	0	0
750-800	17.5	4.4	329.5 +/- 1.6	8.5	0	0
800-850	19.1	4.8	328.8 +/- 1.2	6.5	0	0
850-900	34	8.6	329.4 +/- .9	4.3	0	0
900-950	83	13.4	328.5 +/- 1.3	1.9	0	0
950-1000	58.2	14.7	325.9 +/- .6	2.9	0	0
1000-1030	42	10.6	323.4 +/- .9	3.1	0	0
1030-1100	29	7.3	321 +/- 1.5	5.2	0	0
1100-1150	4	1	333.9 +/- 7.6	23.8	0	0

TOTAL GAS AGE = 324.8 MY.

% I.I.C. = INTERFERING ISOTOPES CORRECTION

ERROR ESTIMATES AT ONE SIGMA LEVEL

PE84-39A K-FELDSPAR SUMMARY

TEMP. (DEG.C)	aV Ar39	% Ar39	AGE (Ma)	% ATMOS.	Ar37/Ar39	% I.I.C.
			J = 1.877E-03			
200-300	12.2	8.1	219.5 +/- 1.4	26.9	0	0
300-330	13	4.3	215.6 +/- 1.5	14.1	0	0
330-400	21.8	7.3	249.2 +/- .9	8.9	0	0
400-430	15.3	5.1	237.5 +/- 1.1	9.9	0	0
450-700	15.9	5.3	274.4 +/- 1.1	5.9	0	0
700-730	31.7	10.6	283.3 +/- .5	3.8	0	0
730-800	25.1	8.4	277.3 +/- .7	3.9	0	0
800-830	23	7.7	273.1 +/- 3.1	5.6	0	0
830-900	28	9.4	277.8 +/- .8	4.7	0	0
900-930	27.6	9.2	283 +/- .3	5.3	0	0
930-1000	21.1	7	281 +/- .8	7	0	0
1000-1050	32	10.7	282.4 +/- .4	10.2	0	0
1050-1100	18.7	6.3	287.8 +/- .8	13.9	0	0
1100-1140	9	3	290.3 +/- 2.7	22.8	0	0

TOTAL GAS AGE = 271.3 MY.

% I.I.C. - INTERFERING ISOTOPES CORRECTION
ERROR ESTIMATES AT ONE SIGMA LEVEL

PE84-39B BIOTITE SUMMARY

TEMP. (DEG.C)	aV Ar39	% Ar39	AGE (Ma)	% ATMOS.	Ar37/Ar39	% I.I.C.
			J = 1.837E-03			
200-300	7.8	1.8	244.9 +/- 3.3	39.8	0	0
300-330	26.7	6.2	302.3 +/- .8	12.1	0	0
330-400	61.2	14.2	318.3 +/- .4	4.4	0	0
400-430	98.1	22.7	317.9 +/- .3	3.2	0	0
450-700	82.1	19	317.8 +/- .3	4.3	0	0
700-730	37.8	8.7	320.4 +/- .8	9.5	0	0
730-800	16.2	3.7	314.1 +/- 1.4	20.5	0	0
800-830	24	6	319 +/- 1.4	14.3	0	0
830-900	39	9	322.4 +/- .5	10.9	0	0
900-930	25	5.8	320.7 +/- .9	18.3	0	0
930-1000	7.4	1.7	309.8 +/- 3.9	43.8	0	0
1000-1130	2.7	.6	273.3 +/- 92.6	89.2	0	0

TOTAL GAS AGE = 314 MY.

% I.I.C. - INTERFERING ISOTOPES CORRECTION
ERROR ESTIMATES AT ONE SIGMA LEVEL

PE84-114B BIOTITE SUMMARY

TEMP.(DEG.C)	aV Ar39	% Ar39	AGE(Ma)	% Ar40S.	Ar37/Ar39	% I.I.C.
			J = 1.9488E-03			
200-300	1.7	.3	138.9 +/- 49.8	94.4	0	0
300-400	3.7	.7	313.1 +/- 10.3	37.6	0	0
400-450	5.4	1.1	282.5 +/- 10.7	40.8	0	0
450-700	7.8	1.5	330.1 +/- 4	30.9	0	0
700-750	19.3	3.8	340.3 +/- 1.7	18.3	0	0
750-800	60	12	347.7 +/- .8	6.8	0	0
800-850	136.3	27.3	348.9 +/- .9	4.8	0	0
850-900	65.1	13	341.3 +/- .6	10.7	0	0
900-950	73.1	15	347.2 +/- 1.4	10.7	0	0
950-1000	56.6	11.3	343.9 +/- 1.5	16.4	0	0
1000-1150	67.5	13.5	345.3 +/- .7	21.9	0	0

TOTAL GAS AGE = 344.4 MY.

% I.I.C. - INTERFERING ISOTOPES CORRECTION
ERROR ESTIMATES AT ONE SIGMA LEVEL

PE84-114H HORNBLENDE SUMMARY

TEMP.(DEG.C)	aV Ar39	% Ar39	AGE(Ma)	% Ar40S.	Ar37/Ar39	% I.I.C.
			J = 1.9638E-03			
200-750	6.6	6.2	412.8 +/- 5	30.4	.5	0
750-850	2.9	2.8	311.9 +/- 7	36.1	1.6	.2
850-900	1.7	1.6	321.7 +/- 12.3	44.1	2.3	.3
900-950	4.1	3.9	340.2 +/- 5.6	35.3	4.6	.5
950-1000	22.2	21.1	381.8 +/- 1	9.6	8.7	1.1
1000-1050	49.3	46.8	368.8 +/- .6	7.4	8.9	1.1
1050-1100	7.6	7.2	369.4 +/- 3.3	30.3	9.6	1.2
1100-1130	3.4	3.3	358.6 +/- 7.4	47	9.9	1.3
1130-1190	7	6.6	377.6 +/- 3.9	36.7	9.8	1.2

TOTAL GAS AGE = 372.3 MY.

% I.I.C. - INTERFERING ISOTOPES CORRECTION
ERROR ESTIMATES AT ONE SIGMA LEVEL

PE84-118B BIOTITE SUMMARY

TEMP.(DEG.C)	aV Ar39	% Ar39	AGE(Ma)	% Al/K	Ar37/Ar39	% I.I.C.
			J = 1.965E-03			
200-600	18.3	3.6	294.8 +/- 2	37.1	0	0
600-650	115	27.4	317 +/- 1.7	4.8	0	0
650-700	38.5	6.8	316 +/- .9	4.6	0	0
700-750	59.2	14.1	318.2 +/- .4	7	0	0
750-800	21	5	317.1 +/- .8	9.8	0	0
800-850	17	4	318.1 +/- 1.1	8.4	0	0
850-900	24.3	5.8	319.5 +/- .9	4.5	0	0
900-950	83	20.2	320.8 +/- .4	3.5	0	0
950-1000	39.5	9.4	320.7 +/- .9	3.1	0	0
1000-1150	13.8	3.2	319.3 +/- 1.7	22.1	0	0

TOTAL GAS AGE = 317.6 MY.

% I.I.C. - INTERFERING ISOTOPES CORRECTION
ERROR ESTIMATES AT ONE SIGMA LEVEL

PE84-118C PLAGIOCLASE SUMMARY

TEMP.(DEG.C)	aV Ar39	% Ar39	AGE(Ma)	% Al/K	Ar37/Ar39	% I.I.C.
			J = 1.874E-03			
200-600	4.9	8.9	476.8 +/- 9.3	43.6	1.3	.1
600-700	6.8	12.3	261.2 +/- 2.4	43.3	1.9	.2
700-800	7.2	13	231.5 +/- 3.1	43.2	1.9	.2
800-850	4.2	7.6	239.8 +/- 7.9	36.2	1.3	.1
850-900	3.8	6.9	249.1 +/- 8.9	69.3	0	0
900-950	3.6	6.6	253 +/- 10.7	72.3	0	0
950-1000	5.8	10.6	234.7 +/- 9.9	79.1	.9	.1
1000-1150	18.3	33.6	263.9 +/- 5.5	84.3	.9	.1

TOTAL GAS AGE = 279.7 MY.

% I.I.C. - INTERFERING ISOTOPES CORRECTION
ERROR ESTIMATES AT ONE SIGMA LEVEL

PE84-119 MUSCOVITE SUMMARY

TEMP.(DEG.C)	mV Ar39	% Ar39	AGE(Ma)	% atmos.	Ar37/Ar39	% I.I.C.
			J = 1.966E-03			
200-600	3	.8	332 +/- 18.9	62.7	0	0
600-650	5.7	1.1	331.7 +/- 9.6	30.2	0	0
650-700	7.8	2	332.7 +/- 4.2	24.4	0	0
700-750	12.7	3.7	342.6 +/- 1.8	11.3	0	0
750-800	83.8	25	347.5 +/- 1.3	3.8	0	0
800-850	118	34.4	348.9 +/- .5	1.8	0	0
850-900	48	14	343.5 +/- 4.4	3.1	0	0
900-950	20.9	6.1	344.2 +/- .8	4.6	0	0
950-1000	23.1	6.7	347.8 +/- 2.4	3.3	0	0
1000-1150	19.3	5.6	349.9 +/- 2.4	9.2	0	0

TOTAL GAS AGE = 346.8 MY.

% I.I.C. - INTERFERING ISOTOPES CORRECTION

ERROR ESTIMATES AT ONE SIGMA LEVEL

PE 84-27 MUSCOVITE SUMMARY

J = 1.877E-03

TEMP. (DEG.C)	aV Ar39	% Ar39	AGE (Ma)	% ATMOS.	Ar37/Ar39	% I.I.C.
200-300	2.7	.6	243.9 +/- 9.9	48.2	0	0
300-350	8.3	1.2	332 +/- 2.6	26.6	0	0
350-400	19.6	4.7	317.1 +/- .7	10.8	0	0
400-450	61.4	14.7	334.8 +/- .4	4.8	0	0
450-700	81.3	19.5	337.8 +/- .3	4.8	0	0
700-750	45.7	10.9	338.3 +/- .5	9.1	0	0
750-800	27.9	6.7	335 +/- .8	17.9	0	0
800-850	18	4.3	341.4 +/- 1.2	13.2	0	0
850-900	32.7	7.8	342.1 +/- .6	9.8	0	0
900-950	32.4	12.5	337.9 +/- .5	6.1	0	0
950-1000	40	9.5	339.2 +/- .5	6.8	0	0
1000-1140	29.3	7	341.5 +/- .8	10.2	0	0

TOTAL GAS AGE = 333.8 MY.

% I.I.C. - INTERFERING ISOTOPES CORRECTION

ERROR ESTIMATES AT ONE SIGMA LEVEL

PE84-28 MUSCOVITE SUMMARY

J = 2.787E-03

TEMP. (DEG.C)	aV Ar39	% Ar39	AGE (Ma)	% ATMOS.	Ar37/Ar39	% I.I.C.
200-600	4.6	1.5	353.6 +/- 7.3	58.1	0	0
600-650	5.4	1.8	357.8 +/- 3.4	37.1	0	0
650-700	9	3.1	359.3 +/- 3.1	29.3	0	0
700-750	28	9.6	357.3 +/- 4.3	17	0	0
750-800	42.8	14.7	372.2 +/- .8	8.7	0	0
800-850	61.9	21.3	369.4 +/- 1.3	8.3	0	0
850-900	53	18.2	372.4 +/- 1.8	8.1	0	0
900-950	29.8	10.3	372 +/- 1.6	11.2	0	0
950-1000	21.2	7.3	372.9 +/- 1.4	13.3	0	0
1000-1050	21.3	7.3	371.4 +/- 1.2	14.3	0	0
1050-1100	12.3	4.2	370.3 +/- 2.4	32.4	0	0

TOTAL GAS AGE = 369.2 MY.

% I.I.C. - INTERFERING ISOTOPES CORRECTION

ERROR ESTIMATES AT ONE SIGMA LEVEL

PE84-29 MUSCOVITE SUMMARY

TEMP. (DEG.C)	nV Ar39	% Ar39	AGE (Ma)	% ATMOS.	Ar37/Ar39	% I.I.C.
			J = 1.077E-03			
200-500	1.7	.3	275.6 +/- 26.6	83.4	0	0
500-550	1.2	.2	332 +/- 16.2	57.1	0	0
550-600	2.4	.5	343.4 +/- 9.2	40.9	0	0
600-650	5.2	1.1	347 +/- 3.4	28.2	0	0
650-700	9.6	2	357.7 +/- 1.3	18.7	0	0
700-730	18	3.8	362 +/- 1.5	16.2	0	0
730-800	38.2	8.1	363.6 +/- .4	7.8	0	0
800-830	146.1	31	366 +/- .7	3.9	0	0
830-900	94.5	20	366.1 +/- .6	4.2	0	0
900-930	54	11.4	368.1 +/- .5	4.5	0	0
930-1000	40	8.4	366.8 +/- .6	14.3	0	0
1000-1150	60	12.7	363.9 +/- .5	21.5	0	0

TOTAL GAS AGE = 364.8 MY.

% I.I.C. - INTERFERING ISOTOPES CORRECTION
ERROR ESTIMATES AT ONE SIGMA LEVEL

PE84-30 MUSCOVITE SUMMARY

TEMP. (DEG.C)	nV Ar39	% Ar39	AGE (Ma)	% ATMOS.	Ar37/Ar39	% I.I.C.
			J = 2.842E-03			
200-400	3.9	2.2	332.1 +/- 8.1	58	0	0
400-650	4.9	2.7	341.8 +/- 4.2	35.9	0	0
650-700	8.3	4.8	350.3 +/- 2.5	20.1	0	0
700-730	12.6	7.1	367.6 +/- 1.8	18.9	0	0
730-800	28.3	16.2	369.6 +/- .8	8.5	0	0
800-830	51.9	29.4	370 +/- .5	9.1	0	0
830-900	30	17	373 +/- 4.1	12.7	0	0
900-930	13.2	7.5	372.3 +/- 3.3	22.9	0	0
930-1000	14.1	8	374 +/- 6.8	17.6	0	0
1000-1030	8.3	4.7	373.9 +/- 3.8	27.9	0	0

TOTAL GAS AGE = 369.8 MY.

% I.I.C. - INTERFERING ISOTOPES CORRECTION
ERROR ESTIMATES AT ONE SIGMA LEVEL

BQ-1-B BIOTITE SUMMARY

TEMP.(DEG.C)	mV Ar39	% Ar39	AGE(Ma)	% Atmos.	Ar37/Ar39	% I.I.C.
			J = 3.315E-03			
200-650	91.8	13.3	360.2 +/- 1.5	32.8	0	0
650-750	60.1	8.7	369.8 +/- .7	17.7	0	0
750-850	34.1	4.9	366.1 +/- 1.4	24.3	0	0
850-900	55	7.9	367.4 +/- 3.1	27.3	0	0
900-1000	61.7	8.9	379.6 +/- .9	31.6	0	0
1000-1100	313.6	45.8	377.7 +/- .3	12.1	0	0
1100-1150	27	3.9	374.4 +/- .3	9.8	0	0
1150-1200	42.9	6.2	372.3 +/- 1.3	36.6	0	0

TOTAL GAS AGE = 370.3 MY.

% I.I.C. - INTERFERING ISOTOPES CORRECTION

ERROR ESTIMATES AT ONE SIGMA LEVEL

BQ-2-B BIOTITE SUMMARY

TEMP.(DEG.C)	mV Ar39	% Ar39	AGE(Ma)	% Atmos.	Ar37/Ar39	% I.I.C.
			J = 3.3E-03			
200-300	2.8	.3	102 +/- 265.7	99.3	0	0
300-350	6.3	.7	349.6 +/- 4.5	24.8	0	0
350-400	8.9	.9	363.7 +/- 3	14.3	0	0
400-450	51.6	5.6	370.3 +/- .6	10.9	0	0
450-700	68.4	7.4	370.3 +/- .6	9.4	0	0
700-750	76.5	8.3	370.7 +/- .5	12.6	0	0
750-800	48.1	5.2	370.2 +/- .4	8.7	0	0
800-850	26.8	2.9	369.2 +/- 1.2	32	0	0
850-900	29.7	3.2	371.2 +/- 1.3	38.9	0	0
900-950	34.5	3.9	372.2 +/- 1.2	34	0	0
950-1000	63.3	7	370.9 +/- .6	20.4	0	0
1000-1030	79	8.5	374.2 +/- .6	5.8	0	0
1030-1100	125	13.5	371.3 +/- .3	5.9	0	0
1100-1150	227.1	24.6	370.5 +/- .3	7.3	0	0
1150-1200	68	7.3	371.6 +/- 1.8	13.8	0	0

TOTAL GAS AGE = 370.7 MY.

% I.I.C. - INTERFERING ISOTOPES CORRECTION

ERROR ESTIMATES AT ONE SIGMA LEVEL

PE 84-34 MUSCOVITE SUMMARY

TEMP.(DEG.C)	mV Ar39	% Ar39	AGE(Ma)	% AlnO3	Ar37/Ar39	% I.I.C.
			J = 1.030E-03			
200-500	3.3	.6	270 +/- 9.8	44.8	0	0
500-830	2.8	.5	313.7 +/- 7.8	34.6	0	0
830-400	5.1	1	323.4 +/- 4.6	23.3	0	0
400-450	10.7	2.2	324 +/- 1.7	18.4	0	0
450-700	16.8	3.5	333.5 +/- 1.1	14.3	0	0
700-750	28.6	5.9	334.4 +/- 1.3	10.2	0	0
750-800	140	29	340.9 +/- .3	4.6	0	0
800-850	151.7	31.5	340.3 +/- .4	3.6	0	0
850-900	58	12	338.5 +/- .4	6.4	0	0
900-950	27.3	5.6	338.9 +/- .7	18.1	0	0
950-1000	20.8	4.3	318.8 +/- 1.6	48.1	0	0
1000-1030	11.6	2.4	337.7 +/- 2.4	41.5	0	0
1030-1150	4	.8	287.9 +/- 8.3	73.1	0	0

TOTAL GAS AGE = 337.2 MY.

% I.I.C. - INTERFERING ISOTOPES CORRECTION
ERROR ESTIMATES AT ONE SIGMA LEVEL

PE84-45B MUSCOVITE SUMMARY

TEMP.(DEG.C)	mV Ar39	% Ar39	AGE(Ma)	% AlnO3	Ar37/Ar39	% I.I.C.
			J = 1.07E-03			
600-700	24	4.6	334 +/- 3.3	39.2	0	0
700-800	133	25.9	340.4 +/- 1.3	6.6	0	0
800-900	243.8	47.5	342.4 +/- 1.1	4.3	0	0
900-950	50	9.7	341.2 +/- 1.5	12.3	0	0
950-1000	32.9	6.4	342.1 +/- 2	21.8	0	0
1000-1050	19	3.7	344.1 +/- 2.7	31.1	0	0
1050-1150	10	1.9	336.6 +/- 4.2	44.6	0	0

TOTAL GAS AGE = 341.4 MY.

% I.I.C. - INTERFERING ISOTOPES CORRECTION
ERROR ESTIMATES AT ONE SIGMA LEVEL

PE-46-M MUSCOVITE SUMMARY

TEMP.(DEG.C)	mV Ar39	% Ar39	AGE(Ma)	% ATMOS.	Ar37/Ar39	% I.I.C.
			J = 2.985E-03			
200-300	1.2	.2	374.9 +/- 94.9	83.3	0	0
300-350	1.1	.2	380.3 +/- 31.4	39	0	0
350-400	2.6	.5	334.4 +/- 16	30.5	0	0
400-700	7.7	1.6	340.6 +/- 4.6	28.8	0	0
700-750	22	4.6	350.8 +/- 2.2	9.7	0	0
750-800	71.7	15	357.3 +/- .4	3.3	0	0
800-850	157.8	33.1	361.3 +/- .3	3.3	0	0
850-900	26.7	5.6	360.9 +/- 1.4	4.3	0	0
900-950	31.9	6.7	360.4 +/- .9	3.7	0	0
950-1000	48	10	362.2 +/- 1.1	2.9	0	0
1000-1050	74	15.5	363.2 +/- .8	2	0	0
1050-1100	31	6.3	364.9 +/- 1.1	3.8	0	0

TOTAL GAS AGE = 341.2 MY.

% I.I.C. - INTERFERING ISOTOPES CORRECTION ERROR ESTIMATES AT ONE SIGMA LEVEL

PE84-46P K-FELDSPAR SUMMARY

TEMP.(DEG.C)	mV Ar39	% Ar39	AGE(Ma)	% ATMOS.	Ar37/Ar39	% I.I.C.
			J = 3E-03			
150-300	9.7	1.9	392.3 +/- 4.8	10.7	0	0
300-350	26	5.1	246.4 +/- 3.7	3.3	0	0
350-400	17.7	3.4	230.7 +/- 4	8.6	0	0
400-650	30.6	6.2	242.3 +/- 1.2	4.1	0	0
650-700	32.8	6.7	246.8 +/- .8	3.5	0	0
700-750	30	6.1	245.1 +/- .5	3.3	0	0
750-800	34.8	7.1	247.6 +/- .8	3.8	0	0
800-850	30.6	6.2	249.9 +/- 1.1	5.5	0	0
850-900	38.4	7.8	251.8 +/- 1.4	3.8	0	0
900-950	33.9	7.3	255.4 +/- .6	6.7	0	0
950-1000	23.4	5.2	260.2 +/- 1.3	7.3	0	0
1000-1050	29.2	6	266.7 +/- 1.6	7.1	0	0
1050-1100	26.6	5.4	271.1 +/- 1.1	9.5	0	0
1100-1150	35.9	7.3	273.6 +/- .9	10.2	0	0
1150-1200	82.8	17	276 +/- .4	6.1	0	0

TOTAL GAS AGE = 260.3 MY.

% I.I.C. - INTERFERING ISOTOPES CORRECTION ERROR ESTIMATES AT ONE SIGMA LEVEL

PE84-53F MUSCOVITE SUMMARY

TEMP. (DEG.C)	mV Ar39	% Ar39	AGE (Ma)	% ATMOS.	Ar37/Ar39	% I.I.C.
			J = 1.9676-03			
300-600	8.2	1.1	280.3 +/- 10.6	65.8	0	0
600-650	6.6	1.4	320 +/- 4.1	29.8	0	0
650-700	8.9	1.9	342.8 +/- 3.8	13.3	0	0
700-750	16.5	3.6	335.7 +/- 3.1	14.3	0	0
750-800	45.4	9.9	337.1 +/- .7	10.8	0	0
800-850	122.2	26.6	343.7 +/- .4	9.3	0	0
850-900	115	25	342.1 +/- .4	2.8	0	0
900-930	46	10	344.4 +/- 1.2	3.5	0	0
930-1000	30.9	6.7	344.3 +/- 1	4.8	0	0
1000-1150	61.3	13.3	348.2 +/- .6	3.5	0	0

TOTAL GAS AGE = 342 MY.

% I.I.C. - INTERFERING ISOTOPES CORRECTION

ERROR ESTIMATES AT ONE SIGMA LEVEL

PE84-53B BIOTITE SUMMARY

TEMP. (DEG.C)	mV Ar39	% Ar39	AGE (Ma)	% ATMOS.	Ar37/Ar39	% I.I.C.
			J = 1.9636-03			
200-500	1.8	.3	87.3 +/- 80.2	96.8	0	0
500-550	4	.8	122.5 +/- 9.3	79	0	0
550-600	9	1.9	291 +/- 3.4	27	0	0
600-650	22.2	4.8	309.5 +/- 1.1	15.9	0	0
650-700	102.2	22.1	313.3 +/- .4	5.4	0	0
700-750	77.4	16.7	312.3 +/- .5	7.3	0	0
750-800	22.4	4.8	308.7 +/- 1	20.1	0	0
800-850	17.6	3.8	307.2 +/- 1.7	27.7	0	0
850-900	32.4	7	310.9 +/- .8	9.9	0	0
900-950	92.8	20	314.7 +/- .3	6.1	0	0
950-1000	58.8	12.7	311.3 +/- .5	10.8	0	0
1000-1150	21.2	4.5	299 +/- 1.4	41.1	0	0

TOTAL GAS AGE = 309.3 MY.

% I.I.C. - INTERFERING ISOTOPES CORRECTION

ERROR ESTIMATES AT ONE SIGMA LEVEL

PEG4-5481 MUSCOVITE SUMMARY

TEMP.(DEG.C)	mV Ar39	% Ar39	AGE(Ma)	% ATMOS.	Ar37/Ar39	% I.I.C.
			J = 3.62E-03			
150-300	1.4	.1	63 +/- 412.6	99	0	.1
300-850	1.5	.1	100.3 +/- 223.9	97.3	0	0
350-600	2.7	.3	216.3 +/- 60.7	91.7	0	0
600-650	5	.6	309.2 +/- 29	83.1	0	0
650-700	14	1.6	333.7 +/- 7.7	65.6	0	0
700-750	29.3	3.3	341.2 +/- 3.4	48.1	0	0
750-800	78	9.4	348.1 +/- 1.7	30.1	0	0
800-850	233	28	344.5 +/- 2.1	16.5	0	0
850-900	98	11.8	350.2 +/- 3.9	49	0	0
900-950	49	5.9	346.4 +/- 3.3	46.6	0	0
950-1000	79	9.5	333.3 +/- 2.2	32	0	0
1000-1050	130	15.6	356.1 +/- 1.1	24	0	0
1050-1100	98	11.8	359.1 +/- 3.6	31.1	0	0
1100-1150	9.8	1.1	280.1 +/- 8.1	86.2	0	0

TOTAL GAS AGE = 347.5 MY.

% I.I.C. - INTERFERING ISOTOPES CORRECTION
ERROR ESTIMATES AT ONE SIGMA LEVEL

PEG4-5482 K-FELDSPAR SUMMARY

TEMP.(DEG.C)	mV Ar39	% Ar39	AGE(Ma)	% ATMOS.	Ar37/Ar39	% I.I.C.
			J = 2.62E-03			
200-300	30.6	4.2	426.3 +/- 1.7	33.4	0	0
300-350	34.3	4.7	234.4 +/- 1.3	14.8	0	0
350-400	40.8	5.6	240.2 +/- .9	13	0	0
400-450	32.6	4.5	241.7 +/- .9	13	0	0
450-700	37.6	5.2	241.4 +/- .6	20.7	0	0
700-750	33.3	4.6	241.5 +/- 1.1	19.5	0	0
750-800	45.2	6.3	246.2 +/- .6	16.5	0	0
800-850	48.9	6.8	248 +/- .6	16.9	0	0
850-900	55.5	7.7	251 +/- .5	16.4	0	0
900-950	60.3	8.4	253.3 +/- .5	15.6	0	0
950-1000	61.9	8.6	253.3 +/- .6	19.1	0	0
1000-1100	73.3	10.2	254.3 +/- .6	22.3	0	0
1100-1200	163	22.7	244.4 +/- .5	18.6	0	0

TOTAL GAS AGE = 239.8 MY.

% I.I.C. - INTERFERING ISOTOPES CORRECTION
ERROR ESTIMATES AT ONE SIGMA LEVEL

PE84-127A MUSCOVITE SUMMARY

TEMP.(DEG.C)	aV Ar39	% Ar39	AGE(Ma)	% Atmos.	Ar37/Ar39	% I.I.C.
			J = 1.9846E-03			
200-600	22.9	5.7	241.5 +/- 2	54.1	0	0
600-650	52.5	13.1	318.7 +/- .7	13.4	0	0
650-700	85.9	21.4	324.5 +/- .5	7	0	0
700-750	35	8.7	323.7 +/- 1.2	13.1	0	0
750-800	21.7	5.4	319.8 +/- 1.7	26.8	0	0
800-825	24	6	322.8 +/- 3.3	22	0	0
825-850	46.9	11.7	327.8 +/- 2.3	13	0	0
850-900	77	19.2	321.8 +/- 1.8	15	0	0
900-950	6.8	1.7	325 +/- 9.5	10.8	0	0
950-1000	18	4.4	307.2 +/- 6.7	31.8	0	0
1000-1140	9.5	2.3	303.5 +/- 4.7	49.4	.3	0

TOTAL GAS AGE = 318.3 MY.

% I.I.C. - INTERFERING ISOTOPES CORRECTION
ERROR ESTIMATES AT ONE SIGMA LEVEL

PE84-127A1 K-FELDSPAR SUMMARY

TEMP.(DEG.C)	aV Ar39	% Ar39	AGE(Ma)	% Atmos.	Ar37/Ar39	% I.I.C.
			J = 2.632E-03			
200-500	32.3	4	295.7 +/- 1.7	37.3	0	0
500-550	43.2	5.7	232.7 +/- 1	41.7	0	0
550-600	46.9	5.9	240.3 +/- .9	41.7	0	0
600-650	47.2	5.9	243.1 +/- 1.1	43.9	0	0
650-700	44.7	5.6	243.4 +/- .8	48.2	0	0
700-750	46.6	5.8	243.7 +/- 1.1	52.7	0	0
750-800	45.7	5.7	243.3 +/- 1	52.8	0	0
800-850	64	8	248.9 +/- 1.1	53.3	0	0
850-900	61.9	7.8	252.8 +/- 1.2	51.1	0	0
900-950	69	8.7	256.1 +/- .9	50.8	0	0
950-1000	64	8	255.5 +/- 1	53.7	0	0
1000-1030	49.3	6.2	257.6 +/- 1.3	60.8	0	0
1030-1100	49.8	6.3	258.7 +/- 1.1	60	0	0
1100-1150	53	6.6	268 +/- .9	57	0	0
1150-1200	71	8.9	275.5 +/- .8	46	0	0

TOTAL GAS AGE = 259.6 MY.

% I.I.C. - INTERFERING ISOTOPES CORRECTION
[illegible]

PE84-125 MUSCOVITE SUMMARY

TEMP.(DEG.C)	aV Ar39	% Ar39	AGE(Ma)	% ATMOS.	Ar37/Ar39	% I.I.C.
			J = 1.844E-03			
200-300	3.4	.9	201.3 +/- 8.3	45.3	0	0
300-350	3.8	1	211.3 +/- 6.6	30.8	0	0
350-600	9.8	2.7	286.3 +/- 2.4	13.1	0	0
600-650	17.6	4.9	341.8 +/- 1	4.4	0	0
650-700	28.2	7.9	343.6 +/- .8	4.8	0	0
700-750	37.3	10.4	344 +/- .6	4.8	0	0
750-800	25.7	7.2	344.1 +/- .7	5.2	0	0
800-850	31	8.7	347.2 +/- .6	4.8	0	0
850-900	76.5	21.3	349 +/- .4	1.7	0	0
900-950	50	14	349.4 +/- .4	3.1	0	0
950-1000	45	12.6	346.2 +/- .4	4.4	0	0
1000-1150	27.2	7.6	351.8 +/- .8	9.7	0	0

TOTAL GAS AGE = 342.6 MY.

% I.I.C. - INTERFERING ISOTOPES CORRECTION
ERROR ESTIMATES AT ONE SIGMA LEVEL

B-454 BIOTITE SUMMARY

TEMP.(DEG.C)	aV Ar39	% Ar39	AGE(Ma)	% ATMOS.	Ar37/Ar39	% I.I.C.
			J = 2.819E-03			
200-600	22.8	5.5	312.4 +/- 1.2	19.3	0	0
650-700	23.2	6.1	326.8 +/- 2.5	6.3	0	0
700-750	149.5	36.5	321.6 +/- .9	4.2	0	0
750-800	41.4	10.1	320.7 +/- .6	10.9	0	0
800-850	15.3	3.7	318.4 +/- 2.3	22.1	0	0
850-900	29	7.1	322.5 +/- 1.2	11.9	0	0
900-950	65.8	16.1	321.9 +/- .6	7.9	0	0
950-1000	23.2	6.1	330.4 +/- 1.6	12.2	0	0
1000-1050	18.9	4.6	322.6 +/- 1.7	19.4	0	0
1050-1150	13.1	3.7	303.4 +/- 1.8	34.7	.8	.1

TOTAL GAS AGE = 320.6 MY.

% I.I.C. - INTERFERING ISOTOPES CORRECTION
ERROR ESTIMATES AT ONE SIGMA LEVEL

PE84-43B BIOTITE SUMMARY

TEMP. (DEG.C)	mV Ar39	% Ar39	AGE (Ma)	% Atmos.	Ar37/Ar39	% I.I.C.
			J = 1.877E-03			
300-500	1.2	.2	203.6 +/- 38.8	85.9	0	0
500-550	.8	.1	273.1 +/- 80.5	82.3	0	0
550-600	1.4	.3	282.3 +/- 23.4	74.7	0	0
600-650	3.1	.6	309.8 +/- 9.6	61	0	0
650-700	6.3	1.3	312.1 +/- 3.6	43.5	0	0
700-750	10.3	2.1	331.4 +/- 2.9	19.8	0	0
750-800	17.2	3.5	338.5 +/- 1	14.8	0	0
800-850	47.9	9.9	343.5 +/- .4	5.6	0	0
850-900	109.3	22.6	349.9 +/- .4	3.7	0	0
900-950	68	14.1	349 +/- .2	3.2	0	0
950-1000	73	15.1	349.8 +/- .3	5.1	0	0
1000-1140	142.8	29.6	352.3 +/- .3	6.8	0	0

TOTAL GAS AGE = 347.8 MY.

% I.I.C. - INTERFERING ISOTOPES CORRECTION

ERROR ESTIMATES AT ONE SIGMA LEVEL

PE-20-P MUSCOVITE SUMMARY

TEMP. (DEG.C)	mV Ar39	% Ar39	AGE (Ma)	% Atmos.	Ar37/Ar39	% I.I.C
			J = 2.865E-03			
300-650	12.6	.8	349.4 +/- 12.9	87.3	0	0
650-750	22.4	1.6	339.8 +/- 2.8	67.8	0	0
750-850	100.2	7.7	346.1 +/- .4	15.2	0	0
850-900	174.4	12.4	349 +/- .4	6.1	0	0
900-950	173	12.4	351.1 +/- .4	3.6	0	0
950-1000	268.7	19.1	350.6 +/- .3	26.1	0	0
1000-1050	275.7	19.6	351.3 +/- .3	12.4	0	0
1050-1100	56.9	4	350.1 +/- .4	14.8	0	0
1100-1150	137	9.7	352 +/- .4	4.9	0	0
1150-1200	172.8	12.3	353.2 +/- .7	31.2	0	0

TOTAL GAS AGE = 350.7 MY.

% I.I.C. - INTERFERING ISOTOPES CORRECTION

ERROR ESTIMATES AT ONE SIGMA LEVEL

APPENDIX A - 6

BIOTITE AND K-FELDSPARS FROM THE SOUTH MOUNTAIN BATHOLITH

(BIOTITE STANDARD NS-231)

B4B CAN 57 N.S. BIOTITE SUMMARY

TEMP. (DEG.C)	aV Ar39	% Ar39	AGE (Ma)	% ATMOS.	Ar37/Ar39	% I.I.C
			J = 2.76E-03			
500-550	4.2	2.7	315.1 +/- 10.6	53.7	0	0
550-600	11.3	7.4	370.9 +/- 2.7	27.3	0	0
600-650	32.1	20.9	371 +/- .9	13.8	0	0
650-700	17.6	11.4	348 +/- 1.8	12.7	0	0
700-750	21.4	13.9	372 +/- 1.3	17.5	0	0
750-800	8.3	5.4	348.3 +/- 3.6	33.7	0	0
800-850	6	3.9	343.8 +/- 7.1	47.7	0	0
850-900	12	7.8	372.7 +/- 3.7	31.4	0	0
900-950	17.7	11.5	370.1 +/- 2	20.9	0	0
950-1000	12.6	8.2	348.7 +/- 2.8	27.6	0	0
1000-1050	3.9	2.5	341.6 +/- 5.8	49.5	0	0
1050-1150	5.8	3.8	341 +/- 8.2	58.4	0	0

TOTAL GAS AGE = 348 MY.

% I.I.C. - INTERFERING ISOTOPES CORRECTION

ERROR ESTIMATES AT ONE SIGMA LEVEL

PE85-142 K-FELDSPAR SUMMARY

TEMP. (DEG.C)	aV Ar39	% Ar39	AGE (Ma)	% ATMOS.	Ar37/Ar39	% I.I.C
			J = 2.795E-03			
200-300	17.2	3.3	313.8 +/- 2.8	28.3	0	0
300-550	20.4	4	262.8 +/- 1.7	11	0	0
550-600	17.3	3.4	320.9 +/- 1.9	13.5	0	0
600-650	17.4	3.4	334.1 +/- 1.9	14.4	0	0
650-700	16	3.1	378 +/- 1.7	13.2	0	0
700-750	21.7	4.2	350.6 +/- 1	14.2	0	0
750-800	18	3.5	345.1 +/- 1.5	22.3	0	0
800-850	25.4	4.9	332.7 +/- 1.7	17.5	0	0
850-900	31.5	6.1	333.8 +/- .6	13.1	0	0
900-950	41.6	8.1	334.5 +/- .8	12.6	0	0
950-1000	38.6	7.5	335.6 +/- .9	13	0	0
1000-1050	40.5	7.9	337.6 +/- .8	14	0	0
1050-1100	61.1	12	347.3 +/- .4	13	0	0
1100-1140	78	15.3	356.5 +/- .4	11.9	0	0
1140-1180	64.3	12.6	342.3 +/- .4	14.8	0	0

TOTAL GAS AGE = 342.8 MY.

% I.I.C. - INTERFERING ISOTOPES CORRECTION

ERROR ESTIMATES AT ONE SIGMA LEVEL

PE85-143 K-FELDSPAR SUMMARY

TEMP.(DEG.C)	aV Ar39	% Ar39	AGE(Ma)	% ATMOS.	Ar37/Ar39	% I.I.C.
			J = 2.838E-03			
200-500	29.4	4.3	317.5 +/- .9	33	0	0
500-550	38.6	5.7	294.4 +/- .6	9.9	0	0
550-600	40.7	6	329.5 +/- .7	9	0	0
600-650	36.2	5.3	339.5 +/- .7	10.4	0	0
650-700	23.8	3.5	352.1 +/- 1.7	13.3	0	0
700-750	13.9	2	344 +/- 1.6	19.2	0	0
750-800	20.6	3	346.7 +/- 1.6	16	0	0
800-850	28.4	4.2	344.1 +/- 1.1	18.5	0	0
850-900	62.9	9.3	350 +/- .8	11.7	0	0
900-950	57.7	8.5	357.9 +/- .8	10.1	0	0
950-1000	46.7	6.9	353.9 +/- .6	13.5	0	0
1000-1050	48.4	7.1	359.1 +/- .8	13.1	0	0
1050-1100	42.4	9.2	347.9 +/- .6	11.1	0	0
1100-1140	92.8	13.7	370.7 +/- .3	9.6	0	0
1140-1180	73.2	10.8	370.5 +/- .8	12.2	0	0

TOTAL GAS AGE = 351.8 MY.

% I.I.C. - INTERFERING ISOTOPES CORRECTION
ERROR ESTIMATES AT ONE SIGMA LEVEL

PE85-144 K-FELDSPAR SUMMARY

TEMP.(DEG.C)	aV Ar39	% Ar39	AGE(Ma)	% ATMOS.	Ar37/Ar39	% I.I.C.
			J = 2.9E-03			
150-450	8.2	1.5	384.9 +/- 5.3	49	0	0
450-500	14.7	2.7	306.4 +/- 1.6	18.7	0	0
500-530	5.4	.9	273.1 +/- 9.5	21.2	0	0
530-560	9.3	1.7	316.8 +/- 2.5	19	0	0
560-590	5	.9	325.3 +/- 6.5	23.7	0	0
590-630	12.3	2.2	352 +/- 2.3	23.1	0	0
630-690	16.2	2.9	371.7 +/- 2.6	17.2	0	0
690-750	28.7	5.2	352.8 +/- 1.3	13	0	0
750-810	29.8	5.4	333.6 +/- 1.4	18.1	0	0
810-870	55.9	10.2	334.8 +/- .6	12.7	0	0
870-930	121.9	22.3	340.8 +/- .3	11.7	0	0
930-990	64.8	11.8	341.5 +/- .5	14.7	0	0
990-1050	49.7	9.1	341.7 +/- .6	17.6	0	0
1050-1170	123.2	22.5	356.1 +/- .7	8.7	0	0

TOTAL GAS AGE = 343.9 MY.

% I.I.C. - INTERFERING ISOTOPES CORRECTION
ERROR ESTIMATES AT ONE SIGMA LEVEL

PE85-151 K-FELDSPAR SUMMARY

TEMP.(DEG.C)	mV Ar39	% Ar39	AGE(Ma)	% ATMOS.	Ar37/Ar39	% I.I.C.
			J = 2.783E-03			
200-500	21.1	4.3	349.9 +/- 2.8	24.7	0	0
500-550	19.1	3.8	276.2 +/- 2.1	15.8	0	0
550-600	8.3	1.7	311.6 +/- 3.3	21.2	0	0
600-650	9.2	1.8	333.8 +/- 3.4	24.1	0	0
650-700	8.1	1.6	343.6 +/- 4.9	24.4	0	0
700-750	23.5	4.7	372.4 +/- 1.6	14.6	0	0
750-800	16.6	3.3	356.6 +/- 1.3	12.9	0	0
800-850	18.5	3.7	348.9 +/- 1.3	11.7	0	0
850-900	28.2	5.7	340.1 +/- 1.3	12.2	0	0
900-950	33.8	6.8	341.4 +/- .9	8.1	0	0
950-1000	45.6	9.2	339.5 +/- 1.1	9.1	0	0
1000-1050	47.3	9.6	343.5 +/- 1.2	11.1	0	0
1050-1100	52.6	10.7	350.6 +/- 1	9.5	0	0
1100-1140	93.1	18.9	359 +/- .6	6.7	0	0
1140-1180	65.4	13.3	360.9 +/- .7	9.2	0	0

TOTAL GAS AGE = 348.2 MY.

% I.I.C. - INTERFERING ISOTOPES CORRECTION

ERROR ESTIMATES AT ONE SIGMA LEVEL

APPENDIX B. MICROPROBE ANALYSES OF SELECTED SAMPLES.

AMPHIBOLES.

	PE84-130 RIM	PE84-130 CORE	PE83-9 RIM	PE83-9 CORE
SiO2	39.46	39.38	44.87	45.13
TiO2	.40	.38	.83	.38
Al2O3	18.20	17.45	10.17	11.45
FeO	21.80	21.72	15.61	16.94
MnO	.31	.30	.28	.25
MgO	5.01	4.89	11.56	10.26
CaO	11.05	11.28	11.80	11.44
Na2O	2.01	1.74	1.22	1.06
K2O	.43	.40	.47	.38
H2O	1.98	1.95	2.00	2.01
SUM	100.65	99.61	98.86	99.38
Si	5.982	6.036	6.715	6.724
Al	2.018	1.964	1.285	1.276
Al	1.233	1.187	.509	.734
Ti	.046	.044	.093	.043
Mg	1.132	1.117	2.579	2.278
Fe	2.764	2.784	1.954	2.111
Mn	.040	.039	.035	.032
Ca	1.795	1.852	1.892	1.826
Na	.591	.517	.354	.306
K	.083	.078	.090	.072
H	2.000	2.000	2.000	2.000
O	24.000	24.000	24.000	24.000
F/FM	.712	.716	.435	.485

	PE84-114 RIM	PE84-114 CORE	PE84-64C RIM	PE84-64C CORE	PE83-11 RIM	PE83-11 CORE
SiO2	45.75	44.63	39.81	39.93	44.75	44.93
TiO2	.93	.99	.25	.27	.31	.32
Al2O3	9.12	9.68	20.47	18.57	13.17	13.01
FeO	16.89	17.02	20.12	20.96	14.93	14.68
MnO	.61	.51	.28	.26	.22	.11
MgO	10.92	10.61	4.23	4.52	10.87	10.84
CaO	11.93	11.99	10.88	11.29	11.73	11.77
Na2O	1.18	1.40	1.57	1.38	1.01	.98
K2O	.39	.53	.30	.41	.21	.19
H2O	4.20	4.16	1.99	1.97	2.03	2.03
SUM	101.92	101.52	99.97	99.65	99.31	98.92
Si	6.531	6.422	5.984	6.066	6.602	6.640
Al	1.469	1.578	2.016	1.934	1.398	1.360
Al	.065	.064	1.610	1.391	.891	.906
Ti	.100	.107	.028	.031	.034	.036
Fe	2.016	2.048	2.529	2.663	1.842	1.814
Mn	.074	.062	.036	.033	.027	.014
Mg	2.323	2.276	.948	1.024	2.390	2.388
Na	.327	.391	.458	.406	.289	.281
K	.071	.097	.058	.079	.040	.086
H	4.000	4.000	2.000	2.000	2.000	2.000
O	24.000	24.000	24.000	24.000	24.000	24.000
F/FM	.474	.481	.730	.725	.439	.434

RMT Biotite

	PE82-2	PE83-2	PE82-4	PE83-4	PE82-5
SiO2	35.55	36.33	35.90	36.16	34.91
TiO2	1.77	1.79	2.07	1.45	1.88
Al2O3	18.66	18.59	18.45	20.00	19.02
Feo	19.46	17.45	21.44	20.95	22.97
MnO	0.18	.20	0.18	.02	.06
MgO	9.23	11.13	7.92	8.18	7.42
CaO	0.00	0.00	0.00	0.00	0.00
Na2O	0.08	0.13	0.03	0.14	
K2O	10.00	11.01	9.60	7.94	10.27
H2O	3.91	4.00	3.91	3.94	3.90
SUM	98.84	100.63	99.50	98.78	100.43
Si	5.454	5.447	5.501	5.494	5.365
Al	2.546	2.553	2.499	2.506	2.635
Al	.827	.732	.832	1.075	.809
Ti	.204	.202	.239	.166	.217
Fe	2.497	2.188	2.747	2.662	2.952
Mn	0.023	0.025	0.023	0.003	.008
Mg	2.111	2.487	1.809	1.852	1.700
Na	0.024	0.38	0.009	0.041	0.000
K	1.957	2.106	1.876	1.539	2.013
H	4.000	4.000	4.000	4.000	4.000
O	24.00	24.000	24.00	24.00	24.000
F/FM	.544	0.471	0.605	0.590	.635

	PE83-5
SiO2	35.02
TiO2	1.62
Al2O3	19.28
FeO	18.97
MnO	0.00
MgO	9.66
Na2O	0.18
K2O	10.92
H2O	3.92
SUM	99.57
Si	5.351
Al	2.649
Al	.823
Ti	.186
Fe	2.424
MG	2.200
Na	.053
K	2.128
H	4.000
O	24.000
F/FM	.524

	PE83-10	PE82-8	PE83-7	PE82-19
SiO2	35.78	35.82	34.04	36.89
TiO2	1.76	1.86	1.97	1.66
Al2O3	19.60	19.15	18.22	20.12
FeO	18.41	19.99	18.68	14.90
MnO	.07	.13	.10	.10
MgO	10.02	9.44	11.06	11.81
Na2O	.08	.11	.09	.26
K2O	11.19	11.35	10.63	10.26
H2O	3.99	3.99	3.88	4.06
SUM	101.00	101.84	98.67	100.26
Si	5.372	5.377	5.262	5.441
Al	2.628	2.623	2.738	2.559
Al	.839	.765	.581	.973
Ti	.199	.210	.229	.184
Fe	2.311	2.510	2.415	1.838
Mn	.009	.017	.013	.012
Mg	2.242	2.112	2.548	2.596
Na	.023	.032	.027	.074
K	2.162	2.173	2.096	1.930
H	4.000	4.000	4.000	4.000
O	24.000	24.000	24.000	24.000
F/FM	.509	.545	.488	.416

	PE82-10	PE84-76	PE82-17	PE84-108	PE84-100	PE83-12
SiO2	35.91	35.87	37.14	36.26	36.52	37.63
TiO2	1.90	1.82	2.71	1.76	1.69	1.79
Al2O3	17.11	18.60	16.74	18.34	18.70	17.33
FeO	22.89	20.98	18.94	20.84	21.00	19.70
MnO	.17	.19	.34	.20	.12	.30
MgO	8.24	8.83	10.78	8.54	7.95	10.03
Na2O	.06	.10	.13	.09	.05	.07
K2O	9.95	10.02	10.43	9.89	9.46	9.23
H2O	3.89	3.94	4.00	3.93	3.93	3.98
SUM	100.12	100.35	101.21	99.85	99.42	100.06
Si	5.528	5.453	5.561	5.527	5.570	5.661
Al	2.472	2.547	2.439	2.473	2.430	2.339
Al	.632	.784	.514	.822	.931	.734
Ti	.220	.208	.305	.202	.194	.203
Fe	2.947	2.667	2.372	2.657	2.679	2.479
Mn	.022	.024	.043	.026	.016	.038
Mg	1.891	2.001	2.406	1.940	1.807	2.249
Na	.018	.029	.038	.027	.015	.020
K	1.954	1.943	1.992	1.923	1.840	1.771
H	4.000	4.000	4.000	4.000	4.000	4.000
O	24.000	24.000	24.000	24.000	24.000	24.000
F/FM	.611	.574	.501	.580	.599	.528

	PE83-10	PE82-8	PE83-7	PE82-19
SiO2	35.78	35.82	34.04	36.89
TiO2	1.76	1.86	1.97	1.66
Al2O3	19.60	19.15	18.22	20.12
FeO	18.41	19.99	18.68	14.90
MnO	.07	.13	.10	.10
MgO	10.02	9.44	11.06	11.81
Na2O	.08	.11	.09	.26
K2O	11.19	11.35	10.63	10.26
H2O	3.99	3.99	3.88	4.06
SUM	101.00	101.84	98.67	100.26
Si	5.372	5.377	5.262	5.441
Al	2.628	2.623	2.738	2.559
Al	.839	.765	.581	.973
Ti	.199	.210	.229	.184
Fe	2.311	2.510	2.415	1.838
Mn	.009	.017	.013	.012
Mg	2.242	2.112	2.548	2.596
Na	.023	.032	.027	.074
K	2.162	2.173	2.096	1.930
H	4.000	4.000	4.000	4.000
O	24.000	24.000	24.000	24.000
F/FM	.509	.545	.488	.416

	PE82-10	PE84-76	PE82-17	PE84-108	PE84-100	PE83-12
SiO2	35.91	35.87	37.14	36.26	36.52	37.63
TiO2	1.90	1.82	2.71	1.76	1.69	1.79
Al2O3	17.11	18.60	16.74	18.34	18.70	17.33
FeO	22.89	20.98	18.94	20.84	21.00	19.70
MnO	.17	.19	.34	.20	.12	.30
MgO	8.24	8.83	10.78	8.54	7.95	10.03
Na2O	.06	.10	.13	.09	.05	.07
K2O	9.95	10.02	10.43	9.89	9.46	9.23
H2O	3.89	3.94	4.00	3.93	3.93	3.98
SUM	100.12	100.35	101.21	99.85	99.42	100.06
Si	5.528	5.453	5.561	5.527	5.570	5.661
Al	2.472	2.547	2.439	2.473	2.430	2.339
Al	.632	.784	.514	.822	.931	.734
Ti	.220	.208	.305	.202	.194	.203
Fe	2.947	2.667	2.372	2.657	2.679	2.479
Mn	.022	.024	.043	.026	.016	.038
Mg	1.891	2.001	2.406	1.940	1.807	2.249
Na	.018	.029	.038	.027	.015	.020
K	1.954	1.943	1.992	1.923	1.840	1.771
H	4.000	4.000	4.000	4.000	4.000	4.000
O	24.000	24.000	24.000	24.000	24.000	24.000
F/FM	.611	.574	.501	.580	.599	.528

	PE84-64D
SiO2	34.55
TiO2	1.23
Al2O3	19.77
FeO	25.27
MnO	.06
MgO	6.90
CaO	.03
Na2O	.20
K2O	9.39
H2O	3.91
SUM	101.31
Si	5.293
Al	2.707
Al	.863
Ti	.142
Fe	3.238
Mn	.008
Mg	1.576
Na	.059
K	1.835
H	4.000
O	24.000
F/FM	.673

	PE85-161	PE85-162
SiO2	35.69	35.26
TiO2	1.57	1.64
Al2O3	19.55	19.78
FeO	21.75	22.39
MnO	0.00	0.00
MgO	8.52	7.40
Na2O	0.26	0.29
K2O	8.96	8.67
H2O	3.95	3.91
SUM	100.26	99.34
Si	5.408	5.405
Al	2.592	2.595
Al	.900	.977
Ti	.179	.189
Fe	2.758	2.870
MG	1.924	1.691
Na	.076	.086
K	1.732	1.695
H	4.000	4.000
O	24.000	24.000
F/FM	.589	.629

	PE83-11	PE84-72	PE82-9
SiO2	37.81	37.13	35.03
TiO2	1.87	1.78	2.16
Al2O3	18.12	19.17	18.14
FeO	15.44	17.45	19.60
MnO	0.00	.14	0.00
MgO	13.28	11.04	8.94
Na2O	.19	.15	.11
K2O	8.93	7.73	10.51
H2O	4.06	4.01	3.86
SUM	99.70	98.60	98.35
Si	5.580	5.554	5.430
Al	2.420	2.446	2.570
Al	.732	.933	.744
Ti	.208	.200	.252
Fe	1.906	2.183	2.541
Mn	0.000	.018	0.000
Mg	2.921	2.461	2.066
Na	0.054	0.044	0.033
K	1.681	1.475	2.078
H	4.000	4.000	4.000
O	24.000	24.000	24.000
F/FM	.395	.472	.552

BALD MOUNTAIN MUSCOVITE

	PE84-27	PE84-28	PE84-29	PE84-30
SiO2	47.28	47.26	46.96	46.99
TiO2	.53	1.01	.78	.66
Al2O3	35.47	34.69	35.24	35.83
FeO	1.39	1.46	1.25	1.38
MgO	.63	.79	.69	.81
Na2O	.59	.35	.65	.25
K2O	10.07	11.02	10.32	10.19
H2O	4.55	4.55	4.54	4.56
Sum	100.51	101.13	100.43	100.67
Si	6.222	6.220	6.198	6.174
Al	1.778	1.780	1.802	1.826
Al	3.722	3.601	3.678	3.722
Ti	.052	.100	.077	.065
Fe	.153	.161	.138	.152
Mg	.124	.155	.136	.159
Na	.151	.089	.166	.064
K	1.690	1.850	1.737	1.708
H	4.000	4.000	4.000	4.000
O	24.000	24.000	24.000	24.000
F/FM	.531	.509	.504	.489

BALD MOUNTAIN PLAGIOCLASE.

	PE84-27	PE84-28	PE84-29	PE84-30
SiO2	68.21	69.46	68.72	68.54
Al2O3	20.35	19.94	19.74	20.09
CaO	.65	.48	.28	.37
Na2O	12.31	11.14	12.22	12.08
K2O	.13	.09	.14	.15
SUM	101.65	101.13	101.10	101.25
Si	11.791	11.978	11.914	11.867
Al	4.145	4.052	4.033	4.099
Ca	.120	.089	.052	.069
Na	4.126	3.725	4.107	4.055
K	.029	.020	.031	.035
O	32.000	32.000	32.000	32.000
OR	.671	.516	.739	.797
AB	96.513	97.170	98.020	97.552
AN	2.816	2.314	1.241	1.651

APPENDIX C. OTHER DATA.

XRD DATA FOR SMB K-FELDSPARS

SAMPLE	2θ			NAME	% OR*
	060	$\bar{2}04$	$\bar{2}01$		
PE85-142	41.73±.02	50.67±.05	21.04±.02	int. microcline	89±2
PE85-143	41.71±.05	50.66±.03	21.04±.02	int. microcline	89±2
PE85-144	41.74±.04	50.61±.06	21.00±.02	int. microcline	93±3
PE85-151	41.77±.05	50.68±.04	21.00±.02	int. microcline	93±3

PLOTS OF XRD DATA FROM SMB K-FELDSPARS

(After Wright, 1968)

Boxes represent uncertainty in peak measurements.

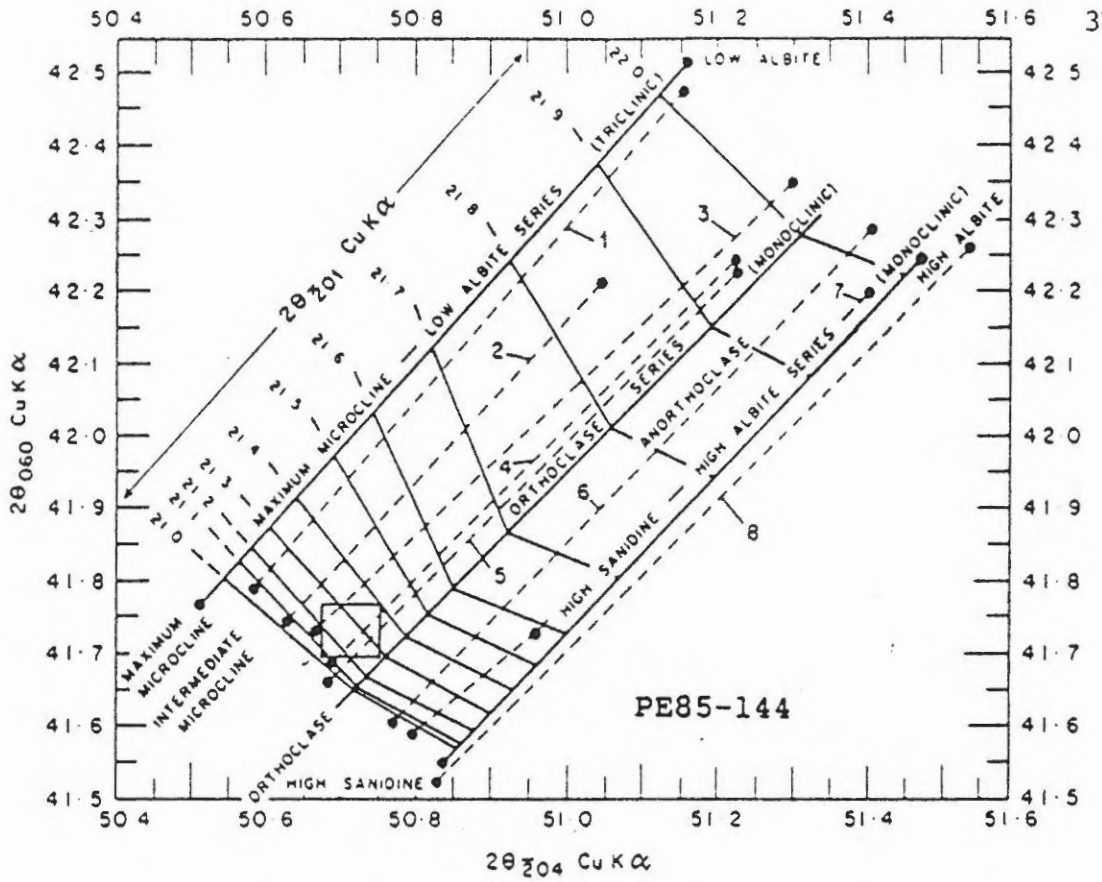
PE85-144
LOW ALBITE
(TRICLINIC)
(MONOCLINIC)
HIGH ALBITE
LOW ALBITE SERIES
HIGH ALBITE SERIES
ANORTHOCLASE SERIES
MAXIMUM MICROCLINE
INTERMEDIATE MICROCLINE
ORTHOCLASE
HIGH SANIDINE
$2\theta_{060}$ Cu Kα
$2\theta_{\bar{2}04}$ Cu Kα

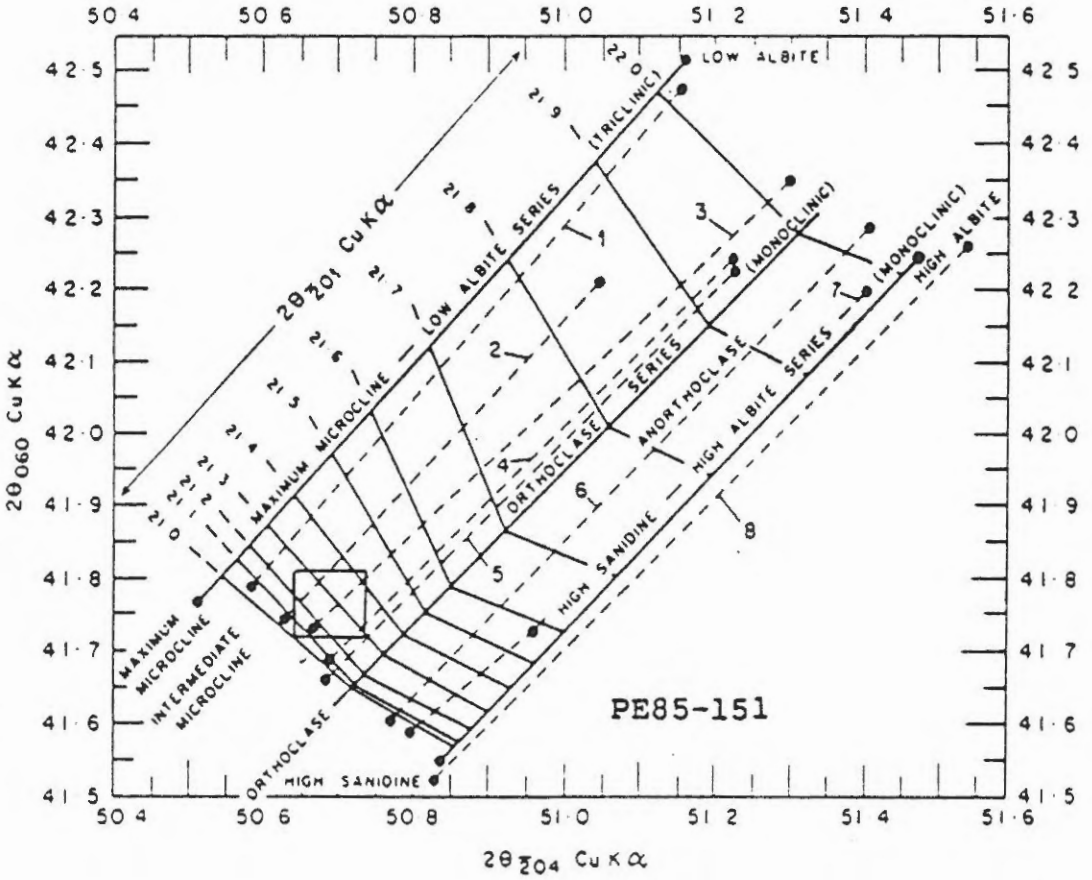
PE85-151
LOW ALBITE
(TRICLINIC)
(MONOCLINIC)
HIGH ALBITE
LOW ALBITE SERIES
HIGH ALBITE SERIES
ANORTHOCLASE SERIES
MAXIMUM MICROCLINE
INTERMEDIATE MICROCLINE
ORTHOCLASE
HIGH SANIDINE
$2\theta_{060}$ Cu Kα
$2\theta_{\bar{2}04}$ Cu Kα

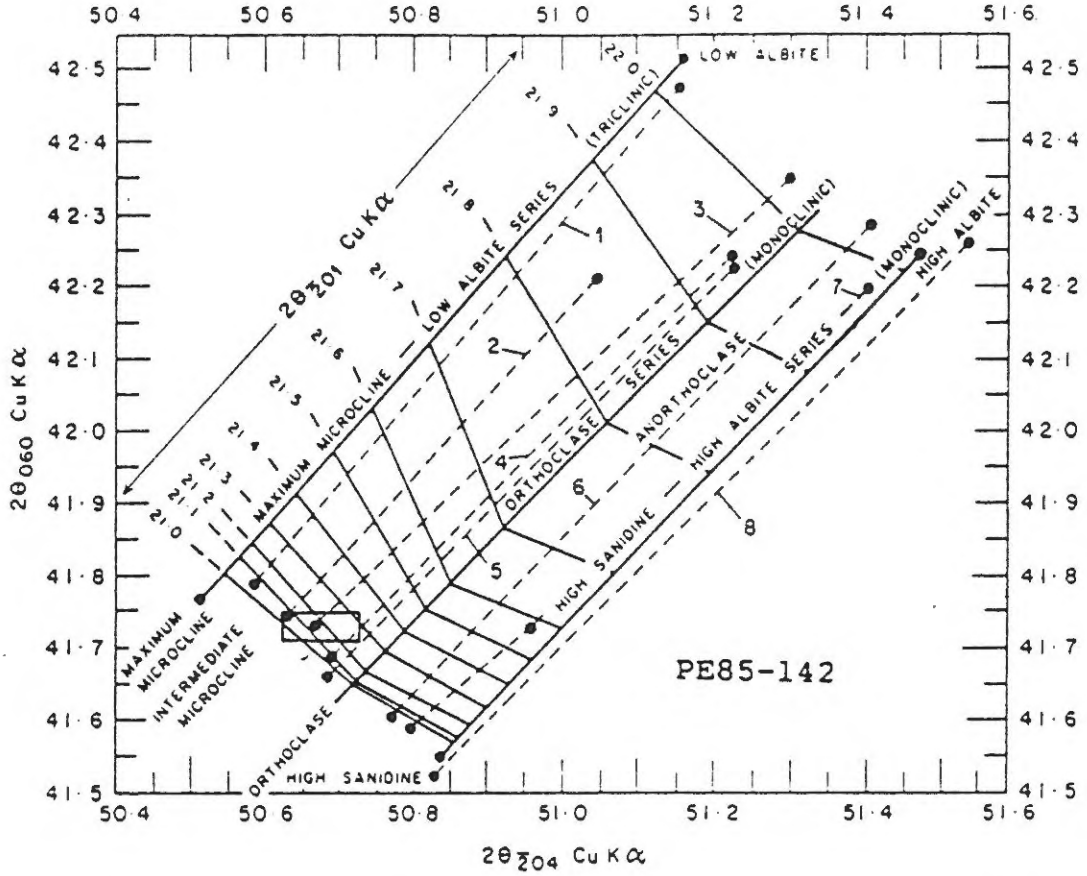
50·4
50·6
50·8
51·0
51·2
51·4
51·6
42·5
42·4
42·3
42·2
42·1
42·0
41·9
41·8
41·7
41·6
41·5
LOW ALBITE
(TRICLINIC)
LOW ALBITE SERIES
MAXIMUM MICROCLINE
(MONOCLINIC)
ANORTHOCLASE SERIES
HIGH ALBITE SERIES
HIGH ALBITE
ORTHOCLASE
HIGH SANIDINE
MAXIMUM MICROCLINE
INTERMEDIATE MICROCLINE
ORTHOCLASE
HIGH SANIDINE
PE85-142
$2\theta_{060}$ Cu Kα
$2\theta_{\bar{2}01}$ Cu Kα
$2\theta_{\bar{2}04}$ Cu Kα

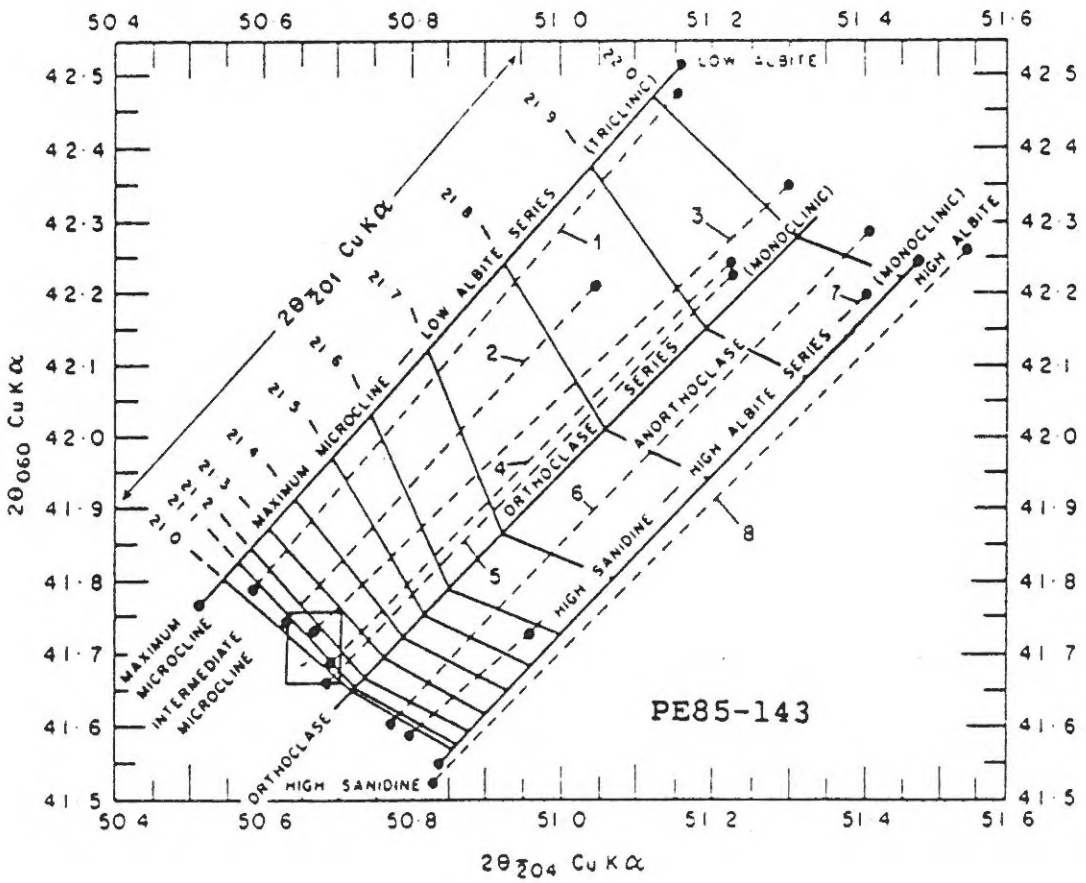
50·4
50·6
50·8
51·0
51·2
51·4
51·6
42·5
42·4
42·3
42·2
42·1
42·0
41·9
41·8
41·7
41·6
41·5
LOW ALBITE
(TRICLINIC)
LOW ALBITE SERIES
MAXIMUM MICROCLINE
(MONOCLINIC)
ANORTHOCLASE SERIES
HIGH ALBITE SERIES
HIGH ALBITE
ORTHOCLASE
HIGH SANIDINE
MAXIMUM MICROCLINE
INTERMEDIATE MICROCLINE
ORTHOCLASE
HIGH SANIDINE
PE85-143
$2\theta_{060}$ Cu Kα
$2\theta_{\bar{2}01}$ Cu Kα
$2\theta_{\bar{2}04}$ Cu Kα

XRD DATA FOR SSP K-FELDSPARS

SAMPLE	2θ			NAME	%OR*
	060	$\bar{2}04$	$\bar{2}01$		
PE84-39A	41.83 +/-.05	50.53 +/-.05	21.07 +/-.02	Maximum microcline	89+/-2
PE84-46	41.79 +/-.05	50.55 +/-.05	21.03 +/-.01	Maximum microcline	93+/-2
PE84-54B	41.78 +/-.05	50.52 +/-.05	21.01 +/-.01	Maximum microcline	95+/-2
PE84-127	41.79 +/-.05	50.52 +/-.05	21.06 +/-.02	Maximum microcline	91+/-2

PLOTS OF XRD DATA FROM SSP K-FELDSPARS

(After Wright, 1968)

Boxes represent uncertainty in peak measurements.

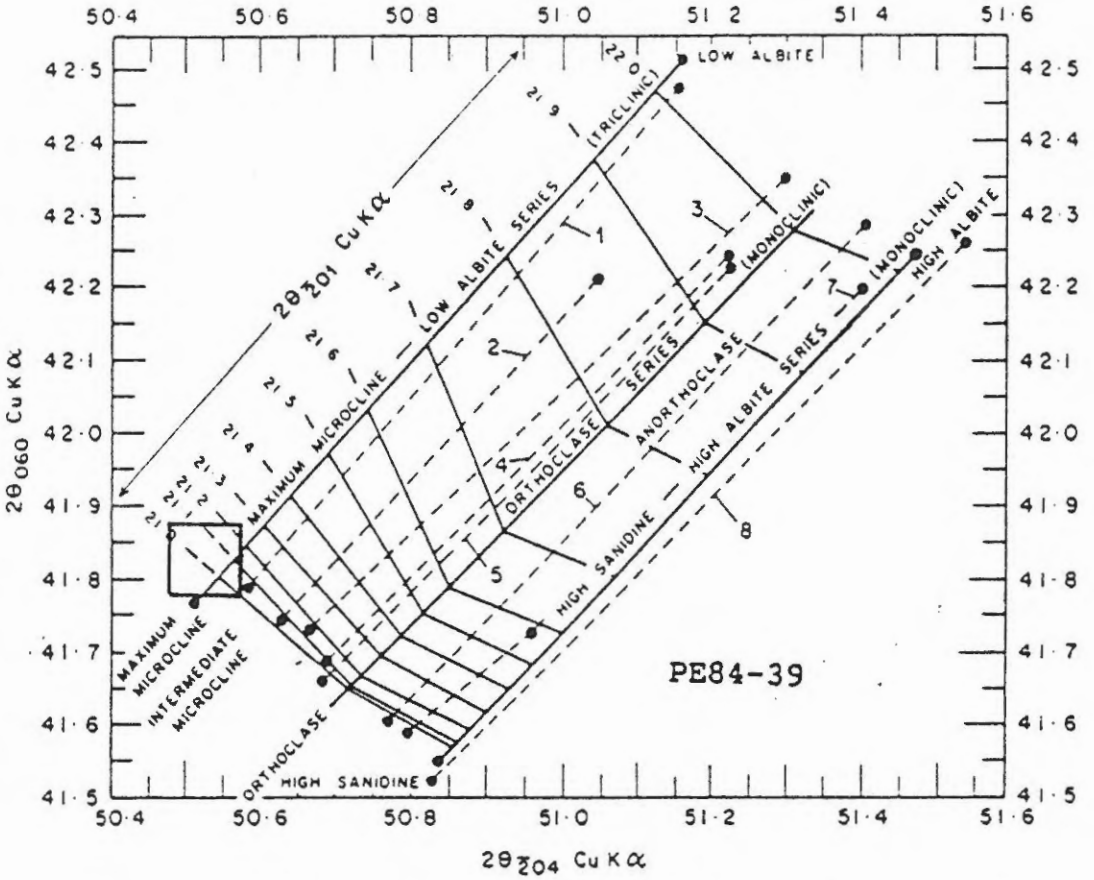
50·4
50·6
50·8
51·0
51·2
51·4
51·6
42·5
42·4
42·3
42·2
42·1
42·0
41·9
41·8
41·7
41·6
41·5
2θ060 Cu Kα
2θ̄04 Cu Kα
2θ̄01 Cu Kα
LOW ALBITE
(TRICLINIC)
LOW ALBITE SERIES
MAXIMUM MICROCLINE
ORTHOCLASE SERIES
ANORTHOCLASE SERIES
HIGH ALBITE SERIES
(MONOCLINIC)
HIGH ALBITE
HIGH SANIDINE
ORTHOCLASE
MAXIMUM MICROCLINE
INTERMEDIATE MICROCLINE
PE84-39

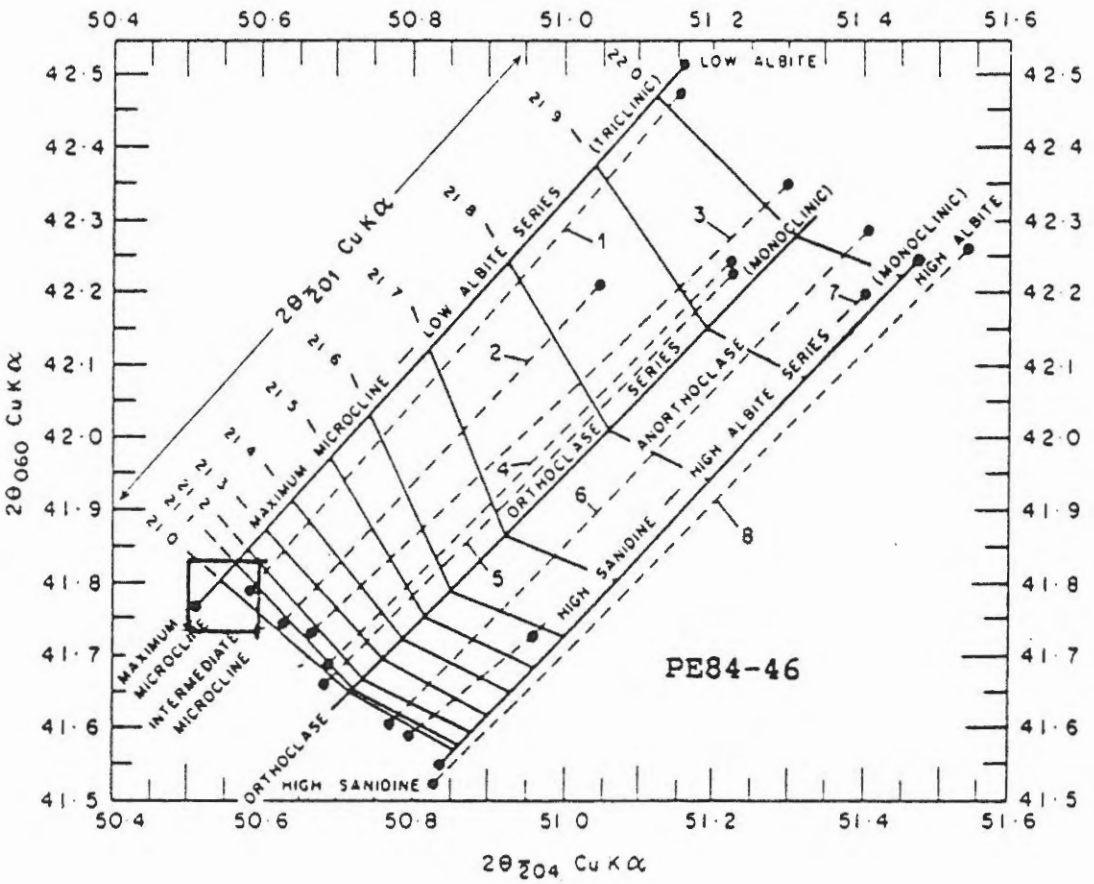
50·4
50·6
50·8
51·0
51·2
51·4
51·6
42·5
42·4
42·3
42·2
42·1
42·0
41·9
41·8
41·7
41·6
41·5
2θ060 Cu Kα
2θ̄04 Cu Kα
2θ̄01 Cu Kα
LOW ALBITE
(TRICLINIC)
LOW ALBITE SERIES
MAXIMUM MICROCLINE
ORTHOCLASE SERIES
ANORTHOCLASE SERIES
HIGH ALBITE SERIES
(MONOCLINIC)
HIGH ALBITE
HIGH SANIDINE
ORTHOCLASE
MAXIMUM MICROCLINE
INTERMEDIATE MICROCLINE
PE84-46

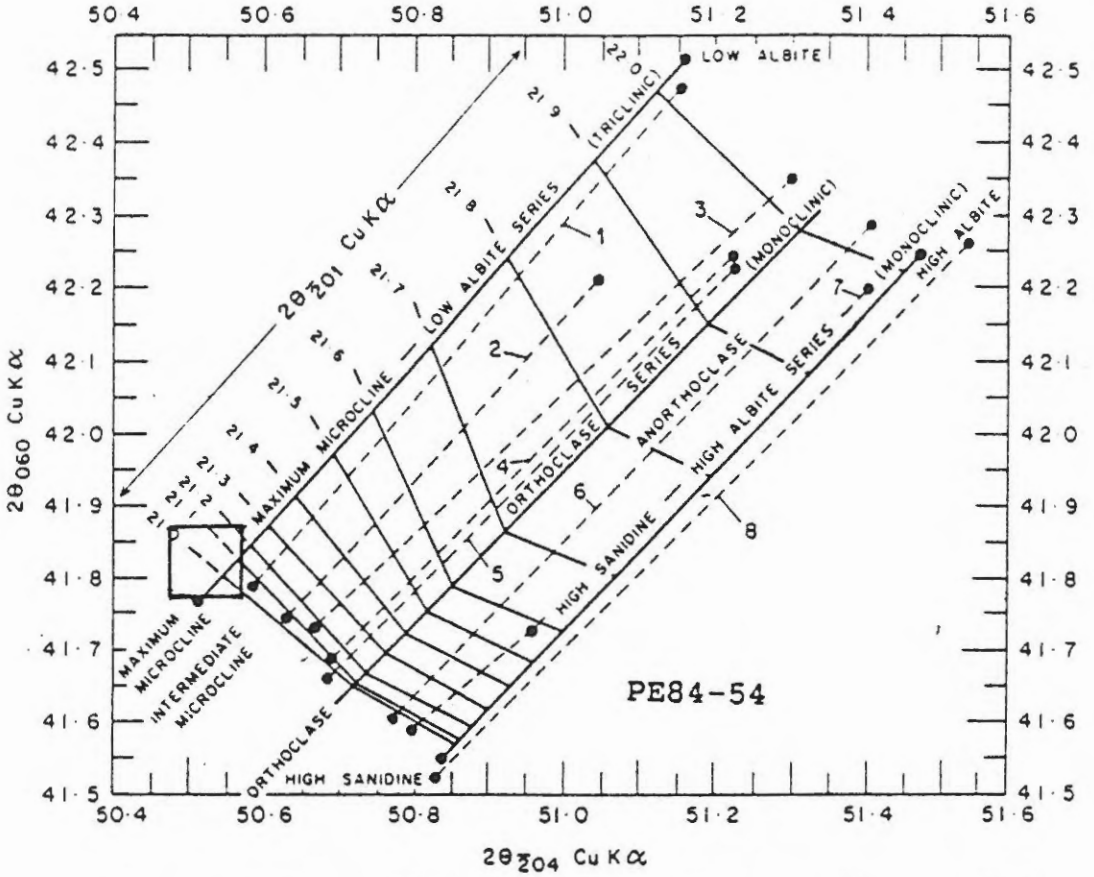
50·4
50·6
50·8
51·0
51·2
51·4
51·6
42·5
42·4
42·3
42·2
42·1
42·0
41·9
41·8
41·7
41·6
41·5
LOW ALBITE
(TRICLINIC)
LOW ALBITE SERIES
MAXIMUM MICROCLINE
ORTHOCLASE SERIES
ANORTHOCLASE
HIGH ALBITE SERIES
HIGH SANIDINE
(MONOCLINIC)
(MONOCLINIC)
HIGH ALBITE
MAXIMUM MICROCLINE
INTERMEDIATE MICROCLINE
ORTHOCLASE
HIGH SANIDINE
PE84-54
$2\theta_{\bar{2}01}$ Cu Kα
$2\theta_{060}$ Cu Kα
$2\theta_{\bar{2}04}$ Cu Kα

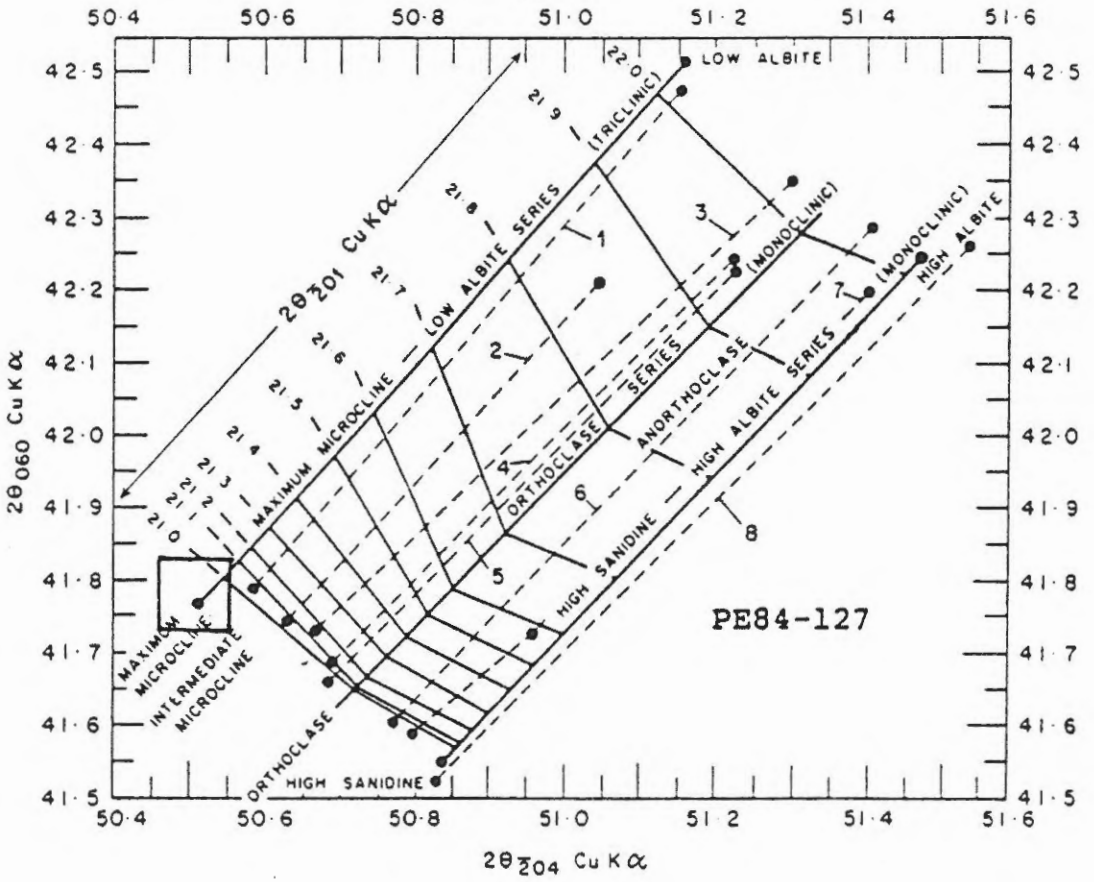
50·4
50·6
50·8
51·0
51·2
51·4
51·6
42·5
42·4
42·3
42·2
42·1
42·0
41·9
41·8
41·7
41·6
41·5
LOW ALBITE
(TRICLINIC)
LOW ALBITE SERIES
MAXIMUM MICROCLINE
ORTHOCLASE SERIES
ANORTHOCLASE
HIGH ALBITE SERIES
HIGH SANIDINE
(MONOCLINIC)
(MONOCLINIC)
HIGH ALBITE
MAXIMUM MICROCLINE
INTERMEDIATE MICROCLINE
ORTHOCLASE
HIGH SANIDINE
PE84-127
$2\theta_{\bar{2}01}$ Cu Kα
$2\theta_{060}$ Cu Kα
$2\theta_{\bar{2}04}$ Cu Kα

APPENDIX C-2

PETROGRAPHIC SUMMARY OF SAMPLES DATED

The principal NE to NNE foliation in the metamorphic rocks is designated S_2.

SAMPLES FROM THE SSP

PE84-27: Medium-grained equigranular 2-mica monzogranite. Biotite (1mm) extensively chloritized; muscovite (2mm) moderately kinked; feldspars saussuritized, with fractures and deformation twins; strong anastomosing tectonic foliation defined by lenticular quartz, feldspar, and muscovite; brown hematitic staining from alteration.

PE84-28: Medium-grained equigranular two -mica monzogranite. Biotite (1mm) extensively chloritized; muscovite (2mm) moderately kinked; feldspars saussuritized with fractures and deformation twins; Strong anastomosing tectonic foliation defined by lenticular quartz, feldspar and muscovite.

PE84-29: Medium-grained equigranular two-mica monzogranite. Biotite (1mm) extensively chloritized; muscovite (2mm) moderately kinked; feldspars saussuritized, with fractures and deformation twins; strong anastomosing tectonic foliation defined by lenticular quartz, feldspar and muscovite.

PE84-30: Medium-grained equigranular two-mica monzogranite. Biotite (1mm) extensively chloritized; muscovite (2mm) moderately kinked; feldspars saussuritized, with fractures and deformation twins; strong anastomosing tectonic foliation defined by lenticular quartz, feldspar and muscovite.

PE83-9: Medium-grained equigranular hornblende - biotite - tonalite. Hornblende (1.5mm) and biotite (3mm) are fresh. Besides essential quartz and plagioclase, this rock contains accessory apatite, sphene, and epidote. Weak to moderate foliation defined by biotite and hornblende.

PE4-39A: Muscovite Pegmatite. Perthitic microcline with lamellae of albite 0.25-1mm thick; feldspar slightly turbid; muscovite (2cm) slightly kinked; fracture filled by quartz vein.

PE84-39B: Medium-grained equigranular biotite tonalite.

Biotite (1mm), mildly chloritized with minor muscovite overgrowth; Plagioclase moderately saussuritized. Weak foliation defined by biotite.

PE84-114: Medium-grained Hornblende-Biotite tonalite. Hornblende (4mm) with few inclusions of quartz. Biotite (5mm) very slightly chloritized, with minor recrystallization around the edges; partly replaced by sphene and epidote. Plagioclase grains (5mm) very slightly saussuritized. Quartz partly recrystallized, displaying slight undulose extinction. Moderate foliation defined by alignment of biotite and quartz ribbons.

PE84-118: Medium-grained equigranular biotite tonalite. Biotite (1mm) apparently fresh, except for peripheral replacement by minor muscovite, epidote and sphene; peripheral replacement of plagioclase by carbonate, muscovite and epidote; accessory apatite, and zircon. Weak foliation defined by biotite.

PE84-119: Coarse-grained pegmatitic two mica monzogranite. Biotite (2mm) partly overgrown by muscovite. Muscovite (4mm) strongly kinked; feldspar with bent lamellae partly altered to fine muscovite. partly recrystallized quartz ribbons indicate moderate shearing; accessory apatite,and zircon.

PE84-125: Medium-grained biotite-muscovite monzogranite. Muscovite (1mm) kinked and moderately sheared; biotite kinked, sheared and partly chloritized; quartz substantially recrystallized. Plagioclase shows deformation twins and is partly overgrown by muscovite.

PE84-127A: Muscovite pegmatite. Perthitic microcline with patches and streaks of albite 50-200 um wide; muscovite (2cm) slightly wrinkled; fracture filled by quartz vein.

S456: Medium-grained equigranular biotite tonalite. Biotite (1mm) kinked, slightly altered around edges to muscovite, and rutile; plagioclase moderately saussuritized with twin lamellae bent; accessory apatite and zircon. Moderate tectonic foliation defined mainly by biotite and quartz ribbons.

81-BQ-1: Medium-grained biotite-hornblende quartz diorite. Biotite (2mm) in clusters, apparently has replaced hornblende. Accessory apatite, sagenite, sphene and opaque oxide. Minor saussuritization of plagioclase; myrmekitic; no foliation.

81BQ-2: Medium-grained equigranular biotite-hornblende quartz diorite. Biotite (2mm) in clusters, apparently has replaced hornblende. Accessory apatite, rutile, zircon, and opaque oxide. Minor saussuritization of plagioclase; no foliation.

PE84-34: Medium-grained equigranular two-mica monzogranite. Muscovite (1mm) slightly kinked, partly has overgrown biotite (1mm) which is slightly chloritized. Plagioclase mildly saussuritized, microcline appears unaltered. Moderate foliation defined by muscovite and biotite.

PE84-45: Gouge from brittle fault. Weathered granular aggregate (2 - 20 mm) of equigranular medium-grained two-mica granite. Muscovite apparently unaltered; with minor kinking. Biotite completely chloritized, feldspars partly altered to clays.

PE84-46: Muscovite Pegmatite. Perthitic microcline with patches of albite 0.5-1mm thick. Muscovite (2cm) slightly kinked. Very minor alteration of microcline to muscovite.

PE84-53: Medium-grained equigranular 2-mica monzogranite. Muscovite (1mm) slightly kinked; biotite (1mm) fresh, coarse (0.2mm) apatite. No foliation.

PE84-54B: Muscovite pegmatite. Perthitic microcline with albite lamellae 0.5mm thick; muscovite (2cm) slightly wrinkled; fracture filled by quartz vein.

PE84-43B: Medium-grained equigranular biotite tonalite. Biotite (1mm) slightly kinked, slightly chloritized, partly overgrown by secondary muscovite. Accessory sillimanite (possibly xenolithic), apatite, and zircon.

PE82-20P: Muscovite Pegmatite. Muscovite (5mm) strongly kinked. Quartz with strongly sutured grain boundaries; feldspars with deformation twins are slightly turbid.

SAMPLES FROM THE SMB

NS-231: Coarse-grained porphyritic biotite granodiorite. Biotite (5 mm), slightly chloritized; plagioclase saussuritized. K-feldspar perthitic, up to 1 cm long. Accessory muscovite, apatite and iron oxides.

PE85-142: Coarse-grained porphyritic biotite monozogranite.

Perthitic microcline (3cm), turbid, partly replaced by muscovite. Plagioclase is strongly saussuritized; biotite is partly chloritized, and cordierite is pinitized. No evidence of deformation. Moderate brown staining from alteration.

PE85-143: Coarse-grained porphyritic biotite granodiorite. Perthitic microcline (3cm), slightly turbid, partly replaced by muscovite. Plagioclase is strongly saussuritized and biotite is partly chloritized and partly recrystallized. Garnet and sphene are secondary minerals. No evidence of deformation. Minor brown (hematitic) staining from alteration.

PE85-144: Coarse-grained porphyritic biotite monzogranite. Perthitic K-feldspar (3cm), turbid, partly replaced by muscovite. Plagioclase is strongly saussuritized, biotite is partly chloritized and cordierite is pinitized. No evidence of deformation. Moderate brown staining from alteration.

PE85-150: Medium-grained porphyritic monzogranite. Plagioclase extensively saussuritized. Biotite extensively replaced by chlorite, sphene and muscovite. K-feldspar partly replaced by muscovite. Accessory zircon and apatite.

PE85-151: Coarse-grained porphyritic biotite monzogranite. Perthitic K-feldspar (3cm), turbid, partly replaced by muscovite. Plagioclase is strongly saussuritized; biotite is partly chloritized, cordierite is pinitized and andalusite is partly replaced by muscovite. No evidence of deformation.

SAMPLES FROM THE RMT

PE82-1: Biotite schist. Poikiloblastic partly chloritized biotite (0.3mm) with quartz inclusions, has overgrown S_2; lepidoblastic muscovite (0.03mm) forms the matrix with quartz and chlorite.

PE82-4: Biotite schist. Poikiloblastic biotite (0.3mm), with quartz inclusions has overgrown S_2; matrix of fine muscovite and quartz define foliation. Biotite shows no internal strain.

PE82-5: Biotite Schist. Poikiloblastic biotite (0.3mm) with quartz inclusions, has overgrown S_2. Matrix

consists of fine muscovite and quartz, which define the foliation. Biotite shows no internal strain.

PE82-20N: Biotite-cordierite-sillimanite metapelite. Poikiloblastic decussate biotite (2.5mm) with quartz inclusions, has overgrown S_2, which is weakly defined by muscovite and fine biotite. Mineral assemblage also include plagioclase, tourmaline, and garnet. Biotite is slightly kinked and partly recrystallized.

PE82-22: Biotite-andalusite-cordierite metapelite. Poikiloblastic decussate biotite (1mm) with quartz inclusions; decussate muscovite (1mm) with quartz inclusions; cordierite partly pinitized; garnet, plagioclase and minor tourmaline also present. Porphyroblasts have overgrown S_2, which is weakly defined by fine biotite and muscovite. Moderate shearing resulting in partial granulation of andalusite, and kinking of micas. Matrix of fine muscovite and granoblastic quartz. Biotite moderately kinked.

PE83-2: Biotite-garnet schist. Poikiloblastic biotite (2mm) with few quartz inclusions, has overgrown S_2, which is defined by fine muscovite and quartz. Moderately sheared, with rotation, kinking, and breaking of biotite porphyroblasts. Chlorite porphyroblasts have overgrown the shear fabric. Biotite moderately kinked. Matrix of quartz, muscovite and sericitized plagioclase.

PE83-4: Biotite-garnet schist. Slightly chloritized, poikiloblastic biotite (1.5mm), with quartz inclusions, has overgrown S_2. Moderate Kinking of biotite; matrix of muscovite and quartz define poor foliation.

PE84-64C: Metabasite. Poikiloblastic hornblende, with inclusions of quartz and opaque oxides. Matrix with quartz, muscovite and saussuritized plagioclase. Strong foliation defined by parallel alignment of hornblende.

PE84-64D: Garnet-mica schist. Biotite (1mm) fresh, with few inclusions of quartz and opaque oxides; Biotite sheared into fish structures with long tails. Strong foliation defined by parallel alignment of muscovite, lenticular quartz, and biotite. Garnet with inclusion trails, some of which are sigmoidal and apparently continuous with the external foliation. Very minor chlorite overgrows foliation.

Biotite shows no internal strain.

PE84-72: Biotite schist. Biotite (0.5mm) moderately altered to an aggregate of quartz, chlorite and rutile. Biotite overgrows S_2, defined by fine muscovite and quartz. A later foliation crenulates S_2, causing rotation and minor kinking of biotite crystals.

PE84-76: Garnet-mica-schist. Decussate biotite (0.5mm), strongly kinked, has overgrown S_2, and is set in matrix of muscovite and quartz. Later overgrowth of chlorite porphyroblasts (1mm).

PE84-78: Biotite schist. Biotite (0.5mm) with minor peripheral chloritization. S_2 wraps around biotite porphyroblasts, which show little internal strain. Few biotite porphyroblasts rotated. S_2 defined by fine muscovite and quartz.

PE84-97: Massive Peridotite. Phlogopite (5mm), has overgrown orthopyroxene; olivine slightly serpentinised. No sign of deformation.

PE84-100: Biotite semipelite. Biotite porphyroblasts (0.2mm), with few quartz inclusions, has overgrown S_2, defined by fine muscovite and quartz. Biotite shows no internal strain. Matrix consists of fine muscovite, quartz, feldspar and epidote.

PE84-108: Biotite metapelite. Poikiloblastic biotite (0.5mm) with quartz inclusions. S_2, defined by fine muscovite and quartz wraps around biotite porphyroblasts, which show no internal strain; matrix of muscovite, quartz and opaque oxides.

PE85-161: Biotite-garnet-staurolite schist. Biotite (.5mm) sheared, forming 'fish' structures. Garnets and staurolite with inclusion trails, some of which are sigmoidal and apparently continuous with the external foliation. Strong foliation defined by biotite, fine muscovite, and lenticular quartz aggregates. Staurolite partly replaced by muscovite and chlorite, which appear undeformed. Biotite shows no internal strain.

PE85-162: Biotite-garnet schist. Biotite (.5mm) sheared, forming 'fish' structures. Garnets with inclusion trails, some of which are sigmoidal and continuous with the external foliation. Strong foliation defined by biotite, fine muscovite and quartz ribbons. Very minor chlorite overgrows foliation. Biotite shows no internal strain.

MC-1: Gabbronorite. Fresh biotite (2mm) has replaced pyroxene. Plagioclase overgrown by fibrolite. No sign of deformation except for minor bending of plagioclase twin lamellae. Biotite unaltered.

PE82-2: Biotite Schist. Inclusion free, fresh biotite (.3mm), sheared into elongate fish structures; partly recrystallized. Strong fabric defined by biotite, fine muscovite, and lenticular quartz. No visible alteration. Biotite shows no internal strain.

PE83-5: Biotite-andalusite-staurolite-schist. Biotite (1mm), staurolite, andalusite, and garnet have overgrown S_2, weakly defined by fine muscovite and quartz. Mild overgrowth of chlorite and muscovite. Biotite shows minor kinking.

PE83-7: Biotite-muscovite schist (migmatitic). Biotite (3mm), with few quartz inclusions, strongly kinked, broken, and rotated by shearing; plagioclase granulated and saussuritized. Plagioclase and biotite replaced by chlorite and coarse muscovite, which have overgrown the shear fabric, with minor crenulation.

PE82-8: Biotite schist. Poikiloblastic biotite (0.8mm) with quartz inclusions; moderately sheared; S_2 wraps around biotite porphyroblasts; biotite mildly kinked; matrix consists of muscovite, quartz and chlorite.

PE82-9: Biotite schist. Biotite (0.25mm) very slightly chloritized. Minor crenulation of biotite which overgrows S_2, defined by fine muscovite and quartz. Very minor chloritization of biotite, which is mildly kinked.

PE82-10: Micaceous psammite. Biotite (0.3mm) defining weak foliation (S_2); biotite free of inclusions and very slightly chloritized. Other minerals are quartz, feldspar, muscovite, epidote and opaque oxides. Biotite very mildly kinked.

PE83-10: Biotite-cordierite schist. Porphyroblasts of biotite (1mm), with few quartz inclusions has overgrown S_2; moderate kinking and rotation of biotite porphyroblasts; peripheral chloritization of biotite. Cordierite and opaque oxide have overgrown a matrix of muscovite quartz and chlorite.

PE83-11: Metabasite. Poikiloblastic hornblende (1cm), moderately aligned, defining S_2. Poikiloblastic

biotite (2mm), has overgrown S_2; recrystallized after brittle deformation. Both with inclusions of opaque oxide and quartz. Carbonate porphyroblasts have overgrown a matrix of chlorite, quartz, rare plagioclase and opaque oxide.

PE83-12: Biotite schist. Biotite (0.2mm) has overgrown S_2, defined by fine muscovite, quartz and chlorite. Very minor alteration of biotite to chlorite. Minor kinking of biotite.

PE82-14: Muscovite-biotite schist. Muscovite (0.5mm) defining strong foliation; biotite strongly sheared into fish structures; partly replaced by muscovite and chlorite; quartz, plagioclase, and tourmaline are also present and parallel to the foliation.

PE82-17: Biotite schist. Inclusion-free biotite (1mm) moderately sheared into fish structures, and substantially chloritized. Foliation defined by biotite, fine muscovite and lenticular quartz. Biotite slightly kinked.

PE82-18: Biotite-staurolite-cordierite metapelite. Poikliloblastic biotite (3mm) with quartz inclusions, strongly kinked, mildly chloritized, has overgrown S_2. Staurolite, cordierite, and garnet have overgrown a matrix of quartz and muscovite. In outcrop, this rock grades from a granofels to a schist.

PE82-19: Biotite-staurolite-cordierite-garnet metapelite. Poikiloblastic biotite (3mm) with inclusions of quartz; biotite strongly kinked, mildly chloritized; staurolite partly replaced by chlorite and muscovite. Porphyroblasts have overgrown S_2, which is weakly defined by fine muscovite and quartz.

PE82-21: Biotite-andalusite-garnet metapelite. Decussate biotite (2mm), and muscovite (2mm), partly enclosed within andalusite have overgrown S_2. Micas poikiloblastic with inclusions of quartz. S_2 defined by fine muscovite, biotite, and lenticular quartz. Strong kinking of micas, moderate chloritization of biotite.

PE84-33: Cordierite-garnet metapelite. Poikiloblastic biotite (1mm) with quartz inclusions, has overgrown S_2, which is weakly defined by fine biotite. Cordierite partly replaced by muscovite and rosettes of chlorite. Biotite shows no internal strain, partly recrystallized.

PE84-41: Biotite-andalusite-garnet-sillimanite metapelite. Poikiloblastic biotite (1mm) with quartz inclusions, partly enclosed by andalusite; biotite partly recrystallized and moderately kinked. Fibrolite partly rims andalusite. Inclusion trails within andalusite discordant with external foliation. Strong shearing, forming augen of andalusite enclosed by biotite.

PE84-65: (No TS) Muscovite-chlorite vein. Muscovite (5mm) intergrown with chlorite. Post tectonic vein cuts main foliation (S_2) in White Rock Formation metabasite.

PE84-77: Garnet-mica schist. Lepidoblastic biotite (0.5mm) and muscovite (0.25mm). Micas free of inclusions, partly overgrown by chlorite rosettes. Biotite moderately kinked.

PE84-121: Biotite-sillimanite schist. Biotite (2mm) strongly kinked, sheared and chloritized. Muscovite (1cm), has partly replaced staurolite and biotite. Matrix of quartz and fine muscovite is crenulated.

PE84-129: Migmatite lens. Muscovite (1cm) strongly kinked; graphic texture; andalusite, fibrolitic sillimanite and plagioclase are the other minerals.

PE84-130: Metabasite. Nematoblastic, poikiloblastic amphibole (4mm) with inclusions of quartz, epidote and opaque oxides; matrix consists of quartz, biotite, epidote, chlorite, plagioclase and opaque oxides. Chlorite partly overgrows amphibole.

NS71-139: Slate. White mica (10-30um) with frayed edges, defining weak foliation . Quartz , chlorite, albite and opaque oxides constitute the remaining mineralogy; mica/quartz=2.

NS72-31: Slate. White mica (10-30um) with frayed edges defining single foliation. Quartz, chlorite, albite and opaque oxides constitute the remaining mineralogy; mica/quartz=3.

NS72-33: Slate. White mica (10-30um) with frayed edges defining single foliation. Quartz, chlorite, albite and opaque oxides constitute the remaining mineralogy; mica/quartz=3.

..KB-1: Slate. White mica (10-50um) with rectangular edges defining single foliation. Other minerals are quartz, chlorite, tourmaline and opaque oxides;

mica/quartz=1.

..KB-3: Laminated metasiltstone. White mica (10-60um) with rectangular edges define weak foliation. Other minerals are quartz, chlorite, albite and opaque oxides; mica/quartz=0.7.

..KB-6: Metasiltstone. White mica (20-80um) with rectangular edges define single weak foliation. Other minerals are quartz, chlorite and opaque oxides; mica/quartz=0.07.

PE85-137: Slate. White mica (10-30um) with frayed edges defining single foliation. Quartz, albite, chlorite and opaque oxides constitute the rest of the rock; mica/quartz=3.

PE85-138: Slate. White mica (10-90um) with frayed edges. Consists of quartz-rich and mica-rich domains, with overall mica/quartz=3. Strong crenulation fabric superimposed on original slately cleavage; chlorite, albite and opaque oxides are the other minerals.

REFERENCES

Abramov, V. A., Brandt, S. B., and Anfilogov, V. N. 1972. Kinetics of homogenization of microcline perthite between 400 and 1000 degrees C. Doklady Akademii Nauk SSSR, 202, pp. 166-168.

Albarede, F. 1978. The recovery of spatial isotope distributions from stepwise degassing data. Earth and Planetary Science Letters 39, pp. 387-397.

Aleinikoff, J. N., Moench, R. H., and Lyons, J. B. 1985. Carboniferous U-Pb age of the Sebago batholith, southwestern Maine: metamorphic and tectonic implications. Geological Society of America Bulletin, 96, pp. 990-996.

Alexander, E. C., Jr., Michelson, G. M., and Lanphere, M. A. 1978. MMhb-1: A new $^{40}Ar/^{39}Ar$ dating standard. Short Paper, 4th international conference on geochronology and cosmochronology, Isotope Geology. United States Geological Survey Open-File Report 78-701, pp. 6-8.

Arthaud, F., and Matte, P. 1977. Late Paleozoic strike-slip faulting in southern Europe and northern Africa: result of right-lateral shear zone between the Appalachians and the Urals. Geological Society of America Bulletin, 88, pp. 1305-1320.

Bailey, D. K. 1983. The chemical and thermal evolution of rifts. Tectonophysics, 94, pp. 585-597.

Bailey, L. W. 1898. Report on the geology of southwest Nova Scotia. Geological Survey of Canada Annual Report, IX, part M.

Bedard, J. H. 1985. The opening of the Atlantic, the Mesozoic New England igneous Province and mechanisms of Continental breakup. Tectonophysics, 113, pp. 209-232.

Bell, K., and Blenkinsop, J. 1977. Geochronological evidence of Hercynian activity in Newfoundland. Nature 265, pp. 616-618.

Bell, K., Blenkinsop, J., Berger, A. R., and Jayasinghe, N. R. 1979. The Newport granite: its age, geological setting, and implications for the geology of northeastern Newfoundland. Canadian Journal of Earth Sciences 16, No. 2, pp. 264-269.

Bell, K., Blenkinsop, J., and Strong, D. F. 1977. The geochronology of some granite bodies from eastern Newfoundland and its bearing on Appalachian evolution. Canadian Journal of Earth Sciences, 14, pp. 456-476.

Belt, E. S. 1968. Post-Acadian rifts and related facies, Eastern Canada. In STUDIES OF APPALACHIAN GEOLOGY: NORTHERN AND MARITIME. Ed. E-An Zen, W. S. White, J. B. Bradley, and J. B. Thompson, Jr., pp. 95-139.

Berger, G. W. 1975. $^{40}Ar/^{39}Ar$ step heating of thermally overprinted biotite, hornblende and potassium feldspar from Eldorado, Colorado. Earth and Planetary Science Letters, 26, pp. 387-408.

Berger, G. W., York, D., Buchan, K. L., and Dunlop, D. J. 1978. $^{40}Ar/^{39}Ar$ dating of Grenville paleopoles. Canadian Geophysical Union, Program with Abstracts, Fifth Annual Meeting, p. 41.

Berger, G. W., and York, D. 1981. Geothermometry from $^{40}Ar/^{39}Ar$ dating experiments. Geochimica et Cosmochimica Acta 45 pp. 795-811.

Bird, J. M. and Dewey, J. F. 1970. Lithosphere plate continental margin tectonics and the evolution of the Appalachian orogen. Geological Society of America Bulletin, 81, pp. 1031-1060.

Boucot, A. J. 1960. Implications of Lower Devonian brachiopods from Nova Scotia. International Geological Congress Report, Twenty-first session, part xii, pp. 129-137.

Boucot, A. J. 1968. Silurian and Devonian of the northern Appalachians. In STUDIES OF APPALACHIAN GEOLOGY: NORTHERN AND MARITIME, ed. E. Zen, W. S. White, J. B. Hadley, and J. B. Thompson, Jr. Interscience, pp. 83-94.

Bradbury, H. J. and Nolen-Hoeksema, R. C. 1985. The Lepontine Alps as an evolving metamorphic core complex during A-type subduction: evidence from heat flow, mineral cooling ages, and tectonic modelling. Tectonics, 4, pp. 187-211.

Bradley, D. C. 1982. Subsidence in Late Paleozoic Basins in the northern Appalachians. Tectonics, 1, pp. 107-123.

Brandt, S. B., and Voronovskiy, S. N. 1967. Dehydration and diffusion of radiogenic argon in micas.

International Geology Review, 9, pp. 1504-1507.

Brereton, N. R. 1970. Corrections for interfering isotopes in the $^{40}Ar/^{39}Ar$ method. Earth and Planetary Science Letters, 8, pp. 427-433.

Brereton, N. R. 1972. A reappraisal of the $^{40}Ar/^{39}Ar$ stepwise degassing technique. Royal Astronomical Society Geophysical Journal, 27, pp. 449-478.

Brown, D. E. (in press). The Bay of Fundy: Thin-skinned tectonics and resultant Early Mesozoic sedimentation. In EASTERN CANADA BASINS AND WORLDWIDE ANALOGUES, symposium volume. Ed. C. Beaumont and A. J. Tankard.

Butler, J. R. 1973. Paleozoic deformation and metamorphism in part of the Blue Ridge thrust sheet, North Carolina. American Journal of Science, 273-A, pp. 72-88.

Calder, L. M., and Barr, S. M. 1982. Petrology of the Mavillette Intrusion, Digby County, Nova Scotia. Maritime Sediments and Atlantic Geology, 18, pp. 29-40.

Carslaw, H. S., and Jaeger, J. C. 1959. CONDUCTION OF HEAT IN SOLIDS. Oxford Clarendon Press, 510 pp.

Chatterjee, A. K., and Keppie, J. D. Polymetallic mineralization in the endo- and exo-contact of the Wedgeport pluton, Yarmouth County. Nova Scotia Dept of Mines and Energy, Report 81-1, pp. 43-46.

Chu, P. 1978. Metamorphism of the Meguma Group in the Shelburne area, Nova Scotia. Unpublished MSc thesis, Acadia University, Wolfville, Nova Scotia, 206 pp.

Clarke, D. B., and Halliday, A. N. 1980. Strontium Isotope geology of the South Mountain batholith, Nova Scotia. Geochimica et Cosmochimica Acta, 44, pp. 1045-1058.

Clarke, D. B., and Halliday, A. N. 1985. Sm/Nd isotopic investigation of the age and origin of the Meguma Zone metasedimentary rocks. Canadian Journal of Earth Sciences, 22, pp. 102-107.

Clarke, D. B., and Muecke, G. K. 1980. Trip 21: Igneous and metamorphic geology of southern Nova Scotia. GAC-MAC Field Trip Guidebook, 101 pp.

Clarke, D. B., and Muecke, G. K. 1985. Review of the

petrochemistry and origin of the South Mountain Batholith and associated plutons, Nova Scotia, Canada. In HIGH HEAT PRODUCTION GRANITES, HYDROTHERMAL CIRCULATION AND ORE GENESIS. Institute of Mining and Metallurgy, London, pp. 41-54.

Cliff, R. A. 1985. Isotopic dating in metamorphic belts. Journal of the Geological Society of London, 142, pp. 97-110.

Cormier, R. F., and Smith, T. E. 1973. Radiometric ages of granitic rocks, southwestern Nova Scotia. Canadian Journal of Earth Sciences, 10, pp. 1201-1210.

Crank, J. 1957. THE MATHEMATICS OF DIFFUSION. Oxford University Press, Oxford, 414 pp.

Criss, R. E., Lanphere, M. A., and Taylor, H. P. Jr. 1982. Effects of regional uplift, deformation, and meteoric-hydrothermal metamorphism on K-Ar ages of biotites in the southern half of the Idaho Batholith. Journal of Geophysical Research, 87, pp. 7029-7046.

Crosby, D. G. 1962. Wolfville map area, Nova Scotia (21 H 1). Geological Survey of Canada, Memoir 325, 67 pp.

Cullen, J. D. 1983. Metamorphic petrology and geochemistry of the Goldenville Formation metasediments, Yarmouth, Nova Scotia. Unpublished MSc Thesis, Dalhousie University, Halifax, Nova Scotia, 241 pp.

Cumming, L. M. 1985. A Halifax slate graptolite locality, Nova Scotia; in Current Research, Part A, Geological Survey of Canada, Paper 85-1A, pp. 215-221.

Currie, K. L. 1977. A note on post-Mississippian thrust faulting in northwestern Cape Breton Island. Canadian Journal of Earth Sciences, 14, pp. 2973-2941.

Dallmeyer, R. D. 1975. $^{40}Ar/^{39}Ar$ ages of biotite and hornblende from a progressively remetamorphosed basement terrane: their bearing on interpretation of release spectra. Geochimica et Cosmochimica Acta, 39, pp. 1655-1669.

Dallmeyer, R. D. 1978. $^{40}Ar/^{39}Ar$ incremental-release ages of hornblende and biotite across the Georgia Inner Piedmont: Their bearing on Late Paleozoic-Early Mesozoic tectonothermal history. American Journal of Science, 278, pp. 214-238.

Dallmeyer, R. D. 1979. $^{40}Ar/^{39}Ar$ Dating: principles,

techniques and applications in orogenic terranes. In LECTURES IN ISOTOPE GEOLOGY, ed. E. Jager and J. C. Hunziker, Springer-Verlag, pp. 77-104.

Dallmeyer, R. D. 1982. $^{40}Ar/^{39}Ar$ incremental-release ages of biotite from a progressively remetamorphosed Archean basement terrane in southwestern Labrador. Earth and Planetary Science Letters, 61, pp. 85-96.

Dallmeyer, R. D. 1982. $^{40}Ar/^{39}Ar$ ages from the Narragansett Basin and southern Rhode Island basement terrane: Their bearing on the extent and timimg of Alleghenian tectonothermal events in New England. Geological Society of America Bulletin, 93, pp. 1118-1130.

Dallmeyer, R. D., and Keppie, J. D. 1984. Geochronological constraints on the accretion of the Meguma Terrane with North America. Geological Society of America Abstracts with Programs, Northeastern Section, p 11.

Dallmeyer, R. D., Keppie, J. D. 1986. Polyphase late Paleozoic tectonothermal evolution of the Meguma terrane, Nova Scotia. Geological Society of America Abstracts with Programs, Northeastern Section, pp. 11.

Dallmeyer, R. D., and Rivers, T. 1982. Recognition of extraneous argon components through incremental-release $^{40}Ar/^{39}Ar$ analysis of biotite and hornblende across the Grenville metamorphic gradient in southwestern Labrador. Geochimica et Cosmochimica Acta, 47, pp. 413-428.

Dallmeyer, R. D., Sutter, J. F.,and Baker, D. J. 1975. Incremental $^{40}Ar/^{39}Ar$ ages of biotite and hornblende from the northeastern Reading Prong: Their bearing on late Proterozoic thermal and tectonic history. Geological Society of America Bulletin, 86, pp. 1435-1443.

Dallmeyer, R. D., and VanBreeman, O. 1981. Rb-Sr Whole-Rock and $^{40}Ar/^{39}Ar$ mineral ages of the Togus and Hallowell quartz monzonite and Three Mile Pond granodiorite plutons, south-central Maine: their bearing on post-Acadian cooling history. Contributions to Mineralogy and Petrology, 78, pp. 61-73.

Dallmeyer, R. D., VanBreemen, O., and Whitney, J. A. 1982. Rb-Sr whole-rock and $^{40}Ar-^{39}Ar$ mineral ages of the Hartland stock, south-central Maine: A post-Acadian representative of the New Hampshire Plutonic Series. American Journal of Science, 282, pp. 79-93.

Dalrymple, G. B., Alexander, E. C. Jr., Lanphere, M. A., and Kramer G. P. 1981. Irradiation of samples for $^{40}Ar/^{39}Ar$ dating using the Geological Survey TRIGA reactor. United States Geological Survey Professional Paper 1176.

Dalrymple, G. B., and Lanphere, M. A. 1974. $^{40}Ar/^{39}Ar$ age spectra of some undisturbed terrestrial samples. Geochimica et Cosmochimica Acta, 38, pp. 715-738.

De Albuquerque, C. A. R. 1977. Geochemistry of the tonalitic and granitic rocks of the Nova Scotia southern plutons. Geochimica et Cosmochimica Acta, 41, pp. 1-13.

De Albuquerque, C. A. R. 1979. Origin of the plutonic mafic rocks of southern Nova Scotia. Geological Society of America Bulletin, 90, pp. 719-731.

Del Moro, A., Puxeddu, M., Radicati di Brozolo, F., and Villa, I. M. 1982. Rb-Sr and K-Ar ages on minerals at temperatures of 300-400 ^{o}C from deep wells in the Larderello geothermal field (Italy). Contributions to Mineralogy and Petrology, 81, 340-349.

Dempster, T. J. 1985. Uplift patterns and orogenic evolution in the Scottish Dalradian. Journal of the Geological Society of London, 142, pp. 111-128.

Dempster, T. J., and Harte, B. 1986. Polymetamorphism in the Dalradian of the central Scottish Highlands. Geological Magazine, 123, pp. 95-104.

Dodson, M. H. 1973. Closure temperature in cooling geochronological and petrological systems. Contributions to Mineralogy and Petrology, 40, 259-274.

Dodson, M. H. 1979. Theory of cooling ages. In LECTURES IN ISOTOPE GEOLOGY, ed. E. Jager and J. C. Hunziker, Springer-Verlag, pp. 194-202.

Eggleton, R. A., and Banfield, J. F. 1985. The alteration of granitic biotite to chlorite. American Mineralogist, 70, pp. 902-910.

Ellis, A. J., and Mahon, W. A. J. 1977. CHEMISTRY AND GEOTHERMAL SYSTEMS. Academic Press, New York, 392 pp.

Evernden, J. F., Curtis, G. H., Kistler, R. W., and Obradovich, J. 1960. Argon diffusion in glauconite, microcline, sanidine, leucite, and phlogopite. American Journal of Science, 258, pp. 583-604.

Fairbairn, H. W., Hurley, P. M., Pinson, W. H., and Cormier, R. F. 1960. Age of granitic rocks of Nova Scotia. Geological Society of America Bulletin, 71, pp. 399-419.

Fairbairn, H. W., Hurley, P. M., and Pinson, W. H. 1964. Preliminary age study and initial $^{87}Sr/^{86}Sr$ of Nova Scotia granitic rocks by the Rb-Sr whole rock method; Geological Society of America Bulletin, 75, pp. 253-258.

Faribault, E. R. 1908. Lunenburg County, Nova Scotia; Geological Survey of Canada Summary Report, pp. 78-83.

Faribault, E. R. 1910. Gold-bearing series of LaHave Basin, Lunenburg County, Nova Scotia; Geological Survey of Canada Summary Report, p 253.

Faribault, E. R. 1912. Gold-bearing series of Medway River, Nova Scotia. Geological Survey of Canada Summary Report, pp. 339-340.

Faribault, E. R. 1914. Geology of the Port Mouton Map Area, Queen's County Nova Scotia; Geological Survey of Canada Summary Report, pp. 251-258.

Faribault, E. R., Armstrong, P., and Wilson, J. T. 1938a. Malaga Lake sheet (East Half), Queen's and Lunenburg counties, Nova Scotia; Geological Survey of Canada, Map 435A.

Faribault, E. R., Armstrong, P., and Wilson, J. T. 1938b. Malaga Lake sheet (West Half), Queen's and Lunenburg counties, Nova Scotia; Geological Survey of Canada, Map 436A.

Fechtig, H., and Kalbitzer, S. 1966. The diffusion of argon in potassium-bearing solids. In POTASSIUM-ARGON DATING, ed. O. A. Schaeffer, and J. Zahringer, pp. 68-107. Berlin: Springer-Verlag. 234 pp.

Ferry, J. M. 1985. Hydrothermal alteration of Tertiary igneous rocks from the Isle of Skye, northwest Scotland. Contributions to Mineralogy and Petrology, 91, pp. 283-304.

Fitch, F. J., Miller, J. A., and Mitchell, J. G. 1969. A new approach to radio isotopic dating in orogenic belts. In TIME AND PLACE IN OROGENY, ed. P. E. Kent, G. E. Satterthwaite and A. M. Spencer. Geological Society of London Special Publication No. 3, pp. 157-195.

Fleck, R. D., Sutter, J. F., and Elliot, E. 1977. Interpretation of discordant $^{40}Ar/^{39}Ar$ age spectra of Mesozoic tholeiites from Antarctica. Geochimica et Cosmochimica Acta, 41, pp. 15-32.

Fleischer, R. L., Price, P. B., and Walker, R. M. 1975. NUCLEAR TRACKS IN SOLIDS: PRINCIPLES AND APPLICATIONS. University of California Press, Berkeley, California, 605 pp.

Foland, K. A. 1974. ^{40}Ar diffusion in homogeneous orthoclase and an interpretation of Ar diffusion in K-feldspars. Geochimica et Cosmochimica Acta, 38, pp. 151-168.

Foland, K. A. 1983. $^{40}Ar/^{39}Ar$ Incremental heating plateaus for biotites with excess argon. Isotope Geoscience, 1, pp. 3-21.

Foland, K. A. and Faul, H. 1977. Ages of the White Mountain intrusives - New Hampshire, Vermont, and Maine, U. S. A. American Journal of Science, 277, pp. 888-904.

Fralick, P. W. and Schenk, P. E. 1981. Molasse deposition and basin evolution in a wrench tectonic setting: the Late Paleozoic, eastern Cumberland Basin, Maritime Canada. In SEDIMENTATION AND TECTONICS IN ALLUVIAL BASINS, ed. A. D. Miall, Geological Association of Canada, Special Paper, 23, pp. 77-97.

Fullager, P. D., and Butler, J. R. 1979. 325 to 265 m.y. old granitic plutons in the Piedmont of the southeastern Appalachians. American Journal of Science, 279, pp. 161-185

Fyffe, L. R., Pajari, G. E. Jr., and Cherry, M. E. 1981. The Acadian plutonic rocks of New Brunswick. Maritime Sediments and Atlantic Geology, 17, pp. 23-36.

Fyson, W. K. 1966. Structures in the Lower Paleozoic Meguma Group, Nova Scotia. Geological Society of America Bulletin, 77, pp. 931-944.

Fyson, W. K. 1967. Gravity sliding and cross-folding in Carboniferous rocks, Nova Scotia. American Journal of Science, 265, pp. 1-11.

Gates, A. E., Simpson, C., and Glover, L., III. 1986. Appalachian Carboniferous dextral strike-slip faults: an example from Brookneal, Virginia. Tectonics, 5, pp. 119-133.

Gerling, E. K., Kol'tsova, T. V., Petrov, B. V., and Zul'fikarova, Z. K. 1965. On the suitability of amphiboles for age determination by the K-Ar method. Geokhimiya, no. 2, pp. 219-226.

Gerling, E. K., Levskii, L. K., and Morozova, I. M. 1963. On the diffusion of radiogenic argon from minerals. Geokhimiya, no. 6, pp. 539-543.

Gerling, E, K., Petrov, B. V., and Kol'tsova, T. V. 1966. A comparative study of the activation energy of argon liberation and dehydration energy in amphiboles and biotites. Geokhimiya, no. 4, pp. 379-389.

Gerling, E. K. 1984. Remiminiscences about some works connected with the study of noble gases, their isotopic composition and Geochronology. Isotope Geoscience, 2, pp. 271-289.

Gibling, M. R., Boehner, R. C., and Rust, B. R. (in press). The Sydney Basin of Atlantic Canada: an Upper Paleozoic extensional basin in a strike-slip setting. In EASTERN CANADA BASINS AND WORLDWIDE ANALOGUES, symposium volume. Ed. C. Beaumont and A. J. Tankard.

Giles, P. S. 1981. Major transgressive-regressive cycles in Middle to Late Visean rocks of Nova Scotia. Nova Scotia Department of Mines and Energy, Paper 81-2, 27 pp.

Giles, P. S. 1985. A major post-Visean sinistral shear zone-new perspectives on Devonian and Carboniferous rocks of southern Nova Scotia; in Guide to the granites and mineral deposits of southwestern Nova Scotia, ed. A. K. Chatterjee and D. B. Clarke; Nova Scotia Department of Mines and Energy, Paper 85-3.

Giletti, B. J. 1974. Diffusion related to geochronology. In GEOCHEMICAL TRANSPORT AND KINETICS, ed. A. W. Hofmann, B. J. Giletti, H. S. Yoder Jr., and R. A. Yund. pp. 61-76. Carnegie Institution, Washington. 353 pp.

Gleadow, A. J. W. 1981. Fission track dating: what are the real alternatives? Nuclear Tracks, 5, pp. 3-14.

Gleadow, A. J. W., and Duddy, I. R. 1981. A long-term track annealing experiment for apatite. Nuclear Tracks, 5, pp. 169-174.

Glover, L. III, Speer, J. A., Russell, G. S., and Farrar, S. S. 1983. Ages of regional metamorphism and

ductile deformation in the central and southern Appalachians. Lithos, 16, pp. 223-245.

Grist, A. 1986. Low-temperature geochronology of the South Mountain Batholith, Nova Scotia, using $^{40}Ar/^{39}Ar$ and fission track dating techniques. Unpublished BSc thesis, Dalhousie University, Halifax, Nova Scotia, 70 pp.

Hammerschmidt, Von K., and Wagner, H. 1983. K/Ar determination on biotites from the crystalline rocks of the research drilling project Urach III. Neues Jahrbuch fur Mineralogie Monatschefte, pp. 35-48.

Hanson, G. N., and Gast, P. W. 1967. Kinetic studies in contact metamorphic zones. Geochimica et Cosmochimica Acta, 31, pp. 1119-1153.

Hanson, G. N., Simmons, K. R., and Bence, A. E. 1975. $^{40}Ar/^{39}Ar$ spectrum ages for biotite, hornblende and muscovite in a contact metamorphic zone. Geochimica et Cosmochimica Acta, 39, pp. 1269-1277.

Harrison, T. M. 1981. Diffusion of ^{40}Ar in hornblende. Contributions to Mineralogy and Petrology, 78, pp. 324-331.

Harrison, T. M. 1983. Some observations on the interpretation of $^{40}Ar/^{39}Ar$ age spectra. Isotope Geoscience, 1, pp. 319-338.

Harrison, T. M. 1984. A reassessment of fission track annealing behavior in apatite. The Fourth International Fission Track Dating Workshop, Troy, New York.

Harrison, T. M., and Be, K. 1983. $^{40}Ar/^{39}Ar$ Age spectrum analyses of detrital microclines from the southern San Joaquin Basin, California: An approach to determining the thermal evolution of sedimentary basins. Earth and Planetary Science Letters, 64, pp. 244-256.

Harrison, T. M., Duncan, I. J., and McDougall, I. 1985. Diffusion of ^{40}Ar in biotite: temperature, pressure and compositional effects. Geochimica et Cosmochimica Acta, 49, pp. 2461-2468.

Harrison, T. M., and Fitzgerald, J. D. 1986. Exsolution in hornblende and its consequences for $^{40}Ar/^{39}Ar$ age spectra and closure temperature. Geochimica et Cosmochimica Acta, 50, pp. 247-253.

Harrison, T. M., and McDougall, I. 1980a. Investigations

of an intrusive contact, northwest Nelson, New Zealand-I. Thermal, chronological and Isotopic constraints. Geochimica et Cosmochimica Acta, 44, pp. 1985-2004.

Harrison, T. M., and McDougall, I. 1980b. Investigations of an intrusive contact, northwest Nelson, New Zealand-II: Diffusion of radiogenic and excess ^{40}Ar in hornblende revealed by $^{40}Ar/^{39}Ar$ age spectrum analysis. Geochimica et Cosmochimica Acta, 44, pp. 2005-2020.

Harrison, T. M., and McDougall, I. 1982. The thermal significance of potassium feldspar. K-Ar ages inferred from $^{40}Ar/^{39}Ar$ age spectrum. Geochimica et Cosmochimica Acta, 46, 1811-1820.

Hayatsu, A. 1979. K-Ar isochron age of the North Mountain Basalt, Nova Scotia. Canadian Journal of Earth Sciences, 16, pp. 973-975.

Hope, T. L., and Woodend, S. L. 1986. Geological mapping and igneous and metamorphic petrology, Queen's and Shelburne counties, Nova Scotia; in Current Research, Part A, Geological Survey of Canada, Paper 86-1A, pp. 429-433.

Huneke, J. C., and Smith, S. P. 1976. The realities of recoil: ^{39}Ar recoil out of small grains and anomalous patterns in ^{39}Ar-^{40}Ar dating. Proceedings of the 7th Lunar Science Conference, pp. 1987-2008.

Hunziker, J. C., Frey, M., Clauer, N., Dallmeyer, R. D., Friedrichsen H., Flehmig, W., Hochstrasser, K., Roggwiler, P., and Schwander, H. 1986. The evolution of illite to muscovite: mineralogical and isotopic data from the Glarus Alps, Switzerland. Contributions to Mineralogy and Petrology, 92, pp. 157-180.

Hurford, A. J., and Green, P. F. 1982. A user's guide to fission track dating calibration. Earth and Planetary Science Letters, 59, pp. 343-354.

Hurford, A. J., and Green, P. F. 1983. The zeta age calibration of fission track dating. Isotope Geoscience, 1, pp. 285-317.

Hurford, A. J., and Hammerschmidt, K. 1985. $^{40}Ar/^{39}Ar$ and K/Ar dating of the Bishop and Fish Canyon Tuffs: Calibration ages for fission-track dating standards. Chemical Geology (Isotope Geoscience Section), 58, pp. 23-32.

Hutchinson, H. E. 1982. Geology, geochemistry, and

genesis of the Brazil Lake pegmatites, Yarmouth County, Nova Scotia. Unpublished BSc thesis, Dalhousie University, Halifax, Nova Scotia, 95 pp.

Hwang, S. G., and Williams, P. F. 1985. Preliminary geology of the Barrington area, southwest Nova Scotia. Nova Scotia Department of Mines and Energy, Program and Summaries, Ninth Annual Open House and Review of Activities, pp. 115-116.

Irving, E., and Strong, D. F. 1984. Evidence against large-scale Carboniferous strike-slip faulting in the Appalachian-Caledonian orogen. Nature, 310, pp. 762-764.

Jahns, R. H., and Burnham, C. W. 1969. Experimental studies of pegmatite genesis: a model for the derivation and crystallization of granitic pegmatites: Economic Geoloogy, 64, pp. 843-864.

Jansa, L. F. and Pe-Piper, G. 1985. Early Cretaceous volcanism on the northeastern American margin and implications for plate tectonics. Geological Society of America Bulletin, 96, pp. 83-91.

Jayasinghe, N. R., and Berger, A. R. 1976. On the plutonic evolution of the Wesleyville area, Bonavista Bay, Newfoundland. Canadian Journal of Earth Sciences, 13, pp. 1560-1570.

Jellinek, R. 1986. Discovery of Earliest Jurassic reptile assemblages from Nova Scotia imply catastrophic end to the Triassic. Lamont Newsletter, no. 12, Lamont Doherty Geological Observatory, pp. 1-3.

Jost, W. 1960. DIFFUSION IN SOLIDS, LIQUIDS, AND GASES. Academic Press Inc., New York, 558 pp.

Keen, C., and Cordsen, A. 1981. Crustal structure, seismic stratigraphy, and rift processes of the continental margin off eastern Canada: Ocean bottom seismic refraction results off eastern Canada. Canadian Journal of Earth Sciences, 18, pp. 1523-1538.

Keppie, J. D. 1977. Tectonics of southern Nova Scotia. Nova Scotia Department of Mines and Energy, Paper 77-1, 34 pp.

Keppie, J. D. 1982. The Minas Geofracture. In MAJOR STRUCTURAL ZONES AND FAULTS OF THE NORTHERN APPALACHIANS. Ed. P. St. Julien and J. Beland. Geological Association of Canada, Special Paper 24, pp. 263-280.

Keppie, J. D. 1983. Geological history of the Isaacs Harbour area, parts of 11F/3 and 11F/4, Guysborough county, Nova Scotia. Nova Scotia Department of Mines and Energy Report of Activities, 83-1, pp. 109-143.

Keppie, J. D. 1984. Geology of the easternmost Meguma terrane of Nova Scotia, Canada. Nova Scotia Department of Mines and Energy, Report of Activities 84-1, pp. 193-196.

Keppie, J. D, Dallmeyer, R. D., Krogh, T. E., Cormier, R. F., and Halliday, A. N. 1985. Geochronological constraints for mineralization in the easternmost Meguma terrane, Nova Scotia. Nova Scotia Department of Mines and Energy, Program and Summaries, Ninth Annual Open House and Review of Activities, pp. 39-40.

Keppie, J. D., and Muecke, G. K. 1979. Geologic Map of the Province of Nova Scotia. Nova Scotia Department of Mines and Energy, Halifax.

Keppie, J. D., Odom, L., and Cormier, R. F. 1983. Tectonothermal evolution of the Meguma Terrane: radiometric controls. Geological Society of America, Abstracts with Programs, Northeastern Section, p. 136.

Keppie, J. D., and Smith, P. K. 1978. Compilation of isotopic age data of Nova Scotia. Nova Scotia Dapartment of Mines and Energy, Report 78-4.

Klein, G. D. 1962. Triassic sedimentation, Maritime Provinces, Canada. Geological Society of America Bulletin, 73, pp. 1127-1146.

Kulp, J. L., and Eckelmann, F. D. 1960. Potassium-argon isotopic ages on micas from the southern Appalachians. Annals of the New York Academy of Science, 91, pp. 408-419.

Kunk, M. J., Sutter, J. F., and Naeser, C. W. 1985. High-precision $^{40}Ar/^{39}Ar$ ages of sanidine, biotite, hornblende, and plagiclase from the Fish Canyon Tuff, San Juan volcanic field, south central Colorado. Geological Society of America Abstracts with Programs, pp. 636.

Lanphere, M. A., and Dalrymple, G. B. 1971. A test for the $^{40}Ar/^{39}Ar$ age spectrum technique on some terrestrial materials. Earth and Planetary Science Letters, 12, 359-372.

Lanphere, M. A., and Dalrymple, G. B. 1976. Identification of excess ^{40}Ar by the $^{40}Ar/^{39}Ar$ age

spectrum technique. Earth and Planetary Science Letters, 32, pp. 141-148.

Lefort, J. P. and Van der Voo, R. 1981. A kinematic model for the collision and complete suturing between Gondwanaland and Laurussia in the Carboniferous. Journal of Geology, 89, pp. 537-550.

Lewis, A. E. 1984. BIOSTATISTICS. Van Nostrand, 198 pp.

Lister, G. S., and Snoke, A. W. 1984. S-C mylonites. Journal of Structural Geology, 6, pp. 617-638.

Lux, D. R., and Guidotti, C. V. 1985. Evidence for extensive Hercynian metamorphism in western Maine. Geology, 13, pp. 696-700.

Mak, E. K., York, D., Grieve, R. A. F., and Dence, M. R. 1976. The age of the Mistastin Lake crater, Labrador, Canada. Earth and Planetary Science Letters, 31, pp. 345-357.

Mchone, J. G. 1978. Distribution, orientations and ages of mafic dikes in central New England. Geological Society of America Bulletin, 89, 1645-1655.

McKenzie, C. C., and Clarke, D. B. 1975. Petrology of the South Mountain batholith. Canadian Journal of Earth Sciences, 12, pp. 1209-1218.

Merrihue, C. M. 1965. Trace element determinations and potassium-argon dating by mass spectroscopy of neutron-irradiated samples. Transactions of the American Geophysical Union, 46, p. 125.

Merrihue, C. M., and Turner, G. 1966. Potassium-argon dating by activation with fast neutrons. Journal of Geophysical Research, 71, pp. 2852-2857.

Morel, P., and Irving, E. 1978. Tentative paleocontinental maps for the Early Phanerozoic and Proterozoic. Journal of Geology, 86, pp. 535-561.

Mosher, S., and Rast, N. 1984. The deformation and metamorphism of Carboniferous rocks in Maritime Canada and New England. In VARISCAN TECTONICS OF THE NORTH ATLANTIC REGION, ed. D. H. W. Hutton and D. J. Sanderson. Geological Society of London Special Publication, no. 14, pp. 233-243.

Muecke, G. K. 1973. Meguma Group metamorphism - a progress report. Geological Association of Canada, Annual Meeting Newfoundland Section, Abstract.

Muecke, G. K. 1984. Metamorphic evolution of the Meguma terrane, Nova Scotia. Geological Society of America Abstracts with Programs, Northeastern Section, p. 52.

Mussett, A. E. 1969. Diffusion measurements and the potassium-argon method of dating. Royal Astronomical Society Geophysical Journal, 18, pp. 257-303.

Naeser, C. W. 1967. The use of apatite and sphene for fission track age determinations. Geological Society of America Bulletin, 78, pp. 1523-1526.

Naeser, C. W. 1979. Fission track dating and geological annealing of fission tracks; in LECTURES IN ISOTOPE GEOLOGY, ed. E. Jager and J. C. Hunziker, pp. 154-169, Springer-Verlag, New York.

Naeser, C. W., and Forbes, R. B. 1976. Variation of fission track ages with depth in two deep drill holes (abstract). EOS, Transactions of the American Geophysical Union, 57, p. 353.

Nance, D. 1985. Alleghenian deformation in the Mispec group, Saint John Harbour, New Brunswick; in Current Research, Part A, Geological Survey of Canada, Paper 85-1A, pp. 7-13.

Nance, R. D., and Warner, J. B. 1986. Variscan tectonostratigraphy of the Mispec Group, southern New Brunswick: structural geometry and deformation history; in Current Research, Part A, Geological Survey of Canada, Paper 86-1A, pp. 351-358.

Naylor, R. S. 1971. Acadian orogeny: an abrupt and brief event. Science, 172, pp. 558-560.

Nur, A. 1983. Accreted terranes. Reviews of Geophysics and Space Physics 21, pp. 1779-1785.

O'Brien, B. H. 1983. The structure of the Meguma Group between Gegogan Harbour and Country Harbour, Guysborough County, Nova Scotia. Nova Scotia Department of Mines and Energy, Report of Activities 83-1, pp. 145-181.

O'Reilly, G. A. 1976. The petrology of the Brenton Pluton, Yarmouth County, Nova Scotia. Unpublished BSc thesis, Dalhousie University, Halifax, Nova Scotia, 69 pp.

O'Reilly, G. A., Gauthier, G., and Brooks, C. 1985. Three Permo-Carboniferous Rb/Sr age determinations from the South Mountain Batholith, southwestern Nova Scotia.

Nova Scotia Department of Mines and Energy, Report of Activities 85-1, pp. 143-152.

Ozima, M., Kaneoka, I., and Yanagisawa, M. 1979. Temperature and pressure effects on $^{40}Ar/^{39}Ar$ systematics. Earth and Planetary Science Letters, 42, pp. 463-472.

Palmer, A. R. 1983. The decade of North American geology: 1983 geologic time scale. Geology, 11, pp. 503-504.

Pankhurst, R. J., Moorbath, S., Rex, D. C., and Turner, G. 1973. Mineral age patterns in ca. 3700 my old rocks from West Greenland. Earth and Planetary Science Letters, 20, pp. 157-170.

Poole, W. H. 1967. Tectonic evolution of the Appalachian region of Canada. In GEOLOGY OF THE ATLANTIC REGION. Ed. E. R. W. Neale and H. Williams. Geological Association of Canada, Special Paper 4, pp. 9-51.

Poole, W. H. 1971. Graptolites, copper and potassium-argon in Goldenville Formation, Nova Scotia, in Report of activities, part A, Geological Survey of Canada, Paper 71-1A, pp. 9-11.

Poole, W. H. 1970. Plate tectonic evolution of the Canadian Appalachian region. Geological Survey of Canada, Paper 76-1B, pp. 113-126.

Poole, W. H., Sanford, B. V., Williams, H., and Kelly, D. G. 1970. Geology of southeastern Canada. In GEOLOGY AND ECONOMIC MINERALS OF CANADA. Ed. J. W. R. Douglas. Geological Survey of Canada, Economic Geology Report 1, pp. 229-304.

Purdy, J. W., and Jager, E. 1976. K-Ar ages on rock-forming minerals from the Central Alps. Memoir of the Institute of Geology and Mineralogy, University of Padova, Padova, Italy, 30, pp. 1-31.

Rast, N., Kennedy, M. J., and Blackwood, R. F. 1976. Comparison of some tectonostratigraphic zones in the Appalachians of Newfoundland and New Brunswick. Canadian Journal of Earth Sciences, 13, pp. 868-875.

Reynolds, P. H., Kublick, E. E., and Muecke, G. K. 1973. Potassium-argon dating of slates from the Meguma Group, Nova Scotia. Canadian Journal of Earth Sciences, 10, pp. 1059-1067.

Reynolds, P. H., and Muecke, G. K. 1978. Age studies on slates: applicability of the $^{40}Ar/^{39}Ar$ stepwise

outgassing method. Earth and Planetary Science Letters 40, pp. 111-118.

Reynolds, P. H., Zentilli, M., and Muecke, G. K. 1981. K-Ar and $^{40}Ar/^{39}Ar$ geochronology of granitoid rocks from southern Nova Scotia: its bearing on the geological evolution of the Meguma Zone of the Appalachians. Canadian Journal of Earth Sciences, 18, pp. 386-394.

Richardson, J. M. G., Spooner, E. T. C., and McAuslan, D. A. 1982. The East Kemptville tin deposit, Nova Scotia: an example of a large tonnage, low grade, greisen-hosted deposit in the exocontact zone of a granite batholith. In Current Research, part B, Geological Survey of Canada, Paper 82-1B, pp. 27-32.

Riding, R. 1974. Model of the Hercynian foldbelt. Earth and Planetary Science Letters, 24, pp. 125-135.

Roddick, J. C. 1983. High precision intercalibration of $^{40}Ar-^{39}Ar$ standards. Geochimica et Cosmochimica Acta, 47, pp. 887-898.

Rogers, H. D. 1985. Geology of the igneous-metamorphic complex of Shelburne and eastern Yarmouth counties, Nova Scotia, in Current Research, Part A, Geological Survey of Canada, Paper 85-1A, pp. 773-777.

Rogers, H. D. 1986. Geology and Igneous Petrology of Shelburne and eastern Yarmouth counties, Nova Scotia. Unpublished MSc thesis, Acadia University, Wolfville, Nova Scotia, 150 pp.

Sarkar, P. K. 1978. Petrology and geochemistry of the White Rock metavolcanic suite, Yarmouth, Nova Scotia. Unpublished PhD thesis, Dalhousie University, Halifax, Nova Scotia, 188 pp.

Savell, M. J. 1980. The Applicability of the $^{40}Ar/^{39}Ar$ stepwise outgassing method to the dating of slates. Unpublished BSc thesis, Dalhousie University, Halifax, Nova Scotia, 63 pp.

Schenk, P. E. 1970. Regional variation of the flysch-like Meguma Group (Lower Paleozoic) of Nova Scotia compared to recent sedimentation off the Scotia Shelf. Geological Association of Canada, Special Paper 7, pp. 127-153.

Schenk, P. E. 1971. Southeastern Atlantic Canada, northwestern Africa and continental drift. Canadian Journal of Earth Sciences, 8, pp. 1218-1251.

Schenk, P. E. 1976. A regional synthesis (of Nova Scotia geology). Maritime Sediments, 12, pp. 17-24.

Schenk, P. E. 1978. Synthesis of the Canadian Appalachians. Geological Survey of Canada, Paper 78-13, pp. 113-136.

Schenk, P. E. 1980. Paleogeographic implications of the Meguma Group, Nova Scotia, - a chip of Africa? In "The Caledonides in the USA", Proceedings. Ed. D. R. Wones, IGCP 27: The Caledonide orogen. Virginia Polytechnic Institute and State University, Department of Geological Sciences, Memoir 2, pp. 27-32.

Schenk, P. E. 1981. The Meguma Zone of Nova Scotia - a remnant of western Europe, South America or Africa? In GEOLOGY OF THE NORTH ATLANTIC BORDERLANDS. Ed. J. W. Kerr and A. J. Ferguson. Canadian Society of Petroleum Geologists, Memoir 7, pp. 119-148.

Schenk, P. E. 1983. The Meguma terrane of Nova Scotia, Canada - an aid in trans-Atlantic correlation. In REGIONAL TRENDS IN THE GEOLOGY OF THE APPALACHIAN - CALEDONIAN - HERCYNIAN - MAURITANIDE OROGEN. Ed. P. E. Schenk. D. Reidel publishing, Dordrecht, The Netherlands, pp. 121-130.

Schenk, P. E. (in press). Sedimentation of a Cambrian to Devonian passive margin - the Meguma Zone of Nova Scotia. American Journal of Science.

Schenk, P. E., and Lane, T. E. 1982. Pre-Acadian sedimentary rocks of the Meguma zone, Nova Scotia- a passive continental margin juxtaposed against a volcanic island arc. International Association of Sedimentologists, Excursion 5B Guidebook, 85 pp.

Scotese, C. R., Van der Voo, R., Johnson, R. E., and Giles, P. S. 1984. Paleomagnetic results from the Carboniferous of Nova Scotia. In PLATE RECONSTRUCTION FROM PALEOZOIC PALEOMAGNETISM. Ed. R. Van der Voo, C. R. Scotese, and N. Bonhommet. American Geophysical Union, Geodynamics Series, 12, pp. 63-81.

Secor, D. T., Jr., Snoke, A. W., Bramlett, K. W., Costello, O. P., and Kimbrell, O. P. 1986a. Character of the Alleghanian orogeny in the southern Appalachians: Part I. Alleghanian derformation in the eastern Piedmont of South Carolina. Geological Society of America Bulletin, 97, pp. 1319-1328.

Secor, D. T., Jr., Snoke, A. W., and Dallmeyer, R. D. 1986b. Character of the Alleghanian orogeny in the

southern Appalachians: Part III. Regional tectonic relations. Geological society of America Bulletin, 97, pp. 1345-1353.

Shepherd, T. J., Miller, M. F., Scrivener, R. C., and Darbyshire, D. P. F. 1985. Hydrothermal fluid evolution in relation to mineralization in southwest England, with special reference to the Dartmoor-Bodmin area. In HIGH HEAT PRODUCTION (HHP) GRANITES, HYDROTHERMAL CIRCULATION AND ORE GENESIS. Institute of Mining and Metallurgy, London, pp. 345-364.

Smith, P. K. 1985. Mylonitization and fluidized breccation in southern Nova Scotia. Nova Scotia Department of Mines and Energy, Report 85-1, pp. 119-133.

Smitheringale, W. G. 1973. Geology of parts of Digby, Bridgetown and Gaspereau Lake map-areas. Geological Survey of Canada Memoir, 375, 78 pp.

Spariosu, D. J., Kent, D. V., and Keppie, D. J. 1984. Late Paleozoic motions of the Meguma terrane, Nova Scotia: new paleomagnetic evidence. In PLATE RECONSTRUCTION FROM PALEOZOIC PALEOMAGNETISM, ed. R. Van der Voo, C. R. Scotese, and N. Bonhommet. American Geophysical Union, Geodynamics Series 12. pp. 82-98.

Steiger, R. H., and Jager, E. 1977. Subcommission on Geochronology: Convention on the use of decay constants in geo- and cosmochronology. Earth and Planetary Science Letters, 36, pp. 359-362

Strong, D. F. 1979. The Mount Peyton batholith, central Newfoundland: A bimodal calc-alkaline suite. Journal of Petrology, 20, pp. 119-138.

Strong, D. F. 1980. Granitoid rocks and associated mineral deposits of eastern Canada and western Europe. Geological Association of Canada, Special Paper 20, pp. 741-770.

Strong, D. F., Dickson, W. L., and Pickerill, R. K. 1979. Chemistry and prehnite-pumpellyite facies metamorphism of calkalkaline Carboniferous volcanic rocks of southeastern New Brunswick. Canadian Journal of Earth Sciences, 16, pp. 1071-1085.

Tankard, A. J., and Welsink, H. J. (In press). Extensional tectonics and stratigraphy of the Mesozic Grand Banks of Newfoundland. American Association of Petroleum Geologists Memoir.

Taylor, F. C. 1965. Silurian stratigraphy and Ordovician-Silurian relationships in southwestern Nova Scotia. Geological Survey of Canada, Paper 64-13, 24 pp.

Taylor, F. C. 1967. Reconnaisance geology of Shelburne map area, Queens, Shelburne and Yarmouth Counties, Nova Scotia; Geological Survey of Canada, Memoir 349, 83 pp.

Taylor, F. C. 1969. Geology of the Annapolis-St. Mary's Bay map area, Nova Scotia (21A, 21B East Half); Geological Survey of Canada, Memoir 358, 65 pp.

Taylor, F. C., and Schiller, E. A. 1966. Metamorphism of the Meguma Group of Nova Scotia. Canadian Journal of Earth Sciences, 3, pp. 959-974.

Tetley, N. W., and McDougall, I. 1978. Anomalous $^{40}Ar/^{39}Ar$ release spectra for biotites from the Berridale Batholith, New South Wales, Australia. United States Geological Survey Open-File Report, 78-701, pp. 427-430.

Thorndike, R. M. 1978. CORRELATIONAL PROCEDURES FOR RESEARCH. New York, Gardner Press, 340 pp.

Turner, G. 1968. The distribution of potassium and argon in meteorites. In ORIGIN AND DISTRIBUTION OF THE ELEMENTS, ed. L. H. Ahrens, pp. 387-397. London, Pergamon, 1178 pp.

Turner, G. 1969. Thermal histories of meteorites by the $^{40}Ar/^{39}Ar$ method. In METEORITE RESEARCH, ed. P. M. Millman, pp. 407-417, Dordrecht, Reidel, 940 pp.

Turner, G and Cadogan, P. H. 1974. Possible effects of ^{39}Ar recoil in $^{40}Ar/^{39}Ar$ dating. Proceedings of the Fifth Lunar Science Conference, 2, pp. 1601-1615

Turner, D. L., and Forbes, R. B. 1976. K-Ar studies in two deep basement drill holes (abstract). EOS, Transactions of the American Geophysical Union, 57, p. 353.

Turner, G., Miller, J. A., and Grasty, R. L. 1966. Thermal history of the Bruderheim meteorite. Earth and Planetary Science Letters, 1, pp. 155-157.

Uchupi, E. and Austin, J. A., Jr. 1979. The geologic history of the passive margin off New England and the Canadian Maritimes. Tectonophysics, 59, pp. 53-69.

Van Houten, F. B. 1977. Triassic-Liassic deposits,

Morocco and eastern North America: comparison. American Association of Petroleum Geologists Bulletin, 61, pp. 79-99.

Villa, I. M., Huneke, J. C., and Wasserburg, G. J. 1983. ^{39}Ar recoil losses and presolar ages in Allende inclusions. Earth and Planetary Science Letters, 63, pp. 1-12.

Wagner, G. A., Reimer, G. M., and Jager, E. 1977. Cooling ages derived by apatite fission-track, mica Rb-Sr and K-Ar dating: the uplift and cooling history of the central Alps. Memoir of the Institute of Geology and Mineralogy, University of Padova, Padova, Italy, 30, 27 pp.

Wark, J. M., and Clarke, D. B. 1980. Geochemical discriminators and the palaeotectonic environment of the North Mountain basalts, Nova Scotia. Canadian Journal of Earth Sciences, 12, pp. 1740-1745.

White, C. E., Wentzell, B. D., and Raeside, R. P. 1985. Repeated metamorohism of the Meguma zone, southwest Nova Scotia. Atlantic Geoscience Society, 1985 Symposium, Program with Abstracts.

Williams, G. L., Fyffe, L. R., Wardle, R. J., Colman-Sadd, S. P., and Boehner, R. C. 1985. LEXICON OF CANADIAN STRATIGRAPHY, VOL. VI, ATLANTIC REGION. Canadian Society of Petroleum Geologists.

Williams, H. 1980. Structural telescoping across the Appalachian orogen and the minimum width of the Iapetus Ocean. In THE CONTINENTAL CRUST AND ITS MINERAL DEPOSITS. ed. D. W. Strangway, Geological Association of Canada Special Paper 20.

Williams, H., and Hatcher, R. D. Jr. 1982. Suspect terranes and accretionary history of the Appalachian orogen. Geology, 10, pp. 530-536.

Wilson, J. T. 1966. Did the Atlantic close and re-open? Nature, 211, pp. 676-681.

Wolfson, I. K. 1983. A study of the tin mineralization and lithogeochemistry in the area of the Wedgeport pluton, southwestern Nova Scotia. Unpublished MSc Thesis, Dalhousie University, Halifax, Nova Scotia, 376 pp.

Wones, D. R., and Eugster, H. P. 1965. Stability of biotite: experiment, theory, and application. American Mineralogist, 50, pp. 1228-1272.

Wright, T. L. 1968. X-ray and optical study of alkali feldspar: Part2. American Mineralogist, 53, pp. 88-104.

Yeo, G. M., and Ruixing, G. 1986. Late Carboniferous dextral movement on the Cobequid-Hollow fault system, Nova Scotia: evidence and implications; in Current Research, Part A, Geological Survey of Canada Paper 86-1A, pp. 399-410.

York, D. 1984. Cooling histories from $^{40}Ar/^{39}Ar$ spectra: implications for Precambrian Plate Tectonics. Annual Review of Earth and Planetary Sciences, 12, pp. 383-409.

Zentilli, M., and Reynolds, P. H. 1985. $^{40}Ar/^{39}Ar$ dating of micas from the East Kemptville tin deposit, Yarmouth County, Nova Scotia. Canadian Journal of Earth Sciences, 22, pp. 1546-1548.

METAMORPHIC MAP OF NOVA SCOTIA, 1979

Compiled by J. Duncan Keppie & G. K. Muecke
Nova Scotia Department of Mines and Energy

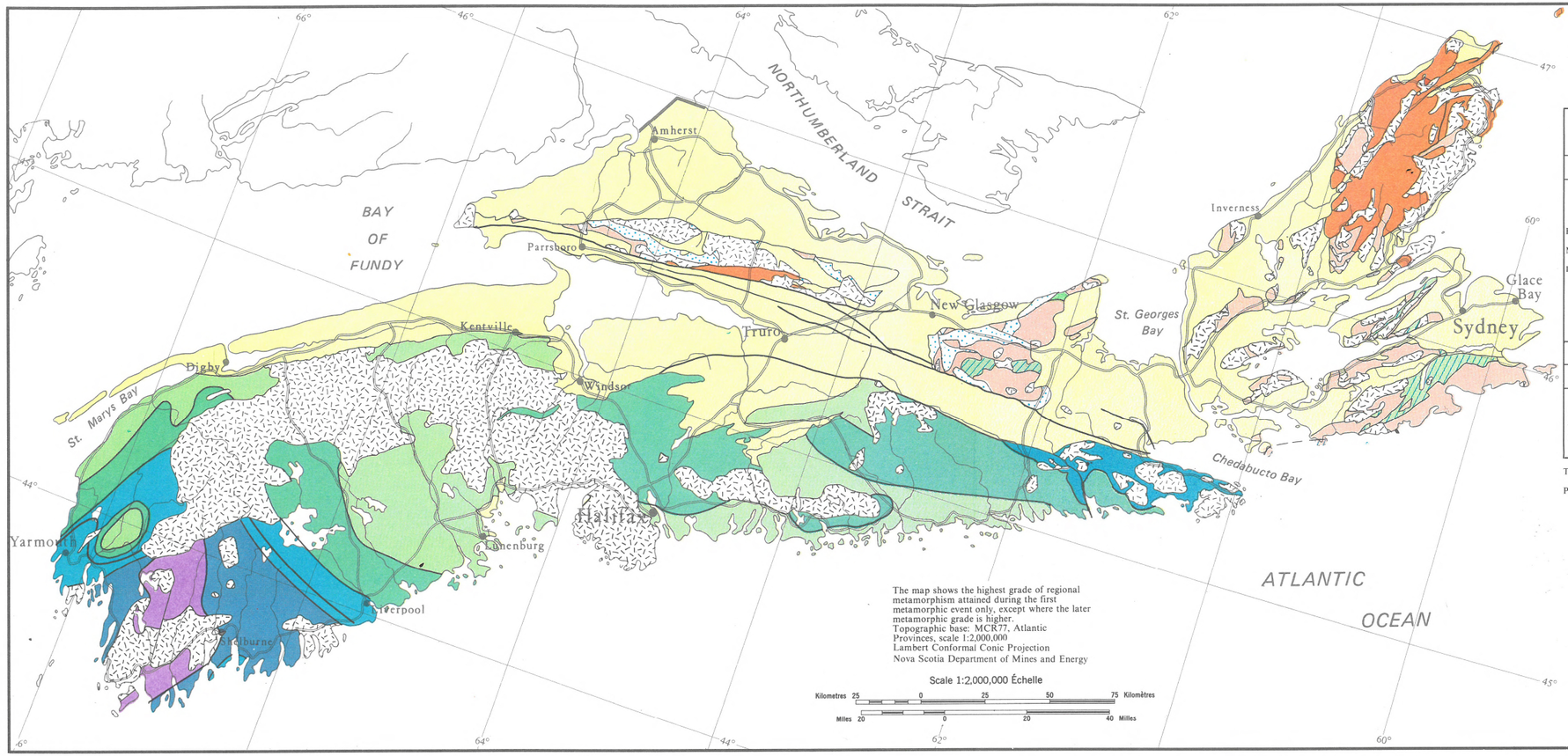

The map shows the highest grade of regional metamorphism attained during the first metamorphic event only, except where the later metamorphic grade is higher.
Topographic base: MCR77, Atlantic Provinces, scale 1:2,000,000
Lambert Conformal Conic Projection
Nova Scotia Department of Mines and Energy

Scale 1:2,000,000 Échelle

Kilometres 25 0 25 50 75 Kilomètres
Miles 20 0 20 40 Milles

LEGEND

AGE	METAMORPHIC FACIES	CODE	METAMORPHIC ZONE	OROGENY, TYPE OF METAMORPHISM
	Sub-greenschist			Post-ACADIAN
EARLY MIDDLE DEVONIAN	Sub-greenschist			ACADIAN High T Low P
	Greenschist		Chlorite	
			Biotite	
	Amphibolite		Garnet	
			Andalusite-staurolite - cordierite	
			Sillimanite	
	Amphibolite upon Hadrynian greenschist			
	Greenschist			ACADIAN OR TACONIAN
ORDOVICIAN	Greenschist			TACONIAN
LATE HADRYNIAN & EARLIER	Greenschist		Variable	CADOMIAN High T Medium P (some low P)
	Amphibolite		Zonal	
	Granulite		Succession	

T: temperature
P: pressure

Plutonic igneous rocks

GEOLOGICAL MAP OF NOVA SCOTIA, 1979

Compiled by J. Duncan Keppie
Nova Scotia Department of Mines and Energy

Abbreviations

K	CRETACEOUS	a.	anhydrite
J	JURASSIC	b.	basalt
T	TRIASSIC	c.	coal
P	PERMIAN	cg.	conglomerate
C	CARBONIFEROUS	cl.	clay
D	DEVONIAN	g.	gypsum
S	SILURIAN	gn.	gneiss
O	ORDOVICIAN	gw.	greywacke
Ꞓ	CAMBRIAN	lst.	limestone
H	HADRYNIAN	m.	marble
H	HELIKIAN	q.	quartzite
L	LATE	sch.	schist
M	MIDDLE	sh.	shale
E	EARLY	sl.	slate
		ss.	sandstone
		v.	volcanic rocks
		Ma.	million years
		~~	Unconformity
		≈≈≈	Orogeny

LEGEND

PLUTONIC IGNEOUS ROCKS

- granite
- granodiorite
- diorite
- granite granodiorite diorite gabbro

	K	E		s. cl.
140				ss. lst. b.
210	J	E		b.
	T	L		ss. sh.
247	P			
290				
HERCYNIAN OROGENY		L	*PICTOU*	ss. sh. c. cg.
			CUMBERLAND	
			RIVERSDALE	
			CANSO	
			WINDSOR	
340	C	E		ss. lst. g. a. salt
			HORTON	ss. sh. cg.
370				ss. sh. cg. v.
		L		cg. ss.
ACADIAN OROGENY	D	M		cg. ss. v.
		E		ss. lst. sh.
415	S			ss. sh. lst. v.
TACONIAN OROGENY	436 O		*MEGUMA*	cg. ss. sh. lst. v. sl. gw. gn. sch.
500	Ꞓ			
CADOMIAN OROGENY	580			Undivided ss. sh. v.
				v. sl. q. sch. m.
	H			q. m. v. sl. gn.
MICMACIAN OROGENY	900			Undivided gn. sch.
Ma	H or older			gn. sch.

Topographic base: MCR77, Atlantic Provinces, scale 1:2,000,000
Lambert Conformal Conic Projection

Scale 1:2,000,000 Échelle

Kilometres 25 0 25 50 75 Kilomètres
Miles 20 0 20 40 Milles

NORTHUMBERLAND STRAIT
BAY OF FUNDY
ATLANTIC OCEAN
Amherst
Parrsboro
Windsor
New Glasgow
Truro
Halifax
Yarmouth
Lunenburg
Liverpool
Shelburne
St. Marys Bay
Inverness
St. Georges Bay
Glace Bay
Sydney
Chedabucto Bay
66°
64°
62°
60°
47°
46°
45°
44°